TRG-81-3
77-1125866-00

June 1981

-Study Guide-

OPERATOR TRAINING-DEGRADED CORE RECOGNITION AND MITIGATION

Phase 1

Volume 2

Babcock & Wilcox
a McDermott company

TRG-81-3
77-1125866-00
June 1981

- STUDY GUIDE -

OPERATOR TRAINING-DEGRADED CORE RECOGNITION AND MITIGATION

Phase 1

Volume 2

BABCOCK & WILCOX
Nuclear Power Group
Nuclear Power Generation Division
P. O. Box 1260
Lynchburg, Virginia 24505

Babcock & Wilcox

Lesson 6 — CONSEQUENCES OF INADEQUATE CORE COOLING AND LIKELY CORE DAMAGE EFFECTS

Introduction

1. Lecturer —

2. Purpose — To give the operator necessary background information on the likely consequences of sustained inadequate core cooling and the resulting progression of core damage.

Objectives

The following material will be presented during this lesson:

1. General physical and thermochemical description of the fuel and cladding.

2. Normal operating parameters, then accident (LOCA) conditions that effect the integrity of this system.

3. Direct consequences to the cladding and fuel of major decrease in cooling capacity at cladding surface and/or partial core uncovering.

4. Primary consequences of loss of fuel integrity.

Key points to be retained are as follows:

1. The general configuration of the fuel/fuel assembly.

2. Operational (i.e., pressure/temperature) limits of fuel assembly materials.

3. Mechanics of fuel failure under accident conditions.

4. The consequences of fuel failure to the primary system.

Lesson 6 Outline

1. Introduction

2. Fuel and Cladding System Description

   2.1. Fuel
   2.2. Cladding and Assembly Materials

3. Loss-of-Coolant Conditions

   3.1. Manual Operation
   3.2. LOCA

4. Direct Consequences of Core Uncovering to Cladding/Fuel

   4.1. Cladding Rupture
   4.2. Cladding Oxidation/Hydrogen Generation
      4.2.1. Zircaloy Oxidation
      4.2.2. Stainless Steel Oxidation
      4.2.3. Radiolytic Decomposition of Water
   4.3. Fuel/Cladding Eutectic Formation

5. Core LOCA Consequences and TMI-2 Estimates

   5.1. General Consequences
   5.2. TMI-2 Estimates

6. Summary

CONTENTS

Lesson 6 – CONSEQUENCES OF INADEQUATE CORE COOLING AND LIKELY CORE DAMAGE EFFECTS

1. Introduction

The rate of power generation in a nuclear power reactor core is not limited by nuclear considerations; rather, the upper bounds on operating parameters are dictated by the thermal, thermal-hydraulic, and material limitations of the system. The reactor core must be maintained at a power level sufficient for the heat removal system to maintain temperatures within the system below specified safe limits. In a pressurized water reactor (PWR) core, the heat source is the uranium dioxide fuel contained in Zircaloy cladding and grouped with appropriate structural, control, and perhaps diagnostic materials, into fuel assemblies. During normal core operation the major portion of the energy produced in the fuel material is the product of the neutron-induced fission of the uranium-235 (and to a lesser extent plutonium nuclei within the fuel); it is this fission process that is rapidly terminated by a reactor scram. However, a smaller but still significant portion of the core heat generation is the result of beta- and gamma-decay of fission-product nuclides, which are also by-products of the fission process. These decay reactions are not terminated by a reactor shutdown or the presence of neutron poison materials; they provide the primary heat source for core material damage under loss-of-coolant circumstances.

The main parameters affecting core material damage in a loss-of-coolant situation is temperature. In a reactor core there are four basic resistances to heat transport: the thermal resistivity of the fuel material itself, the resistance across the gap separating the fuel material from the cladding, the resistance across the cladding itself, and the resistance between the outer cladding surface and the reactor coolant. It is the large increase in this last thermal resistance, from the outer cladding surface to the coolant, that is the initial result of a loss-of-coolant situation. The resulting inadequate or lowered cooling capability gives rise to the increase in fuel

temperature that can result in damage to the fuel material. The capability of the coolant to remove heat in a loss-of-coolant accident (LOCA) that involves the water level dropping below the core is drastically reduced; this is the reason "core uncovering" is a major loss-of-coolant consequence.

2. Fuel and Cladding System Description

2.1. Fuel

Pressurized water reactor (PWR) fuel generally consists of sintered uranium dioxide pellets stacked and sealed within Zircaloy tubes, which are themselves grouped with appropriate structural and control components into fuel assemblies. A Babcock & Wilcox Mark B fuel assembly is a square 15 by 15 array of such fuel and control material rods (208 fuel rods per assembly, 16 guide tubes for control materials, and one central instrument tube). A B&W "177 series" reactor core, such as the TMI-2 unit, contains 177 such assemblies. The uranium dioxide fuel in PWRs is generally enriched in the fissile uranium-235 isotope to 1.5 to 4.0% from the natural enrichment level of about 0.7% ^{235}U.

A number of factors, the explanation of which is beyond the scope of the present discussion, enter into the selection of uranium dioxide — as opposed to other uranium materials or compounds, such as uranium metal alloys, uranium carbide, uranium nitride — as the most appropriate fuel for a PWR.

The uranium dioxide fuel is in the form of sintered right-cylindrical pellets, which are fabricated by the powder metallurgical technique of cold pressing and sintering. In this technique uranium dioxide powder is compressed under high pressure and room temperature in a die press into approximately 50% dense cylindrical compacts. These compacts are then baked at approximately 1700C under a reducing atmosphere of hydrogen and nitrogen to densify and harden (or sinter) into 95% dense pellets. This fabrication technique thus produces a material of low but controlled porosity and fine (approximately 10 micron) grain structure. In terms of fission product migration, swelling, dimensional changes, thermal stability, etc., the behavior of nuclear fuel under irradiation is closely dependent on impurities and the precise microstructural nature of the fuel, and thus impurity levels and microstructure are very closely controlled in the fabrication process.

Figure 6-1 is an approximate description of a typical uranium dioxide nuclear fuel pellet. Uranium dioxide is the form of uranium oxide used as nuclear fuel, although uranium can exist in four different oxidation states: +3, +4, +5, and +6. The +4 oxidation state is the one that corresponds to uranium dioxide. A change in the oxidation state — for instance, to U_3O_8 or UO_3 — would involve complete destruction of pellet integrity. The melting point of uranium dioxide is about 2800C (or 5100F).

The uranium dioxide powder from which fuel pellets are fabricated is the product of a sequence of manufacturing operations which (including pellet fabrication) are termed the front end of the full cycle:

- Mining uranium ore (U_3O_8).
- Conversion of U_3O_8 to gaseous UF_6.
- Enrichment of natural UF_6 to UF_6 higher in ^{235}U content.
- Conversion of UF_6 to UO_2 powder.

During irradiation in a reactor core, some of the uranium atoms (^{235}U and ^{238}U) undergo the following reactions:

- ^{235}U thermal neutron capture and subsequent fission to form fast neutrons, fission products, and energy.
- ^{238}U fast neutron capture to form, after a sequence of intermediate steps, plutonium-239.
- ^{239}Pu thermal neutron capture and subsequent fission to form fast neutrons, fission products, and energy.

When a reactor core is shut down, whether under normal or abnormal conditions, the reactions above essentially cease, thus eliminating the major source of energy release in the core (fuel) materials. However, a significant amount of energy release continues in the gamma- and beta-decay of the fission product residues of the main fission process. Although this decay energy decreases fairly rapidly with time after shutdown, it can still provide, particularly in the event of a loss of water coolant around the core materials, enough energy to result in major thermal damage to core components. Thus, the uranium dioxide fuel material, even while not undergoing fission, still provides (through the decay of the fission product materials within its structure) the initial energy driving force for core damage in the case of a LOCA.

2.2. Cladding and Assembly Materials

The function of the fuel assembly is to provide a mechanical framework that facilitates transfer of the energy generated within the fuel material to the primary coolant while simultaneously restricting the migration of fuel and fission product materials out of the fuel element. The primary structural component of the fuel assembly is the fuel rod, which consists of a stack of approximately 230 uranium dioxide pellets sealed inside a Zircaloy-4 tube. Springs at either end of the pellet stack position and restrain the stack.

The springs and the stack are separated by Zircaloy spacers. The interior of the rod is pressurized with helium to minimize the pressure drop across the cladding (and thus its creep collapse) during normal operation and to enhance heat transfer across the pellet/cladding gap. Zircaloy is an alloy of zirconium consisting of approximately 98.4% zirconium, 1.3% tin, 0.2% iron, and 0.1% chromium. It has a melting point of approximately 1850C (3361F). A zirconium alloy is chosen for the cladding material primarily because of the relatively transparent nature of the zirconium nucleus to neutron radiation; that is, zirconium activates in a neutron flux to a lesser extent than other candidate cladding materials, such as stainless steel. In some older PWRs, however, stainless steel cladding is used because of its high strength compared to zircaloy.

A B&W Mark B fuel assembly (Table 6-1) consists of 208 fuel rods dispersed in a square 15 by 15 array with 16 (control/poison) guide tubes and a central instrumentation tube. The guide tubes admit either control rods (CRs), axial power shaping rods (APSRs), burnable poison rods (BPRs), or neutron source rods. All the assemblies are completely interchangeable. The rods are spaced and held in place by stainless steel upper and lower end fittings and eight Inconel spacer grids. A typical fuel assembly contains approximately 525 kg of uranium dioxide, 125 kg of Zircaloy, and 70 kg of stainless steel.

A control rod assembly (CRA) for a B&W PWR consists of 16 rods of silver-indium-cadmium (Ag-In-Cd) alloy neutron poison material sealed in cladding of type 304 stainless steel. The alloy has a melting point of approximately 1500C (2730F). The poison material length per rod is about 135 inches.

A burnable poison rod assembly (BPRA) consists of 16 rods of sintered alumina-boron carbide (Al_2O_3-B_4C) pellets inside Zircaloy-4 cladding. The burnable poison length is approximately 125 inches.

An axial power shaping rod assembly (APSRA) is made up of Ag-In-Cd alloy poison material in stainless steel cladding. The poison material length is approximately 3 ft, it is located near the lower ends of the rods.

Therefore, the number of materials contained in a fuel assembly, and that can thus conceivably interact in a temperature excursion caused by an extended loss of coolant, can be seen to include more than just the fuel material UO_2. However, as will be shown in the balance of this discussion, the UO_2 and its Zircaloy cladding constitute the primary heat sources in such an accident, and

thus any core degradation analysis will focus primarily on the UO_2 pellet-Zircaloy cladding materials.

Table 6-1. Typical Fuel Assembly Parameters (Approximate)

Weight, lb	1515
Displaced volume, ft^3	2.85
Axial length, in.	165.63
No. of fuel rods	208
No. of guide tubes	16
No. of instrument tubes	1
No. of spacer grids	8
UO_2 loading, kg	526
Total Zircaloy, kg	131

Figure 6-1. Typical Uranium Dioxide Fuel Pellet

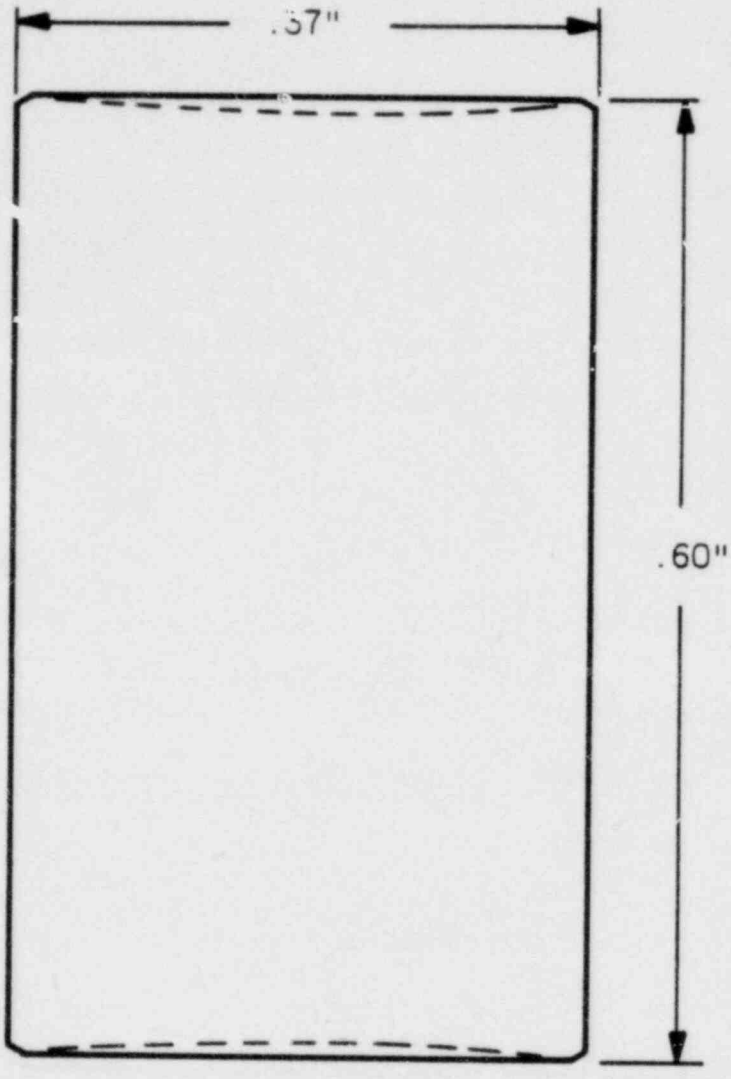

- MATERIAL - SINTERED URANIUM DIOXIDE, 95% DENSE
  - OXYGEN-TO-URANIUM RATIO 2.00 - 2.02
- DENSITY - 10.41 GRAMS/CC
- WEIGHT - 10.8 GRAMS
- PELLET DISHED AND CHAMFERED AT EACH END
- DIAMETER - .37 INCHES
- HEIGHT - .60 INCHES
- OPEN POROSITY - 1%

3. Loss-of-Coolant Condition*

3.1. Normal Operation

During normal operation of a PWR core, the reactor coolant temperature reaches a maximum of about 605F (319C), the fuel (cladding) surface temperature about 650F (344C), the volume average fuel temperature about 1100F (593C), and the maximum fuel centerline temperature around 3000F (1649C). These values are well below any level where significant material damage occurs. The linear power rating for fuel rods during normal operation is about 5.5-6.0 kW/ft, whereas an approximate design limitation for a normally operating core would be 15 kW/ft. Thus, it can be seen that under normal operating conditions the thermal design of the core assemblies is such that the energy produced within the core materials is more than adequately transferred to the reactor coolant, keeping material temperatures well below damage/deformation limits.

The thermal energy generated within a fuel rod needs to be transported across four general thermal resistances to reach the primary coolant:

- The thermal resistance of the uranium dioxide pellet itself.
- The thermal resistance of the gap between the pellet and the cladding material.
- The thermal resistance of the cladding itself.
- The thermal resistance across the fluid boundary layer between the outer cladding surface and the bulk coolant.

A simplified equation for the maximum temperature in the fuel/cladding system using solid fuel pellets, that is, the centerline temperature of the fuel pellet itself, can be written:

$$T_{c\ell} = T_f + \frac{qR_o^2}{2}\left\{\frac{1}{2k_f} + \frac{1}{k_g}\ln\frac{R_o}{R} + \frac{1}{k_c}\ln\frac{R_c}{R} + \frac{1}{hR_c}\right\} \qquad (1)$$

---

*TMI-2 based.

where

k_f = fuel pellet thermal conductivity,

k_g = pellet/cladding gap thermal conductivity,

k_c = cladding thermal conductivity,

h = convective heat transfer coefficient of outer cladding surface,

R_o, R, R_c = radii of pellet, inner cladding surface, and outer cladding surface, respectively,

q = volumetric heat generation rate of the fuel, a quantity proportional to the fuel rod linear power rating.

During normal core operation q represents a fairly constant (with time) value for heat generation, accounting for all heat energy generated within the fuel, primarily fission energy. Also, the value for h is large enough to adequately remove heat under core coolant flow conditions. The overall result of the heat transport mechanism is the set of fairly constant temperature values mentioned earlier.

3.2. LOCA

The primary consequence of an extended LOCA of interest here is core uncovering. That is, the primary system loses enough water that the liquid (or liquid-steam mixture) level in the reactor vessel falls below the top of the fuel rods. In general, the farther below the top of the core the level falls and the longer the time core materials remain above the liquid level, the greater the potential for and the extent of fuel damage and core degradation. This can be demonstrated by referring to the heat transfer balance given above.

Upon initiation of the reactor trip, control rod insertion essentially terminates fission reactions within the fuel material. However, the fission products present within the fuel continue to provide a heat source through the mechanism of gamma- and beta-decay, which the control rods do not affect. This heat source is largest near the time of core shutdown and decreases with time thereafter. (For example, at TMI-2 the decay heat in the core about one hour after the shutdown was about 1% of full power, or 32 MW, decreasing to 2.5 MW a little after 2 hours). If not dissipated, this heat is sufficient to cause major core thermal damage.

When the core is uncovered, the heat transfer coefficient between the cladding and the coolant channel, h, drastically decreases. That is, the thermal resistance between the cladding outer surface and the steam is much greater than

that between the cladding and water or a water-steam mixture. This causes the last term in the brackets in equation 1 for $T_{c\ell}$ to increase greatly. Since the equation for $T_{c\ell}$ is an equilibrium equation, this decrease in h does not instantaneously cause an increase in $T_{c\ell}$, but it does show that $T_{c\ell}$ (and therefore the temperatures at all points out to the outer cladding surface) will begin to increase. This temperature increase will in turn have an effect on the other thermal resistances in equation 1 since k_f, k_g, and k_c are themselves temperature-dependent parameters. Figure 6-2 shows the temperature dependence of the thermal conductivity of 95% dense UO_2 (k_f). It can be seen from this curve that the thermal conductivity of the fuel pellet will decrease during a temperature rise excursion, thus increasing the first term inside the brackets of equation 1 and accelerating the tendency of the temperature of the fuel and cladding to rise. Figure 6-3 shows the temperature dependence of the thermal conductivity of Zircaloy-4. In this case the thermal conductivity of the material increases with temperature, causing the third term in the brackets in equation 1 to decrease and damping somewhat the tendency of the fuel/cladding system to heat up.

The thermal resistance of the pellet/cladding gap is a function not only of the thermal conductivity of the helium fill gas (which increases with temperature), but also of the gap width, the amount and thermal conductivity of released fission gas, and the fuel burnup. In general, gap resistivity normally increases with fuel burnup.

However, the overall effects of core uncovering on heat transfer out of the fuel rods is dominated by the drastic lowering of the heat transfer coefficient at the outer cladding surface, which destroys the capability of the fuel element to dissipate the decay heat of the core at a rate fast enough to avoid temperatures high enough to damage the fuel element materials. As the temperature excursion continues to temperatures above 1000C (1831F), additional heat can be generated within the system by metal (primarily zirconium)/steam exothermic chemical reactions. The mechanisms of such reactions are discussed later, but let it suffice at this point to say that the heat produced from these reactions can be a significant component of the total core damage driving force.

Figure 6-4 represents a Sandia Labs example calculation of the temperature history of the TMI-2 core after uncovering. Fuel cladding temperature profiles

were calculated for eight core radial regions using the BOIL computer code. The calculation accounted for the oxidation of Zircaloy as a heat source but did not include the effect of cladding rupture on oxidation rate. However, cladding rupture almost certainly did occur at TMI-2, as is discussed later.

Figure 6-2. Thermal Conductivity of 95% TD UO_2

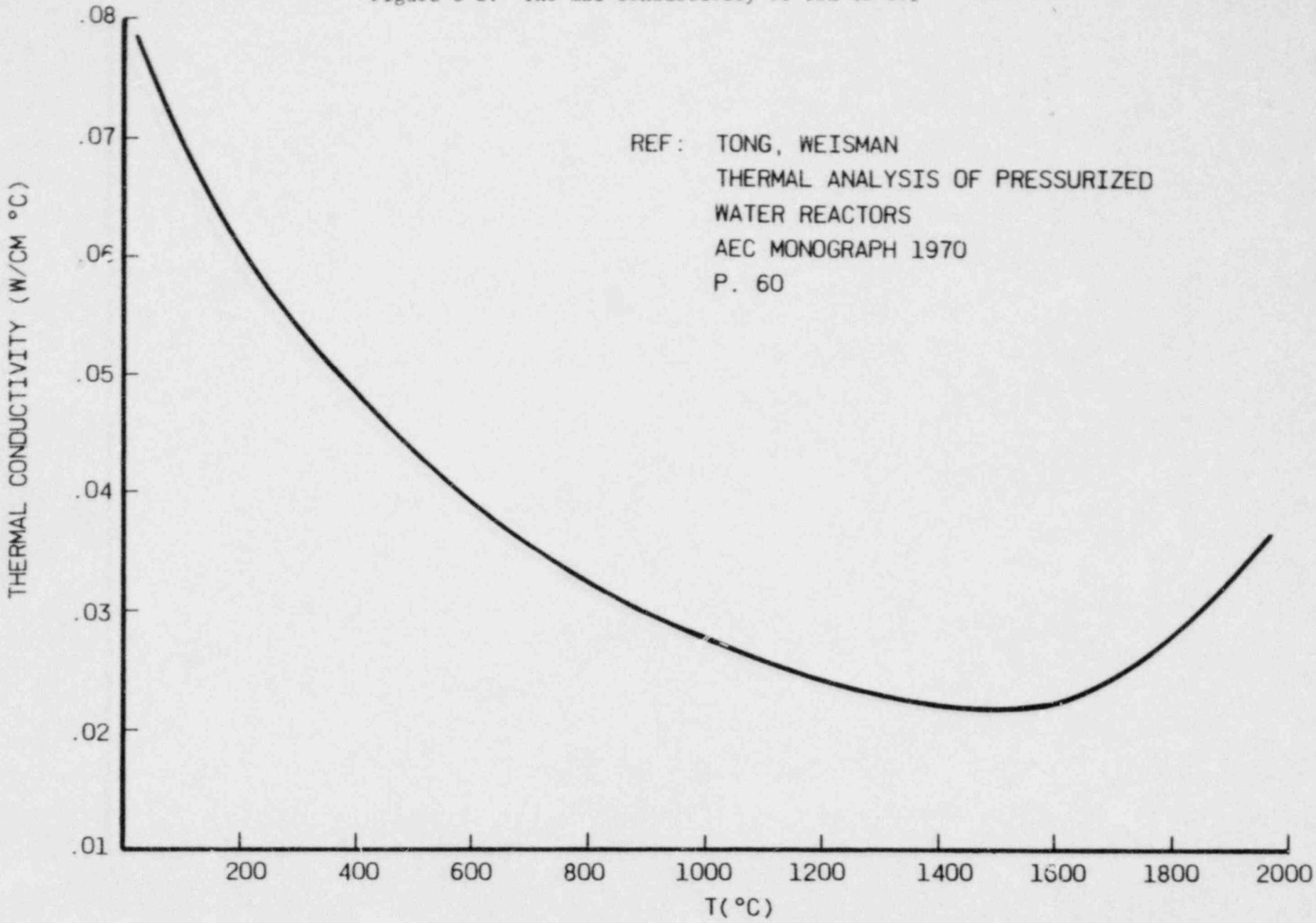

Figure 6-3. Thermal Conductivity of Zircaloy

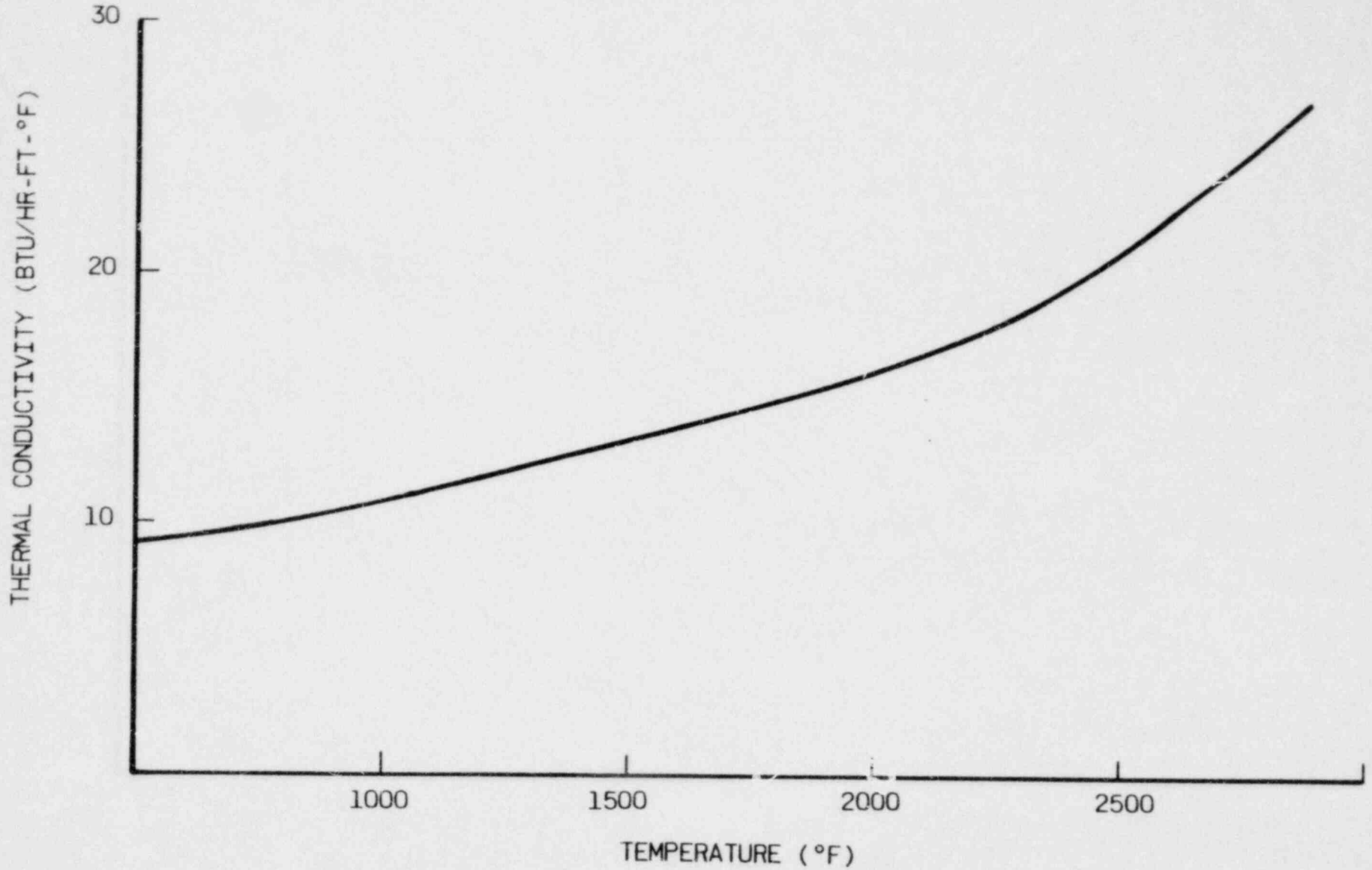

Figure 6-4. TMI-2 Core Temperture Vs Time After Uncovering

Source: NUREG/CR-1561, SAND80-1495

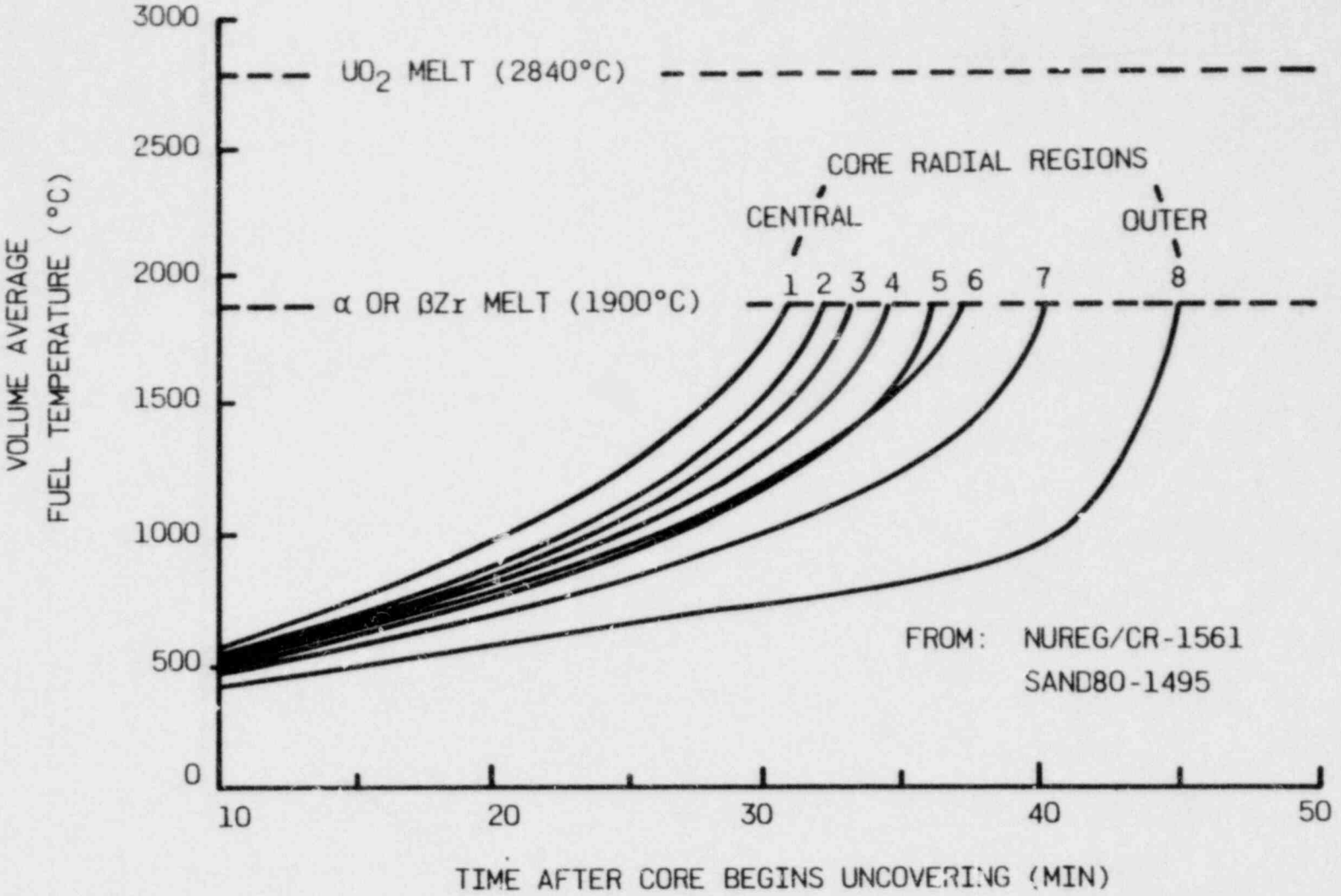

4. Direct Consequences of Core Uncovering to Cladding/Fuel

The damage mechanisms to the reactor core materials resulting from extended loss of coolant are treated here in the following major categories:

- Rupture of the cladding
- Cladding oxidation/hydrogen generation
- Fuel/cladding eutectic formation
- Fuel melting

It should be recognized that although these mechanisms are treated herein as distinct, in an extended core uncovering they would be very interactive. The consequences of these damage mechanisms are varying degrees of loss of fuel element structural integrity, release of radioactive fission products to the core/containment, relocation of fuel materials in the core, blockage of coolant flow channels, hydrogen accumulation, etc. It is well beyond the scope of this discussion to evaluate all the different combinations of potential loss-of-coolant scenarios or potential damage configurations. Instead, the discussion in this section focuses on the nature of the major damage mechanisms noted above, and the next section discusses the extent to which each may have contributed to core damage during the accident at TMI-2.

4.1. Cladding Rupture

The most likely initial form of mechanical fuel rod failure during an extended LOCA is rupture of the Zircaloy cladding caused by the pressure drop across the cladding exceeding the cladding hoop stress limit. That is, the cladding bursts due to excessive internal pressure. The high temperatures that accompany an extended loss of coolant simultaneously increase the internal pressure of the fuel rods while decreasing the capability of the Zircaloy cladding to restrain this pressure. This could result in ballooning and ultimately bursting of the rod. The parameters that contribute to this mode of fuel failure can be discussed separately here while noting that they are cumulative and/or interactive in nature.

It has been noted that during the manufacture of light water reactor (LWR) fuel elements, the fuel rods are pressurized with helium before sealing. This pressurization is performed to improve heat transfer across the fuel pellet/cladding gap and to minimize the pressure drop across the cladding during

normal operation. Minimization of the pressure drop from the coolant side (about 2000 psi) to the interior of the fuel rod (about 1000 psi) is meant to eliminate cladding creep or ovalization, which is a compressive deformation of the Zircaloy cladding. During an extended loss of coolant, however, the greatly increased temperature of the fuel rods, caused by the abnormal heat transfer conditions cited in the last section, causes this helium pressure to increase far past its normal value. In addition, the TMI-2 LOCA involved a significant depressurization of the primary side. Thus, the presence of the helium inside the fuel rods at a high temperature, combined with depressurization outside the fuel rods, can result in tensile loads on the cladding. The contribution of the helium to the internal pressure of the fuel rod can be assumed to follow the ideal gas law in being directly proportional to the absolute temperature.

In addition to the pressure of the helium fill gas inside the fuel rods, additional internal pressure can be generated by the release of gaseous fission products (such as xenon, krypton, and iodine) from the fuel pellet into the rod plenum. During normal reactor core operation, a maximum of approximately 1% of the gaseous fission products is released from the fuel pellets and made available for pressure generation. Figure 6-5 is a plot of the fraction of fission product gas release as a function of fuel temperature and burnup, F(B.U.,T). The normal volume-averaged fuel temperature is about 1000-1100F (540-590C). From Figure 6-4 it can be seen that the temperatures postulated to have been reached in the reactor core during that LOCA were high enough to cause significant fractional release of the fission product gases from the fuel pellets. These release levels not only make fission product gases a significant contributor to the internal rod pressure but also make these radioactive fission products available for release to the primary system in the event of any rod failure involving breach of the cladding.

The capability of the Zircaloy cladding to restrain the internal pressure of the fuel rod is measured by the rupture engineering hoop stress (G), a parameter proportional to the pressure difference (ΔP) across the cladding and inversely proportional to the thickness (t) of the cladding in the following manner:

$$G = (d/2t)\Delta P \qquad (2)$$

where d is the undeformed cladding mid-wall diameter. Figure 6-6 is a plot of rupture engineering hoop stress as a function of cladding temperature. The design curve used by B&W and curves generated by ORNL for various cladding heat-up rates are shown. The ΔP scale shown at the top assumes a cladding thickness of 0.0075 inch. During a LOCA, both the cladding temperature and the hoop stress are increasing. The magnitude of the hoop stress, it will be noted, is also dependent on the primary side pressure. Thus, to give a simple example, if a fuel rod were slowly heated to 800C (1471F), it could be expected to burst when the internal pressure of the rod exceeded the primary side pressure by about 700 psi.

The interactive nature of rod burst failure mechanisms can also show up in another way. Note that the rupture stress or (looked at in another way) the rupture temperature is also a function of the cladding thickness. As is discussed in more detail in the next section, during a LOCA the cladding material (Zircaloy) has the potential for oxidation by steam when the core is uncovered. This oxidation reaction converts the Zircaloy metal to Zirconium oxide, effectively eliminating the structural strength of the converted metal. Thus, the effective thickness of the cladding itself could, under certain loss-of-coolant conditions, decrease during the accident sequence, shortening the time-to-failure of the fuel rods.

It can be seen from the discussion above that the potential for fuel rod rupture during a LOCA is a function of a number of variables particular to the nature of the accident: the rate of core heatup, the duration of core uncovery, the pressure in the primary system, the fuel material temperature, fuel burnup prior to the accident, etc. Prediction or calculation of the time-to-failure in such an accident is thus very sensitive to such parameters and involves detailed analyses of the way these parameters interact. Such calculations have been made by various persons for the TMI-2 case and are covered later in this discussion.

4.2. Cladding Oxidation/Hydrogen Generation

4.2.1. Zircaloy Oxidation

At elevated temperatures during a LOCA that involves core uncovering, zirconium may react with steam to form zirconium oxide and hydrogen by the following chemical reaction

$$Zr + 2H_2O \rightarrow ZrO_2 + 2H_2 + 140 \text{ kcal/mole.} \quad (3)$$

An examination of the right-hand side of equation 3 reveals the following undesirable consequences of such a reaction:

1. Transformation of Zircaloy (primarily zirconium) into ZrO_2 and the consequent loss of cladding structural strength (lowering of rupture hoop stress), making cladding failure more likely to occur, and likely to occur earlier.

2. Formation of hydrogen gas, which enters the primary system. The formation of a large hydrogen bubble creates a flammability/explosion problem if an oxygen source exists and can interfere with placing the primary system into natural circulation (by collecting at the top of the hot leg) even if no oxygen exists.

3. The release of heat into the primary system by means of the exothermic oxidation reaction (140 kcal per g-mole of zirconium oxidized). This heat release can serve to aggravate and accelerate the temperature excursion in the core after a LOCA. It has been shown that in the case of TMI-2, this heat source became the dominant one during the time when the major amount of core damage occurred.

The oxidation of Zircaloy (or zirconium) at the fuel rod cladding surface is thought to proceed via the following steps:

1. Diffusion of steam through a thin hydrogen layer at the cladding surface. This hydrogen layer, while always thin in terms of the inventory of total hydrogen generated, could be expected to become thicker as the Zircaloy oxidizes, thus inhibiting somewhat the zirconium-steam reaction rate.

2. Dissociation of steam at the ZrO_2 surface into hydrogen and oxygen. This is endothermic or energy-absorbing reaction (-58 kcal per g-mole of H_2O) whose energy is provided by the high temperature at the ZrO_2 surface.

3. Diffusion of oxygen through the ZrO_2 layer into the underlying Zircaloy metal.

4. Reaction of the oxygen with the zirconium to form zirconium oxide and the release of 255 kcal energy per g-mole of zirconium oxidized. Figure 6-7 illustrates the phase diagram for the zirconium and oxygen binary system and shows that in an equilibrium situation, no zirconium oxide forms until an oxygen level of approximately 30 at % exists in the metal. That is, oxygen dissolves into zirconium up to approximately 30 at % without chemically reacting with the zirconium to form zirconium oxide (ZrO_2 - 66.7 at % oxygen) and releasing heat. It can be seen that as the zirconium oxide layer on the cladding grows, the oxygen generated at the zirconium oxide surface must diffuse through an increasingly resistant diffusion barrier to get to the base metal. In this way the zirconium oxide layer itself could serve to shield the unoxidized metal from further oxidation.

This somewhat idealized description of cladding oxidation does not take into account other phenomena that may be significant factors in a LOCA, such as microcracking or spallation of the oxide layer, which would expose new base metal surfaces to the steam, localized melting of Zircaloy metal (~1900C/3451F), which obviously would alter the reaction geometry, and limiting of the steam available for reaction with the cladding by core flow blockages. It is in trying to account for these transient effects as well as the thermodynamic equilibrium aspects that the variance (30 to 55%) in the estimates of the extent of Zircaloy oxidation at TMI-2 arises. If all the Zircaloy cladding in a B&W 177-fuel assembly reactor core were to oxidize, the reaction would produce about 1000 kg of hydrogen and 42 MW of energy.

4.2.2. Stainless Steel Oxidation

The stainless steel components of the reactor core can also be oxidized by steam. Although Zircaloy oxidizes much more rapidly than stainless steel at temperatures below about 1000C (1831F), the rate of stainless steel oxidation per unit weight at about 1250C (2281F) is equal to that of zirconium. What would help to retard the stainless steel oxidation contribution to the hydrogen and heat generation compared to the Zircaloy would be the fact that the stainless steel end fittings, etc. would probably be exposed to slightly lower localized temperatures than the Zircaloy, which is in intimate contact with the UO_2 fuel. There is also less stainless steel in the fuel elements than Zircaloy.

The stainless steel oxidation reaction may be represented by equation 4:

$$aFe + bCr + cNi + dH_2O \rightarrow Fe_a\ Cr_b\ Ni_c\ O_d + dH_2 + 155\ \text{kcal/mole}. \qquad (4)$$

It can be seen that the heat contribution and hydrogen contribution of the stainless steel oxidation reaction is on a per-weight basis much like that for Zircaloy.

4.2.3. Radiolytic Decomposition of Water

Besides the metal/steam oxidation reactions that can occur during a LOCA, another potential source of hydrogen in the primary system is the radiolytic decomposition of the water coolant itself. This reaction is of concern because the decomposition of the water molecule could result in the generation of both hydrogen and oxygen, which could then potentially combust in the primary system.

The radiolytic decomposition involves the interaction of decay gamma and beta radiation with water molecules to form solvated electrons (e^-_{aq}), free radicals, and molecules as illustrated in equation 5:

$$H_2O \xrightarrow[\beta,\gamma]{} e^-_{aq},\ OH,\ H,\ HO_2,\ H_2,\ H_2O_2. \qquad (5)$$

Once these species are formed, they could immediately recombine with each other or diffuse into solution for reaction there. The final result of such reactions would be the formation of the molecular products H_2, H_2O_2, O_2, or reformed H_2O. The amount of each of these molecular species formed per unit β or γ energy absorbed is a sensitive function of such parameters as the amount and type of other solutes in the water, the type of radiation absorbed (balance of α, β, γ, and delayed neutrons), the temperature and turbulence of the water, the pH of the water, etc. It is almost impossible to estimate the hydrogen generation accurately by this mechanism in a situation like the LOCA at TMI-2; however, Table 6-2 gives a rough upper bound estimate for the hydrogen generation after shutdown for a 3300-MWt reactor. It can be seen from these results that hydrogen generation from radiolysis is small compared to the contribution of the metal/water oxidation reaction over the early time ranges involved in a LOCA (10^2 to 10^4 seconds). However, the hydrogen generation for a totally sealed system could significantly add to the hydrogen inventory over a more extended time period.

4.3. Fuel/Cladding Eutectic Formation

The melting point of uranium dioxide is approximately 2800C (5071F), for zirconium oxide 2700C (4891F), and for pure Zircaloy 1825C (3316F). The melting point of Zircaloy is also variable as a function of the amount of oxygen dissolved in the metal, as shown in Figure 6-7, increasing from 1825C (3316F) for 0% dissolved oxygen to 1975C (3586F) for about 20 at % dissolved oxygen.

The equilibrium ternary system uranium-zirconium-oxygen, however, has combinations of these elements that form a liquid phase at temperatures as low as 1500C (2731F). This is known as the urania/zirconium eutectic. Figures 6-8a, -8b, and -8c show isothermal sections for this ternary system at 1000C (1831F), 1500C (2731F), and 2000C (3631F). The letter L in these diagrams refers to liquid. The darkened area in Figure 6-8c refers to a region of compositions where nothing but liquid exists under thermodynamic equilibrium conditions.

A detailed analysis of these isothermal phase diagrams is not necessary for the purposes of this discussion, but the following general observations can be noted:

- No liquid phase exists at 1000C (1831F).
- At 1500C (2731F), the liquid phase area, that is, those compositions at which any liquid forms at all, is confined below a line connecting the UO_2 point on the U-O side of the triangle to a point about one third of the distance up the O-Zr side of the triangle. No liquid exists above this line. This means that at 1500C (2731F) the physical condition that must exist for the formation of any eutectic liquid is equilibrium contact between UO_2 and zirconium (Zircaloy) with less than about 33 at % oxygen dissolved in the metal.
- At 2000C (3631F), the liquid phase area is confined below a boundary approximately connecting UO_2 on the U-O side to ZrO_2 on the Zr-O side. This means that at 2000C, eutectic liquid can form given an equilibrium contact condition between uranium dioxide and any Zircaloy metal, irrespective of the level of dissolved oxygen in the metal. No liquid can form, however, between UO_2 and oxidized Zircaloy or ZrO_2.

Note that these diagrams represent a condition of thermodynamic equilibrium between the component materials. This essentially means that the materials must be in intimate physical contact long enough to reach equilibrium. In an extended LOCA, such as occurred at TMI-2, various physical and geometric considerations arise which inhibit the attainment of thermodynamic equilibrium.

Trying to account qualitatively for the various mechanisms that could affect fuel/cladding eutectic formation during a LOCA, both equilibrium and physical, the following observations might be made:

- If the extended loss of coolant involves a slow (<1°C/second) temperature ramp in the core region of interest, extensive Zircaloy oxidation and concurrent oxygen dissolution in Zircaloy metal are likely to have occurred, thereby inhibiting eutectic liquid formation. Even if no cladding has burst, two mechanisms could still exist that would retard eutectic formation at the fuel pellet/inside cladding interface: dissolution of oxygen from the outside cladding surface and diffusion to the inside cladding surface, and the likely existence of a 10-mil ZrO_2 layer on the inside cladding surface due to oxygen transfer from the UO_2 to the Zircaloy during normal operation. The ZrO_2 layer could effectively shield the UO_2 from the Zircaloy metal.

- The cladding is likely to burst due to internal pressure effects before it reaches eutectic formation temperature (~1500C, 2831F). This would allow steam into the fuel/cladding gap, oxidizing the interior cladding surface and thus effectively shielding the UO_2 from the Zircaloy metal and preventing eutectic liquid formation.
- Poor contact between the fuel pellet and inside cladding surface would inhibit eutectic formation below the melting point of the cladding. Once the cladding becomes molten, the potential for eutectic formation increase.
- A fast temperature ramp would increase the probability for eutectic formation by raising the temperature faster than oxygen can diffuse into the Zircaloy.

Table 6-2. Conservative Calculation of Radiolysis Yield

Time after shutdown, s	Integrated decay energy, MJ/MW	Yield, kg H_2
10^2	6	4
10^3	25	17
10^4	160	110
10^5	800	548
10^6	3500	2400

Reference: NUREG/CR-1561, August 1980.

Figure 6-5. Fission Product Gas Release Vs Temperature and Burnup

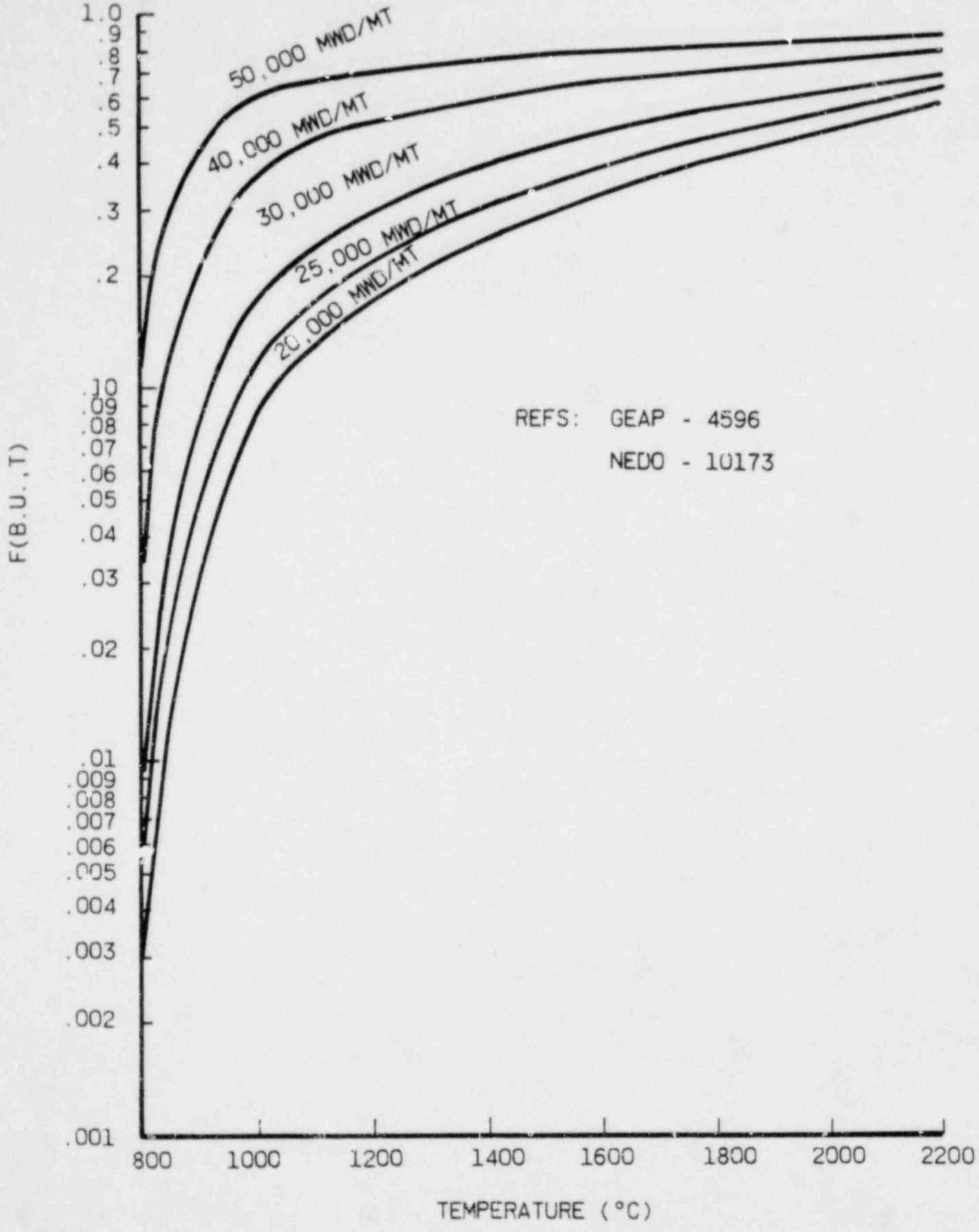

Figure 6-6. B&W Model and ORNL Correlation of Rupture Temperature Vs Engineering Hoop Stress and Ramp Rate

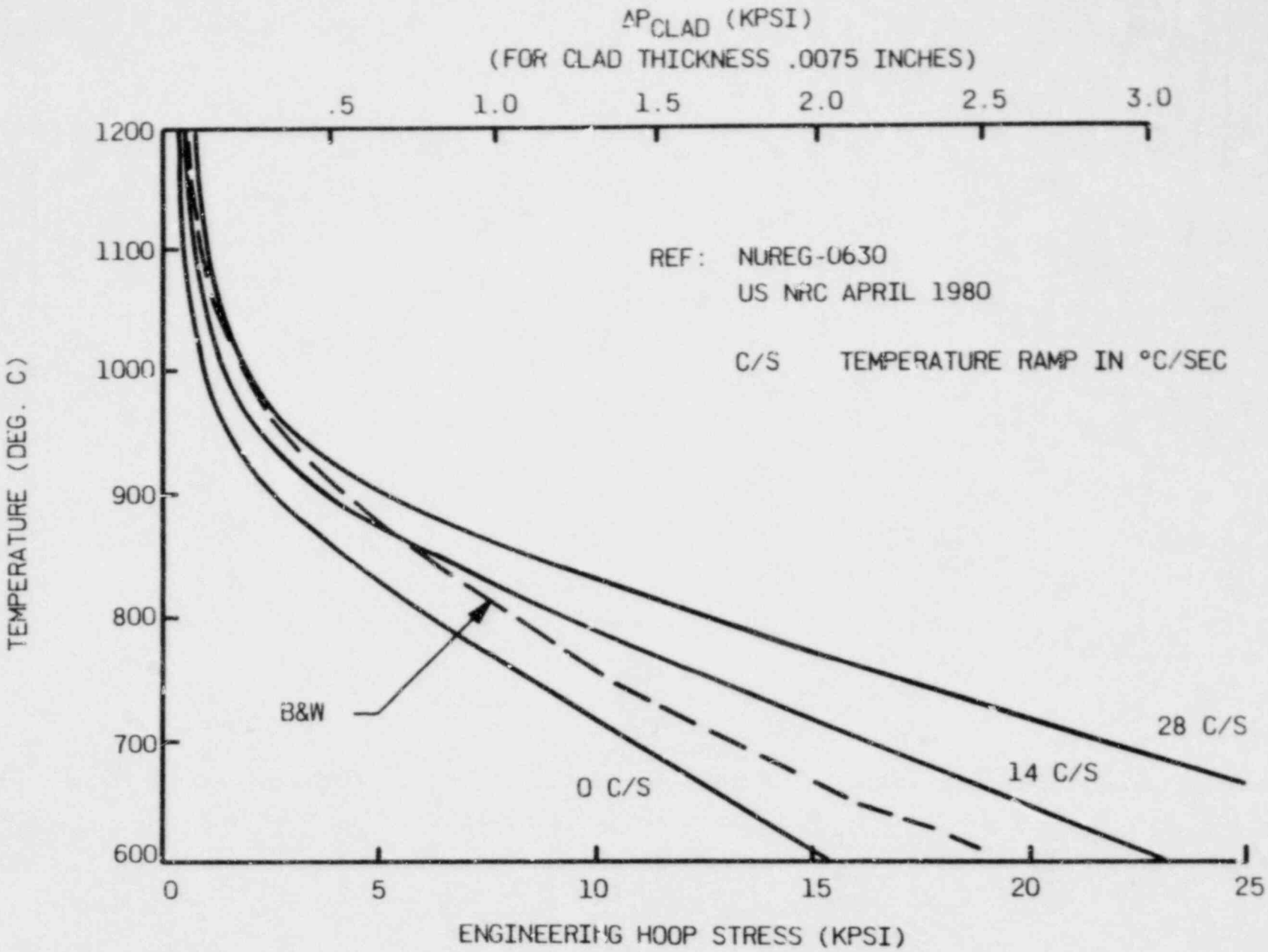

Figure 6-7. Zirconium-Oxygen Phase Diagram

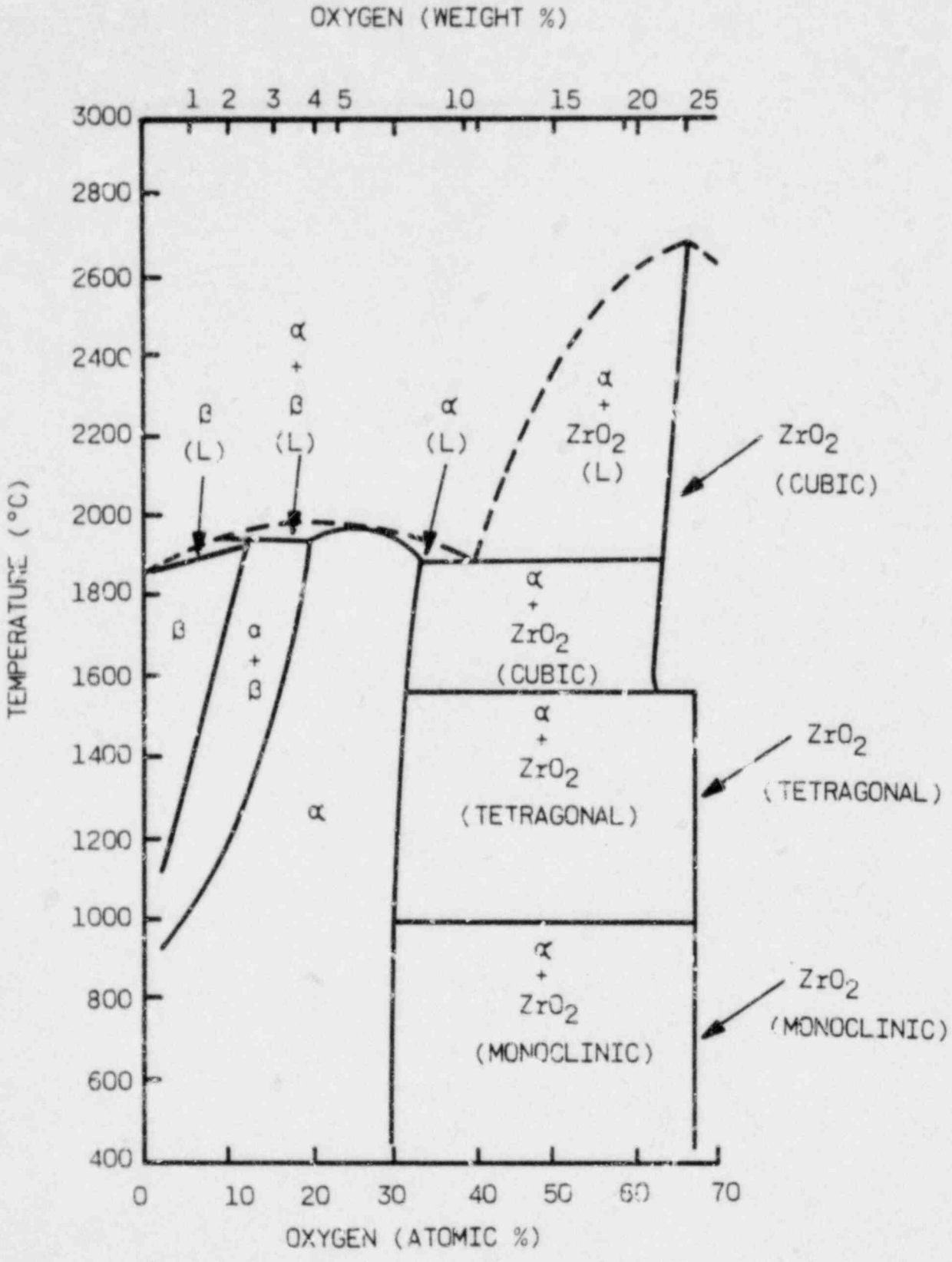

Figure 6-8. Uranium-Oxygen-Zirconium Equilibrium Diagram

Source: J. R. Honekamp, ANA-CO-0041

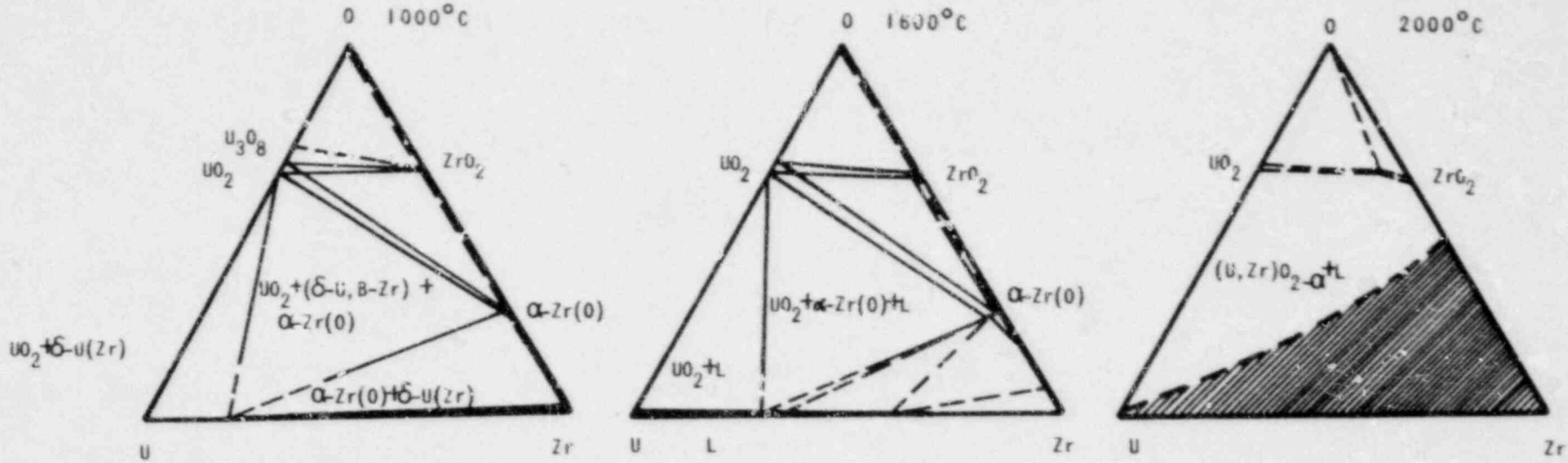

6-8a 6-8b 6-8c

5. Core LOCA Consequences and TMI-2 Estimates

5.1. General Consequences

The consequence to reactor core materials, particularly those constituting the fuel elements, during an extended loss of coolant is essentially extreme overheating due to loss of system capability to remove heat from sources remaining or generated after reactor shutdown. Some of the individual mechanisms for core damage have been discussed in the preceding section. The degree to which each mechanism contributes to core damage and interacts with others to aggravate the high temperature condition depends on the exact nature of the LOCA and the sequence of actions taken (automatically or by the operators) in response to the accident. For example, the TMI-2 accident, because of the stuck PORV, involved a depressurization of the primary side to about 1100 psi, then to 500 psi during the first 2 hours after trip. This depressurization imposed a large pressure drop across the fuel cladding, which undoubtedly contributed to the failure of many or most of the fuel rods by bursting. A LOCA that does not involve significant primary side depressurization could delay the onset of the rod burst effect but at the same time, because of minimal oxidation on the inside of the cladding, contribute to the formation of UO_2-Zircaloy eutectic liquid formation. The exact amount and nature of fuel element damage is thus a sensitive function of a large number of physical and operational variables.

The consequences of the aforementioned damage mechanisms to the fuel materials might be grouped as follows:

- Loss of fuel structural integrity. The mechanisms of rod burst, oxidation, eutectic formation, melting cladding etc. cause the fuel elements themselves to lose the structural and mechanical integrity necessary for their normal operation and installation/removal requirements.

- Release of fission products to the primary system. As has been discussed, a very high temperature in the UO_2 fuel material generally results in a release of a significantly larger fraction of the radioactive fission products from the UO_2 than in normal operation. Failure of the cladding integrity not only would release the gaseous fission products into the primary system but, depending on the magnitude of the cladding failure, release of normally non-volatile fission products by leaching and/or physical relocation.

- Hydrogen bubble formation. The mechanisms for hydrogen formation during the LOCA could result (and did at TMI) in the formation of a significant quantity of non-condensible vapor with a consequent potential for combustion/explosion upon venting and coolant flow blockage.

- Fuel relocation. Large-scale failure of the fuel cladding, either during the course of the high-temperature excursion by bursting or oxidation, or during reflooding of the core by thermal stress on the embrittled cladding, could result in considerable relocation of fuel pellets in the primary system.

5.2. TMI-2 Estimates

The accident at TMI-2 involved an extended loss of coolant to the core, which resulted in a temperature excursion high enough to damage core materials. A number of investigators have analyzed the accident in terms of the extent and nature of the core damage, agreeing on several points and disagreeing on others. This section attempts to present some of the TMI-2 damage estimates as examples of the kind and extent of core damage that might be expected in an extended LOCA. Since the material is compiled from the results of a number of investigators, some of whom disagreed on particulars of the damage results, and since no one can be certain of the exact extent and nature of the damage until the TMI-2 core itself can be observed, these results should be regarded as only examples.

Details of the accident sequence and explanations of the origin and causes of the loss of coolant and core uncovering at TMI-2 are not discussed here. Rather, only the results of these events with regard to core material damage. Figures 6-9, -10, and -11 present Battelle Columbus MARCH code calculations for the vessel pressure, water/steam mixture level, and maximum core temperatures as functions of the time after reactor trip.* The damage mechanisms that occurred in the core can be generally interpreted in terms of these three parameters.

Figure 6-9 shows that the pressure in the primary system over the time period of interest here (0 to 3 hours) rapidly decreased to about 1100 psi, where it held for about one hour, then decreased further to about 600 psi before repressurization.

Figure 6-10 makes the key point that portions of the core became uncovered and remained uncovered for up to nearly 3 hours

---

*MARCH is a development of the BOIL code written at Battelle Columbus Laboratories for use in the reactor safety study.

Figure 6-11 shows the general high-temperature excursion in the core, resulting in temperatures of approximately 4000F (2200C). In contrast, it should be noted that calculations performed with the GRASS-SST code at Argonne National Laboratories and reported by the Nuclear Safety Analysis Center in NSAC-12 (November 1980) showed maximum core temperatures of only about 1750C (3181F).

A study performed by the Fuel Behavior Research Branch of the USNRC (ANA-COO-0025, July 1979) arrived at the following conclusions regarding the fuel damage at TMI-2:

Maximum Damage (Figure 6-12)

- All fuel rods burst at elevations ranging from 1 ft from the top of the core in the center assembly to about 3 ft down in some peripheral assemblies.
- The total amount of Zircaloy oxidized in the first 3 hours of the accident was about 30% of the Zircaloy in the core.
- Embrittlement of cladding by oxidation occurred to a depth between 6 and 7 ft from the top of the core in the center assemblies, to about 5 to 6 ft in most assemblies, and did not occur at all in the lower power corner assemblies.
- Fuel/cladding eutectic formed down to depths of 6 to 7 ft in the center assemblies, to 5 to 6 ft in most assemblies, and did not occur in the corner assemblies.
- No significant oxidation occurred in the lower 5 ft of the core.

Estimates of minimum core damage did not qualitatively differ from the maximum, in the core depths to which damage occurred (Figures 6-13a and 6-13b).

In addition, there is general agreement that the hot oxidized cladding at the top of the core fragmented by thermal shocking when the core was reflooded 174 minutes after reactor trip. This fragmentation and the "slumping" of the core at 225 minutes to which it contributed have resulted in a bed of debris consisting of fragmented cladding and fuel pellets forming near the top of the core.

The fraction (%) of fission products released from the fuel rods to the primary system have been variously estimated as follows:

Xenon, krypton	68 to 71
Iodine	60 to 76
Cesium	60 to 76
Strontium, barium	0.1 to 2.3
Tritium	73
Total fission products	55

From these figures it can be implied that nearly all the volatile fission product materials (xenon, krypton, iodine) released from the UO_2 pellets escaped from the rods to the primary system. Also, the low fractional strontium and barium release fractions indicate that there was no significant fuel liquefaction (eutectic) or melting.

It is also estimated that the core slumping that occurred at 225 minutes resulted in as much as 90% core flow blockage. Temperatures in the core, particularly in the central region near the top, were probably high enough to melt some of the Inconel fuel element spacer grids and the Ag-In-Cd control rod material, although not high enough to cause significant failure of the stainless steel control rod cladding, thus preventing loss of control material from the core region.

6. Summary

1. Discuss and describe the fuel/cladding system: materials, configurations of assemblies and core, and temperature and environmental limitations.

2. Outline the major parametric differences between normal operation and accident conditions and how these differences affect the fuel/cladding system with respect to fuel failure modes.

3. Describe the consequences to the primary system from fuel failure modes: bracket fission product and hydrogen release levels, and discuss the mechanics of fuel failure.

Figure 6-9. TMI-2 Reactor Vessel Pressure

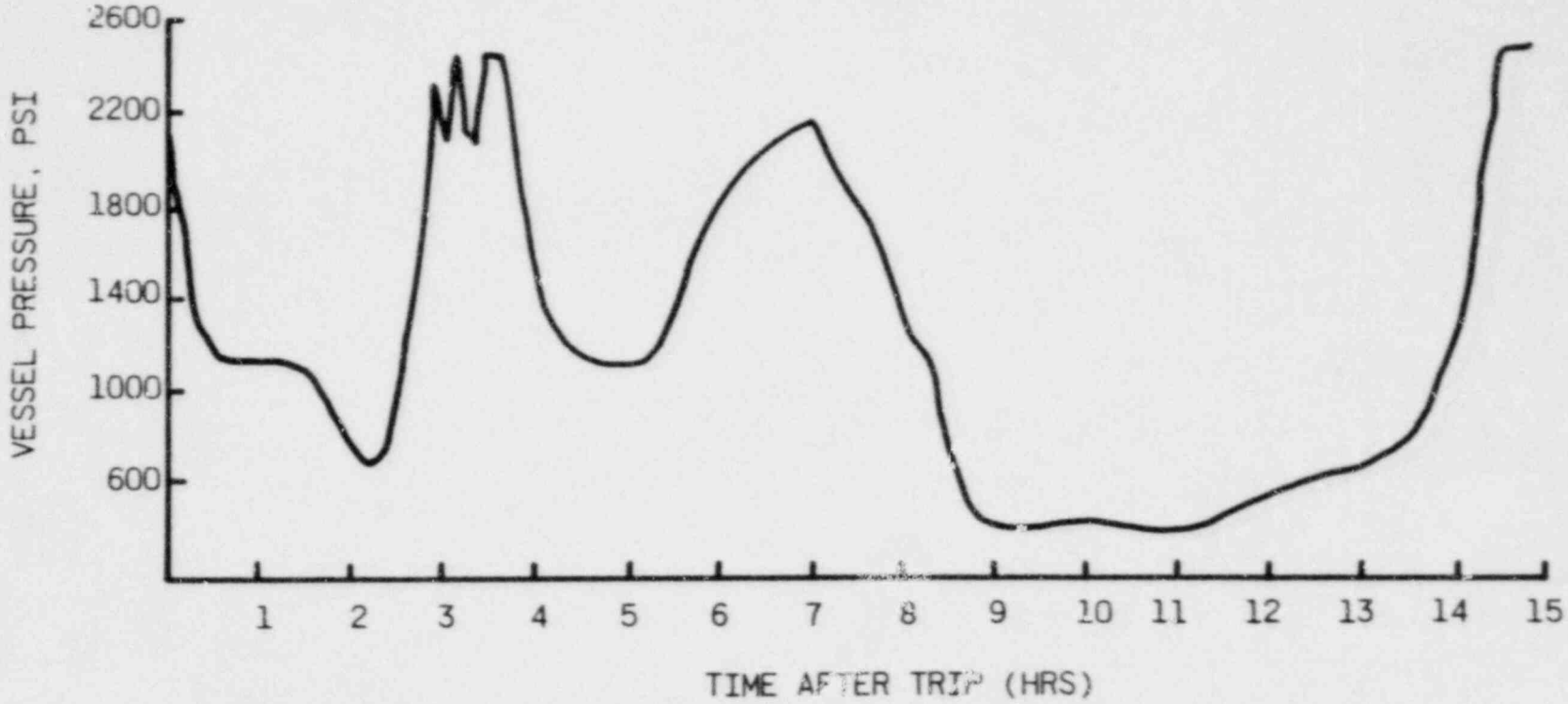

Figure 6-10. TMI-2 Mixture Level, MARCH Code Calculation

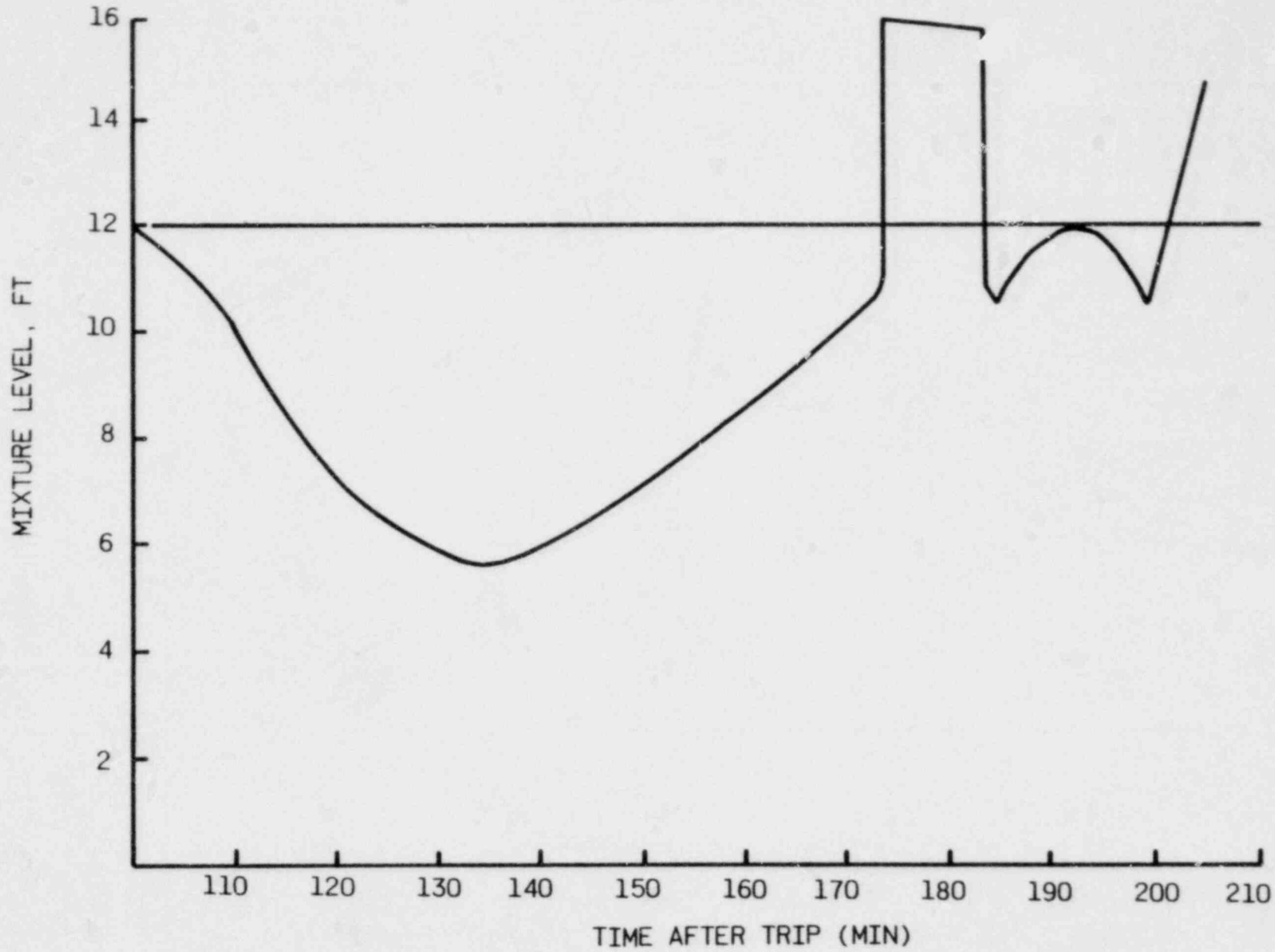

Figure 6-11. TMI-2 Maximum Core Temperature Vs Time

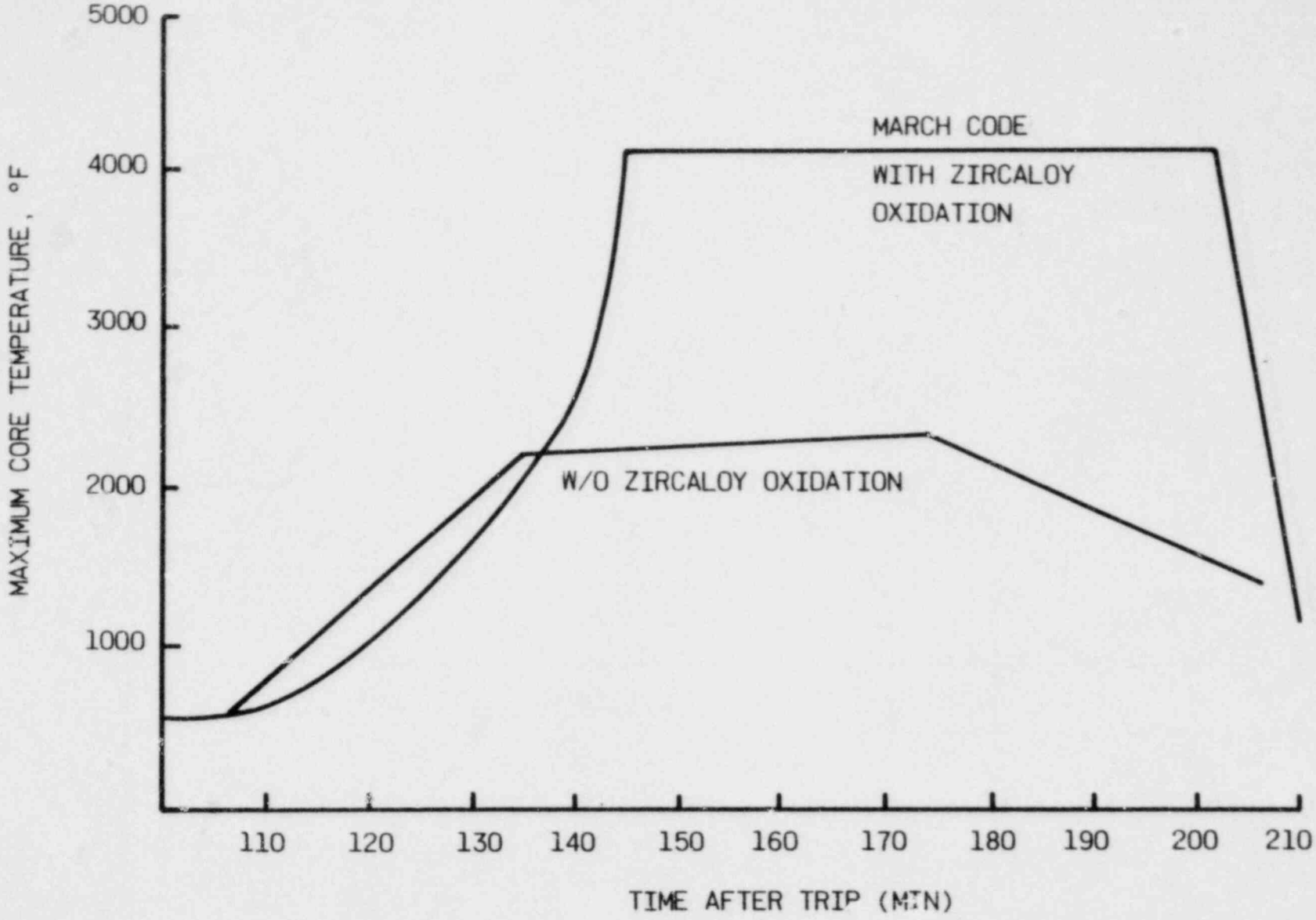

Figure 6-12a. Maximum Damage Estimated to Fuel Rod Cladding, Decay Heat and Oxidation Heat Included

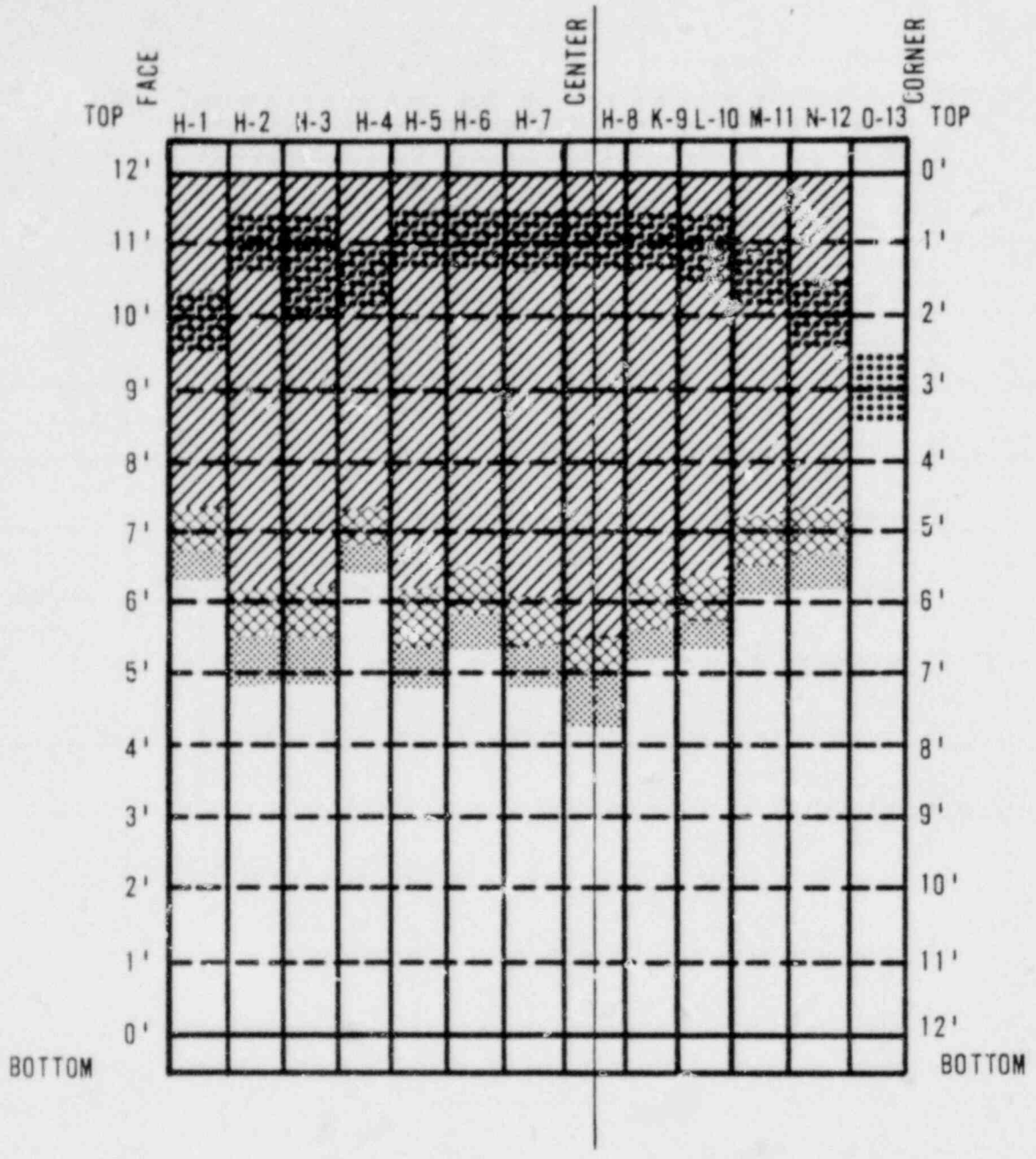

MAXIMUM DAMAGE ESTIMATED TO FUEL ROD CLADDING. DECAY HEAT AND OXIDATION HEAT INCLUDED. HEAT LOSS TO STEAM AND "COLD" RODS SET AT 25% OF TOTAL OF DECAY AND OXIDATION HEAT APPROPRIATE FOR TEMPERATURE. ESTIMATED OXIDE THICKNESS AND POWER LEVEL AT EACH POSITION ON FUEL ROD. ELEVATIONS IN FEET FROM TOP OF CORE.

- NO SIGNIFICANT OXIDATION
- PARTLY OXIDIZED BUT NOT BRITTLE
- OXIDIZED TO BRITTLENESS AND/OR OVER 2500°F
- RUPTURED
- α-Zr + UO_2 LIQUID FORMED

Figure 6-12b. Maximum Damage Estimated to Fuel Rod Cladding, Decay Heat and Oxidation Heat Included

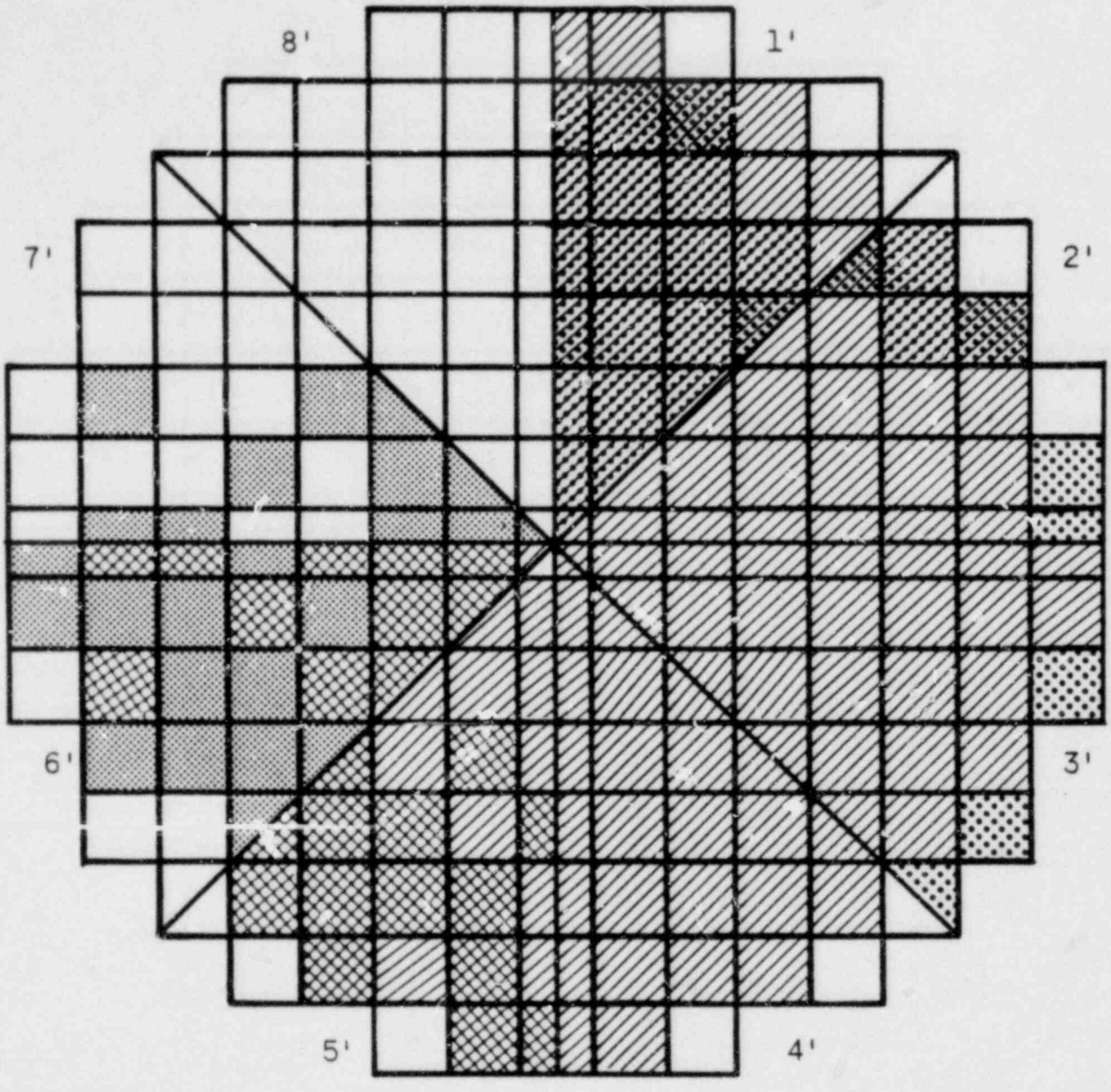

MAXIMUM DAMAGE ESTIMATED TO FUEL ROD CLADDING. DECAY HEAT AND OXIDATION HEAT INCLUDED. HEAT LOSS TO STEAM AND "COLD" RODS SET AT 25% OF TOTAL OF DECAY AND OXIDATION HEAT APPROPRIATE FOR TEMPERATURE, ESTIMATED OXIDE THICKNESS AND POWER LEVEL AT EACH POSITION ON FUEL ROD. ELEVATIONS IN FEET FROM TOP OF CORE.

- NO SIGNIFICANT OXIDATION
- PARTLY OXIDIZED BUT NOT BRITTLE
- OXIDIZED TO BRITTLENESS AND/OR OVER 2500°F
- RUPTURED
- α-Zr + UO_2 LIQUID FORMED

Figure 6-13a. Minimum Damage Estimated to Fuel Rod Cladding, Decay Heat Only — Oxidation Heat Not Included

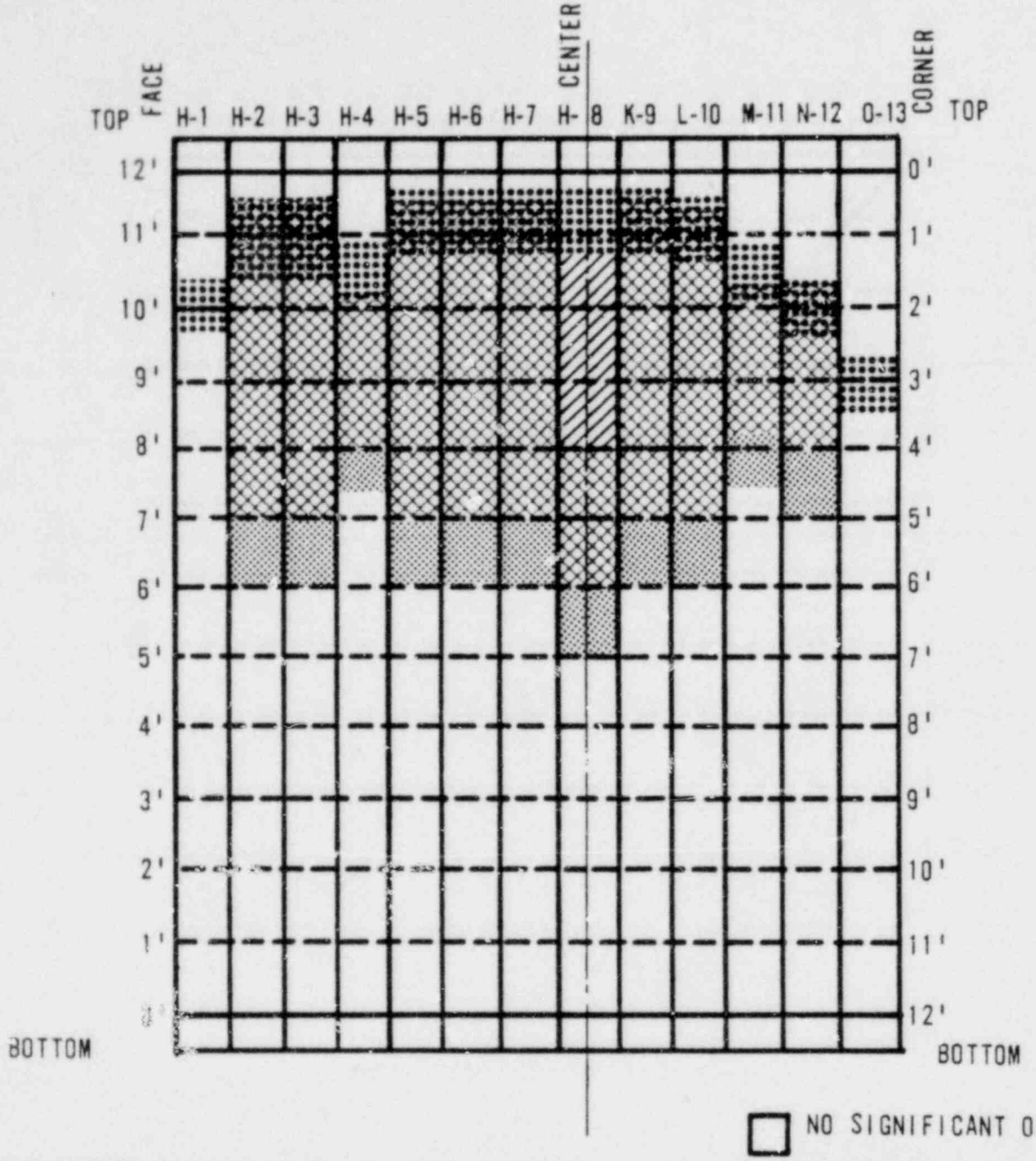

MINIMUM DAMAGE ESTIMATED TO FUEL ROD CLADDING. DECAY HEAT ONLY. OXIDATION HEAT NOT INCLUDED. HEAT LOSS TO STEAM AND "COLD" RODS SET AT 25% OF DECAY HEAT AT EACH POSITION ON FUEL ROD. ELEVATIONS IN FEET FROM TOP OF CORE.

Figure 6-13b. Minimum Damage Estimated to Fuel Rod Cladding, Decay Heat Only — Oxidation Heat Not Included

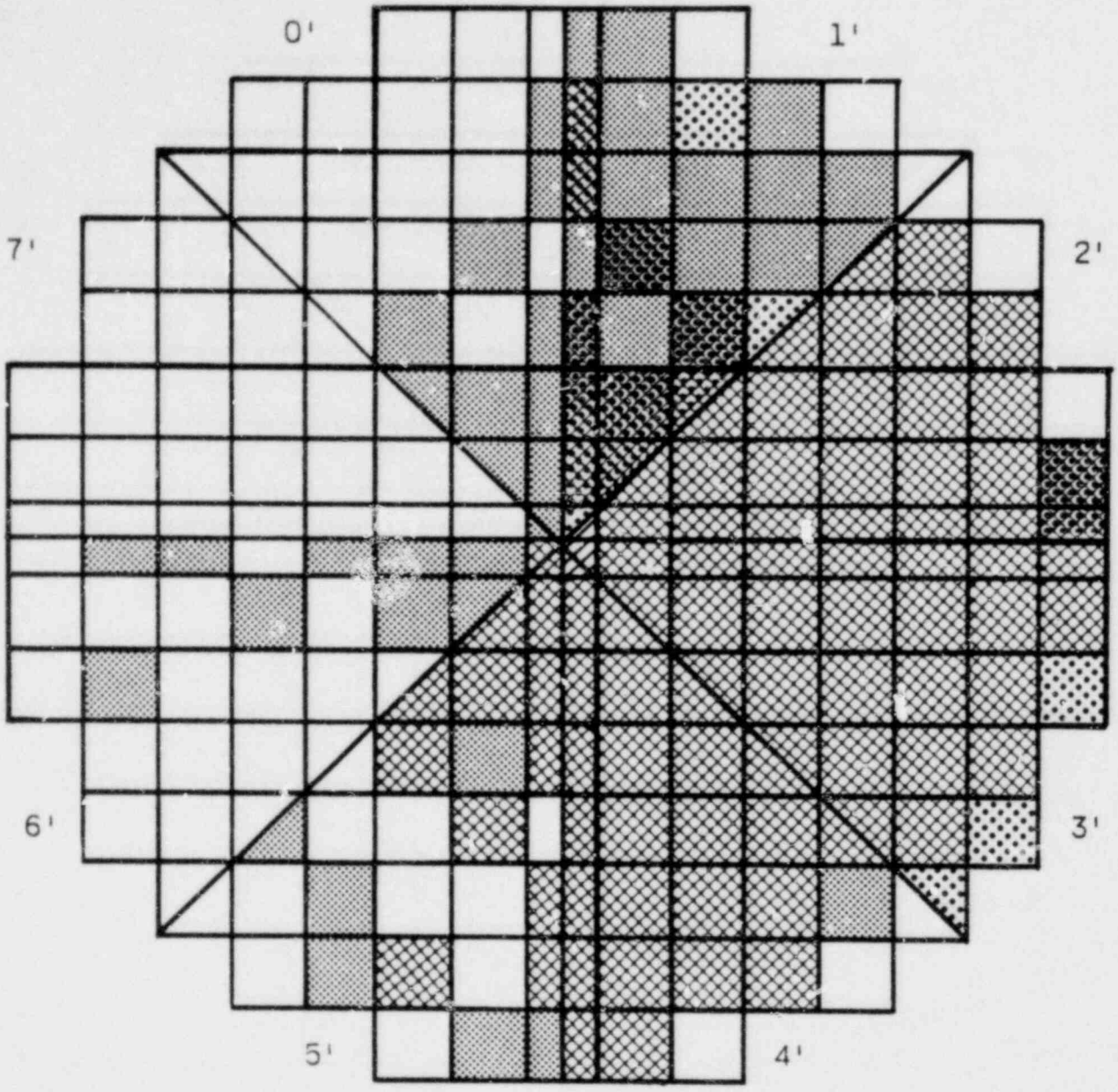

MINIMUM DAMAGE ESTIMATED TO FUEL ROD CLADDING.
DECAY HEAT ONLY. OXIDATION HEAT NOT INCLUDED.
HEAT LOSS TO STEAM AND "COLD" RODS SET AT 25%
OF DECAY HEAT AT EACH POSITION ON FUEL ROD.
ELEVATIONS IN FEET FROM TOP OF CORE.

- NO SIGNIFICANT OXIDATION
- PARTLY OXIDIZED BUT NOT BRITTLE
- OXIDIZED TO BRITTLENESS AND/OR OVER 2500°F
- RUPTURED
- α-Zr + UO_2 LIQUID FORMED

Lesson 7 - USE OF SPNDs IN RECOGNITION OF DEGRADED CORE CONDITIONS

Introduction

1. Lecturer —

2. Purpose — To investigate the use of self-powered neutron detectors (SPNDs) in the analysis of degrading or degraded core conditions.

Objectives

The following material will be presented during this lesson:

1. Description of the incore monitoring system (IMS).
2. Operation of the IMS under normal conditions: at power and during shutdown.
3. Response of SPNDs to high temperatures: thermionic current and release of space charge.
4. Interpretation of SPND alarm data following reactor trips.
5. Limitations of SPND post-trip alarms.

Key points to be retained are as follows:

1. Nuclear and high-temperature responses of the IMS.
2. Use of alarm printer in interpreting SPND alarms.
3. Limitations on SPND post-trip alarms.

Lesson 7 Outline

1. Introduction

2. Description of Self-Powered Neutron Detectors

3. Operation of SPNDs Under Normal Conditions

4. High-Temperature SPND Response

   4.1. Thermionic Emissions — 1979 LRC Experiment
   4.2. Space Charge Release Mechanism
   4.3. Other Phenomena
      4.3.1. Interaction of Thermionic Emissions and Space Charge Release
      4.3.2. Presence of Gamma Radiation and Electronic Circuitry

5. Interpretation of SPND Alarms After Reactor Trips

   5.1. Axial and Radial Distribution
   5.2. High Temperature Vs High Flux

6. Limitations of SPND Post-Trip Alarm Analysis

7. Conclusions

8. Summary

   References

Lesson 7 — USE OF SPNDs IN RECOGNITION OF DEGRADED CORE CONDITIONS

1. Introduction

Large signals can be produced in self-powered neutron detectors (SPNDs) when they are exposed to high temperatures. When the reactor is shut down, these currents are produced either by thermionic emissions or by the release of space charges which build up in the detector insulation. The currents associated with these two phenomena are opposite in direction. Since the detectors are spaced axially along the core height, the existence of high temperatures (and potential core damage) may be judged from an analysis of SPND alarm data. We emphasize that the analysis and interpretation of SPND alarm data are not exact but can be used to confirm indicated core damage.

During the TMI-2 accident, numerous messages concerning the SPNDs were printed by the alarm printer. These messages resulted from high-temperature-induced currents. From these alarms, it has been possible to make a qualitative judgment on the extent of core damage. This lesson is given to share B&W's experience, so that similar alarms can be properly interpreted if a serious accident should happen again.

The alarm printer prints a message whenever an SPND current exceeds a specified range (off-scale) or when it returns to scale after being off-scale. Thus, a message is printed only when a detector's status changes. When going off-scale, the value of the current is not printed, nor is any indication given whether the current is off-scale high or low. When returning to scale, the magnitude of the current is printed. The SPNDs and background wires do not have alarm setpoints; however, the magnitude of the current the plant computer can read is limited by multiplexers. The range of the signals is given in Figure 7-1 along with typical messages. These messages will be referred to as "SPND alarms" rather than as "messages printed by the alarm printer when an SPND changes status."

2. Description of SPNDs

B&W's SPND string comprises seven rhodium emitters, one background wire, and a thermocouple. Each rhodium emitter produces an electron current from neutron absorption ($^{103}Rh + {}_0n^1 \rightarrow {}^{104}Rh \rightarrow {}^{104}Pd$ + electron). The leadwire that carries this signal from the reactor to the control room is made of either Inconel or Zircaloy. The emitter and its leadwire are enclosed in an Inconel sheath and "packed" in a ceramic insulation of either MgO or Al_2O_3, which prevents the leadwire from coming in contact with the sheath. The background wire is similar to a leadwire and is used to account for gamma-induced currents. It extends to the same height as the uppermost emitter, but of course has no emitter. The seven detectors, the background wire, and the thermocouple are all enclosed inside an annulus and collectively make up a detector "string." A cross-sectional view of a detector string is shown in Figure 7-2.

The detectors are spaced along the active fuel height as shown in Figure 7-3. This arrangement allows for three-dimensional power distribution measurements when the reactor is at power.

Current B&W 177-fuel assembly plants have 52 detector strings placed as shown in Figure 7-4. The detector strings are inserted in the central instrument tube of the selected fuel assemblies. They are located so that every fuel assembly either contains or is symmetri to another assembly having a detector string.

3. Operation of SPNDs Under Normal Conditions

SPNDs are used to monitor the power distribution within the reactor core. Their response to neutron and gamma radiation is well understood and can be accurately predicted.

When a rhodium atom in the emitter absorbs a neutron, it is transmitted to rhodium-104, which then β-decays by the following reaction:

$$^{103}Rh + {}_0n^1 \rightarrow {}^{104}Rh \rightarrow {}^{104}Pd + \beta^-.$$

The effective half-life of the β-decay is about 60 seconds. Beta particles that penetrate the ceramic insulation induce a current which is proportional to the local neutron flux and the number of rhodium atoms present. By applying appropriate conversion factors, the local power of the fuel surrounding the SPND can be determined. Typical currents observed in fresh detectors are on the order of +600 nA.

Gamma rays interact with the detector leadwire and sheath primarily by Compton scattering. These interactions also induce currents which must be taken into account during signal processing. This is done using signals from the background wires. Typical currents are -80 nA for Inconel background wires and +80 to -3 nA for Zircaloy background wires. The current for Inconel background wires remains relatively constant over the detector lifetime, while present-generation Zircaloy background currents decrease from about +80 to -3 nA over the first 100 EFPD. The current remains constant thereafter

During power operation the SPNDs and background wires are read by the on-line computer, and a measured three-dimensional power distribution is obtained. The LOCA limit margins are monitored using this power distribution.

After a reactor shutdown, the response of the SPNDs to the neutron flux will decay to zero with a half-life of about 60 seconds. However, the gamma-generated leadwire currents will remain large because the gamma flux within the core decays more slowly. The negative off-scale setpoint for an SPND is -20 nA, and the current in an Inconel leadwire may fall below this value as the neutron-induced positive current quickly decays. Thus, an off-scale negative alarm may be printed even though the shutdown is proceeding normally.

4. High-Temperature SPND Response

Currents are induced in SPNDs by high temperatures via the following mechanisms:

- Thermionic emissions
- Release of a space charge in the insulation

Although experiments have been performed at the Lynchburg Research Center (LRC), our understanding of these phenomena is still limited.

4.1. Thermionic Emissions — 1979 LRC Experiment

When a metal is heated, its valence electrons may be "boiled off" so that they escape from the metal. The thermionic phenomenon is discussed in reference 1.

Five SPNDs and one background wire were heated in an oven at LRC to determine thermionic emission characteristics. The lengths of three of the SPNDs corresponded to level 7 detectors, and the other two SPNDs corresponded to levels 1 and 4. The detectors underwent several cycles of heating during which the temperature and the detector currents were recorded. During three of the heating cycles the SPND signals were measured at 100F intervals while the oven temperature was held constant during the measurements. During the last cycle, the detectors were heated until they failed (at about 2500-2600F).

One unusual result of the experiment was that the thermionic currents were small and positive below about 1000F, while they became increasingly negative above this temperature. Although the currents in individual detectors varied considerably, the results are summarized in Table 7-1. Note that the negative current increases rapidly above 1000F and that the negative setpoint (-20 nA) would be exceeded between 1000 and 1100F. A typical graph of thermionic current versus temperature is shown in Figure 7-5.

One difficulty in using this experiment to interpret SPND alarms is that the positive currents observed were small. The largest positive current in the experiment was 63 nA at 997F (in the background wire). Therefore, off-scale positive alarms would not be caused by thermionic emissions. This experiment is discussed more fully in reference 2.

4.2. Space Charge Release Mechanism

An electric dipole can be induced in the detector insulation by either applying a voltage or exposing the detector to radiation over a period of time. A space charge accumulates in the insulation. A charge of 10 mC was induced on

an SPND at LRC by applying a voltage of 1 V. It is believed that a similar charge would be induced under irradiation. This charge is uniformly distributed axially throughout the insulation.

When the detector is heated, this accumulated charge is released, thereby causing a large positive current. The charge is released at a temperature of 1000-1400F. At temperatures above 1000F, however, the insulation resistance breaks down, shorting out the circuit. The current peaks at about 2200-2400 nA using incore detector circuitry and decays with a half-life of 40-50 seconds as the charge depletes. The current flows when a 1-inch length of detector is heated to the required temperature.

Note that the space charge release phenomenon is not experimentally as well established as thermionic emission.

4.3. Other Phenomena

4.3.1. Interaction of Thermionic Emissions and Space Charge Release

The space-charge release could explain off-scale positive alarms. As the current decays, the detector signal returns to scale, and a value for the current would be printed. The current would then become negative as the thermionic effect becomes dominant. The detector would then alarm off-scale negative if the thermionic current were large enough. This scenario assumes that the temperature remains large enough to induce a thermionic current after the space charge is released. Of course, if the temperature were above 1000F for only a few minutes, the space-charge current would induce an off-scale positive alarm, decay back on-scale, and then not go off-scale negative if the temperature were not high enough.

A detector can repeatedly alarm off-scale positive when the space charges in 1-inch sections of the detector release one after another.

4.3.2. Presence of Gamma Radiation and Electronic Circuitry

Other phenomena, such as the presence of gamma radiation and the electronic circuitry, may influence the high-temperature response of SPNDs. These phenomena have not been investigated in detail (see reference 3).

5. Interpretation of SPND Alarms After Reactor Trips

5.1. Axial and Radial Distribution

When detectors are alarming due to high temperatures, the axial temperature distribution can be roughly determined by analyzing the seven levels in a string. Only those levels that are above 1000F will alarm. Therefore, if only levels 6 and 7 are alarming, it can be inferred that temperatures in excess of 1000F exist in the upper 2/7 of the core.

The detector alarms can also give information on the radial distribution of temperatures. At TMI-2, most of the alarms were from strings in the interior of the core, while strings of the periphery (such as 37, 45, 46, etc.) had fewer alarms. This behavior can be interpreted as evidence that the interior was hotter than the periphery. In addition, only the higher levels alarmed on the periphery, while in the interior all levels of some detectors alarmed. This is confirmatory evidence for the hypothesized inverted-cone damage at TMI-2.

5.2. High Temperature Vs High Flux

The preceding discussion has been directed toward interpretation of SPND alarms once it has been ascertained that high temperatures exist in the core. The in-core insrumentation, however, was designed primarily to monitor neutron flux. Therefore, it must first be determined whether the alarms are being caused by high temperature or large neutron flux.

If the SPND alarms are being caused by an unusually large neutron flux, then all of the following must also be true:

- The reactor is critical or supercritical.
- Because criticality is a corewide phenomena, all SPNDs would exhibit positive currents although not all may be alarming.
- The excore power range nuclear instrumentation would also be responding to the large neutron flux.

As noted earlier, negative off-scale alarms may be observed for Incorel lead-wires a few minutes after shutdown. This is a normal, expected response and would be confined to level 6 and 7 and background detectors.

If it is suspected that the SPNDs are responding to high temperatures, the hot leg temperature instruments and the incore thermocouples can be checked. These instruments will give reliable indications of high temperatures.

We emphasize that the high-temperature response of SPNDs is a complex phenomenon. The explanation presented earlier represents the best understanding currently available. The SPNDs are not stand-alone devices, and other indications of high temperature should be used to diagnose whether and to what extent any core damage has occurred.

6. Limitations of SPND Post-Trip Alarm Analysis

Because the alarm printer uses the same display (????) for both positive and negative alarms, one cannot distinguish between the negative thermionic current and the positive space charge release current. This inability can lead to confusion when analyzing the alarms. Approximately 20 SPNDs are connected to a backup recorder from which one can determine the polarity (sign) of the signals. Thus, we may be able to determine whether an SPND is alarming positive or negative from the backup recorder.

Another problem arises from the lack of information of an SPND alarm. When the current goes off-scale, one cannot determine its magnitude or, therefore, the corresponding temperature. We can be reasonably certain that the temperature is above 1000F, but the temperature could be much higher — there is no way to tell how much higher using only the SPND alarms.

Because only seven 4.75-inch detectors are present in the 12-foot core, axial detail is limited. Since neutron flux behavior is well understood, this is not a limitation under the conditions for which the SPNDs were designed. During abnormal high-temperature conditions, however, the temperature profiles within the core can be very complex, making precise interpretation of the SPND alarms more difficult.

7. Conclusions

Although the temperature response of SPNDs is complex, the high-temperature-induced currents can be used to estimate the distribution of high temperatures (>1000F) in a degraded core and the extent of core damage. Because SPND alarms can result from either high neutron fluxes or high temperatures, however, other indications must be used to determine whether high temperatures exist.

8. Summary

1. Briefly review nuclear and high-temperature responses of the incore monitoring system.
2. Discuss the use of the alarm printer in interpreting SPND alarms and their possible relationship to a degraded core condition.
3. Summarize the limitations on using SPNDs to detect degraded core conditions.

References

[1] M. M. El-Wakil, Nuclear Energy Conversion, Internation Publishing Co. (1971).

[2] H. D. Warren, SPND Thermal Currents in a Furnace, LR:79:4817-01:1, Babcock & Wilcox, July 1979.

[3] M. N. Baldwin and H. D. Warren, "SPND Thermal Currents in a Furnace and Gamma Ray Field," Technical Services Agreement No. 79-307, Final Report, Babcock & Wilcox, February 1980.

Table 7-1. Thermionic Currents in SPNDs

Temperature, F	Current, nA
700	+0.3 ± 0.3
800	+1.9 ± 1.8
900	+5.3 ± 3.6
1000	-7.7 ± 4.6[a]
1100	-77 ± 31
1200	-375 ± 129
1300	-1053 ± 460

[a]Note change in polarity.

Figure 1. SPND Alarm Setpoints

Detector type	Positive setpoint, nA	Negative setpoint, nA
SPND	+2020	-20
Background	+120	-120

Typical SPND Alarms

Time	Status	Address	Description	Reading
06:48:08	NORM	1132	FLUX 7-E LEVEL 5 (nA)	254.
06:48:44	BAD	1491	FLUX 13-C LEVEL 4 (nA)	????

Figure 7-2. Cross Section of SPND String

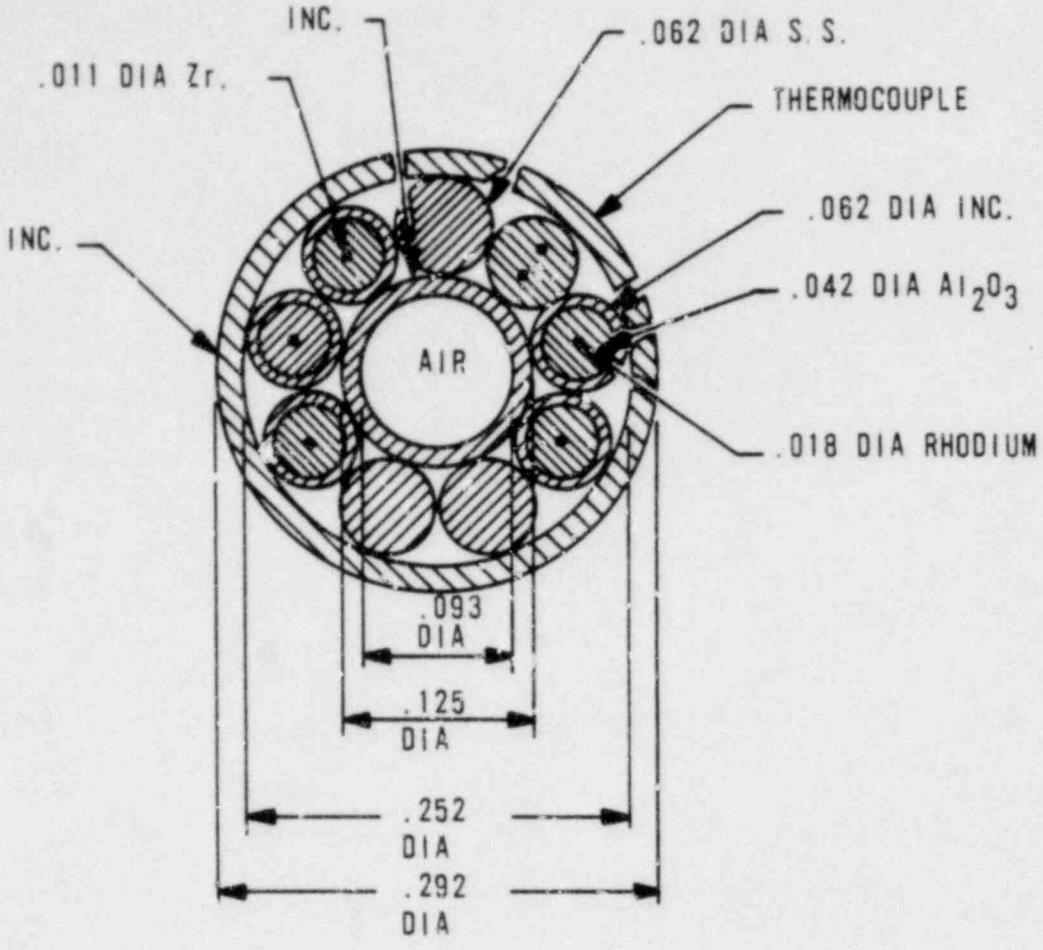

Figure 7-3. Axial Locations of SPNDs

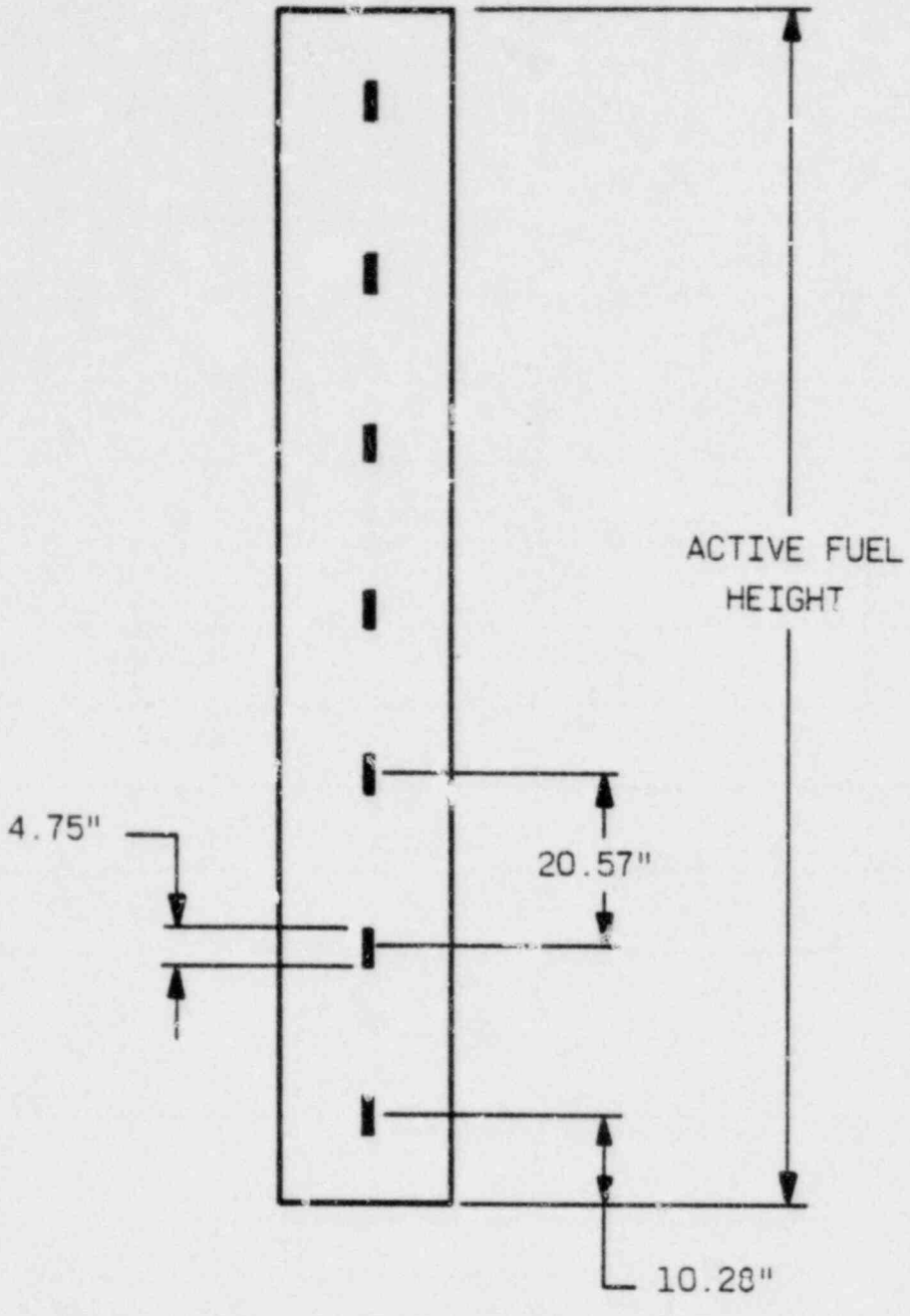

Figure 7-4. Instrument Layout in 177-Fuel Assembly Core

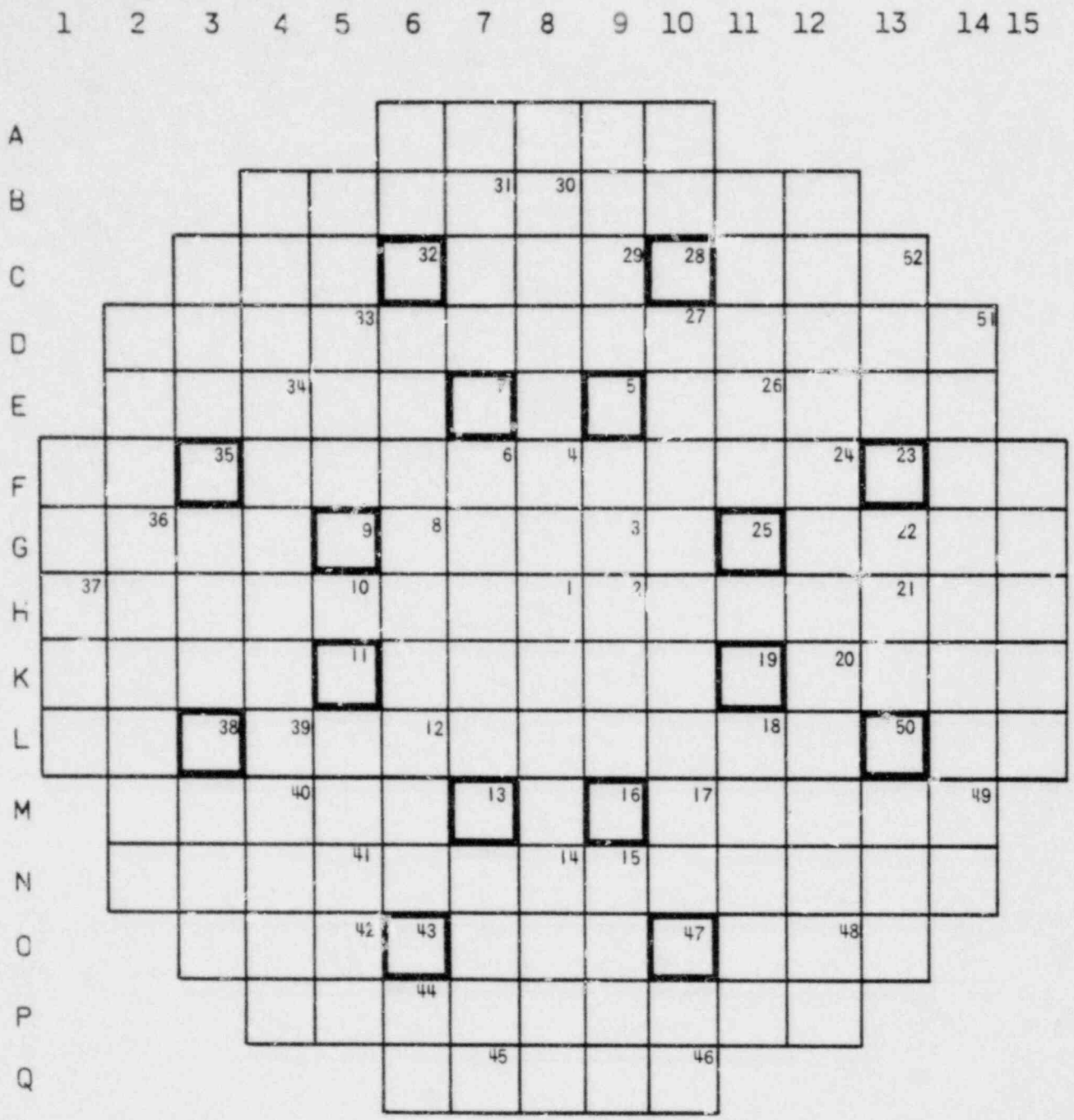

BOLD-FACED ASSEMBLY INDICATES SYMMETRICAL STRING LOCATION

Figure 7-5. Thermionic Emissions in SPNDs

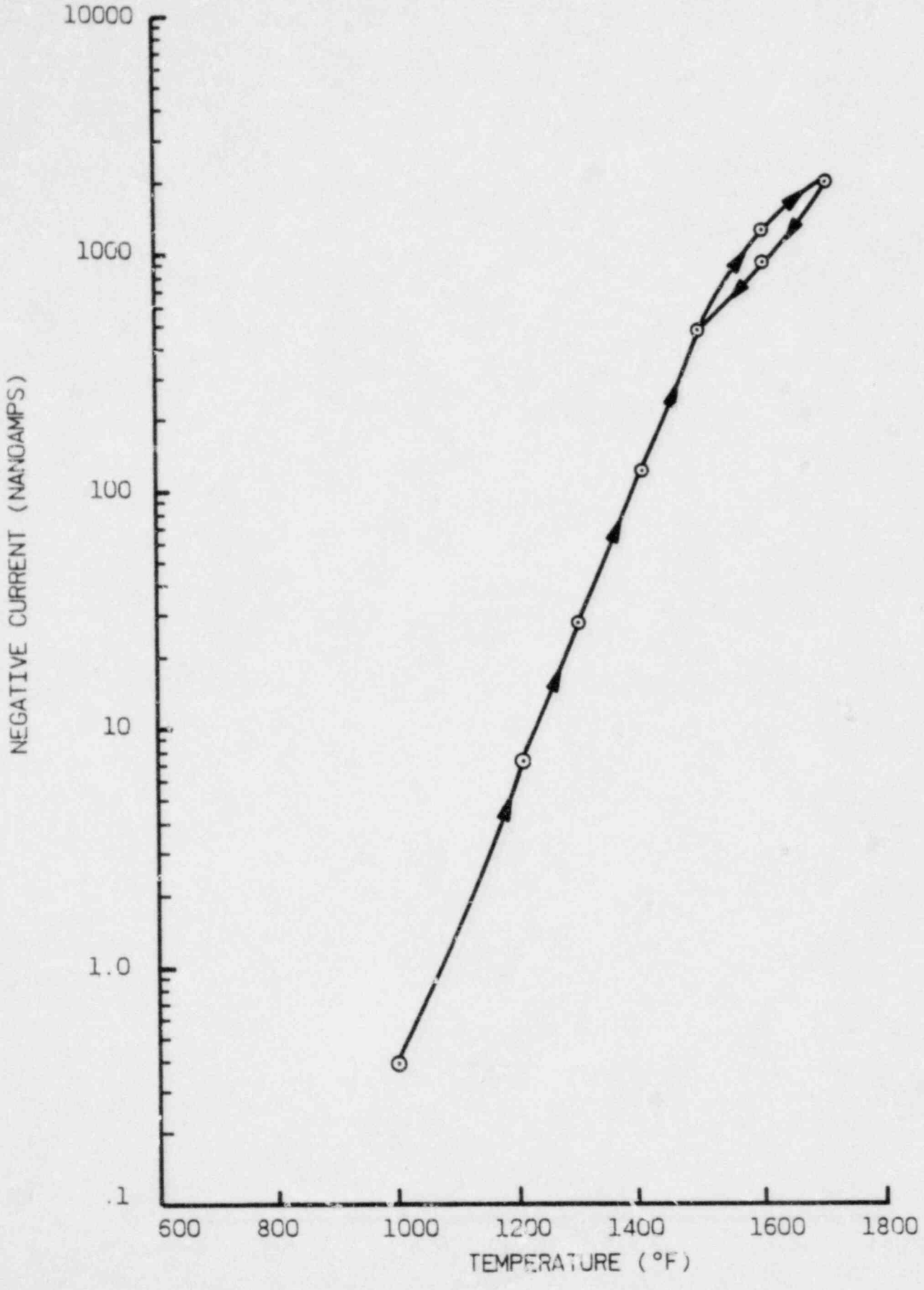

Lesson 8 – DETECTION AND TREATMENT OF INADEQUATE CORE COOLING USING CORE EXIT THERMOCOUPLES

Introduction

1. Lecturer –

2. Purposes –

   a. To discuss the changes in core cooling efficiency as the reactor coolant changes state and flow conditions.

   b. To discuss core exit thermocouple (T_c) use as a means of detecting dangerous conditions in the core.

   c. To describe analyses which resulted in the core exit T_c readings and cladding temperatures (T_{clad}).

   d. To provide instructions for converting T_c readings to T_{clad}.

   e. To discuss required operator actions during high T_{clad} (inadequate core cooling) conditions.

   f. To briefly discuss T_c limitations.

Objectives

The following material will be presented during this lesson:

1. What might cause the reactor coolant to change state and how will that affect core temperatures?

2. How might the operator be able to use T_c's to determine if dangerous conditions exist, and the degree of danger?

3. How are T_c readings and cladding temperature related, and how was relationship established?

4. What actions must operators take based on T_c readings?

5. How might these actions affect the core and the rest of the plant?

6. What are the limitations of the T_c's?

The following key points to be retained are:

1. What influence does the amount of available reactor coolant and the state of that coolant have on core temperatures?

2. What damage would be expected at high core temperatures?

3. How T_c's can measure existence and magnitude of danger to core cooling.

4. Some familiarity with analyses used to develop T_c/T_{clad} correlation.

5. What the operator should be doing for given T_c readings.

6. What the results of these actions might be for the core and the rest of the plant.

7. How T_c readings might be misleading.

8. What to expect for cladding temperatures above 1800F.

Lesson Outline

1. Introduction
2. Causes of Inadequate Core Cooling (ICC) and High Core Temperatures
3. Normal and Off-Normal Modes of Heat Transfer
4. Why and How Cladding Temperature is Measured
5. ICC Guidelines Defining Operator Actions Based on T_{clad}
6. Possible Results and Consequences of Operator Actions
7. Shortcomings of T_c's

Lesson 8 — DETECTION AND TREATMENT OF INADEQUATE CORE COOLING USING CORE EXIT THERMOCOUPLES

1. Introduction

During plant operations, transients and upset conditions can cause an inadequate amount of heat removal from the core. Three elements are directly involved in this core heat removal process: the RCS coolant fluid itself, the circulation of this coolant between the core and steam generators (OTSGs), and the OTSGs operating as a heat sink. Degradation of any or all of these components can result in an inadequate heat removal rate from the core. This can lead to increases in the temperatures of the uranium dioxide (UO_2) fuel and the Zircaloy-4 (Zr-4) cladding surrounding the fuel pellets. Some possible causes of degraded core heat removal, and some possible results of these in terms of fuel and cladding damage, are discussed in the following text. Also discussed are indication to plant operators of the presence and severity of these dangerous conditions, as well as actions to prevent them or to maintain or regain control of the system should they arise.

2. Causes of Inadequate Core Cooling (ICC) and High Core Temperatures

This section lists some possible plant transient conditions that can lead to elevated core temperatures. It also describes some of the mechanisms that can produce elevated fuel and cladding temperatures following these transients.

Loss-of-coolant accidents (LOCAs) affect the first two core cooling components described in the introduction: the RCS coolant fluid and its circulation. LOCAs cause loss of liquid inventory generally in three ways:

1. Loss of fluid out the break.
2. Flashing of liquid to steam if the break is large enough to depressurize the RCS to saturation conditions.
3. Boiling of liquid by core heat if adequate liquid volume, flow rate, and OTSG heat removal are not maintained.

These can lead to partial or complete uncovering if enough makeup or ECCS is not provided. LOCA analyses have shown that core temperatures will remain low if the entire core is kept covered by liquid or by a mixture of saturated steam and liquid. However, if any portion of the core becomes exposed to saturated or superheated steam, elevated cladding temperatures can very quickly result.

LOCAs with reactor coolant (RC) pumps left running can lead to more liquid inventory loss than LOCAs without RC pumps running. For cases without RC pumps running, the liquid loss out of the break would stop as soon as the primary system liquid level dropped below the elevation of the break. After that, liquid loss would be caused just by flashing and core boiloff.

For cases with RC pumps left running, liquid would continually be circulated around the system and, consequently, would be made to flow out of the break. This would allow liquid to continually exit through the break, and, for certain break sizes, could allow essentially all of the system liquid inventory to be lost.

If these conditions were to develop and then the RC pumps were turned off or lost, the circulation and mixing of the steam and liquid in the RCS would cease. This would result in "phase separation." The steam would rise to the higher parts of the RCS and the liquid would fall to the lower portions. The liquid volume in the RCS could have been depleted during RC pump operation to

the point where there is not enough liquid left to cover the core after phase separation. The resulting core uncovery could occur within seconds and could be severe enough to uncover almost all of the core. Of course, this would mean elevated core temperatures if the RC pumps were turned off or inadvertently lost after such dangerous conditions developed within the RCS. The possibility that this might occur is the basis for requiring the operators to stop the RC pumps on ESFAS actuation due to low RCS pressure. This will prevent a pump trip with the system in a low liquid volume condition.

A total prolonged loss of OTSG feedwater will eliminate the RCS heat sink completely. It can also cause the primary system liquid inventory to be boiled away through the pressurizer relief valves if the ECCS is not, or cannot be used to keep the core cooled. Should this occur and the liquid boil-off continue uncorrected, the core would eventually become uncovered, causing rapid increases in core temperatures.

3. Normal and Off-Normal Modes of Heat Transfer

The three elements of core heat removal are described in the introduction. Under normal conditions, heat is being added to the fuel cladding by the fuel at the same rate that it is being removed by the RCS coolant. The coolant then transfers this heat to the OTSGs. The heat removal from the cladding to the RCS fluid is often discussed in terms of a heat transfer coefficient (HTC). HTC is expressed in units of Btu/h-ft^2-°F. If the plant is in full power operation, the HTC is on the order of 10,000-50,000 Btu/h-ft^2-°F (see Figure 8-1) and heat is being transferred via forced convection to subcooled liquid.

If the RCS is in natural circulation, the system is filled with liquid, and RCS flow is on the order of 2-4% of the normal system flow which is 130 million lb/h. The reactor has been shut down and the decay heat rate is about 1% of full core power. The RC pumps have been stopped. The OTSGs are being fed by emergency feedwater (EFW) and the OTSG secondary level is being maintained at about 50% on the operate range (approximately the lower 21 ft of the tubes are covered with liquid). A level of about 8 ft is required for the operating raised loop plant. These are the conditions necessary for maintaining natural circulation. In this case, core HTCs are on the order of 1000-5000 Btu/h-ft^2-°F. This is much less than the HTC for normal operation (see Figure 8-1), but is adequate to remove the reduced core heat output after reactor shutdown. The heat transfer process from the core could be by, for example, forced convection to subcooled liquid, nucleate boiling, or forced convection to vaporization, depending on core heat output, flow rates, and the state of the coolant fluid.

In the latter stages of a LOCA or prolonged loss of feedwater transient, RCS conditions could evolve to the point where the core is covered by a stagnant pool of liquid or steam-liquid mixture. HTCs for this mode of core heat removal are on the order of 100-500 Btu/h-ft^2-°F, which is typical for pool boiling. The core will be boiling away liquid under these conditions and will eventually boil dry unless liquid can be replaced at least as fast as the boiloff rate. This should be within the capability of the ECCS after the initial period following reactor shutdown. Some operator action may be required to obtain more ECCS flow or to decrease RCS pressure to improve ECCS performance.

RCS conditions could deteriorate to the point where the upper part of the core has become uncovered while the lower part remains covered with a saturated mixture of liquid and steam. Following a larger LOCA, the entire core could become uncovered for a short time, and then be recovered by the ECCS, thus evolving to this partial-covering condition. For smaller LOCAs, the RCS could simply drain down or be boiled off until the core is partially uncovered. For the lower part of the core which remains liquid covered, heat removal mechanisms and HTCs would be as described above. For the steam-covered (upper) part of the core, HTCs would be very small (approximately 0.1-10 Btu/h-ft^2-°F) and typical of a forced convection to saturated or superheated vapor heat removal mechanism. Some flow would be expected as steam leaves the mixture-covered portion and rises as it continues to be heated.

In extreme accident situations the core could become completely void of liquid, remaining covered only by saturated/superheated steam. Again, for large LOCAs, if such a condition developed at all, it would only be expected to last for a matter of seconds before being corrected by the ECCS. For small LOCAs or severe loss of OTSG feedwater events, this condition could take a long time (minutes or even hours) to develop and could have a very long duration. This would be the result of an event such as catastrophic equipment failure, incorrect operator actions, or operator inaction. Such long-duration core uncovery, during which there is essentially no heat removal from the cladding while core heat input continues, can result in severe core temperature increases, and possible fuel and cladding damage.

Inadequate core cooling (ICC) results from the latter two conditions described above. As long as the core remains covered with liquid or with a mixture of saturated steam and liquid, core temperatures will stay at safe levels. With partial or full core uncovery come rapidly increasing core temperatures, worsening ICC symptoms (to be discussed later), and increasing likelihood of core damage.

Figures 8-2 and 8-3 show results from LOCA analyses of a series of small cold leg breaks. All cases assumed OTSG feedwater available, RC pumps tripped early in the transient, and one HPI, one LPI, and both CFTs available. Figure 8-2 shows mixture (steam and water) heights in and above the core as a function of time after the LOCA. For three cases, the 0.085, 0.07, and 0.055-ft^2 case. the mixture height drops below the top of the core (as indicated by the solid

horizontal line on Figure 8-2) before the ECCS is able to recover the core. Figure 8-3 shows cladding temperatures, in the portion of the core that is uncovered, for these three cases. Examining the 0.07-ft^2 case in detail, Figure 8-2 shows core uncovery beginning at about 1300 seconds, progressing until as much as the top 2 feet of the core is uncovered, and ending at about 1700 seconds. Figure 8-3 shows that at 1300 seconds (the time core uncovery starts), cladding temperature in the exposed core region begins to increase. The temperature excursion continues until 1700 seconds. At this time, the core has been recovered, and afterward, cladding temperatures decrease, eventually returning to approximately the pre-excursion level.

The importance of keeping the core covered at all times, or failing that, of recovering the core as soon as possible, is obvious from the previous discussion. The existing operator guidelines for small LOCAs are designed to prevent core uncovery. The existing ICC guidelines (to be covered later) are designed to help the operators regain control of core conditions if the small LOCA guidelines cannot be followed or fail for some reason.

4. Why and How Cladding Temperature is Measured

Although no direct cladding temperature (T_{clad}) indicating system exists, thermocouples are available which can be used to indirectly ascertain T_{clad}. As will be explained below, the operators can use these core exit thermocouples (T_c's) to determine the status of the core and the RCS. T_c indications can also give a warning of impending or progressing core damage.

The procedure for determining T_{clad} is very straightforward. Using readings from a number of T_c's (B&W recommends taking an average of approximately the five highest reading T_c's), an accurate indication of the core exit fluid condition can be obtained. To aid operators in determining approximate cladding temperatures, B&W has analytically developed a correlation (see Figure 8-4) based on this average T_c indication and system pressure. As an example to illustrate the use of this correlation, assume that averaging the five hottest T_c readings gives a core exit temperature of 600F and system pressure, as measured by the hot leg pressure sensor, is 600 psig. Using this correlation, as presented in Figure 8-4, implies that T_{clad} is about 1400F.

5. ICC Guidelines Defining Operator Actions Based on T_{clad}

Operator actions are defined, both by the small break operating guidelines (SBOG) and the ICC guidelines, based on system pressures and cladding temperatures. Basically, if the RCS is in a subcooled condition both as measured by the hot leg RTDs and by the T_c's, the SBOGs apply.

However, if conditions degrade to the point where the hot leg RTDs and, especially, the T_c's are indicating superheat (above saturation) temperatures for the existing system pressure, the operators are directed to the ICC guidelines. These instructions define three sets of operator actions based on the level T_{clad} has reached. The curves of Figure 8-4 define three regions — the first between the saturation line and the curve representing a T_{clad} of 1400F, the second between the T_{clad} = 1400F and T_{clad} = 1800F curves, and the third for T_{clad} greater than 1800F. These regions define progressively more severe core conditions and also operator actions which have progressively more severe potential consequences. The specific actions are listed below; the significance of T_{clad}'s of 1400F and 1800F, and the consequences of the corresponding operator action will be discussed later.

When the operators begin to observe superheated RTD and/or T_c readings (Figure 8-5), the ICC guidelines instruct them to:

1. Verify HPI/LPI at maximum flow.
2. Start makeup pump if not running.
3. Verify OTSG level controlled to proper level.
4. Begin depressurizing OTSGs to cause a decrease in OTSG temperature (no faster than 100F/h).
5. Ensure CF isolation valves are open.

If the operators fail to take the required action for T_{clad} in the first region, if the actions taken are inadequate, or if major equipment failures have occured, T_{clad} could increase above 1400F. With T_{clad} in the second region (Figure 8-6), another set of actions is defined by the ICC guidelines:

1. Start one RC pump per loop (do not defeat normal interlocks).
2. Depressurize OTSGs immediately to 400 psig, or as far as necessary to get a 100F decrease in OTSG saturation temperature.
3. Open PORV as necessary to maintain RCS pressure within 50 psig of OTSG pressure (primary to secondary pressure coupling).

4. Immediately begin depressurizing OTSGs to cooldown no faster than 100F/h.

If, for reasons similar to those stated previously, cladding (and core exit) temperatures continue to escalate and reach or exceed 1800F (Figure 8-7) the following operator actions are required:

1. Immediately start all RC pumps (defeat interlocks as necessary).
2. Depressurize OTSGs to atmospheric pressure.
3. Open PORV and leave it open.

Cladding temperatures of 1400 and 1800F are used to define operator actions because they represent significant and increasingly dangerous stages of core degradation.

For example, as T_{clad} rises to 1400F, the rate of cladding failure increases due to hoop stresses. This greatly increases the potential for contamination in the RCS, the reactor building (RB), and possibly the environment. In addition, the cladding becomes plastic at these temperatures, resulting in ballon-like swelling. Such failures and swelling would decrease core flow by increasing flow resistance, thus degrading core cooling.

The zirconium metal-water reaction rate is not yet a concern when T_{clad} is at 1400F. This reaction produces hydrogen, generates heat, and causes an oxide layer to form exposed cladding surfaces. The reaction rate increases with increasing T_{clad}, but the consequences are still negligible at T_{clad}'s of 1400F. The basic objective of the operator actions corresponding to these temperatures is to prevent significant cladding failures and further temperature increases.

Cladding temperatures at and above 1800F indicate that the core is approaching a dangerous condition. The danger could be compounded if the core is allowed to remain at these temperatures for a prolonged period, or to degrade further.

Hydrogen is being generated at a significant rate at this point. The operators must be prepared to deal with loss of circulation to, and heat removal by, the OTSGs if sufficient volumes of hydrogen and other gases are introduced into the RCS. In addition to this, the oxidation of the cladding will also become a concern for sustained 1800F or higher T_{clad}. Significant oxidation could structurally weaken the cladding, to the point where that cladding that has been exposed to steam and is then quenched by liquid could undergo brittle

failure. This would lead to contamination of the RCS, and possibly, the RB and even the environment.

If T_{clad} is allowed to increase beyond 1800F (to 2000F and beyond), the operator must then deal with a serious and rapidly worsening situation. Along with the greater potential for fuel failure and large amounts of hydrogen being generated, the heat produced by the metal-water reaction begins to play a significant role in accelerating the rate of T_{clad} increase.

The primary objectives of the actions corresponding to 1800F are, then, to avoid significant quantities of hydrogen in the RCS and RB, and to prevent massive brittle failure of the cladding with its resultant contamination of the systems. These actions are designed to accomplish this while temperature and time safety margins still exist; that is, before temperatures have become high enough or have been sustained long enough to allow serious core degradation to occur.

If cladding temperatures have reached the 1800F point, it is probably because a large portion of the core has been uncovered for an extended period of time. When these temperatures are observed, the specified actions call for the operator to quickly recover the exposed portion of the core with liquid and to maximize cooling of the RCS. Doing this should return cladding temperatures to a safe level and should also bring the metal-water reaction under control. Again there is a risk that rapid quenching could cause brittle-fracture failure of a significant amount of cladding if extensive oxidation of the cladding has occurred. This risk must be taken in order to prevent further rises in temperature and to halt the progression toward catastrophic fuel and cladding failures that unchecked temperature increases would ultimately produce.

6. Possible Results and Consequences of Operator Actions

The primary objective of each set of temperature-dependent actions is to enable the operators to regain control of core conditions and to prevent further degradation. Ideally, if actions specified by the SBOG are successfully accomplished, superheated conditions should not develop in the core. If this does happen, the accomplishment of each set of actions should make it unnecessary to revert to the next set.

Halting core temperature increases as quickly as possible is desirable in order to minimize core damage. It is also desirable to do this in order to avoid proceeding any deeper into the ICC guidelines than is absolutely necessary. This is because some of the actions, particularly those to be taken when T_{clad} is greater than 1800F, jeopardize other plant equipment.

The actions that the operators are to take when the core temperatures are just beginning to indicate superheat, pose no undue risks to other equipment. Some stresses may be placed on the OTSG tube and shell interface when depressurizing the OTSG. However, these stresses are well within design limits.

Greater hazards exist when operators take the actions specified when T_{clad} exceeds 1400F. The RC pumps may incur some damage upon restart. The initial rapid depressurization of the OTSG, followed thereafter by a controlled depressurization, will stress the tube/shell interface. Again, these stresses will be well within the design limits. Using the pressurizer PORV to control RCS pressure may damage the pressurizer drain tank, particularly the rupture disc. This could also lead to elevated temperatures, pressures, and radiation levels inside the containment. This could affect instrumentation and other RB hardware.

Cladding temperatures must be prevented from increasing above 1800F and must be lowered to the saturation point and below, as quickly as possible. This is necessary, even if it means risking damage to other plant equipment. The primary concern with T_{clad} at these levels, is a rapid and ever increasing rate of hydrogen generation from the cladding metal-water reaction. Actual core integrity is not yet threatened. Hoop-stress failures and weakening of the cladding structure due to oxidation, are progressing. However, such dangers as cladding heatup, fuel and cladding melting, or structural failure of the core supports, are not significant concerns until temperatures exceed 2000F.

Hydrogen, present in the RCS in significant quantities, will hamper efforts to reduce core temperatures that have reached 1800F. The success of operator actions, specified for these conditions, depends heavily upon OTSG cooling. As was discussed in Lesson 2, gases can reduce or halt heat removal from the RCS by the OTSGs by blocking either natural circulation or steam condensation. By preventing cladding temperatures from exceeding 1800F or remaining at those levels for an extended time, hydrogen volumes within the RCS will be controlled and the effectiveness of the OTSGs will be assured.

In performing the required actions, the operators will be affecting other plant equipment. For instance, when overriding interlocks to restart RC pumps, damage to the pumps may occur. Using the PORV to depressurize the RCS could introduce contaminants and potentially explosive quantities of hydrogen into the RB. The pressurizer quench tanks, particularly the rupture disc, will almost certainly be damaged. Equipment, particularly instrument hardware in the RB, may also be damaged. These are potential consequences of the actions required for T_{clad} at and above 1800F; the operator must be aware that they may have to be dealt with while attempting to bring the core conditions under control.

Another result of the operator actions is the exceeding of the 100F/ΔT OTSG tube-to-shell cooldown limit during blowdown of the generators. This is not expected to challenge the actual design limits of these components to the point where OTSG tube ruptures occur. The operator should not have to worry about significant secondary side contamination, offsite doses, or having to contend with OTSG tube leakage while cooling the plant down.

7. Shortcomings of T_c's

Great reliance should be placed on the core exit thermocouples in the situations that have been discussed. This is necessary because of the present level of instrumentation in the plants; these instruments will provide necessary information with reasonable accuracy. However, this equipment does have some shortcomings of which the operators should be aware.

As with any instrumentation, there are errors associated with T_c readouts which simply originate from the hardware and electronics that the systems contain. These may cause the T_c's to read too high in some situations and too low in others. This could lessen their effectiveness for some applications, such as determining locations of potential flow blockages in the core.

Also, readouts may be unavailable from many of the approximately 50 thermocouples in the core; they may simply not be "plugged in" to control room indicators or to the plant computer. The only access to T_c readouts may be through the plant computer, which could be unavailable in post-accident situations. (Other means of obtaining readouts are or will be installed on all plants, however.) For these reasons, readouts from the "hottest" T_c's, which are required by the ICC guidelines, may be unobtainable.

Another significant problem associated with T_c errors is that they may ambiguously indicate saturated or superheated conditions. Present SBOG procedures instruct the operators to turn off RC pumps on low RCS pressure. Future guidelines will require RC pump trip on loss of subcooling. T_c error could lead the operators to believe that the RCS is superheated when it is actually subcooled or saturated. This could cause confusion about whether RC pumps should be stopped or left running.

Generally speaking, the RCS is not likely to evolve immediately to superheated conditions following an upset. There should be ample time following the loss of RCS pressure or subcooling alarms, to trip the pumps before the system liquid inventory becomes so low that pump trip would cause core uncovery. This should be true, even though T_c readings indicate RCS superheating very early in the transient.

Although it is very unlikely to occur, actual superheated conditions in the RCS with the pumps running would be an extremely serious situation. This would signify that the system liquid inventory has been almost entirely lost. At

this point the only means of core cooling is by forced convection to the superheated vapor which is being circulated by the RC pumps. This would only be effective in slowing the rate of cladding temperature increase, but by shutting off the RC pumps even this meager amount of core heat removal would be lost. This would compound an already dangerous LOC condition.

Fortunately, there are other indications available to aid the operators in their decision concerning pump trip. They should consider leaving the RC pumps on if

1. They suspect that more than 2 minutes have elapsed since the low RCS pressure ESFAS alarm or the loss of subcooling alarm.
2. RCP motor currents are low (the higher the steam content of the circulating fluid, the lower the current required to pump it).
3. RC pumps are vibrating excessively, indicating that they are circulating a steam-liquid mixture and, perhaps, cavitating.

Early in a transient, when RC pump tripping is a concern to the operators, the RCS will probably not have evolved to a superheated condition even though this may be indicated by the operators. The above three items provide the operator with additional means of assessing the situation while deciding whether or not to turn off the RC pumps.

The negative aspects of using the T_c's to determine T_{clad} have been stated. They should not lead the operator to believe that the information obtained from the T_c's is valueless. On the contrary, they provide extremely valuable data on core conditions, especially during the early phases of a major upset and when system flows are reduced. They are, in fact, the best and most direct means of assessing core degradation and measuring the effectiveness of actions taken to correct unsafe conditions in the core.

Figure 8-1. Heat Transfer Coefficient
Vs Core Cooling Mode

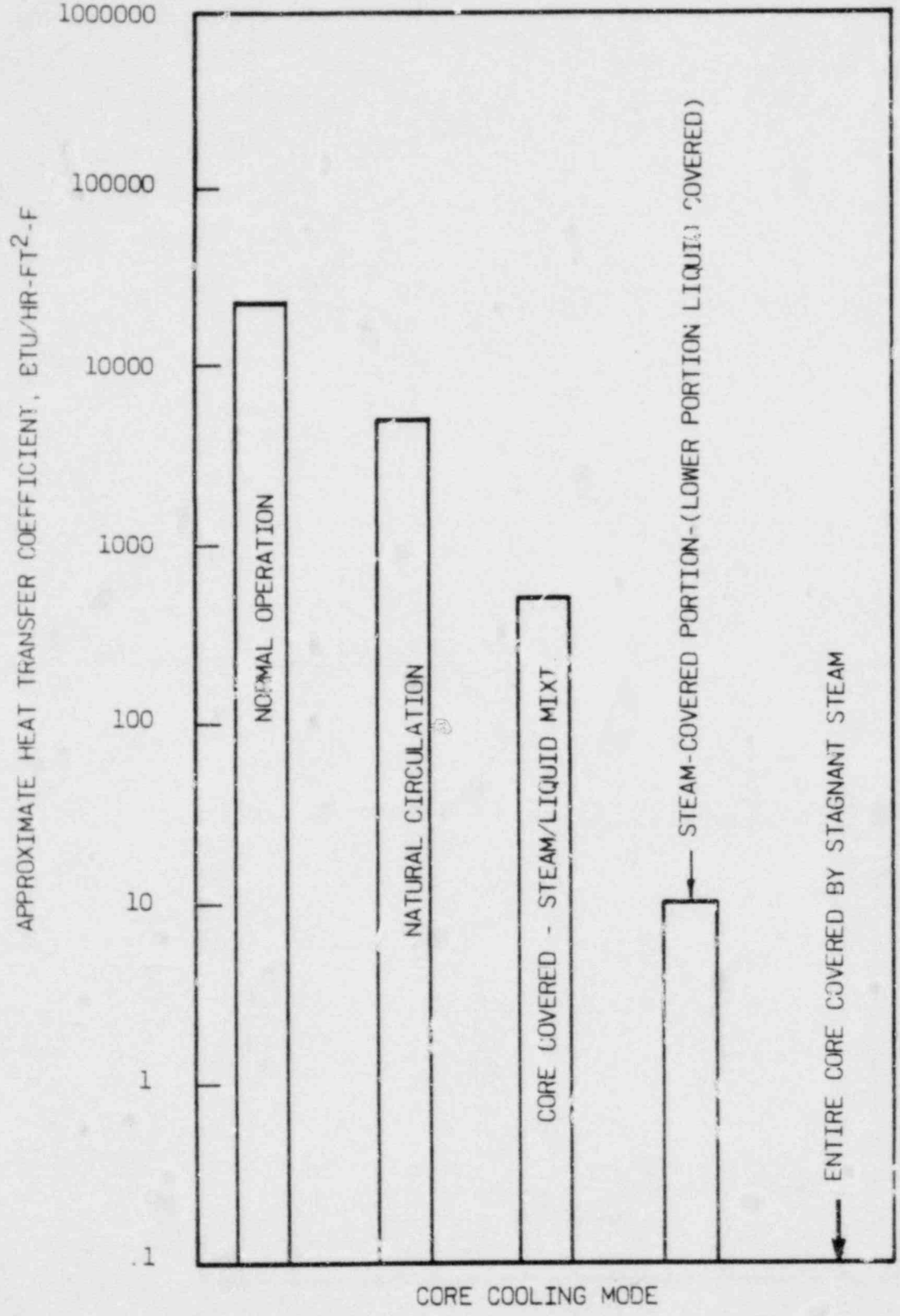

Figure 8-2. Core Mixture Height

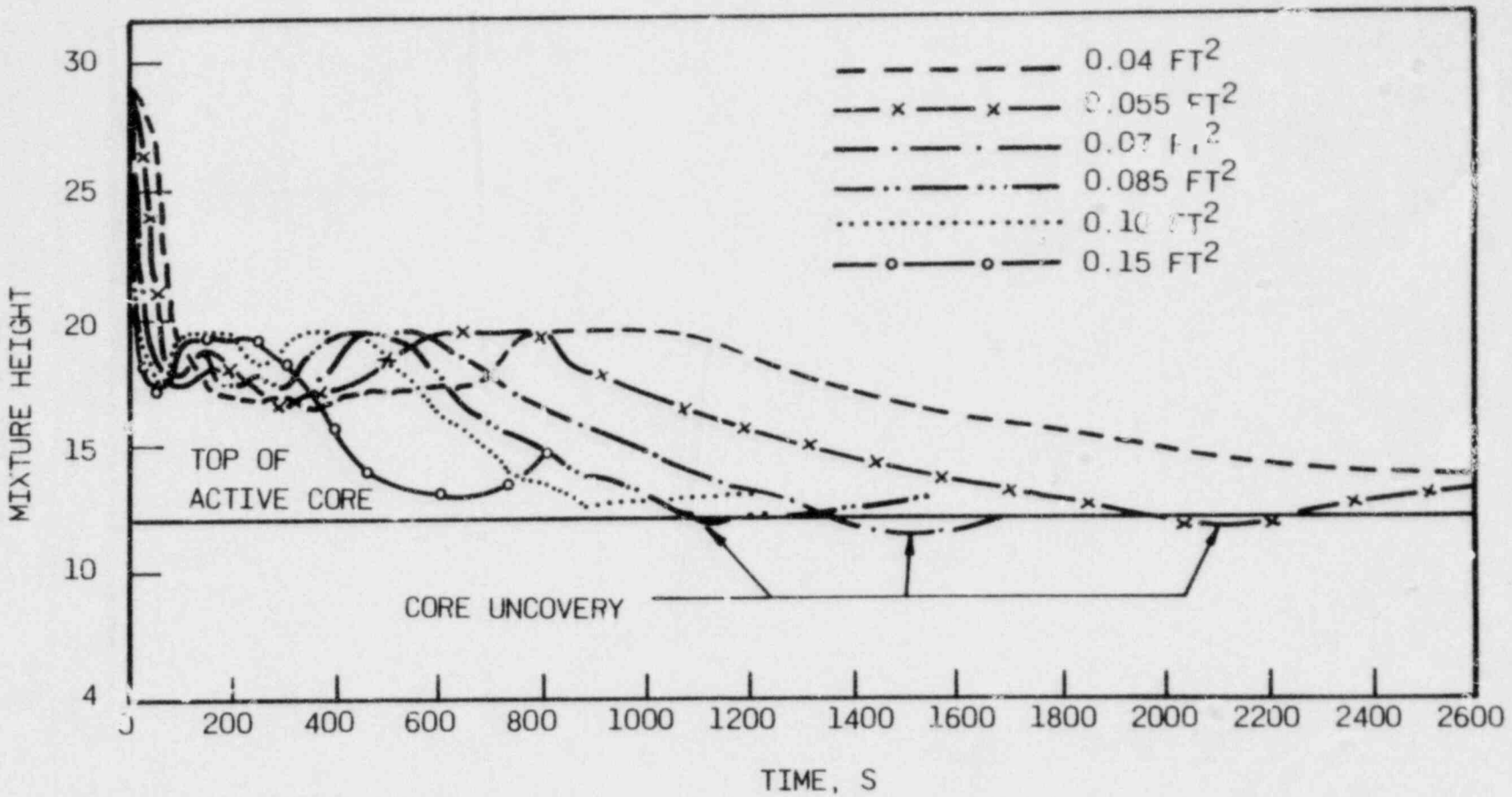

Figure 8-3. Cladding Temperature Vs Time

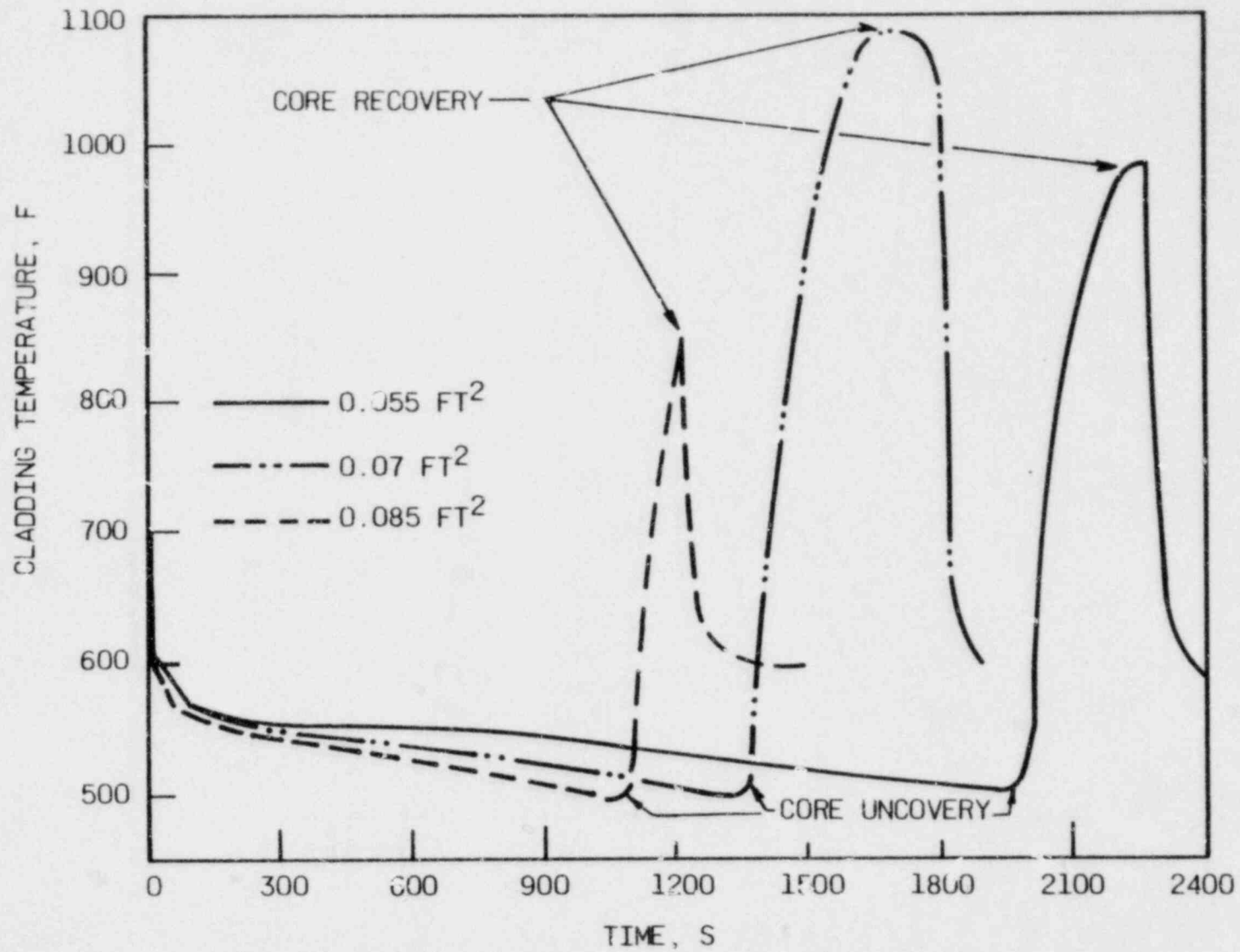

Figure 8-4. Correlation of Core Exit and Cladding Temperatures

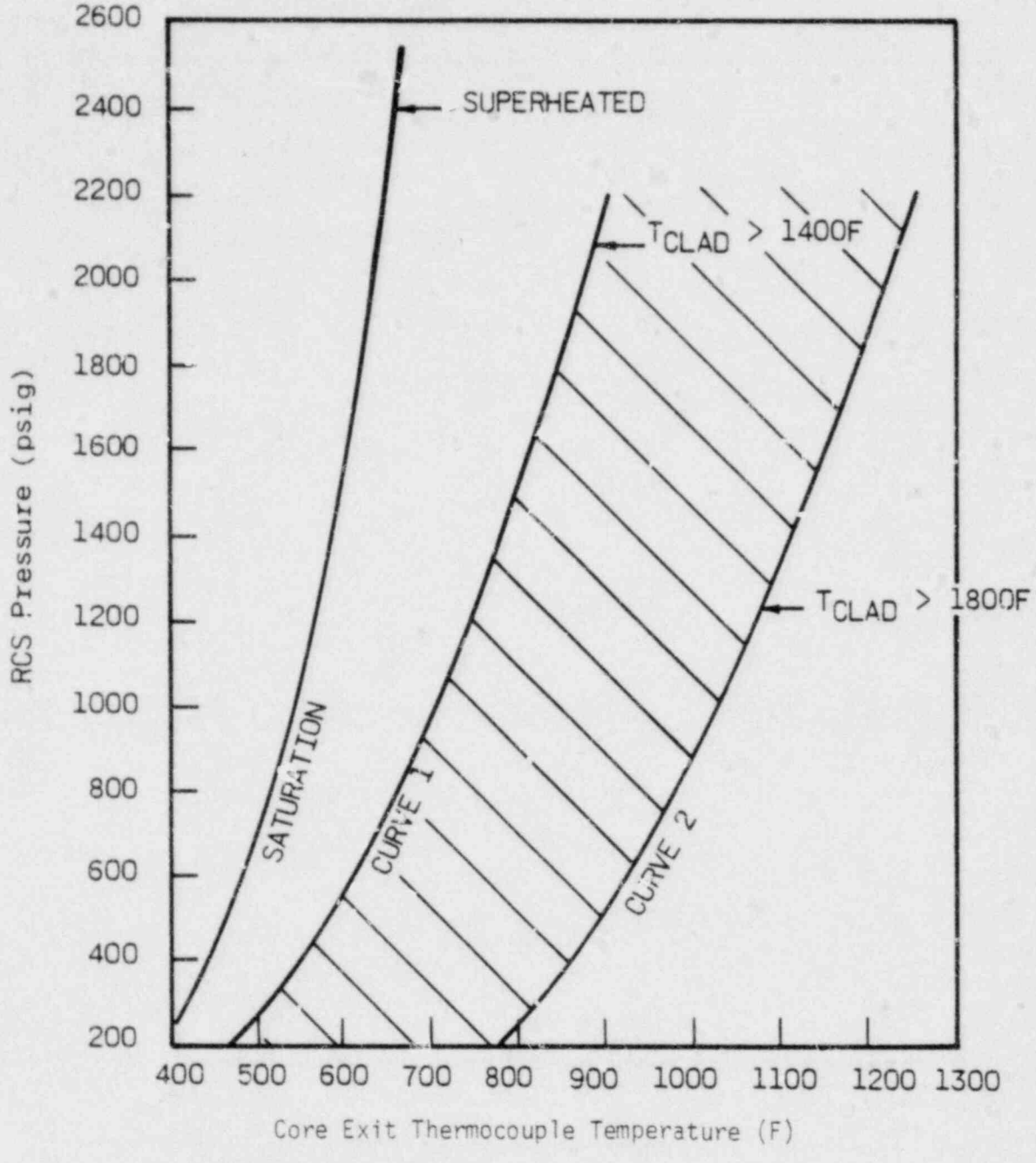

Figure 8-5. RTD and/or T_c Reading Between Saturation and Curve 1

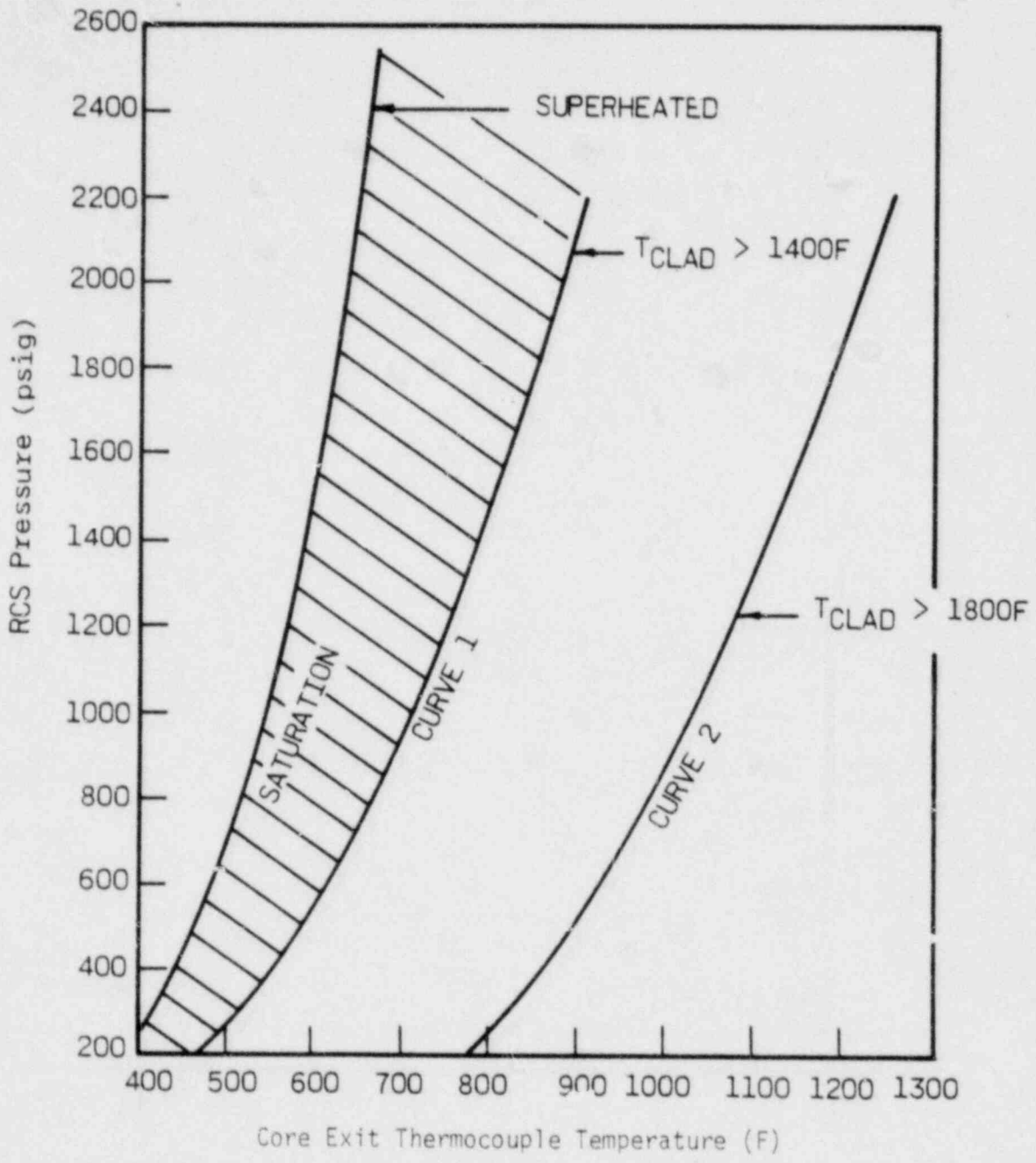

Figure 8-6. RTD and/or T_c Reading Between Curves 1 and 2

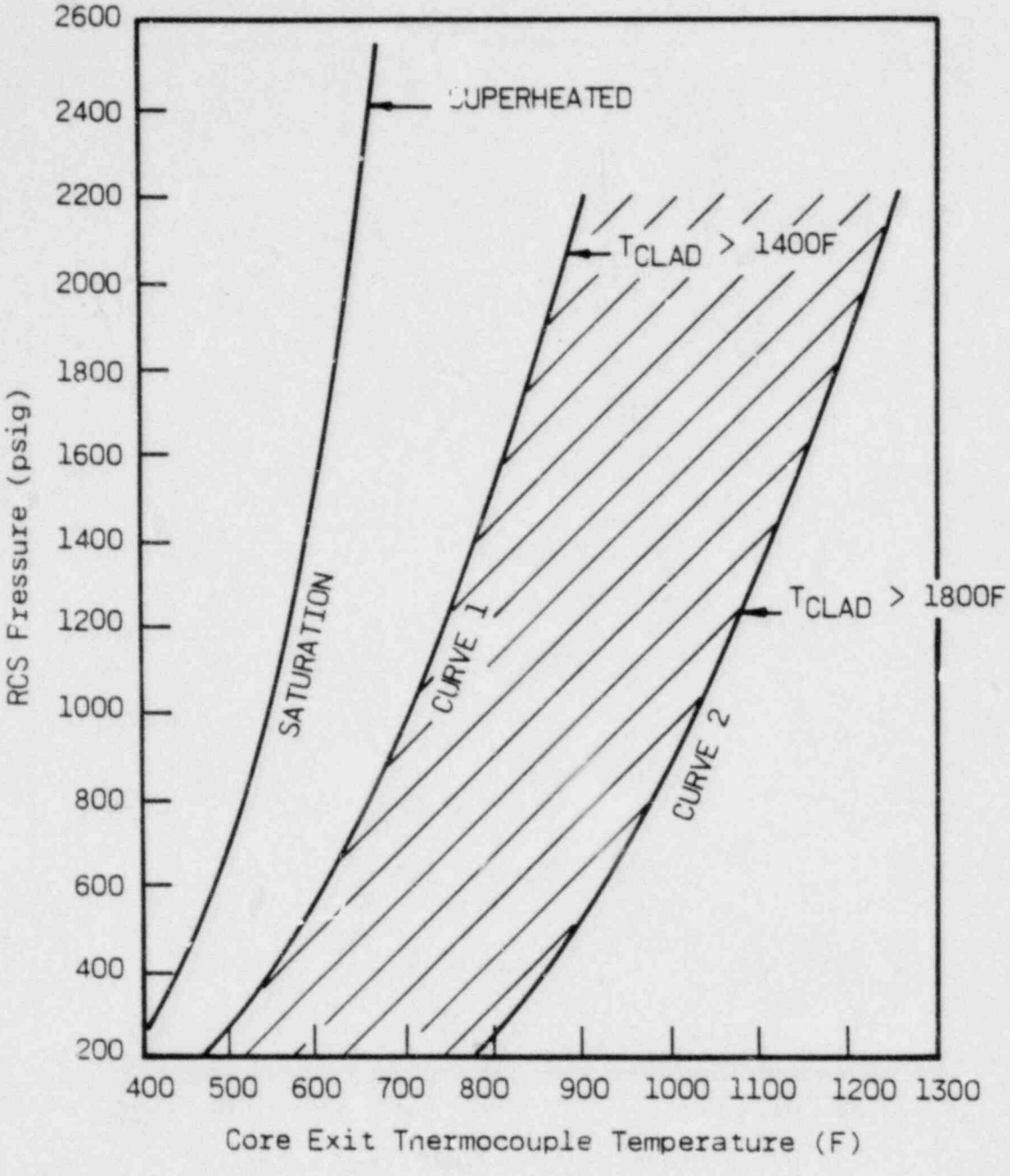

Figure 8-7. RTD and/or T_c Reading More Than 1800F

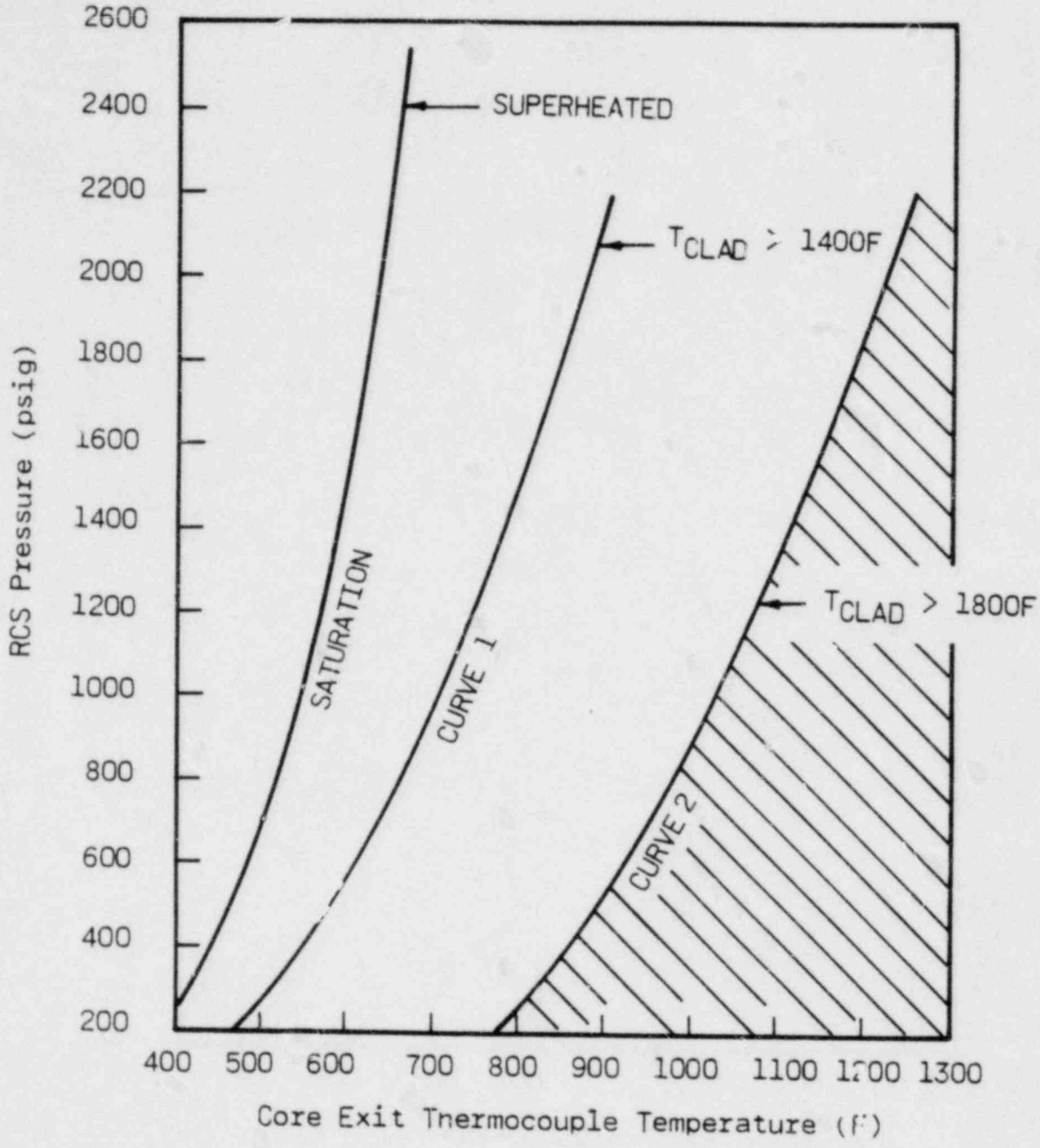

Lesson 9 — RELATIONSHIP OF OCD SOURCE RANGE DETECTORS TO DEGRADED CORE CONDITIONS

Introduction

1. Lecturer —

2. Purpose — To provide interpretations of abnormal source range monitor readings after a reactor trip.

   Although the primary function of out-of-core flux detectors is to monitor reactor flux levels during approach to criticality and power operation, an analysis of post-accident TMI events has indicated that the source range monitors (SRMs) are sensitive to changes in primary coolant "apparent density" and changes in certain core conditions that affect neutron generation.

Objectives

The following material is covered in Lesson 9:

1. General description of out-of-core detector (OCD) system.
2. Brief discussion of physical processes involved — neutron generation in core, criticality, neutron transport.
3. Parametric effect of source generation and void fraction on SRM readings.
4. Discussion of normal and abnormal (TMI-2) SRM readings after a reactor trip.

The following key points are to be retained:

1. Above-normal SRM readings after trip can be caused by any one or a combination of the following: recriticality, fuel failure with fission product release core voiding, downcomer voiding, and/or coolant temperature increase.
2. "Normal" SRM readings after trip can vary due to startup source strength, core multiplication, and/or coolant temperature.
3. SRM readings should decrease continually after trip, and the operator should be wary of any increase in count rate.

LESSON OUTLINE

1. Source Range Monitor Response After Reactor Trip
   1.1. Typical SRM Response (Normal Trip at Oconee 3)
   1.2. SRM Response After TMI-2 Accident
2. Out-of-Core Detector System
3. Neutron Transmission From Core to SRM
   3.1. Neutron Transport
   3.2. Homogeneously Distributed Voids
   3.3. Coolant Temperature
   3.4. Coolant Level
4. Neutron Generation After Reactor Trip
   4.1. Incore Sources
   4.2. Subcritical Multiplication
   4.3. Excore Sources
5. Reactor Events
   5.1. Recriticality
   5.2. Loss of Coolant
   5.3. Coolant Boiling
   5.4. Core Damage
   5.5. False SRM Signals Due to Gamma Radiation
6. SRM Chart Interpretation
7. Summary

References

Lesson 9 — RELATIONSHIP OF OCD SOURCE RANGE DETECTORS TO DEGRADED CORE CONDITIONS

1. Source Range Monitor Response After Reactor Trip

Source range monitors (SRMs) are part of the out-of-core detector (OCD) system in B&W reactors and, as such, are located in the reactor cavity (Figure 9-1). Their major function is to measure a reactor's approach to criticality prior to startup. Observations after the TMI-2 accident indicated that the SRM readings could be confusing, but if properly interpreted, they could be useful monitors of core behavior and system conditions during certain accidents. Because of the SRM locations — away from the harsh environment in the core — SRM signals should be a rapid, reliable measure of neutron flux in the reactor cavity which is normally proportional to core flux. However, interpretation of SRM signals is not straightforward during accidents that could lead to a degraded core because the signal responds to changes in both neutron transmission and neutron generation. Thus, supporting data from other installations must be considered along with operator action to define the cause of anomalous SRM readings following accidents.

Neutrons that are born in the core region must pass through several steel and water regions before reaching the detector locations. The shaded area in Figure 9-1 represents the peripheral fuel assemblies in the core where neutrons that are born have a good chance of escaping the core. The unshaded area represents the inner fuel assemblies (later referred to as the inner core), where changes in neutron generation rate will not significantly affect the core escape flux or the SRM response.

The fraction of neutrons transmitted (or its reciprocal, the attenuation factor) is affected by the mass of water between core and cavity. Water mass can vary due to density changes associated with temperature changes and/or voiding due to loss of coolant via some mechanical malfunction or human error. The neutron generation rate is affected by the mass of coolant in the core region

and any other parameters that alter core reactivity, such as coolant void, coolant temperature, boron concentration, control rod location and integrity, and fuel pin integrity. The complexity of the problem becomes apparent when one considers that these phenomena have competing dependent and/or multiple effects on SRM responses.

In this lesson the SRM responses after a typical reactor trip and after the TMI-2 accident trip are discussed. We will consider some of the reactor conditions that perturb SRM responses and then provide suggestions for interpreting SRM charts in accident situations.

1.1. Typical SRM Response (Normal Trip at Oconee 3)

The SRM response to a normal reactor trip is shown in Figure 9-2. Initially, the power (and therefore the SRM signal) drops with an 80-second period, consistent with the 55-second half-life delayed neutron group. During the first 15 to 20 minutes following reactor trip the delayed neutrons from ^{235}U fission products are the dominant source of neutron flux.

As the delayed neutrons die out (becoming relatively insignificant after about 20 minutes), the photoneutrons from γ,n reactions with D_2O (in the primary coolant) become the dominant source of neturons. This source decays with a variable half-life of 1 to 2 hours (over the time period of about 0.5 to 4 hours after trip) and becomes relatively small by about 10 hours after trip.

After about 10 hours the SRM signal tends to be essentially constant because it is then responding to neutrons from the startup source.

The absolute value of the SRM signal following a normal reactor trip may vary from one reactor to another and even between subsequent trips in the same reactor. However, the general shape should be maintained. Some of the following items could affect the SRM reading:

1. Power history several days prior to trip and, to some extent, burnup — This determines fission product concentration, which is the source of gamma flux for photoneutron production.

2. Coolant temperature variations — This changes the attenuation of neutrons from core to detector.

3. Startup source activity — Depending on the type of startup source, the neutron output may either decrease or increase with time after installation in the reactor.

1.2. SRM Response After TMI-2 Accident

The SRM recorder chart from TMI-2 is shown in Figure 9-3. The abnormal response of the SRM was puzzling to the TMI-2 operators and is the basic reason for presenting this lesson. It should be noted that "after-the-fact" explanations and conclusions seem obvious now, but it took many months of detailed analysis to correlate the SRM response with the TMI-2 accident conditions.[1]

The relevant features of Figure 9-3 are designated by letters:

A – The SRM behavior initially exhibits the typical pattern of delayed neutron decay.

B – After approximately 20 minutes the count rate levels out at a magnitude higher than normal because of the buildup of steam bubbles (voids) in the core and downcomer regions. This is consistent with the fact that reactor coolant system pressure had reached saturation (about 6 minutes after trip) and net flow through the open relief valve continued to empty the system. Void formation is also indicated by the drop in reactor coolant flow rate due to the reduced pumping head produced by the two-phase flow condition. Reduced attenuation of neutron flux due to the reduced coolant density causes an increased count rate.

C – Increasing voidage led to increasing count rates due to continued loss of coolant from the primary system. The "noisy" signal indicates unsteady flow (pump surging) and phase separation characteristic of "slug" flow.

D – Reactor coolant pumps in the B loop are secured by the operator.

E – At 100 minutes the reactor coolant pumps in the A loop were secured. With no forced circulation, phase separation occurred – liquid fell to the bottom of the system and steam voids rose to the upper regions. The combination of back drainage from the hot legs and voids rising to the top produced a "solid" water level above the detector elevation (and probably above the top of the core). This caused an abrupt drop in detector count rate due to increased coolant density in the downcomer (and therefore increased attenuation of neutron flux).

F – The low count rate suggests that the downcomer coolant level was near the top of the core.

G – Coolant began to boil, with a corresponding reduction in core and downcomer levels. Makeup flow of about 18 gpm was insufficient to maintain the coolant level. Transmission of neutron flux from core to detector increased as the coolant level dropped. Also at this time, feedwater addition to the A steam generator was reduced. This reduced condensation in the A loop, leaving the open relief valve as the only pathway for boiloff.

H – A leveling off of the SRM count rate is believed to correspond to a reduction in the rate of core uncovering caused by the makeup flow rate approaching the boiloff rate.

I — The detector was probably uncovered by now (level less than 5 feet above the bottom of the core), and the neutron source reduction in the core counteracted the increased transmission from core to detector. Source reduction resulted from less coolant for photoneutron production and lower core multiplication. At 142 minutes the relief block valve was closed. Increased makeup (36 gpm) may have caused the subsequent signal reduction.

J — The count rate decreased as the coolant level in the core rose.

K — Reactor coolant pump 2B started briefly and partially filled the downcomer.

L — Loop flow data indicated that the pumps worked for only a brief period. When flow ceased, phase separation occurred, with a corresponding drop in downcomer liquid level. Boiloff continued to decrease the downcomer level until equilibrium was established.

M — High-pressure injection (HPI) flow was initiated at 200 minutes. The detector count rate dropped rapidly as the liquid level rose in the downcomer.

N — Continued addition of HPI flow began to quench the core. Possibly, the coolant first wetted the outer core region, bypassing the hot center.

O — Coolant continually entering the core led to an unstable thermal-hydraulic condition. It is speculated that the increased detector signal may have been due to fuel rearrangement and/or coolant flashing to steam.

Because of these complex interactions and the sequence of events, it is essential to understand the neutron generation and attenuation processes as well as the instrumentation response.

2. Out-of-Core Detector System

The out-of-core detector (OCD) system comprises three types of detectors — source range, intermediate range, and power range — which are designed to be sensitive to neutron flux that represents reactor power levels from 10^{-11} to 100% full power. Three types of instruments are needed to provide the required accuracy, with each covering about a third of the total range (including and appropriate overlap). Because the after-shutdown flux levels are of primary interest here, this lesson considers only the source range monitors (SRMs).

SRMs are BF_3 gas-filled ionization chambers which are encased in 0.31 inch of high-density polyethylene and 2 inches of lead. These instruments are sensitive to low-energy neutron (thermal) reactions with ^{10}B.[2] The polyethylene is required to increase the relative number of thermal neutrons by moderating the energy spectrum of neutrons in the reactor cavity. The lead is supplied to reduce the gamma flux that reaches the detector. Gammas can cause anomalous detector signals by creating pulses that are counted as neutrons. The SRMs are housed in 6-inch-diameter steel thimbles and are positioned in the reactor cavity at the elevation of the core midplane. Since the SRM is 26 inches long, the bottom edge of the detector is about 5 feet above the bottom of the core. Typical locations are shown in Figure 9-4. The criterion used to establish these positions was that SRMs should be 90° off-axis from startup sources and separated from each other by 180°. This arrangement enhances sensitivity to fission neutrons (relative to startup source neturons) during the approach to criticality. An elevation view of SRM positions is shown in Figure 9-5.

3. Neutron Transmission From Core to SRM

Of the two major effects on SRM response, this analysis considers first neutron transmission from reactor core to detector location.

3.1. Neutron Transport

When neutron flux passes through a material, the neutrons react with nuclei. Various mechanisms by which neutrons interact with matter are as follows:

1. Elastic scattering — Like a billiard ball collision between the neutron and the nucleus of an atom. Some of the neutron kinetic energy is imparted to the nucleus, but the nucleus is not left in an excited state and the neutron rebounds. This is the moderating or thermalizing process at work in the coolant of a PWR or BWR.

2. Inelastic scattering — In this process the receiving nucleus is excited to a metastable state; upon return to a stable state, it emits excess energy in the form of a neutron and a gamma ray.

3. Capture (or absorption) — The nucleus absorbs the neutron's binding energy, kinetic energy, and mass, creating an isotope of the basic atom. The excited nucleus rids itself of this excess energy by radiation of either charged particles (e.g., alphas, protons, betas, etc.) or gamma emission, but no neutrons. Usually, hard gammas of several Mev are emitted.

The importance of the neutron energy in the interaction of neutrons with matter makes it necessary to classify them according to their energies. The terms thermal, epithermal, and fast represent a broad, rather indefinite range of neutron energies.

Thermal neutrons are those which have reached thermal equilibrium with their surroundings. At 20C the thermal neutrons have a most probable kinetic energy of 0.025 ev in a nonabsorbing medium; most of them have energies less than 1 ev.

Epithermal neutrons are grouped between thermal and fast neutrons. The lower boundary on the fast neutron group is arbitrarily set at about 100 kev.

The initial energy of newborn neutrons can vary from about 0.1 to 10 Mev. This level is then reduced (or moderated) by scattering collisions with nuclei. Neutron energy is of particular importance to attenuation calculations (or its inverse, transmission) because collision cross sections are energy-dependent. (Cross section represents the probability that a collision may occur.) Generally, absorption cross sections are greater at low energies. Thus, low-energy

neutrons are more likely to be absorbed than are high-energy neutrons. A simplified mathematical description of attenuation is

$$\phi/\phi_o = e^{-\Sigma x}$$

where ϕ is flux at the point of interest, ϕ_o is initial flux, Σ is macroscopic removal cross section, and x is distance traversed. Because of the energy dependence of Σ, only high-energy neutrons from the core can reach the detector location, and because of many scattering collisions between core and detector, these neutrons will have lost most of their energy.

Neutron flux transport from core to SRM requires passage through several steel regions (liner, barrel, support cylinder, and pressure vessel), coolant regions (bypass and downcomer), and the reactor cavity (Figure 9-5). Typical line-of-sight distances in a 177-fuel assembly reactor are about 34 cm of steel, 41 cm of coolant, and 112 cm of air. The corresponding attenuation of total neutron flux is approximately 4×10^{-5} due to absorption reactions with steel and water nuclei. Since reactions with coolant nuclei represent a significant part of this attenuation, the potential exists for large variations in SRM readings because of changes in coolant density.

3.2. Homogeneously Distributed Voids

A principal mechanism for changing neutron flux transmission (or attenuation) is the variation in the amount of coolant in the downcomer, core, and bypass regions. Calculations were performed based on a 177-FA reactor model with a constant source of neutrons in the core and all coolant regions at 550F. Homogeneously distributed void formation in coolant regions was simulated by varying the water density. This model should approximate the reactor condition when the reactor coolant pumps are circulating a saturated coolant in a partially filled system. Relative SRM readings (relative transmission of neutrons) are shown in Figure 9-6 as functions of void fraction in the primary coolant. Of significance here is the potential effect on the SRM of voiding different regions. For example, total loss of coolant from the core, bypass, and downcomer regions would increase the SRM reading by a factor of approximately 8300, loss from the downcomer by a fraction of about 100, loss from the core by a factor of about 2.4, and loss from the inner core region by a factor of about 1.1. Also noteworthy is the insensitivity of SRMs to voiding (such as boiling) in the inner core region (all but the outer row of fuel assemblies, the shaded

area in Figure 9-1). Also, the nonlinearity of the effect is shown with the signal tending to increase more rapidly at higher void fractions. It should be emphasized, however, that these are constant source calculations, i.e., the effect of voiding on neutron generation rate is not considered. Voiding in the core region will reduce both the photoneutron production and core multiplication. These effects will first be examined independently and then combined with the transmission analysis to determine a net effect on SRM signal.

3.3. Coolant Temperature

Another condition that affects the attenuation of neutron flux by primary coolant is coolant temperature. Temperature changes cause density changes, which effectively increase or decrease the number of water nuclei in the flux path from core to detector. Analytically, this problem can be treated the same as homogeneously distributed void formations. The data presented in Figure 9-7 were derived from Figure 9-6 for equivalent percent void (density change from reference value at 530F) corresponding to selected tempeatures. (Negative voids correspond to increased density.) The 530F reference temperature was selected as representative of the hot standby condition that should exist after a reactor trip. Consequently, values from Figure 9-6 (modeled at 550F) were adjusted to account for the higher water density.

The data indicate that the SRM signal could increase by a factor of 1.5 to 2.5 for a 100F temperature increase and decrease by a factor of 0.6 to 0.8 for a 100F temperature decrease. Effects on source generation, photoneutrons, and core multiplication will tend to counteract these SRM responses when the temperature of the core coolant changes.

3.4. Coolant Level

When pumps are not operating and no forced circulation exists in a partially filled primary system, the two phases (void and liquid) will separate into a liquid pool and an overhead void space. Published calculational results for the effect of liquid level on SRM response indicate that a maximum increase of a factor of about 100 occurs when the level is 120 cm above the bottom of the core (Figure 9-8).[3] This analysis includes the combined effects of the decreased source and the increased transmission due to decreasing liquid level (increasing void). As liquid level decreases, increasing neutron flux transmission (reduced attenuation) is the dominant effect on SRM response until

about the 120 cm level. Below 120 cm, the decrease in photoneutron generation caused by less coolant in the core and less neutron multiplication in the core due to loss of reactivity overrides the effect of increased transmission.

For comparison, homogeneously distributed void data are also plotted in Figure 9-8. Although the comparison is not rigorous due to some unknown in the modeling detail for the two-phase analysis and in the correlation between downcomer level and homogeneous distribution of voids in the primary system, it does demonstrate the relationship between distributed and collected voids. The data in Figure 9-8 are based on 62% void formation homogeneously distributed in the primary system being equivalent to a liquid level even with the top of the core when the pumps are off. However, Figure 9-8 does show that if the pumps are stopped before the core is uncovered, the SRM will abruptly decrease by as much as a factor of 10. If pumps are stopped after void formation has progressed to the point where the core is uncovered when the liquid and gas phases separate, then the SRM reading will abruptly increase by up to a factor of 5 (except for an almost dry system).

Note that the analysis assumes a dominant photoneutron source and therefore is strictly applicable to the time period of about 15 to 25 minutes after reactor trip. The inclusion of significant flux from delayed neutrons or the startup source would tend to increase both curves, especially at low liquid levels (high percentage voids). Thus, the relative comparison between a separated two-phase system and a homogeneously distributed system should still be valid.

4. Neutron Generation After Reactor Trip

Another major effect on SRM response is the influence of reactor conditions on neutron flux generation after a reactor trip. This phenomenon is first treated independently and then in combination with the transmission effect (where appropriate).

4.1. Incore Sources

The principal mode of neutron production changes as a function of time after trip. Immediately after trip, delayed neutrons from fission products in the reactor fuel are the dominant source of neutrons (Figure 9-9). These neutrons die away rapidly in accordance with the 55-second half-life of the longest-lived delayed neutron group. After about 20 minutes, this source is relatively unimportant.

Photoneutron production becomes the dominant neutron source after the delayed neutron source has decayed and remains so for several hours. Photoneutrons are produced from γ,n reactions in deuterium, which has a natural abundance of 0.016 wt % in water. Therefore, the production of photoneutrons is directly proportional to the mass of coolant in the reactor core, i.e., the number of deuterium nuclei in the core.

Fission products in the reactor fuel provide the gammas for this reaction. However, since the reaction requires a gamma threshhold energy greater than 2.2 Mev, only certain fission products are important. For the first few hours after shutdown, several isotopes — ^{142}La, ^{88}Kr, ^{87}Kr, ^{138}Cs, and ^{84}Br — produce most of the photoneutrons. After several days, ^{140}La and ^{97}Zr are the major sources of high-energy gammas; and at long times ^{140}La is the principal supplier of gammas for γ,n reactions. The decay of the photoneutron source is determined by the decay rate of the gamma-producing isotopes. At short times, when a mixture of isotopes is important, the photoneutron source decays with half-lives of 0.3, 1.4, and 1.7 hours, respectively, over the time spans of 0 to 1 hour, 1 to 2 hours, and 2 to 3 hours after shutdown.[4] At long times after shutdown, the half-life is about 12 days, which is the half-life of ^{140}Ba, the controlling parent isotope in the ^{140}La decay chain. The magnitude of the photoneutron source is directly proportional to the concentration of these key fission products in the reactor core. The fission products, in turn, are proportional to power level and to some extent burnup, i.e., when

activity levels of the key isotopes are below their saturation values. Since fission products tend to reach saturation activities (equilibrium concentrations) after several half-lives of reactor operation, it becomes apparent that the buildup of short-half-life fission products is dependent on burnup for about the first day or two after startup and then is relatively constant. Similarly, the long-half-life fission products saturate after several months of burnup. The same effect occurs in reverse when a reactor comes down in power. For example, a rapid power decrease (such as a trip) will produce a photoneutron-producing gamma source that is characteristic of the power level before trip. However, if the power decrease requires several hours, the magnitude of the short-term photoneutron source will have been reduced because of the decay of short-half-life fission products. Thus, it is necessary to know the reactor power history prior to trip in order to determine the magnitude of the photoneutron source.

After the photoneutron source has decayed, the reactor startup source represents the major source of neutrons in the reactor core. Prior to initial startup, two americium-beryllium-curium (ABC) sources are installed in peripheral fuel assemblies of B&W reactors (Figure 9-4). Each source is about 500 Ci, has a half-life of about 163 days, and is located in an instrument tube at about the core midplane elevation. After installation, SRM readings of about 5 cps are obtained. Prior to the approach to criticality, SRM readings of about 15 cps are observed. However, it is difficult to correlate these data because of uncertainties in core multiplication, coolant temperature, and startup source strength. Because the ABC source strength decays with a 163-day half-life, a regenerative source of antimony-beryllium must be added after cycle 2. Its strength is comparable to that of the ABC source.

Neutron production from α,n reactions in actinides contained in the reactor core was calculated and found to be insignificant compared to other neutron sources.[4] The α,n reaction in oxygen was considered to be a relatively small contributor of neutron flux after reactor trip.

4.2. Subcritical Multiplication

Whenever neutrons are produced from an external source (any source other than fission) in the reactor core, they cause fissions to occur in the reactor fuel, even in a subcritical core. The magnitude of this fission neutron source is the subcritical multiplication factor M (or core multiplication). Since the

value of M will range from 2 (for a dry core) to more than 100 (k = 0.99), it becomes apparent that the largest source of neutron flux will be fissions in the reactor fuel (Figure 9-10). M is a function of core reactivity, which can be represented by a multiplication factor, k. k is related to reactivity by the expression $k = 1/(1 - \rho)$, where ρ is the reactivity change in the core. For valuves of k close to 1.0 (criticality), M is sensitive to small changes in reactivity, and a small change in k can result in large values for M. Conversely, M is less sensitive at lower k values.

A B&W reactor typically has a k of 0.93 to 0.95 after trip. This presents a potential decrease of about a factor of 10 for M (and therefore neutron source generation) but also presents a very large potential increase in M if the core approaches criticality. (Theoretically, M is infinite when k = 1.0.) Increasing M with k near 1.0 appears to be the only mechanism for a large increase in an incore neutron source after reactor trip.

Decreases in M would be less severe because large amounts of negative reactivity would have to be added to attain relatively small reductions in M. For example, a minus 10% change in reactivity would be needed to reduce k from 0.93 to 0.85, with a corresponding reduction in M from 14 to 7 (a factor of 2 reduction in neutron source).

Reactor conditions that can add positive reactivity are deboration, coolant temperature decrease (negative moderator coefficient), xenon decay, and structural damage that could result in loss of fission products, fuel rearrangement, and/or loss of control poison. Negative reactivity could result from a loss of coolant, a coolant temperature increase (negative moderator coefficient), boration, and structural damage that could result in fuel rearrangement and/or loss of fuel.

4.3. Excore Sources

Photoneutrons from γ,n reactions in deuterium can occur in excore coolant regions in the same manner as in incore production. Neutrons produced in the downcomer will have a much better chance of reaching an SRM due to a shorter transport path, but the production rate will be lower due to less gamma flux and no benefit from core multiplication. Although no detailed analysis of this problem has been performed, estimates indicate that excore photoneutron production from core gamma flux does not appear to be important relative to incore photoneutron production.

The release of fission products into the primary coolant, however, could produce a significant excore source of photoneutrons in the downcomer. It has been estimated that a γ,n reaction in the downcomer produces neutrons that are 1000 times more likely to be detected by an SRM than a neutron produced by an incore reaction. This increased sensitivity is counteracted by a dilution factor of 100 from core to primary system. Thus, if fuel cladding were damaged and 10% of the fission product inventory was evenly distributed throughout the primary system, the SRM signal would approximately double. The SRMs would see two approximately equal sources from incore and excore photoneutrons. This SRM behavior pertains only to the time period when the photoneutron source dominates. At other times, any excore photoneutron source would be a partial contributor to total neutron flux.

Certain characteristics of an excore photoneutron source may be used to indicate or confirm the release of fission products from the core. Neutron flux from this source should be insensitive to core reactivity changes and to coolant temperature change and will decay with a half-life corresponding to the important gamma-producing fission product.

5. Reactor Events

Reactor conditions that can affect SRM readings by causing changes in neutron flux transmission and generation are discussed below.

5.1. Recriticality

After reactor trip, certain malfunctions can increase reactivity and cause the core to approach or reach criticality. For a steady addition of positive reactivity, one could expect to see a slow but continuously increasing SRM reading (assuming that initial k is less than about 0.95) with a rising slope on the SRM recorder chart. The SRM reading and chart slope will begin to increase rapidly near criticality. At critical, a spike will occur on the chart because the core is expected to quickly return to a subcritical condition due to its Doppler coefficient, possible structural damage, and/or coolant expansion.

Positive reactivity addition to the core could result from deboration, decreasing coolant temperature (if moderator coefficient is negative), xenon decay or loss, control rod withdrawal, or structural damage resulting in fuel rearrangement, and/or loss of control poison. Deboration could result from various improper valve lineups when using the makeup and purification system and deborating demineralizer system. Xenon loss from damaged fuel pins could amount to 4% reactivity, depending on the time after shutdown. Structural damage could be caused by an overheated core and/or metal/water reactions.

5.2. Loss of Coolant

Primary coolant loss through a broken pipe or stuck-open valve would tend to promote the formation of steam bubbles by depressurization. The SRMs would respond to several competing effects which lead to increased neutron flux transmission and decreased neutron generation. Transmission is increased because of the reduction in the number of water molecules in the neutron's transport path. Generation is decreased due to the reduction in the number of D_2O molecules in the core to produce photoneutrons and to the reduction in core multiplication due to the negative reactivity effect caused by steam voids.

Figure 9-11 illustrates how an SRM response to a loss-of-coolant accident (LOCA) can be estimated. (This analysis assumes that voiding occurs instantaneously.)

1. For a selected void fraction (in the example a dry core, 100% voids, is used), the relative increase in neutron flux transmission can be obtained from Figure 9-6.

2. For a selected time after reactor trip, Figure 9-2 can be used to determine the prevailing method of neutron source generation. That portion of the source due to photoneutrons is reduced in direct proportion to the fraction of steam voids in the coolant, e.g., 100% voids reduces the photoneutron source to zero, whereas the delayed neutron and startup neutron sources are constant relative to void formation. A factor is than calculated that represents the ratio (for all sources) of neutron generation rate after voiding to that before voiding.

3. For an estimated reactivity loss due to voiding, a value for core multiplication can be obtained from Figure 9-10. A factor that represents the change in core multiplication is calculated from the ratio of core multiplication after voiding to that before voiding.

Two results are obtained for case 1 — one near the beginning of the period when photoneutrons are the dominant source (t ≅ 0.3 hour) and one near the end of that time period (t ≅ 5 hours). Note that as the relative importance of photoneutrons decreases, the relative SRM response to a LOCA increases. Additional results for other LOCA conditions are presented in Figure 9-12 to show the typical effects on SRM response of coolant temperature, time after reactor trip, initial k and the specific coolant regions that are voided. These results can be summarized as follows:

1. If the accident started at a lower initial coolant temperature, a greater change in relative neutron flux transmission would occur (and therefore SRM response), i.e., the LOCA removes more water molecules per unit volume of coolant.

2. During the time after trip when photoneutrons are the major source, relative SRM response to coolant loss is less than at other times after trip.

3. A lower initial k for the core tends to increase relative SRM response; i.e., there is less potential for decreasing core multiplication.

4. The effect on SRM response of voiding only the downcomer can exceed the effect of voiding the entire coolant system. Core and bypass region voiding have little tendency to increase SRM response; in fact, a reduction occurs during the period when photoneutrons are the major source.

In this section it is important to remember that we are considering the relative SRM response and not absolute readings. Thus, a case with a larger relative response might have a lower SRM reading. Also, the dry core condition may not represent the maximum effect on SRM response because (as we observed earlier in this lesson) in a non-circulating system with phase separation, the maximum SRM response occurs when the core is partially filled with coolant (Figure 9-8).

5.3. Coolant Boiling

Bulk boiling in the core due to decay heat and/or depressurization may be difficult to detect on the SRM. As in loss of coolant, competing effects of increased transmission and decreased flux generation occur. During the time after shutdown when photoneutrons are the dominant source, the SRM response could decrease unless the downcomer level falls to an elevation below the top of the core. At the TMI Unit 2 plant the SRM response increased by a factor of 100 when the downcomer level uncovered a significant portion of the core. A greater relative response of the SRM should be expected if boiloff causes the core to uncover after the photoneutron source has decayed to near the magnitude of the startup source. As noted earlier, if boiling is localized in the inner core region, there will be essentially no effect on the SRM reading due to the large neutron attenuation that occurs in the coolant in the downcomer.

5.4. Core Damage

If structural damage occurs in the core with subsequent fuel rearrangement, loss of fission products, and/or possibly loss of control poison, the effect on SRM response is somewhat unpredictable. When fuel pin damage occurs, the fuel location in the core could be disrupted (probable negative reactivity) and fission products, including xenon, could be lost (positive reactivity). The net effect on core reactivity would probably be negative, with a corresponding decrease in core multiplication, which would translate into a reduced SRM response. By similar reasoning, the loss of control poison (rods worth about 9% and LBP worth about 4% at beginning of cycle) would cause an increase in SRM reading.

Fission product release to the primary coolant could produce a significant source from photoneutron generation in the downcomer region. This would increase SRM response relative to the pre-damage reading. Obviously, it is not possible to predict a definitive SRM response to core damage because the mode of damage is unknown.

5.5. False SRM Signals Due to Gamma Radiation

BF_3-filled proportional counters (SRMs) are sensitive to high gamma flux. At high gamma dose rates, pulses from gamma reactions may be counted as neutrons.

B&W SRMs are required to operate in gamma fields of 100 R/h. This corresponds to a flux of approximately 10^8 γ/cm^2-s. Since the 2-inch lead shielding around the detector reduces this flux by a factor of about 10, the equivalent cavity flux would be about 10^9 γ/cm^2-s. It is unlikely that such a large gamma flux would occur after reactor trip, even with a dry downcomer and long-term activation of internals.

6. SRM Chart Interpretation

The phenomena discussed herein seldom occur as single events, but rather as consecutive and/or concurrent happenings. For example, loss of coolant could lead to coolant boiling, fuel damage, and/or recriticality. When such events occur in rapid succession, it is quite difficult to interpret SRM readings. However, some general guidelines have been formulated from this study and are presented in Figures 9-13a and 9-13b. The list includes the major SRM responses and their potential causes covered in this lesson. It is worthy of note that the various SRM situations are not mutually exclusive, i.e., the same reactor event sometimes results in different SRM responses depending on its time sequence. Similarly, a particular SRM response can usually be attributed to several possible reactor events. For example, a gradual increase of more than a factor of 10 in SRM response could be caused by the slow voiding of one or more coolant regions via loss of coolant (pipe break or open valve) or by increasing core multiplication via some mechanism for the addition of positive reactivity. This type of situation emphasizes the need for supportive data from other instrumentation and/or operator actions. For the case cited above, coolant loss may be detectable from flow and pressurizer level measurements and primary system pressure and temperature; and core conditions may be assessed from incore thermocouples, SPNDs, and chemical analysis of the coolant. An increase in core reactivity also could cause SRM readings to increase by a factor of more than 10. From an initial condition of $k = 0.95$, the addition of 4.8% reactivity would cause the neutron generation rate from core multiplication to increase by a factor of 10, with a corresponding increase in SRM response. Such a reactivity addition might be caused by a combination of coolant deboration, coolant temperature change, control rod withdrawal, or loss of poison material via core degradation. Any core degradation should be detectable by increased radiation levels in the letdown line.

Some other examples of reactor events and corresponding SRM responses are listed in Figure 9-13 and are considered to be self-explanatory.

7. Summary

1. Review physical phenomena that affect SRM response:
   a. Incore and excore source generation.
   b. Flux attenuation.
2. Discuss SRM behavior after trip:
   a. Normal shutdown.
   b. Abnormal shutdown.
3. Interpretation of high SRM readings:
   a. Recriticality.
   b. Coolant voiding.
   c. Coolant boiling (or heating).
   d. Verification with other instrumentation.
   e. False signals.

References

[1] Analysis of Three Mile Island, Unit 2 Accident, NSAC-1, July 1979; Supplement to Analysis of Three Mile Island, Unit 2 Accident, NSAC-1 Supplement, October 1979.

[2] Babcock & Wilcox Equipment Specification for Neutron Detectors, 08-1006435-01, BWNP-2004(6-76).

[3] R. L. Childs, et al., "Calculation of TMI-2 Source-Range Monitor Reading for Several Core Water Levels," ANS Transactions, Las Vegas, Nevada, June 1980.

[4] C. L. Whitmarsh, Source Range Detector Response After TMI-2 Shutdown, B&W Calculation File 32-1102088-00, June 22, 1979.

Figure 9-1. Layout of Core, Neutron Source, and Source Range and Intermediate Range Detectors

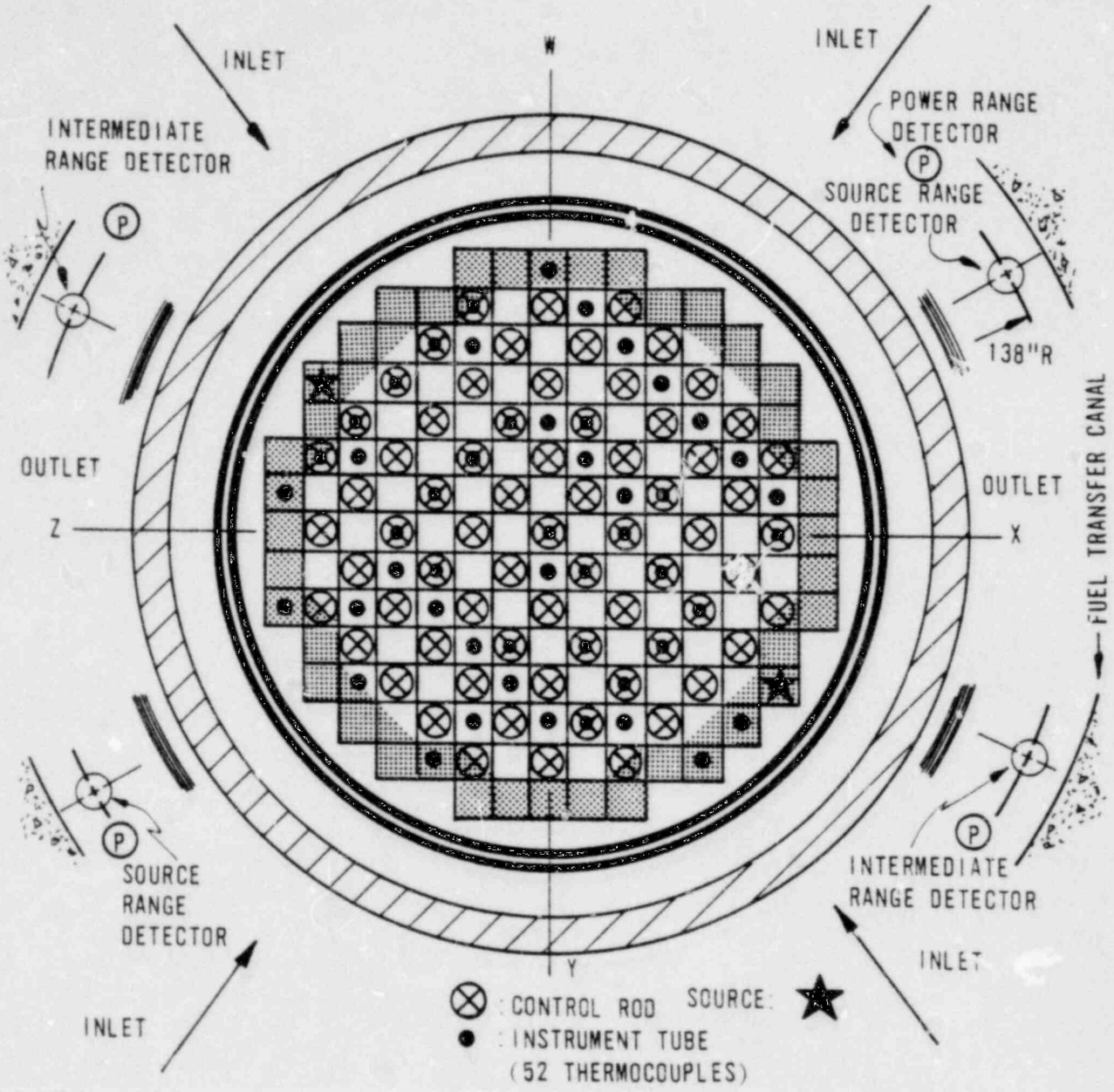

Figure 9-2. Oconee 3 Trip on June 13, 1975, During Shutdown From 87% FP, Reactor Tripped at 19% FP

(1) Loss of Feedwater, (2) Pressurizer Relief Valve Stuck Open

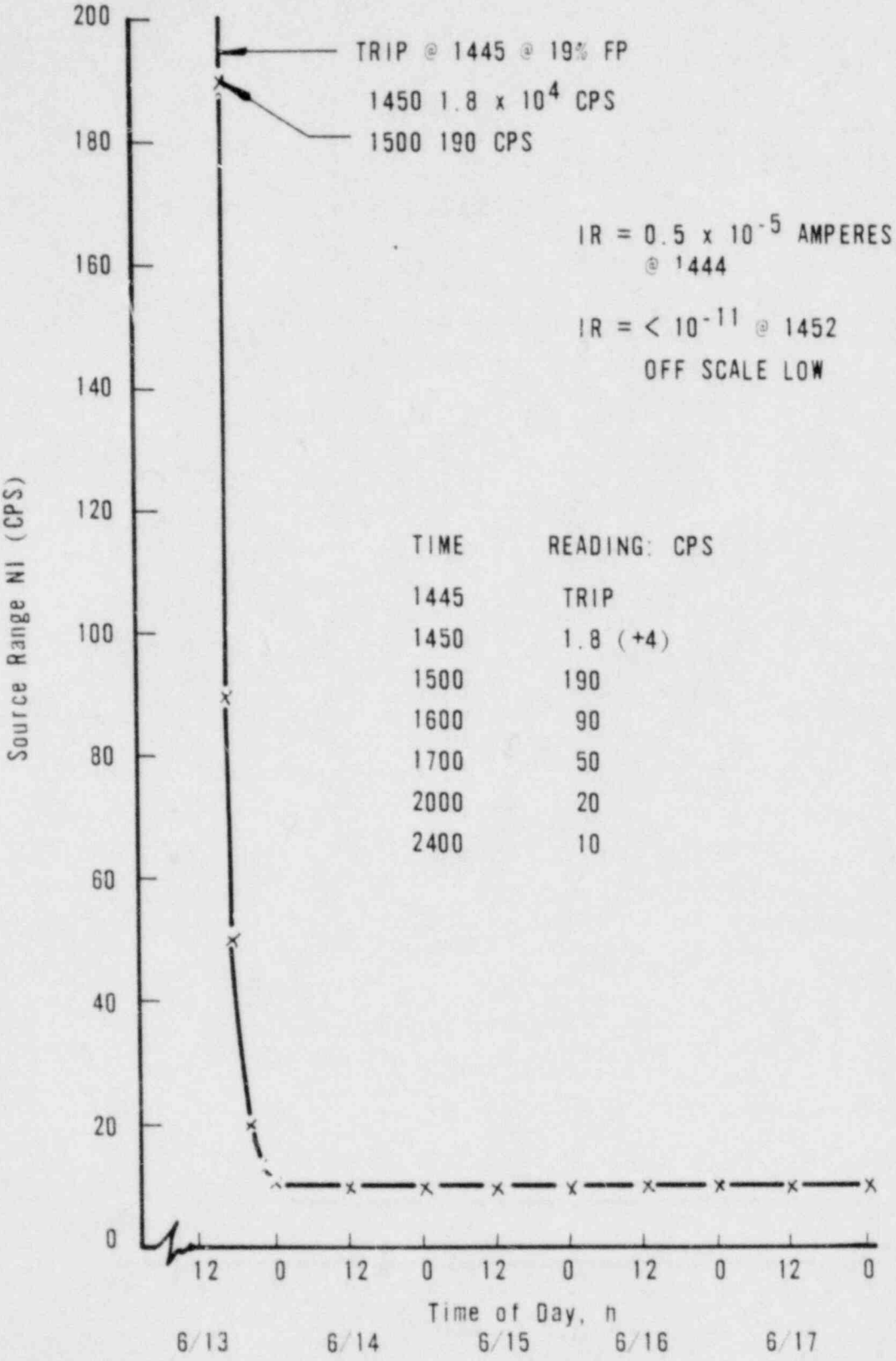

Figure 9-3. TMI-2 Source Range Monitor Readout After Accident

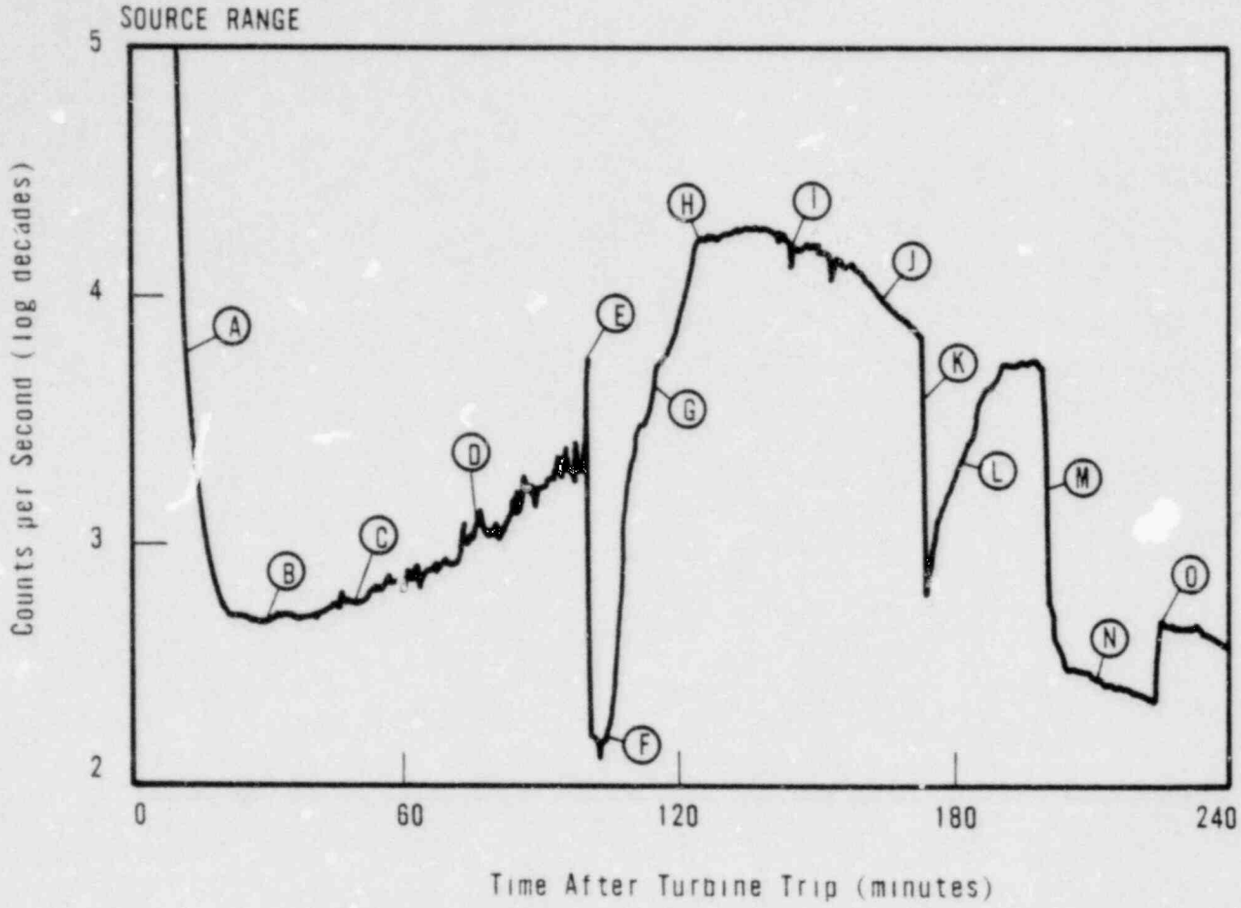

Figure 9-4. Layout of Core, Neutron Source, and Source Range and Intermediate Range Detectors

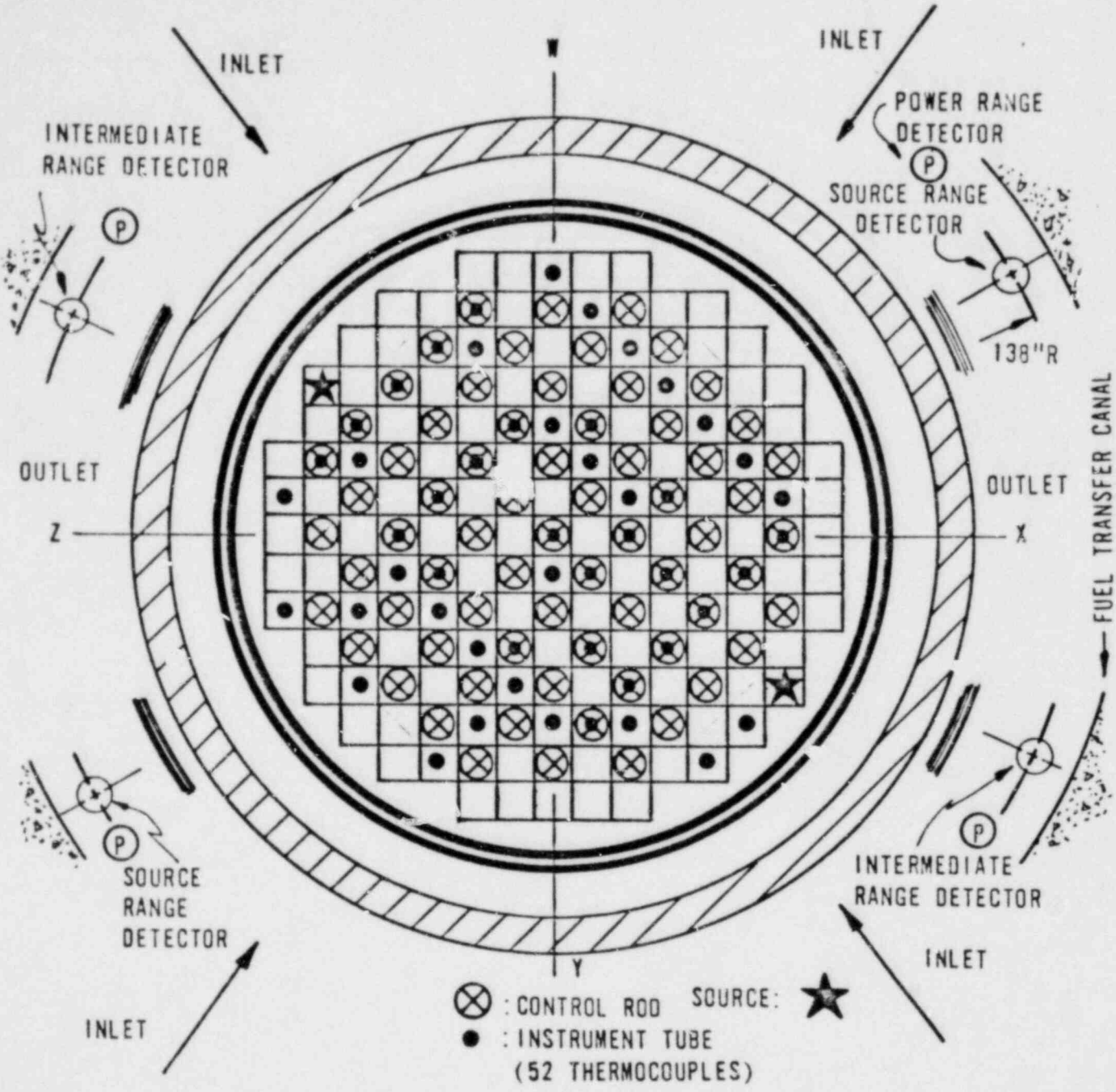

Figure 9-5. Elevation View of 177-Fuel Assembly Reactor

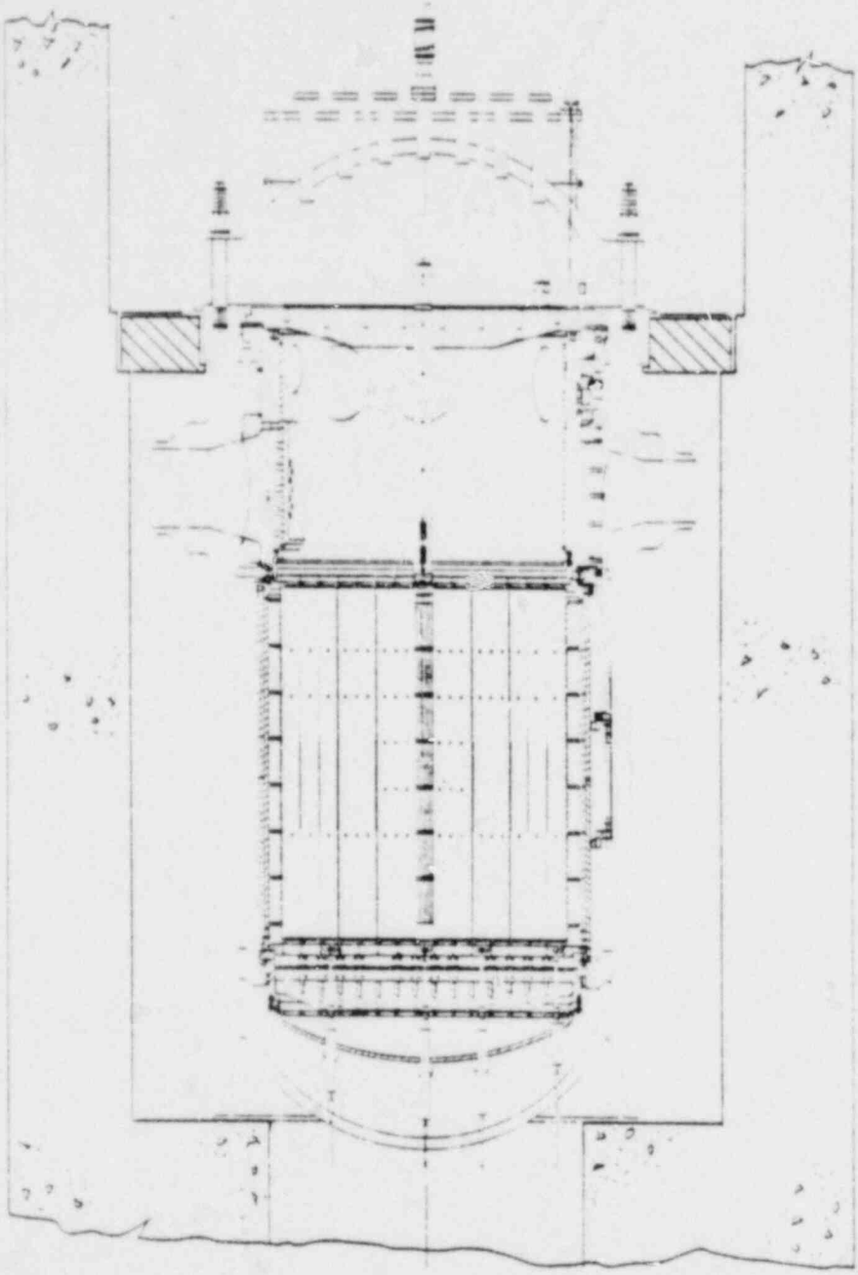

Figure 9-6. Relative Thermal Flux at Source Range Detector Vs Coolant Void Fraction for Constant Source of Fission Neutrons

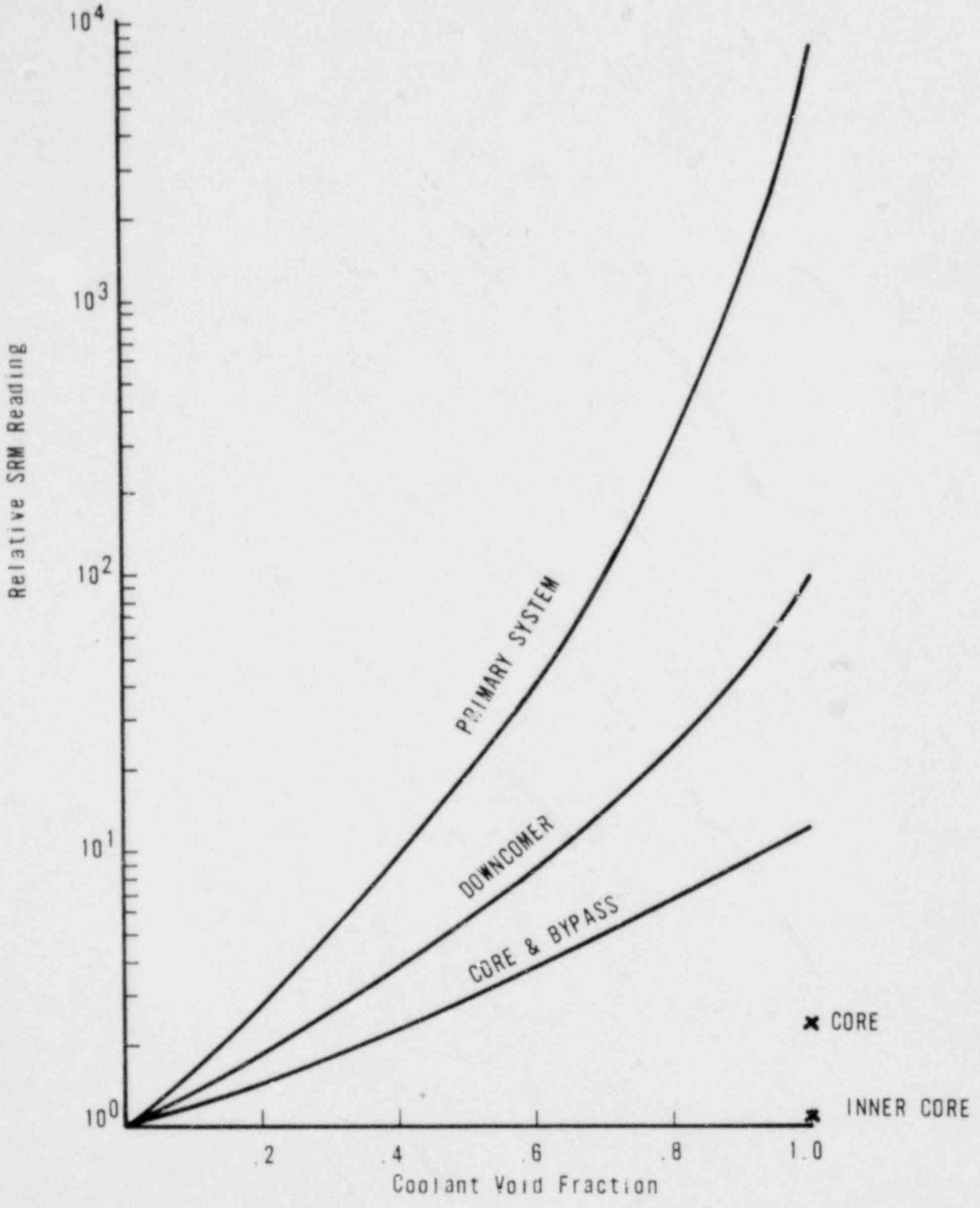

Figure 9-7. Coolant Temperature Effect on Relative SRM Readings

Coolant temp, F	Equivalent % void	Estimated relative SRM reading		
		Primary coolant	Downcomer	Core + bypass
320	-20	0.34	0.53	0.67
375	-16	0.43	0.63	0.71
430	-10	0.63	0.77	0.83
475	-6.2	0.77	0.83	0.91
505	-3.4	0.83	0.91	0.91
530	0	1.0	1.0	1.0
555	3.4	1.2	1.1	1.1
575	6.2	1.3	1.2	1.1
600	10	1.6	1.3	1.4
625	16	2.3	1.6	1.4
640	20	2.9	1.9	1.5

Figure 9-8. Calculated SRM Count Rate Vs Water Level for Photoneutron Source

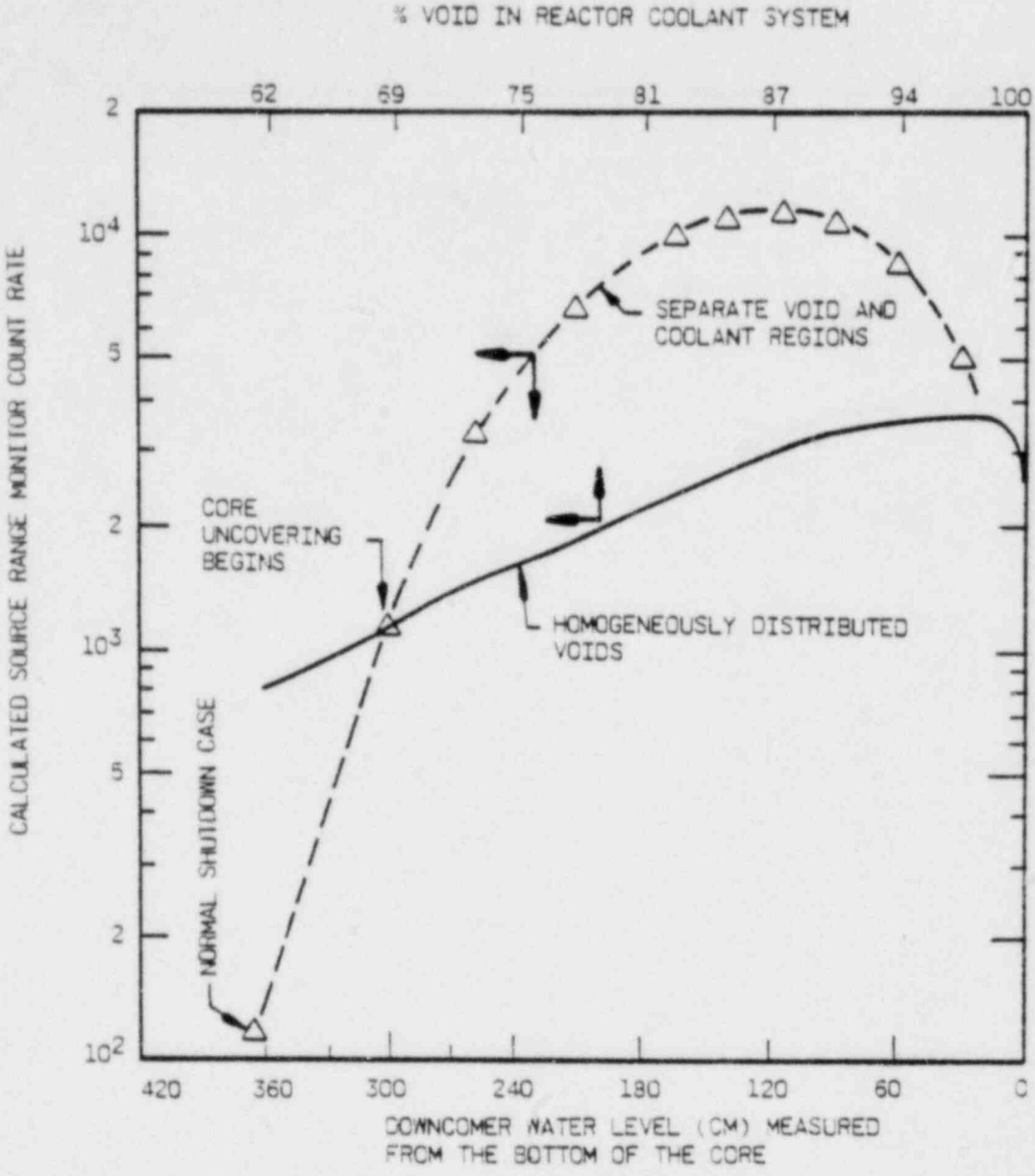

Figure 9-9. Incore Neutron Sources After Shutdown

Source	Time interval of significance	Characteristics	Important parameters
Delayed neutrons	Immediately after trip		
Photoneutrons from D_2O	Dominant source after decay of delayed neutrons	Decays with initial half-life of 1-2 hours, which eventually increases to ∿12 days	Proportional to burnup if < ∿80 days, to power level, and to mass of coolant in core
Startup, primary, and/or regenerative	Dominant source after ∿1 day after shutdown (no fuel damage)	Relatively constant after shutdown with half-life > 60 days	
α,n reactions in actinides and/or oxygen	Relatively small	Essentially constant	
Spontaneous fission	Relatively small	Essentially constant	
Subcritical multiplication in reactor fuel	All times	Major source of neutrons, more than doubles magnitude of all sources	Dependent on factors that affect core multiplication factor: boron, coolant density, fuel integrity, poison integrity, xenon

Figure 9-10. Subcritical Multiplication in a 177-Fuel Assembly Reactor Core

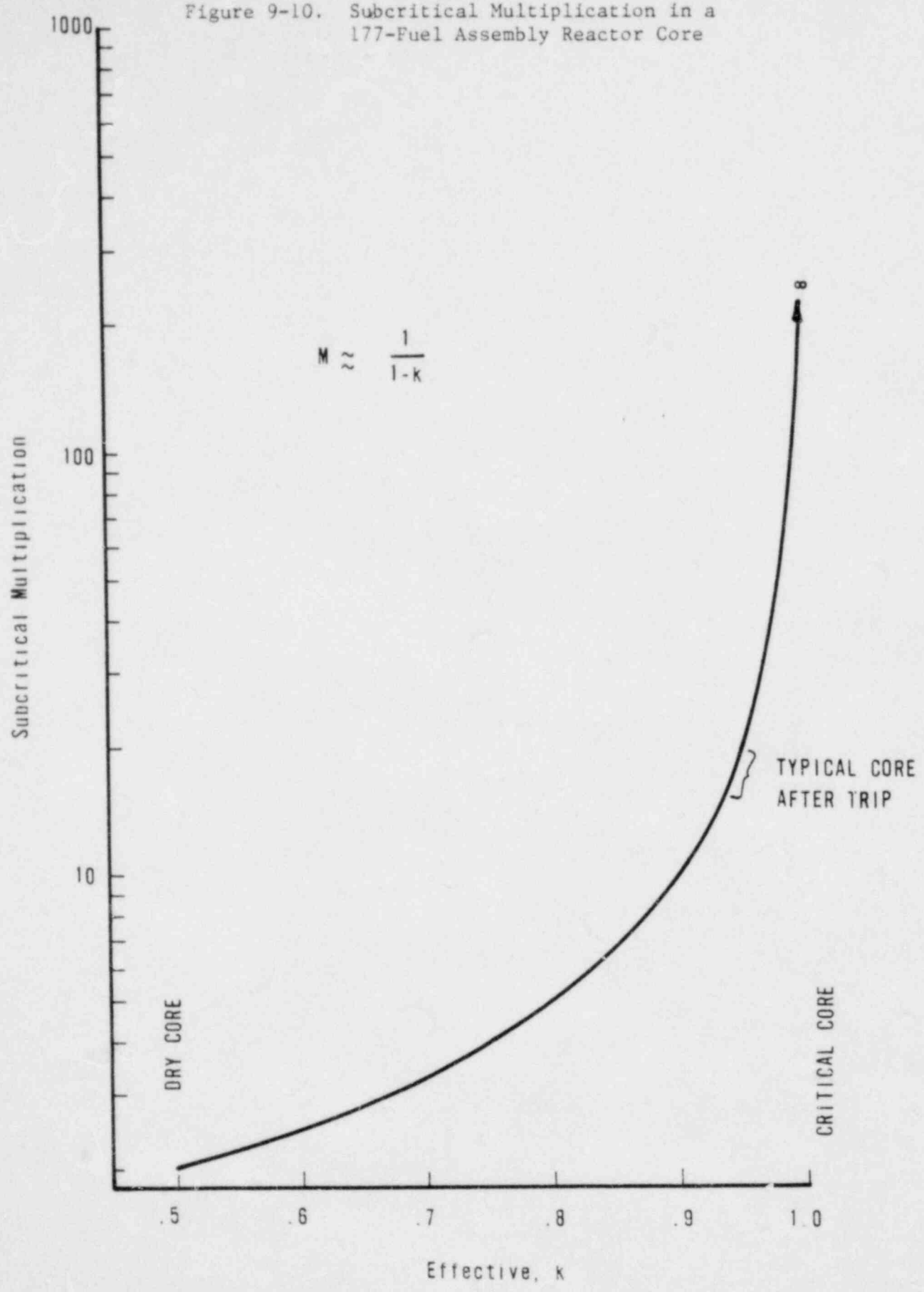

Figure 9-11. Estimation of Total Effect of Loss of Coolant on SRM Response

RELATIVE SRM RESPONSE	=	INCREASE IN NEUTRON FLUX TRANSMISSION DUE TO LOSS OF PRIMARY COOLANT	X	LOSS OF PHOTONEUTRON SOURCE	X	DECREASE IN SUBCRITICAL MULTIPLICATION

CASE 1

$$\text{RELATIVE SRM RESPONSE} = 8300 \times \frac{150-140}{150} \times \frac{2}{20} \quad (t \approx .3n)$$

$$\approx 50$$

$$\text{RELATIVE SRM RESPONSE} = 8300 \times \frac{20-10}{20} \times \frac{2}{20} \quad (t \approx 5n)$$

$$\approx 400$$

Figure 9-12. Relative SRM Response to Loss of Coolant

Approximate time after shutdown, h	Dominant neutron source	Coolant temperature, F	Region voided	Initial k	Relative SRM response
0.3 < t < 5	Photoneutrons	530-550	All	0.95	50-400*
0.3 > t > 10	Delayed neutrons or startup source	530-550	All	0.95	800
0.3 > t > 10	Delayed neutrons or startup source	530-550	All	0.9	2000
0.3 < t < 5	Photoneutrons	~300	All	0.95	50-1200
0.3 < t < 5	Photoneutrons	530-550	Downcomer	0.95	100
0.3 > t > 10	Delayed neutrons or startup source	530-550	Downcomer	0.95	100
0.3 < t < 5	Photoneutrons	530-550	Core + bypass	0.95	1/40-1/2
0.3 > t > 10	Delayed neutrons or startup source	530-550	Core + bypass	0.95	1.2

*Case 1.

Figure 9-13a. Possible Interpretations of SRM Readings

SRM response after reactor trip	Possible cause	Items to check
Gradual increase of factor of <10	Partial voiding of downcomer, downcomer + core, or core	Slow coolant loss via pipe break, open valve, RCS pressure < saturation, coolant temperature (boiling)
	Increasing core reactivity	Deboration, coolant temperature, CR positions, letdown line monitor reading
Rapid increase or decrease of factor of <10	Sudden change in core reactivity	Core temperature, letdown line monitor reading
	Sudden change in coolant inventory	Rapid coolant loss via pipe break, RCS pressure < saturation, HPI and LPI status, RC pump restart, back-drainage from SG loop
	Transition from distributed voids to liquid pool	Loss of RC pump flow
Gradual decrease from normal reading	Photoneutron source in downcomer	Letdown line monitor reading, insensitivity to change in boron concentration and/or coolant temperature
No effect	Boiling in inner core region (full downcomer)	Core outlet temperature, RCS pressure < saturation pressure

Figure 9-13b. Possible Interpretations of SRM Readings

SRM response after reactor trip	Possible cause	Items to check
Gradual increase of factor of >10	Partial to total voiding of downcomer	Slow coolant loss via pipe break or open valve, RCS pressure < saturation
	Partial to total voiding of coolant inventory combined with reduced core source	Core boiling and/or slow coolant loss, RCS pressure < saturation
	Increasing core reactivity	Deboration, coolant temperature, CR positions, letdown line monitor reading
Rapid increase (or spike) of factor of >10	Recriticality	Boron concentration, CR positions, letdown line monitor reading, core temperature
	Rapid drop in coolant level in downcomer	Rapid coolant loss via pipe break or open valve, RCS pressure < saturation
	Transition from distributed voids to liquid pool	Loss of RC pump flow

Lesson 10 — INCORE THERMOCOUPLES AND CORE FLOW BLOCKAGE

Introduction

1. Lecturer —
2. Uniqueness — Incore thermocouples are unique in that they are the only temperature instruments monitoring below a corewide scale.
3. Purpose — To evaluate the capability of incore thermocouple to provide adequate indication for reactor operators to recognize core flow blockage.

Objectives

The following material will be presented during this lesson:

1. Use of incore thermocouples to estimate core flow.
2. Comparing core flow to reactor vessel flow.
3. Estimating core flow blockage.
4. TMI-2 experience.

The key points to be retained are as follows:

1. How to calculate and compare core flow and reactor vessel flow,
2. How to detect and estimate core flow blockage.

Lesson 10 Outline

1. Introduction

2. RC or API Pumps Running

   2.1 Calculation of Effective Core Flow
   2.2. Determination of Reactor Vessel Flow
   2.3. Comparisons and Conclusions

3. Natural Circulation

   3.1. Incore Thermocouple Readings
   3.2. Core Flow Distribution
   3.3. Core Flow Blockage

4. TMI-2 Experience

Lesson 10 — INCORE THERMOCOUPLES
AND CORE FLOW BLOCKAGE

1. Introduction

The use of incore thermocouples to detect core flow blockage is feasible only when the core is covered and the hot legs are full with circulation provided either by reactor coolant (RC) or high-pressure injection (HPI) pumps running or by natural circulation. Under any other conditions, the thermocouples would read near or above saturation temperature and could not easily be related to core flow blockage.

2. RC or HPI Pumps Running

2.1. Calculation of Effective Core Flow

No means exist to measure core flow directly. The flow measuring devices in the reactor coolant system (RCS) hot legs measure RCS flow without distinction as to whether it has passed through or bypassed the core. Similarly, the HPI flow measures flow entering the cold leg, not core flow. Normally there is a well defined proportional relationship between reactor flow and core flow. After a severe accident that has resulted in a core uncovering, however, the core bypass flow might be significantly altered by thermal warpage of the reactor internals opening up the reactor vessel/plenum outlet nozzle seals or open vent valves, providing a direct reactor vessel inlet-to-outlet leakage path. Hence, with the RC or HPI pumps running the hot leg flow or HPI flow indications may not be representative of effective core flow.

The preferred way to calculate core flow is by heat balance. Since $\dot{Q} = \dot{m}\Delta h$, then given the decay heat level ($\dot{Q}$), system pressure, and core ΔT, the core flow rate ($\dot{m}$) can be calculated. The core ΔT should not be calculated as hot leg temperature minus cold leg temperature for the reasons discussed in the preceding paragraph. Instead, the cold leg RTD temperature(s) should be used with the incore thermocouple readings to calculate core flow in the following manner:

$$\dot{m}_i = Q_i/h_i \text{ (for each instrumented assembly)} \quad (1)$$

where

$Q_i = (Q_{core}/177) \times RIA_i$,

Q_{core} = decay heat level, Btu/h,

RIA_i = assembly radial power peak (from the most recent available steady-state core power distribution),

$\Delta h_i = f(P,T_i)$, Btu/lbm,

$\Delta T_i = (T/c)_i - T_{in}$,

T_{in} = cold leg RTD temperature,

$\dot{m}_i$ = assembly flow, lbm/h.

$$\dot{m}_{core} = (177/52) \sum_{i=1}^{52} \dot{m}_i \quad (2)$$

where

$\dot{m}_{core}$ = effective core flow rate, lbm/h,

177/52 = factor assuming proportionality between instrumental assemblies' flow and core flow (simplifying assumption).

The most recent available steady-state core power distribution is appropriate for determining decay heat distribution since the distribution of decay heat is determined by the distribution of fission products that decay with varying half-lives. Hence, the most recent steady-state core power distribution (RIA from the plant computer) will give the best estimate of an assembly's relative power after shutdown.

2.2. Determination of Reactor Vessel Flow

When HPI pumps are running alone, the flow rate should be indicated in the control room. In the absence of an RCS break, the indicated HPI flow can be assumed to be reactor vessel flow.

When RC pumps are running alone, the hot leg flow meters will indicate reactor vessel flow. If one steam generator is idle, then the hot leg flow meter on the active steam generator side will read approximately 20% higher than reactor vessel flow due to idle loop back flow. If the hot leg flow measurements are not available, a reactor vessel heat balance can provide a substitute for the measured flow as follows:

$$\dot{m}_{RV} = Q_{core}/\Delta h_{RV} \qquad (3)$$

where

$\Delta h_{RV} = f(P, \Delta T_{RV})$, Btu/lbm,

$\Delta T_{RV} = T_{hot\ leg} - T_{cold\ leg}$ (RTDs),

Q_{core} = decay heat level, Btu/lbm (including power pump),

$\dot{m}_{RV}$ = reactor vessel flow rate, lbm/h.

It is also possible to calculate the expected reactor vessel flow based on the number of RC pumps running and the design RCS flow split. Table 10-1 summarizes these flows in terms of the measured plant fraction of design flow and the cold leg density (found from $T_{cold\ leg}$ and steam tables).

There are now three flows (one measured and two calculated) with RC pumps operating or two flows (one measured and one calculated) with HPI pumps operating. These flows can be compared in several ways to draw interesting conclusions, as discussed in the next section.

2.3. Comparisons and Conclusions

Figure 10-1 shows block diagrams which provide a means of comparing the flow models from which conclusions can be drawn regarding core blockage. If RC pumps are running, start at point 1 on Figure 10-1. If HPI pumps only are running, start at point 2 on the figure.

The measured-to-expected reactor vessel flow comparison is actually a check of RC system ΔP since RC pump capacity and the RC system idle pump/loop flow split both vary with RC system ΔP. If the reactor vessel flow is as expected, then the RC system is probably unblocked and flowing normally. However, if the measured reactor vessel flow is not as expected, then either the core is being bypassed (low RCS ΔP) or some part of the RC system is blocked (high RCS ΔP). If the core is being bypassed, the incore temperature distribution should be checked for signs of core overheating. To determine which part of the RCS is blocked, a second comparison is made.

The effective core flow should be approximately 95% of the measured reactor vessel flow with 5% normal bypass flow. If this proportion exists, then the core is probably not blocked. Under these circumstances, the incore thermocouples should be used to monitor core cooling. However, if the effective core flow is significantly less than 95% of the measured reactor vessel flow, then the core may be blocked or direct reactor vessel inlet to outlet flow

may exist (or both). Under these circumstances, the incore thermocouples should be used to check for core overheating, which might indicate core flow blockage. If the effective core flow is significantly greater than 95% of the measured reactor vessel flow, then either the measured flow or the incore thermocouple readings are in error. Each should be checked for anomalies and the flow rates recompared.

The distribution of the incore thermocouple readings should be proportional to the assembly flow and heat rate distribution, assuming a flat inlet temperature profile. If it is further assumed that the partial pump flow distribution effects are washed out below the axial location of the incore thermocouples, then the distribution of incore thermocouple readings should be the same as the distribution of the assembly radial power peaks (RIA from the plant computer). Such an equivalence of distributions would imply that the core is free from any large blockage. A thermocouple reading (or preferably readings) would have to be at least 20F higher than normal to be distinguishable as indicating flow blockage rather than just a calibration difference. It would probably be necessary to block more than one fuel assembly to produce such a distribution of thermocouple readings. A non-equivalence of incore thermocouple readings and RIA distributions could mean significant flow blockage or simply that the assumptions of partial pump flow distribution washout and flat inlet temperature profile are invalid. The results of the flow comparisons should guide the interpretation of the incore thermocouple distribution. The amount of core blockage can be very roughly estimated by the number of instrumented assemblies with abnormally high thermocouple readings and their location. This estimate should be consistent with the amount of blockage suggested by the flow rate comparisons. In general, the core would be expected to become blocked near the center first, with subsequent blockage added radially.

3. Natural Circulation

3.1. Incore Thermocouple Readings

In natural circulation, the core average temperature is dependent on the steam generator heat removal which is controlled by the steam generator feedwater temperature and flow rate. Since core average temperature is controlled, the core exit temperature, as reflected in the incore thermocouple readings, can be varied over a wide range without affecting the adequacy of core cooling. The incore thermocouple temperature can, in fact, be saturated or subcooled

depending on the steam generator feedwater conditions. Hence, while the absolute values of the indicated temperatures are important to judge the adequacy of core cooling, it is the distribution of the readings that is useful in determining core flow blockage.

3.2. Core Flow Distribution

The driving force in natural circulation is proportional to the change in density produced by the heat source. Thus, the driving force is proportional to the assembly relative power (RIA).

On the other hand, the hydraulic resistance is proportional to the flow (through an assembly) squared. Since the driving and resistance forces must be equal, the flow through an assembly is proportional to the square root of its relative power. The assembly enthalpy rise and, assuming a flat core inlet temperature distribution, the assembly exit temperature will also be proportional to the square root of the assembly radial peak. Thus, the distribution of the incore thermocouple readings under normal natural circulation conditions should be proportional to the square root of the radial power peak (RIA) distribution.

3.3. Core Flow Blockage

If the incore thermocouple temperature distribution is not the same as the assembly radial peak distribution, then a portion of the core may be blocked. The amount of such core flow blockage can be very roughly estimated by the number and location of instrumented assemblies with abnormally high thermocouple readings. As with RC/HPI pumps running, the thermocouple temperature would have to be at least 20F higher than normal to be distinguishable from calibration differences. Figure 10-2 is a block diagram of the steps to be taken during natural circulation. If a large proportion of the incore thermocouples read saturation temperature, local overheating is possible, particularly if natural circulation is lost. This is undesirable and should be avoided by appropriate control of the steam generator feedwater.

4. TMI-2 Experience

The events at TMI-2 on and after March 28, 1979, added a wealth of knowledge in the area of recognizing degraded core conditions. There was no shortage of data on which to base models after onsite conditions stabilized. Incore thermocouple readings were tracked on a daily basis from March 29 through early May

after natural circulation had been achieved. The thermocouple data were used to monitor the adequacy of core cooling and to estimate the degree of core blockage. The effective core flow rate, calculated as described earlier, was on the order of 1.5×10^6 lbm/h. Under normal conditions the core flow with one RC pump running would be on the order of 30×10^6 lbm/h. With about 95% core bypass flow, it was clear that conditions were not normal.

Both severe core flow blockage and direct reactor vessel inlet-to-outlet leakage were probable. Reinforcing this conclusion were the incore thermocouple temperature distributions. Soon after the accident, a 100F difference in thermocouple readings was observed between the center and the periphery of the core. The high-temperature area bounded approximately 20-25% of the core. Though the temperature difference decreased as decay heat levels dropped, the proportion of the core with high exit temperatures remained essentially constant during the five weeks the incore thermocouples were tracked. Even after natural circulation was achieved, a 30 to 50F temperature difference was still observed between interior and peripheral thermocouples. Figures 10-3 through 10-6 show thermocouple reading distributions from TMI-2 at various times in March and April 1979.

Thus, the TMI-2 data, using the techniques described in this task, strongly implied a severe core flow blockage. This conclusion was entirely consistent with other analytical estimates of core damage.

5. Summary

1. Review the method for estimating core flow based on incore thermocouple readings.

2. Discuss the flow rate and temperature distributions with RC/HPI pumps running and with natural circulation.

3. Review the method for estimating core flow blockage.

Table 10-1. Reactor Vessel Flow

No. of RC pumps running	Expected RV flow, 10^6 lbm/h
4	2.82 MFDF (ρ)[a]
3	2.12 MFDF (ρ)
2	1.41 MFDF (ρ)
1	0.62 MFDF (ρ)

[a]MFDF: Measured fractions of design flow (plant-specific: 1.09 to 1.15), ρ: cold leg coolant density.

Figure 10-1. Flow Model Block Diagram

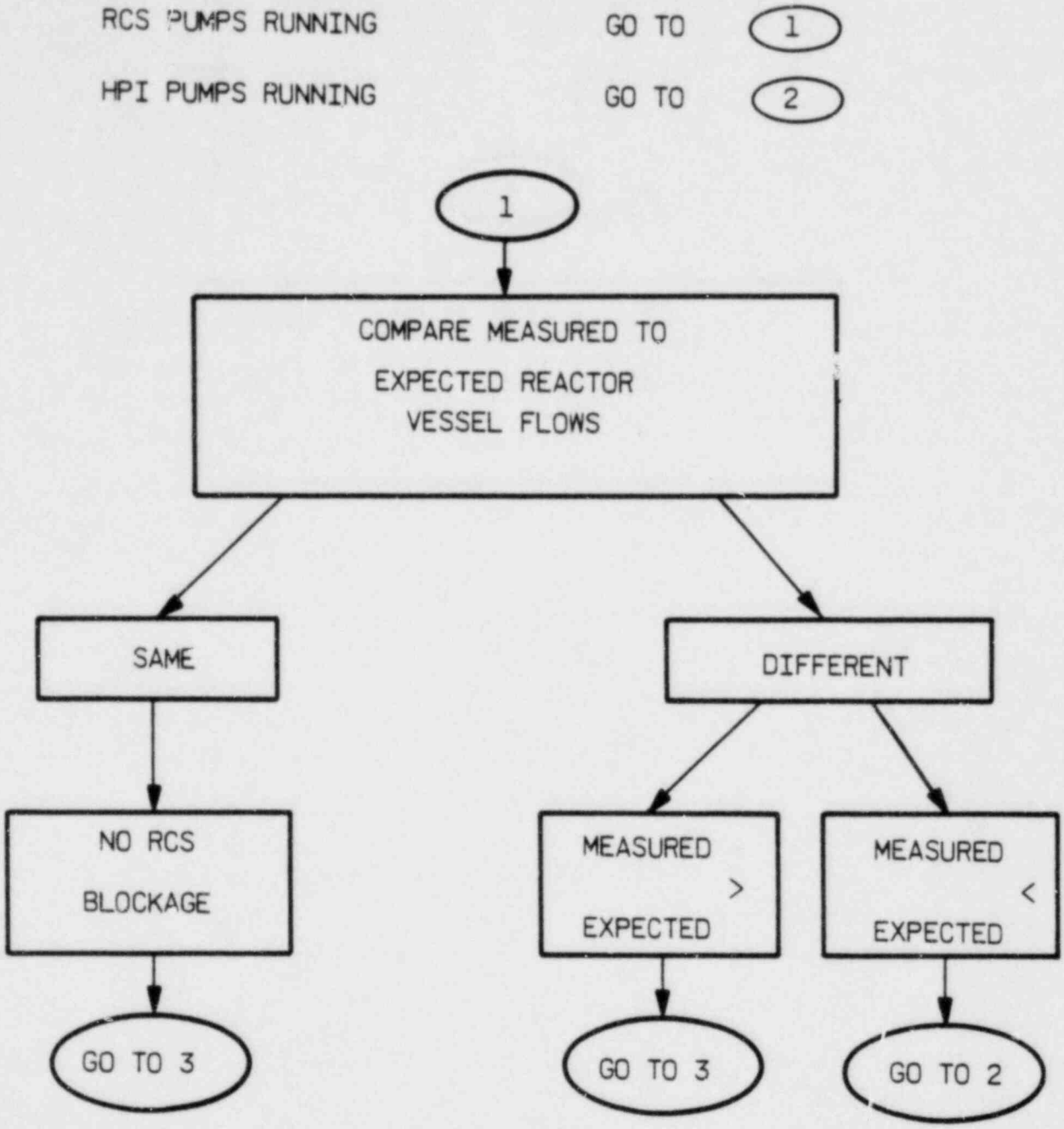

Figure 10-1. (Cont'd)

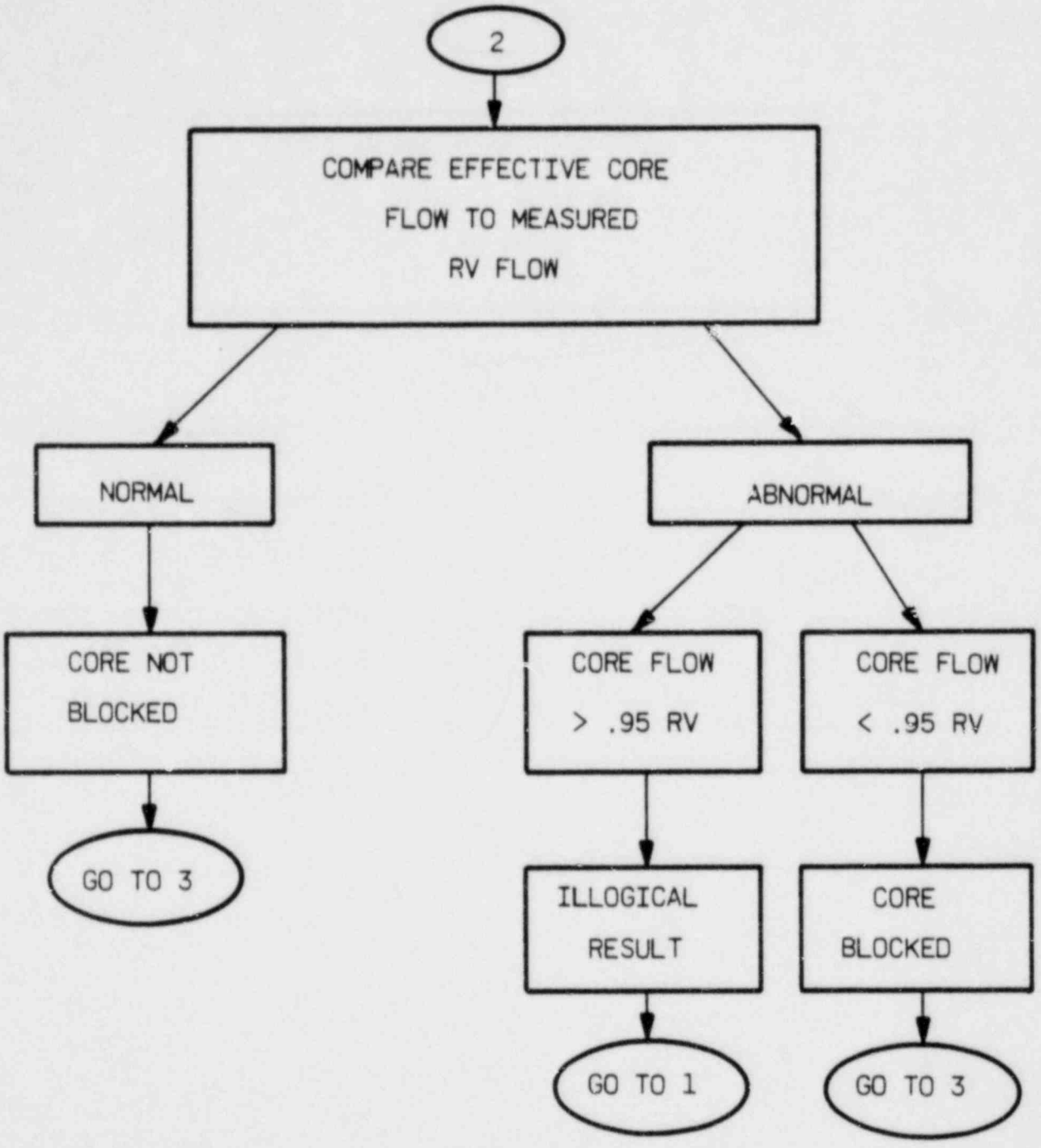

Figure 10-1. (Cont'd)

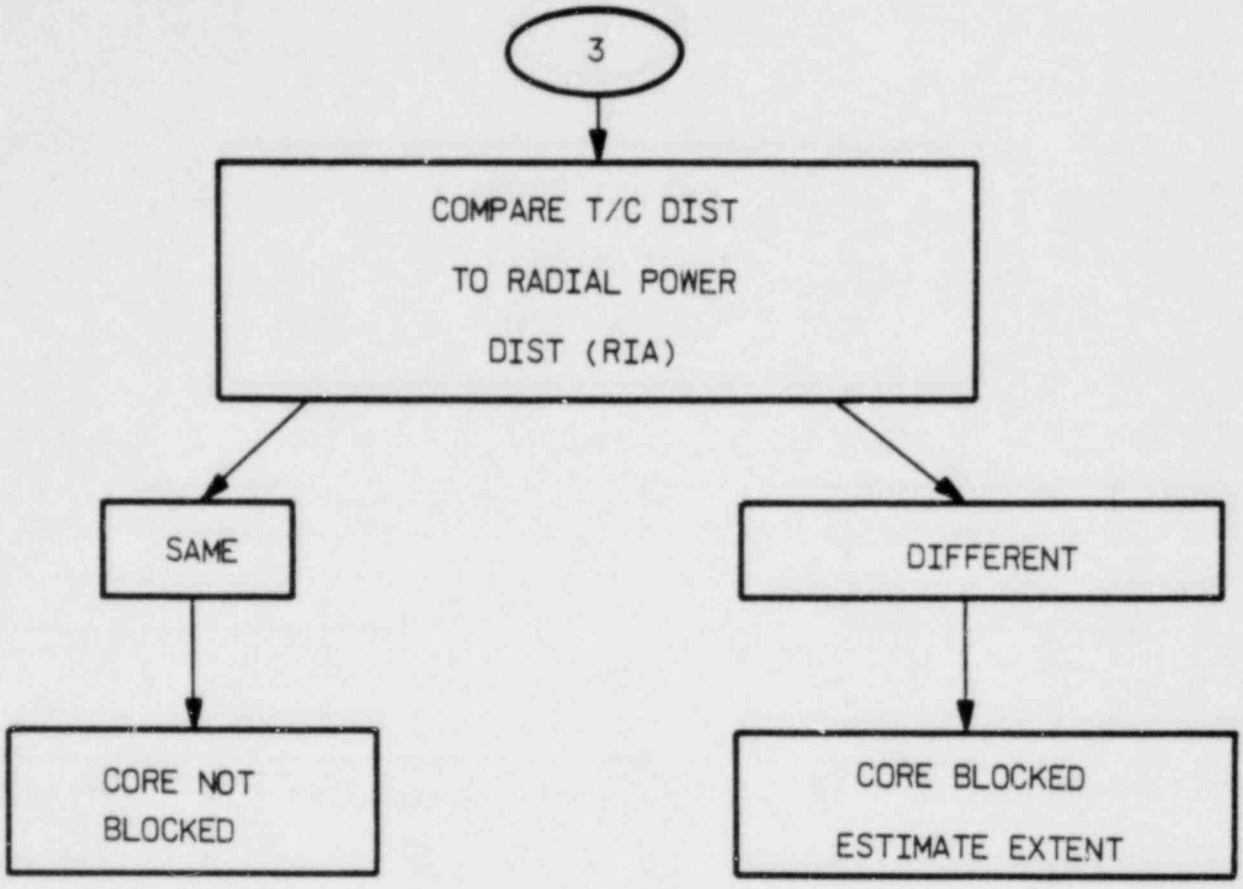

Figure 10-2. Natural Circulation Block Diagram

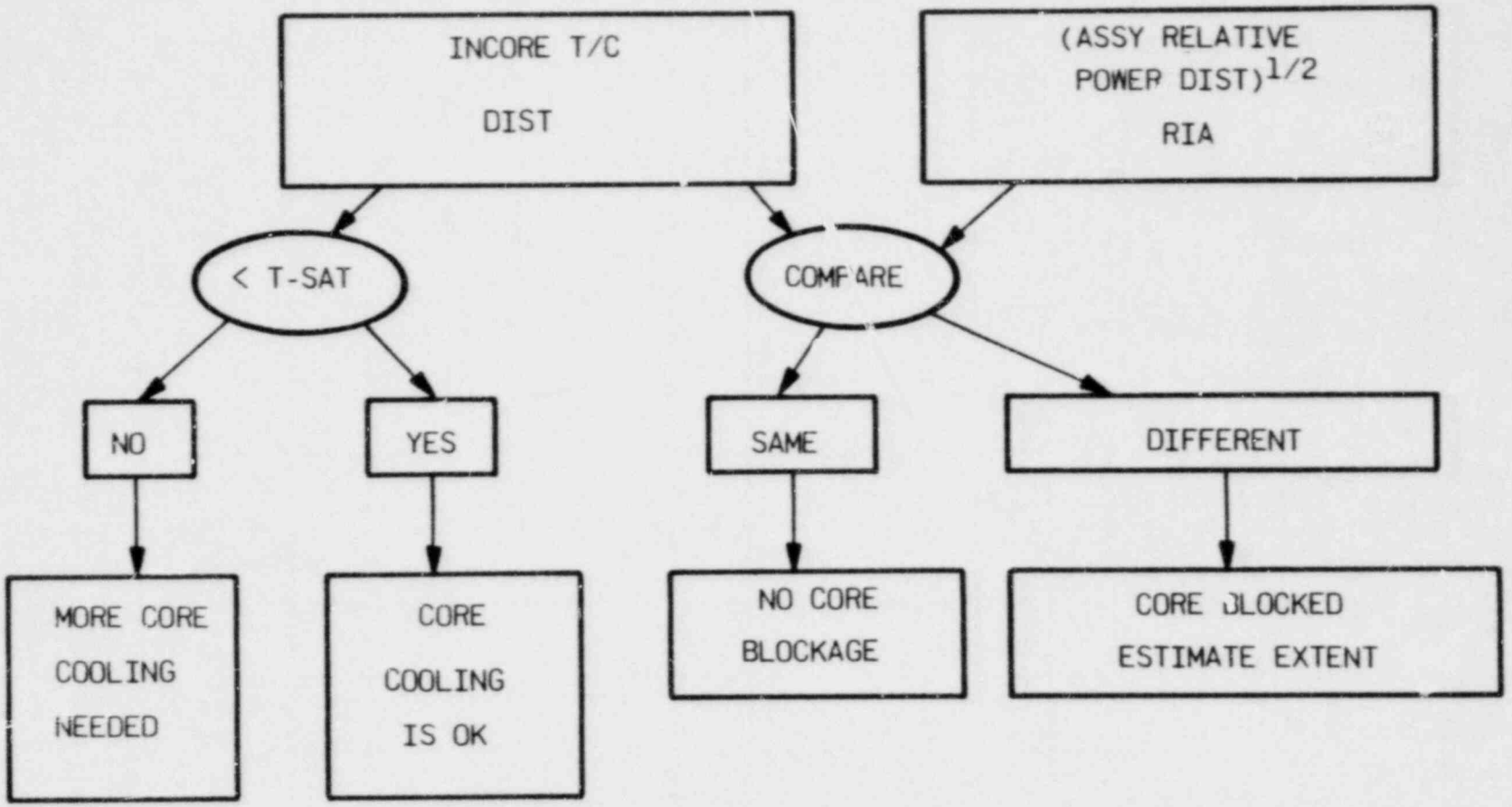

Figure 10-3. TMI-2 SPND String Numbers and Locations, Thermocouple Reading Distributions on March 31, 1979 at 10:45

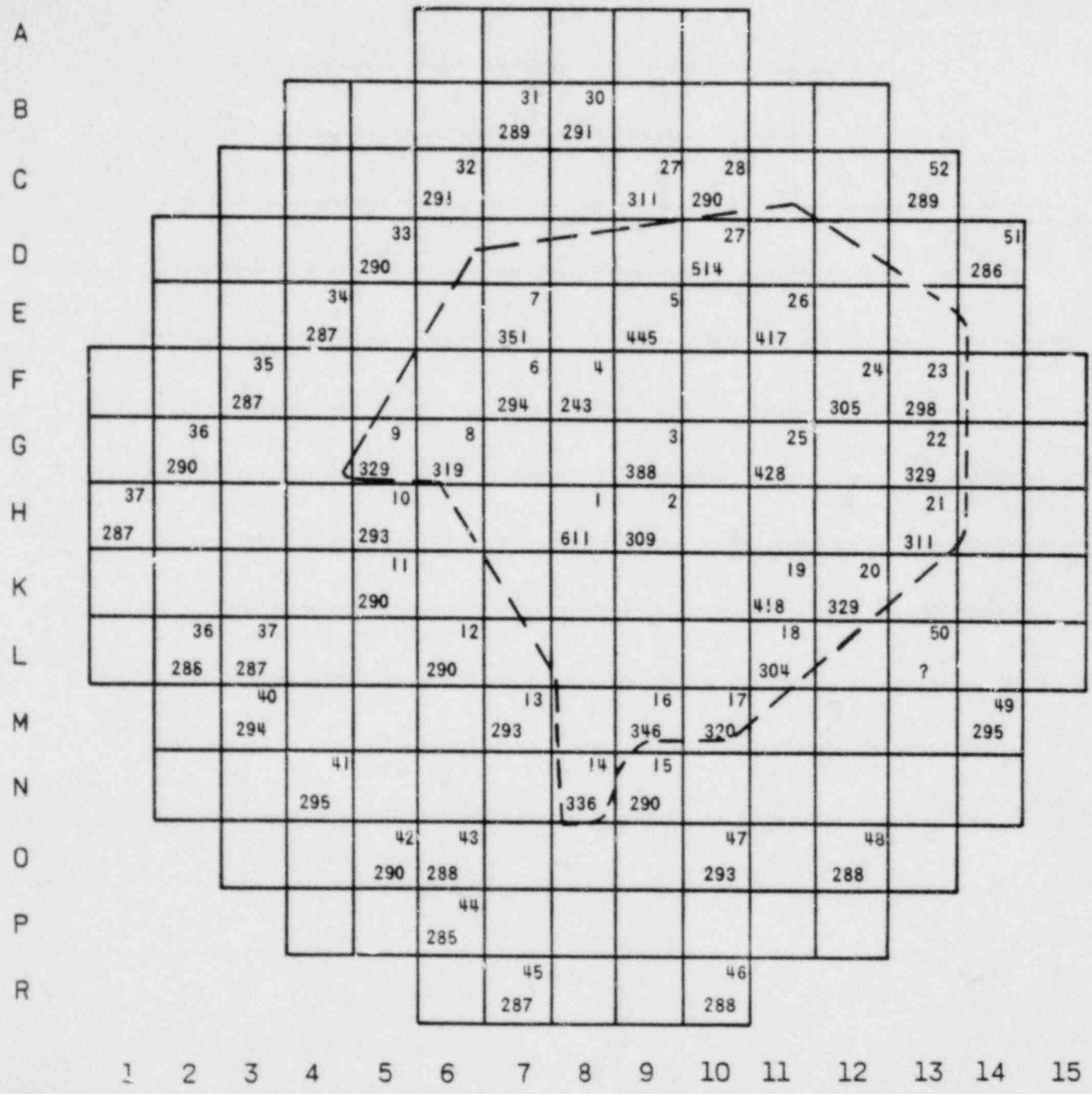

Figure 10-4. TMI-2 SPND String Numbers and Locations, Thermocouple Reading Distributions on April 4, 1979 at 5:32

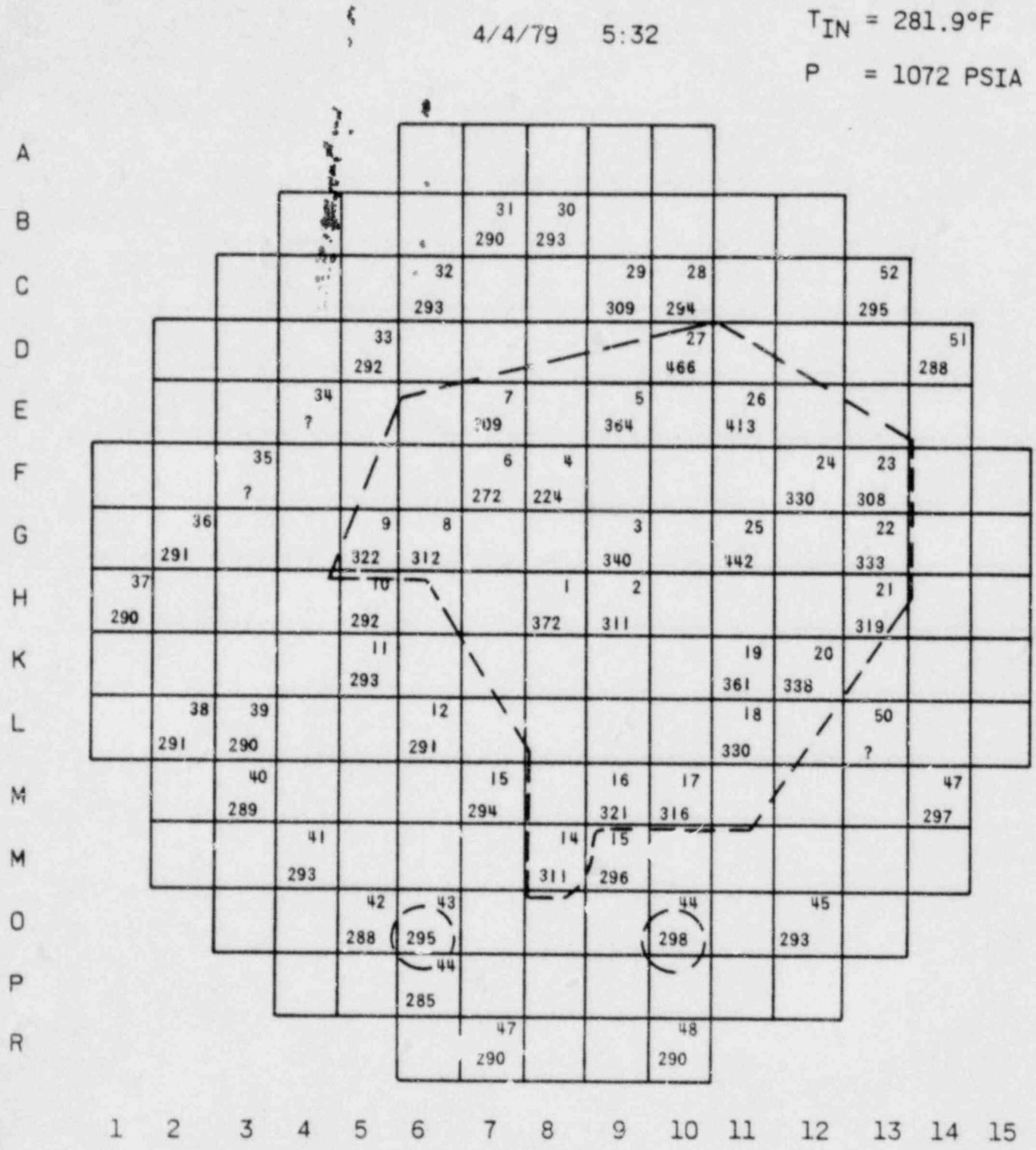

Figure 10-5. TMI-2 SPND String Numbers and Locations, Thermocouple Reading Distributions on April 7, 1979 at 17:00

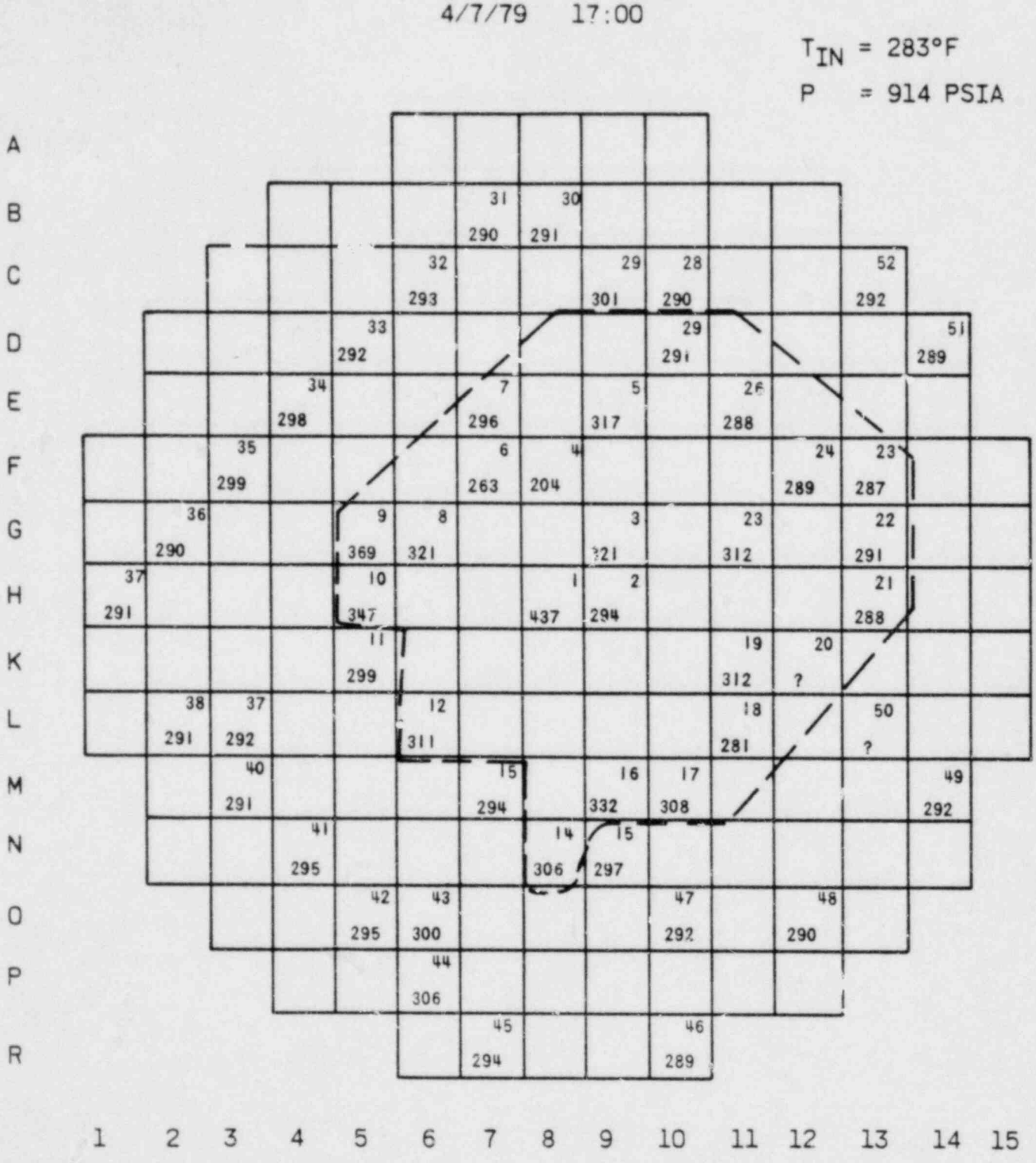

Figure 10-6. TMI-2 SPND String Numbers and Locations, Thermocouple Reading Distributions on April 27, 1979 at 23:45

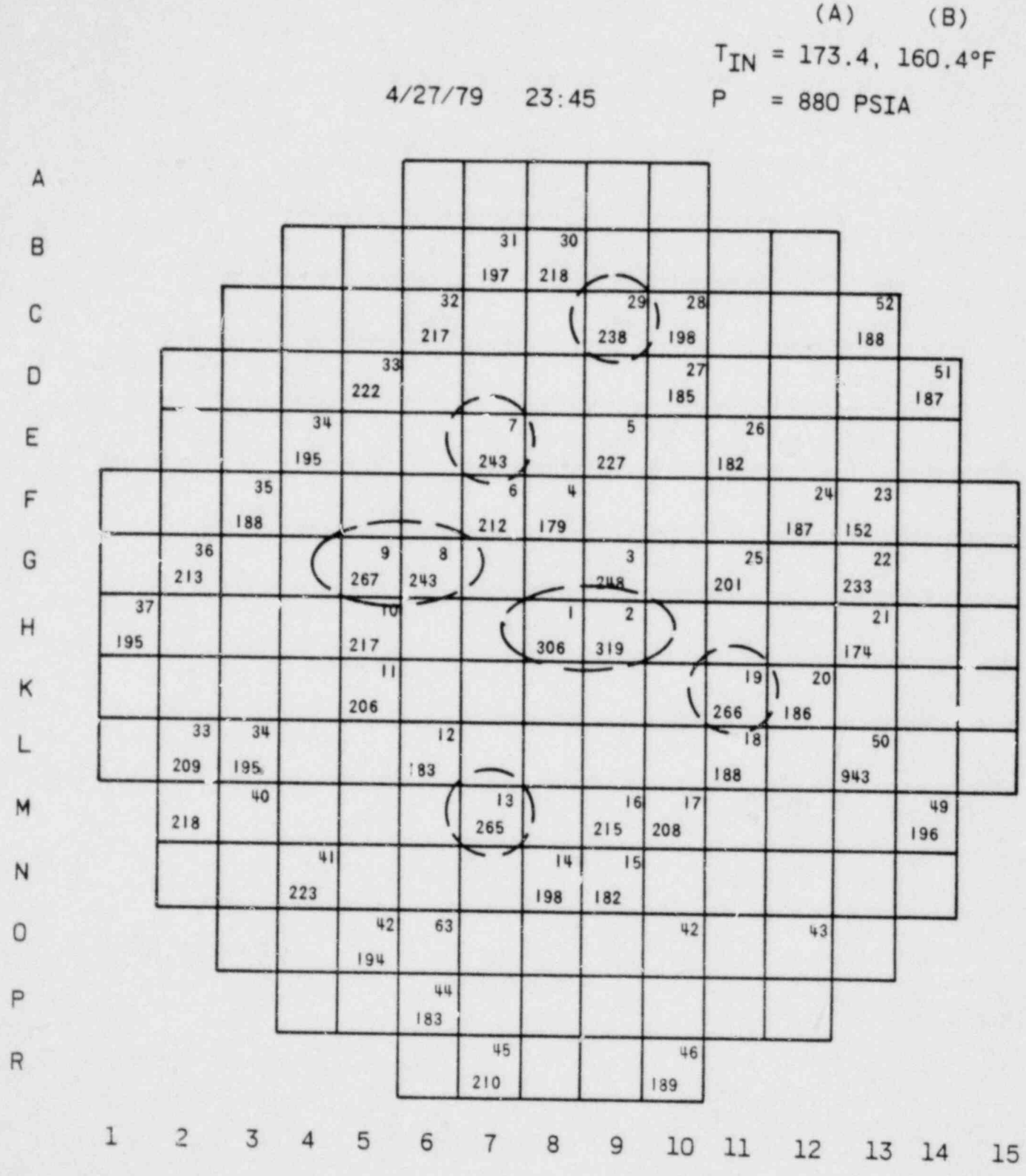

Lesson 11 – RELEASE OF FISSION PRODUCTS FROM DAMAGED FUEL

Introduction

1. Lecturer –

2. Purpose – To describe the buildup and distribution of fission products in the fuel and to quantify the amount of fission product activity expected to be released after various fuel damage scenarios.

Objectives

Lesson 11 covers the following material:

1. The basic characteristics that control the release of key fission products from the fuel (qualitative).

2. The buildup of key fission products as a function of irradiation time and the distribution of fission product activity (quantitative) between the fuel pellets, the fuel rod gaps, and the reactor coolant.

3. The progressive increase in fission product release associated with the various stages of core damage.

4. Rapid assessment of fuel damage based on the amount of key nuclides in the reactor coolant and the ratio of long- to short-half-life nuclides.

LESSON OUTLINE

1. Behavior of Fission Products
2. Fission Product Buildup and Distribution
3. Assessing Degree of Core Damage
4. Summary

Lesson 11 -- RELEASE OF FISSION PRODUCTS FROM DAMAGED FUEL

1. Behavior of Fission Products

The release of 40 fission product elements from the fuel is a very complex process that is affected by many parameters. Appendix 11-A contains excerpts from WASH-1400 and NUREG 0772 that provide a more comprehensive review of the subject of fission product release. However, it is not essential to know why certain fission products are released in greater amounts than others, nor precisely how much will be released in order to take the appropriate actions following a reactor accident. This lesson concentrates only on the behavior of the four fission product elements that are important to the reactor operator during the first hours of the accident because they will dominate the offsite dose consequences. These same four elements will aid him in assessing the extent of damage to the core. The elements are krypton (Kr), xenon (Xe), iodine (I_2) and Cesium (Cs).

The noble gases, Kr and Xe, are shown on the "Periodic Chart of the Elements" (Figure 11-1) in the inert gases column along with He, Ne, Ar, and Rn. This means that all these elements are gaseous (at all temperatures above -92F), that they will behave similarly under given conditions (except for physical differences caused by their different atomic weights), and that they are all chemically unreactive (inert) and thus have no tendency to form chemical compounds with other elements. Thus, Kr and Xe, although slightly soluble in water at high pressures, will usually be found in the gaseous state; therefore, a reactor operator is likely to find any Kr or Xe released as the result of an accident in the steam volume of the pressurizer, the makeup tank, or the reactor building (Figure 11-2).

Iodine is a halogen and will behave in much the same way as fluorine (Fl), chlorine (Cl), and bromine (Br). All halogens are chemically very reactive and thus will form chemical compounds with many chemical elements and other compounds. When in the dry state, all the halogens are quite volatile at and

above room temperature. The halogens are also very soluble in water when in the pure elemental form and even when in most chemical compounds. Thus, in the post-accident environment, the iodine is most likely to be in the liquid phase, i.e., in the reactor coolant or in the containment sump, but a small fraction (less than 0.0001) of the iodine is likely to be airborne in the containment atmosphere. Even though it is small, this airbore fraction may have a significant offsite dose impact, and thus the containment sprays should be used to rapidly remove the airborne fraction. In the event that the iodine activity is released into the containment via a dry pathway [i.e., no water in the reactor coolant system (RCS) at the time of the iodine release], a large fraction of the iodine will become airborne – perhaps 40 to 60% of the release. Thus, in a dry release event, it is absolutely essential that the reactor building sprays be used to remove the airborne iodine and to mitigate the potential offsite dose consequences.

Cesium (Cs) is an alkali metal like sodium. Both are very reactive when in the elemental metallic state, but both are easily oxidized or form other compounds (e.g., NaCl, CsI, Cs_2O). Following a reactor accident, we can normally expect to find Cs in the liquid phase, i.e., in the reactor coolant, or in the containment sump. However, if the accident is such that the Cs release occurs via a dry pathway, a significant portion of the cesium activity may be airborne in the containment in the form of minute aerosol particles. Cesium is volatile at temperatures above 1000F, so if the core is dry and at a temperature above 1000F, most of the Cs will vaporize and subsequently condense as minute particles of metallic Cs, Cs oxide, or Cs iodide as soon as the temperature falls below 1000F. These particles are rapidly absorbed into water, so the pathway must be dry for them to reach the containment atmosphere; once airborne in the containment atmosphere, they could remain airborne for many days. Therefore, it is essential to use the reactor building sprays to remove these Cs particles rapidly.

2. Fission Product Buildup and Distribution

The major offsite dose consequences resulting from reactor accidents that cause severe core damage are due to short-half-life, gaseous nuclides released into the atmosphere. Normally, the liquid pathway is of little concern unless the accident damages the basemat of the containment and causes significant amounts of radioactive liquid to leak from the containment.

All nuclides that have a significant impact on the offsite doses resulting from gaseous pathways saturate (i.e., their production rate equals their removal rate; thus the concentration remains constant) within the fuel after 30 to 60 days of power operation (Table 11-1). Krypton-85 appears to be an exception to this because it does not saturate due to its long half-life (10.72 years), but because of its low gamma yield and low abundance, it has a negligible dose consequence compared to the other gaseous nuclides.

In the event of a liquid pathway release, the offsite dose consequences would be dominated by the Cs activity release, primarily Cs-137 (because of its 30.17-year half-life). Cesium-137 would also have an important offsite dose consequence if the containment were to suffer a gross failure during an accident sequence that produced large quantities of Cs aerosols.

The core inventories shown in Table 11-1 are based on a power level of 2552 MWt; however, they are directly proportional to power and thus can be scaled to any power level. Since all operating B&W plants are within ±10% of this power level, no adjustment is necessary because a 10% error is negligible when compared to the many other uncertainties associated with any accident scenario.

Figure 11-3 shows the diffusion of fission product nuclides from the fuel pellet to the gas plenum in the fuel rod (commonly referred to as the "gap"). The importance of this slow diffusion process is that it provides time for short-half-life nuclides to decay. Since the long-half-life nuclides do not decay to any significant degree during the diffusion period, the radioactive nuclide mixture found in the fuel rod gap appears to be enriched in long-half-life nuclides when compared to the mixture of nuclides in the fuel. This difference in the mixture of nuclides is very helpful in determining the type of fuel damage that might have occurred.

Table 11-2 shows the gap inventory during an equilibrium cycle at 2552 MWt. Note that due to the diffusion time, most short-half-life nuclides take a little longer to saturate (in comparison to Table 11-1), but all saturate within about 120 to 150 days. The important facts to be noted about the gap activity inventory are as follows:

1. The total amount of short-half-life activity in the gap is only a small fraction of the total activity in the core.

2. The total amount of long-half-life activity in the gap is a significant fraction of the total activity in the core.

These points are clearly illustrated in Table 11-3. The gap contains only 4.3% of the Xe-133 and 1.3% of the I-131 (both of which are relatively short-half-life nuclides), whereas it contains 74% of the Kr-85 and 30% of the Cs-137 (both of which are long-half-life nuclides).

Since the extent of fuel damage is initially diagnosed on the basis of radiochemical analysis of reactor coolant samples, it is important to understand how the mixture of fission product nuclides is distributed within the reactor coolant. Figure 11-4 shows schematically that activity leaking from the fuel into the coolant is removed from the coolant by both decay and purification (in either the purification demineralizers or the bleed processing system). The important point of this figure is that the equilibrium activity of a nuclide in the reactor coolant (C_{eq}) is equal to the release rate of that nuclide from the fuel(s) divided by the sum of the decay constant (λ_D) and the purification rate constant (λ_P).

$$\frac{dC}{dt} = S - (\lambda_D + \lambda_P)C ,$$

$$C_{eq} = \frac{S}{\lambda_D + \lambda_P} .$$

This means that for long-half-life nuclides λ_D is very small and usually negligible compared to λ_P; therefore, since S is usually relatively constant, the concentration of long-half-life nuclides (Kr-85 and Cs-137) is inversely proportional to the purification rate. For short-half-life nuclides, λ_P is usually very small compared to λ_D, so the equilibrium concentration is essentially independent of the purification rate and is directly proportional to the release rate from the fuel. Table 11-4 illustrates these points by showing typical values for the activity of key nuclides in the reactor coolant of a

2552-MWt reactor during an equilibrium fuel cycle. It should be noted that, all other factors being equal, these coolant activities are proportional to power level and percent leaking fuel. The important points to be noted with respect to fission product behavior in the reactor coolant are as follows:

1. The relative concentration of long-half-life nuclides is reduced significantly, e.g., the Kr-85 to Kr-88 ratio is approximately 2, whereas in the gap region it was about 5. The reduction is due to the effects of λ_p on the Kr-85 activity.

2. Kr-88, with its 2.84-hour half-life, decays fast enough not to be affected by the value of λ_p, so Kr-88 remains saturated throughout the cycle. The concentration of noble gases with longer half-lives tends to build up during the first part of the cycle, then decrease, and the finally increase to a maximum value at the end of the cycle. This is because the value of λ_p for noble gases is determined by the bleed processing flow because there is (usually) no degassing of the letdown flow. Since bleed flow increases during the cycle, most of the noble gas nuclides first build to saturation and then begin to decrease as the bleed flow increases; however, at about 280 days into the cycle, the bleed flow is diverted to the deborating demineralizers, which offer no opportunity for degassing ($\lambda_p = 0$); thus, the noble gas activity increases between 280 days and the end of the cycle.

3. The iodine nuclides are removed effectively as the letdown passes through the purification demineralizers. This results in a large λ_p for iodine and causes all the iodine nuclides to saturate very quickly.

4. The cesium nuclides are also removed by the purification of the letdown flow, but much less effectively than iodine, so they do not quite saturate during the cycle.

Another important effect that must be considered when examining the radionuclide activity in reactor coolant samples is the phenomenon called "iodine spiking." Figure 11-5 shows the I-131 activity associated with a typical iodine spike. The peak of the illustrated spike is approximately a factor of 5 times the pre-trip concentration. Iodine spikes vary in size depending on operating history and conditions. The spikes could range in size from a factor of 2 to a factor os 1000, but more typically the spiking factor ranges between 5 and 20.

Iodine spikes do not occur when there is no leaking fuel. The spikes are believed to be caused by the belching of activity accumulated in the gap region. The belching occurs during pressure and power transients that create pressure differences between and inside and outside of the cladding.

These transients either cause the steam in the gap region of leaking fuel rods to expand and expel activity into the coolant or cause the steam to contract or condense, thus drawing coolant into the gap. This liquid coolant then drains to hotter portions of the fuel rod where it flashes into steam and expels activity into the circulating reactor coolant.

3. Assessing Degree of Core Damage

Many different sequences of events lead to core damage, each having its own unique probability of occurrence. But if one ignores the details of sequence and probability, all major fuel damage accidents fall into two general categories:

1. Power Burst Events — For example, the ejection of several control rods from the core, which results in immediate fuel damage, regardless of operator actions.

2. Loss of Core Cooling — The loss of core cooling could be due to a loss-of-coolant accident combined with failure of the emergency core cooling system or to a complete loss of all a-c power sources, which results in the loss of all cooling systems and all heat sinks. Fuel failure during loss-of-core-cooling events usually occurs slowly enough for the operator to recognize the situation and to take various actions to mitigate the consequences.

Loss-of-core-cooling events will all go through the following progression of stages, each of which results in the release of increasing amounts of fission product activity:

1. Rupture of the cladding on some of the hottest fuel rods releases the complete gap inventory of these rods.

2. Rupture of the cladding on the remaining fuel rods in the core releases all the gap activity in the core.

3. Release of fission products from the fuel pellets in several of the hottest fuel assemblies.

4. Release of fission products from a major fraction of the fuel pellets in the core.

Figure 11-6 illustrates the status of the water inventory in the RCS during the last stage of this progression. Assuming that the operator is able to restore core cooling, refill the reactor cooling system, and re-establish circulation within the reactor coolant loops, he will then be ready to begin to assess the core damage based on the radiochemical analysis of reactor coolant samples. Table 11-5 shows typical values for the reactor coolant activities to be expected for various degrees of core damage. The coolant activities corresponding to the release of the total inventory from 10 fuel assemblies seems astronomically high but represents less than 10% of the TMI-2 release, as shown in Table 11-6. For some accidents it will be difficult to judge, based on the values in Table 11-5, whether the activity in the coolant came from gross damage to one or two

fuel assemblies, or from gross damage to the cladding of many fuel assemblies. In these cases, a comparison of the nuclide ratios, as shown in Table 11-7, will enable the operator to distinguish between releases from the fuel rod gaps and releases directly from fuel pellets. Note that the ratios are expressed in terms of the long-half-life nuclide divided by the short-half-life nuclide, so high values indicate gap releases, and low values indicate releases from the fuel pellets.

4. Summary

In dealing with degraded core conditions, the operators should:

1. Minimize the fission product release from the core by
   a. Keeping the core covered with water.
2. Minimize the fission product release to the environment by
   a. Utilizing the reactor building sprays.
   b. Minimizing letdown flow.
   c. Cooling with the steam generators and auxiliary feedwater
3. Assess the amount of core damage after refilling the reactor coolant system and re-establishing reactor coolant circulation by taking a reactor coolant sample and performing radiochemical analysis:
   a. The concentrations of individual nuclides will indicate the magnitude of core damage.
   b. The ratio of long- to short-half-life nuclides will distinguish between cladding failures and releases from the fuel pellets.

Table 11-1. Fission Product Inventory in an Equilibrium Cycle Core

Nuclide	Half-life	Curie inventory 30 EFPD	120 EFPD	280 EFPD	310 EFPD
Kr-85	10.72 y	3.1 E5	3.8 E5	5.1 E5	5.3 E5
Kr-88	2.84 h	5.6 E7	5.6 E7	5.6 E7	5.6 E7
Xe-131m	11.92 d	3.3 E5	4.4 E5	4.4 E5	4.4 E5
Xe-133m	2.19 d	3.1 E6	3.1 E6	3.1 E6	3.1 E6
Xe-133	5.25 d	1.3 E8	1.3 E8	1.3 E8	1.3 E8
I-131	8.04 d	6.9 E7	7.4 E7	7.4 E7	7.4 E7
I-132	2.29 h	8.6 E7	8.6 E7	8.6 E7	8.6 E7
I-133	20.8 h	1.3 E8	1.3 E8	1.3 E8	1.3 E8
Cs-136	13.1 d	6.8 E5	8.0 E5	8.0 E5	8.0 E5
Cs-137	30.17 y	2.7 E6	3.5 E6	4.8 E6	5.0 E6

Reference: Midland FSAR (2552 MWt).

Table 11-2. Fission Product Inventory in Gap Region of an Equilibrium Cycle Core

Nuclide	Half-life	Curie inventory 30 EFPD	120 EFPD	280 EFPD	310 EFPD
Kr-85	10.72 y	2.0 E5	2.6 E5	3.7 E5	3.9 E5
Kr-88	2.84 h	5.3 E4	5.3 E4	5.3 E4	5.3 E4
Xe-131m	11.92 d	2.5 E4	4.3 E4	4.4 E4	4.4 E4
Xe-133m	2.19 d	5.9 E4	5.9 E4	5.9 E4	5.9 E4
Xe-133	5.25 d	5.0 E6	5.4 E6	5.4 E6	5.4 E6
I-131	8.04 d	7.4 E5	9.5 E5	9.5 E5	9.5 E5
I-132	2.29 h	4.7 E4	4.8 E4	4.8 E4	4.8 E4
I-133	10.8 h	1.8 E5	1.8 E5	1.8 E5	1.8 E5
Cs-136	13.1 d	1.0 E4	1.6 E4	1.7 E4	1.7 E4
Cs-137	30.17 y	6.4 E5	8.7 E5	1.4 E6	1.5 E6

Table 11-3. Percentage of Fission Product Inventory in Gap Region at end of Equilibrium Core Cycle

Nuclide	Half-life	Percent of core activity in gap[a]
Kr-85	10.72 y	74.0
Kr-88	2.84 h	0.09
Xe-131m	11.92 d	10.0
Xe-133m	2.19 d	2.0
Xe-133	5.25 d	4.3
I-131	8.04 d	1.3
I-132	2.29 h	0.06
I-133	20.8 h	0.14
Cs-136	13.1 d	2.0
Cs-137	30.1 y	30.0

[a]Percentage will change as a function of irradiation time and decay time.

Table 11-4. Fission Product Activity in Reactor Coolant With 0.1% Leaking Fuel in an Equilibrium Cycle Core

		Coolant activity, μCi/g			
Nuclide	Half-life	30 EFPD	120 EFPD	280 EFPD	310 EFPD
Kr-85	10.72 y	0.31	0.45	0.41	0.52
Kr-88	2.84 h	0.24	0.24	0.24	0.24
Xe-131m	11.92 d	0.95 E-1	0.16	0.15	0.17
Xe-133m	2.19 d	0.26	0.26	0.25	0.26
Xe-133	5.25 d	22	24	23	25
I-131	8.04 d	0.36	0.38	0.38	0.38
I-132	2.29 h	0.82 E-1	0.82 E-1	0.82 E-1	0.82 E-1
I-133	20.8 h	0.39	0.39	0.39	0.39
Cs-136	13.1 d	0.62 E-2	0.73 E-2	0.73 E-2	0.74 E-2
Cs-137	30.17 y	0.22 E-1	0.27 E-1	0.34 E-1	0.36 E-1

Table 11-5. Coolant Concentrations Providing Preliminary Indication of Core Damage

Nuclide	Typical coolant activity, Ci/g	1% failed fuel, μCi/g	10% gap inventory, μCi/g	100% gap inventory, μCi/g	Total release from 10 FAs, μCi/g
I-131	0.05	3.8	400	4,000	15,000
I-133	0.15	3.9	80	800	26,000
I-135	0.30	1.9	25	250	26,000
Cs-136	0.001	0.07	7	72	150
Cs-137	0.01	0.36	650	6,500	1,000
Xe-133	12	250	2300	23,000	26,000
Kr-88	0.3	2.5	25	250	11,000

Table 11-6. Fission Product Release From Fuel Following TMI-2 Accident on March 28, 1979

Nuclide	Percent of core inventory	Equivalent No. of fuel assemblies
Xe-133	68	120
Xe-131m	70	124
Kr-85	71	126
Cs-134	63	112
Cs-137	60	106
H-3	73	129

Table 11-7. Key Nuclide Ratios in Reactor Coolant as an Indication of Fuel Damage

Key ratios	Normal coolant	Transient spiking	Gap release	Fuel matrix release
I-131:I-133	1	∿2	5	0.6
I-131:I-135	2	∿4	16	0.6
Cs-137:Cs-136	5	∿10	90	6
Cs-137:Cs-138	0.6	∿4	110	0.04

Figure 11-1. Periodic Chart of the Elements

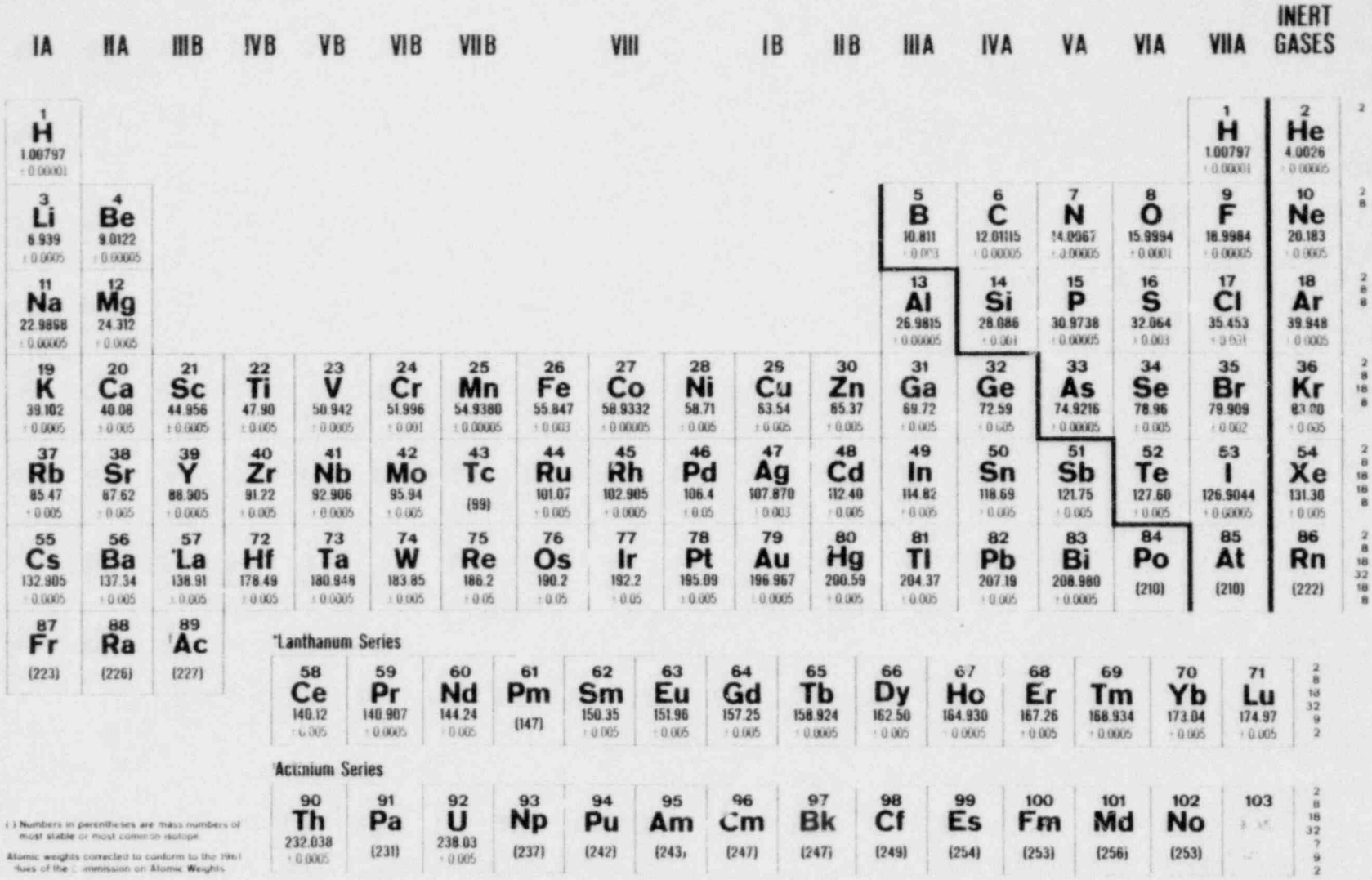

Figure 11-2. Chemical Characteristics of Key Fission Product Elements

1. KRYPTON & XENON

- GASEOUS (UNDER ALL CONDITIONS)
- NOBLE GASES - INERT (NOT CHEMICALLY REACTIVE)
- TRACE SOLUBILITY IN WATER

2. IODINE

- CHEMICALLY REACTIVE (CsI, ZrI_2)
- HIGH SOLUBILITY IN WATER (HIGH AFFINITY FOR WATER)
- HIGHLY VOLATILE UNDER DRY CONDITIONS
- SMALL BUT SIGNIFICANT VOLATILITY IN WATER

3. CESIUM

- VERY VOLATILE AT HIGH TEMPERATURES (> 1000°F)
- VAPOR WILL CONDENSE TO AEROSOL PARTICLES UNDER DRY CONDITIONS
- HIGHLY SOLUBLE IN WATER (VERY HIGH AFFINITY FOR WATER)

Figure 11-3. Diffusion of Fission Products From Fuel Matrix Into Fuel Rod Gap

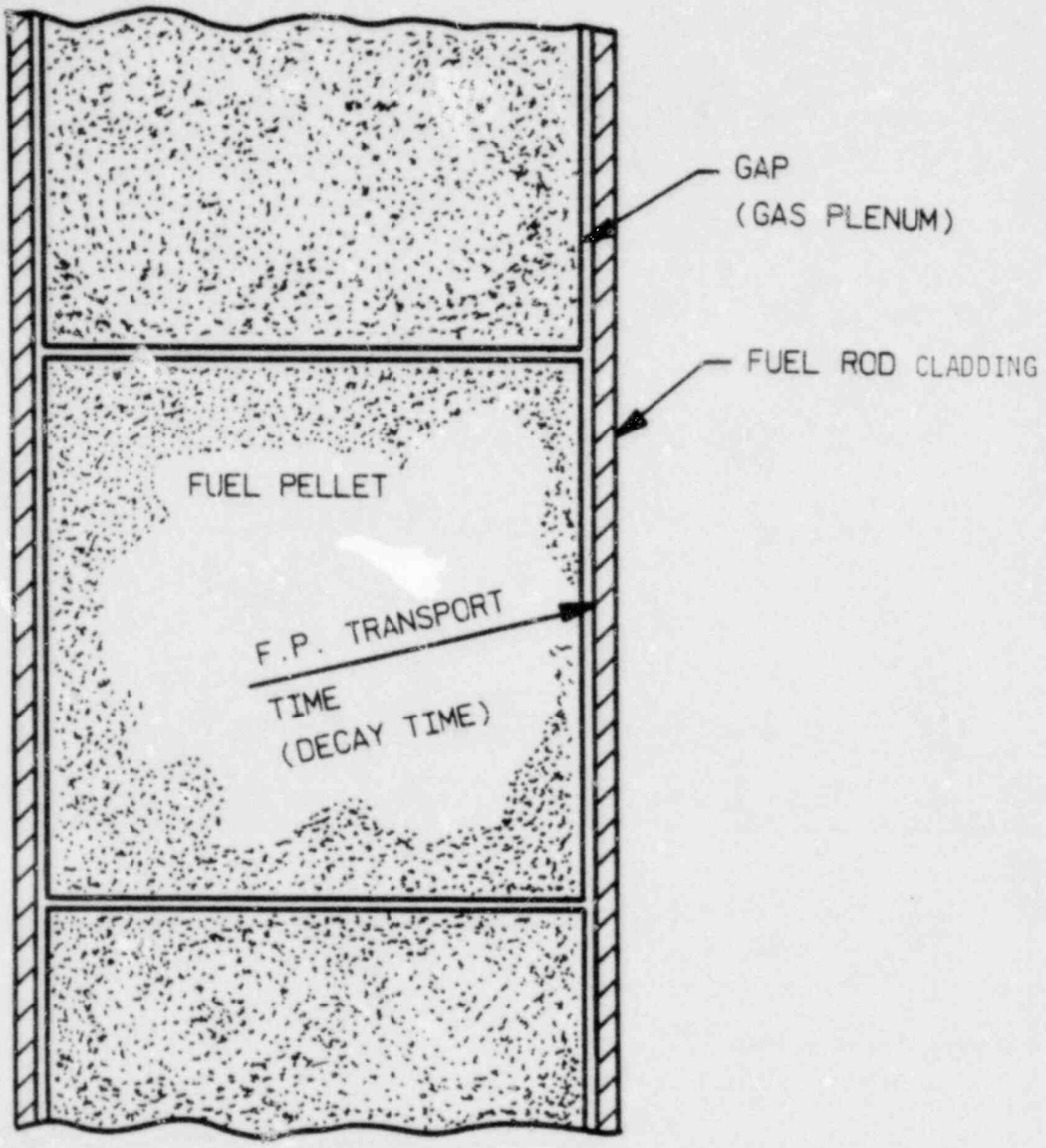

Figure 11-4. Removal of Activity From Coolant

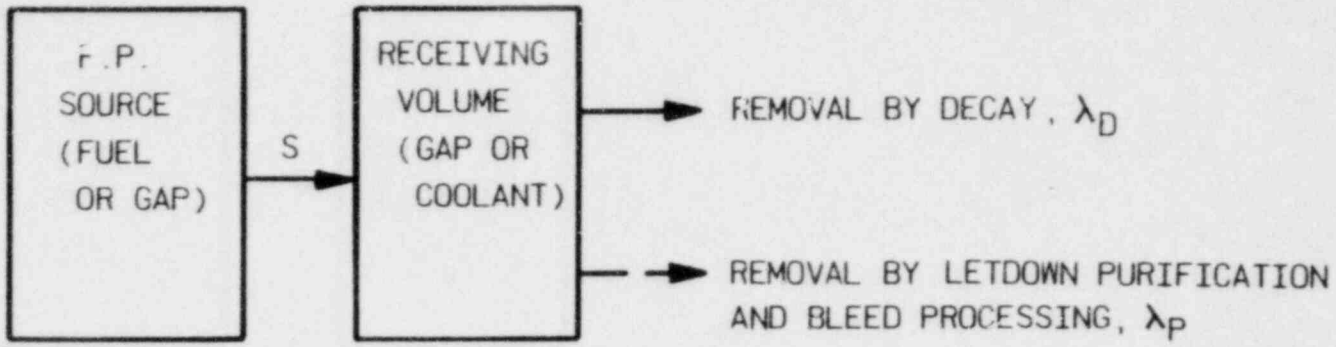

$$\frac{dc}{dt} = S - (\lambda_D + \lambda_P) C = 0$$

$$C_{eq} = \frac{S}{\lambda_D + \lambda_P}$$

Figure 11-5. Iodine Spiking in Reactor Coolant

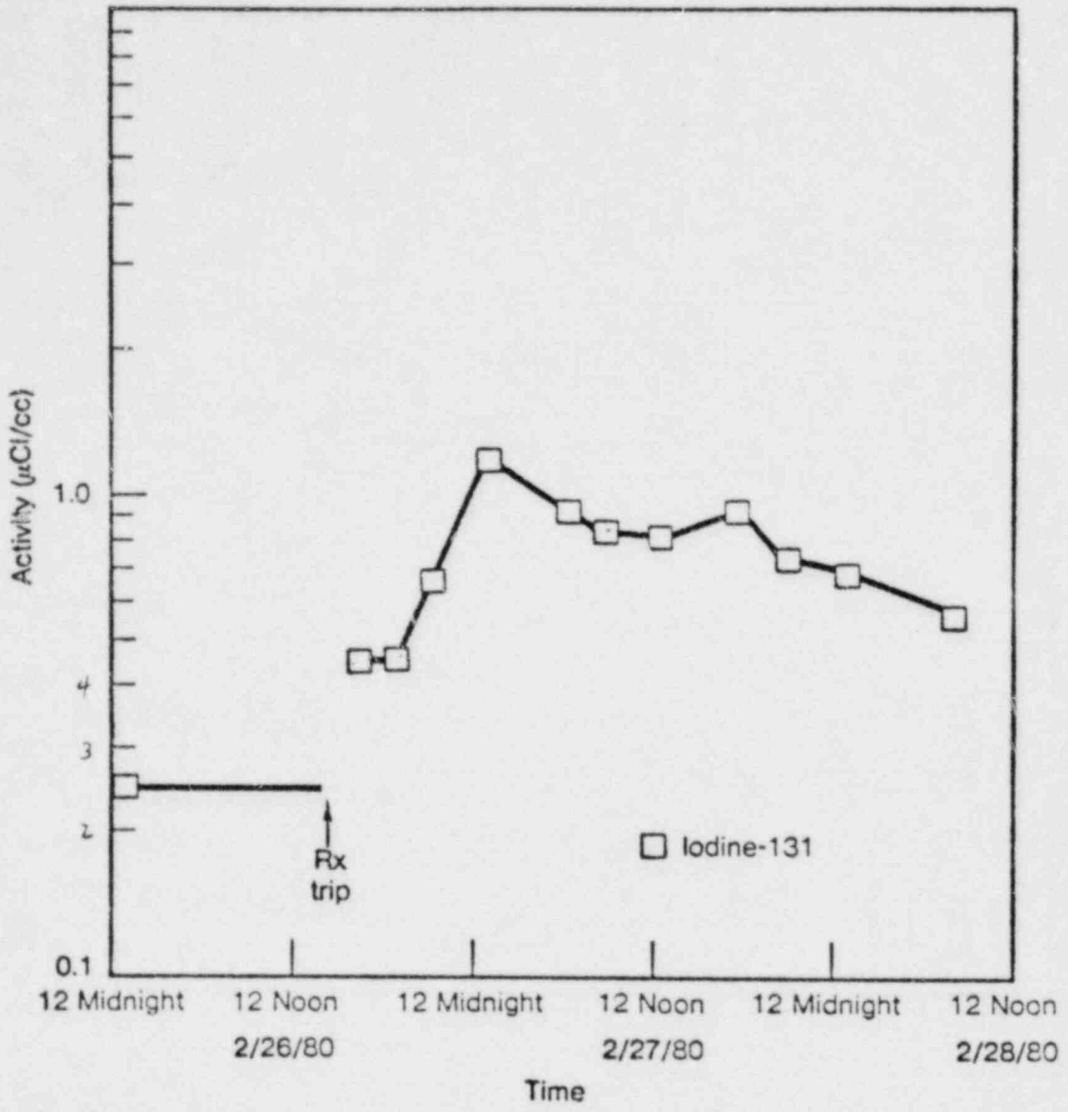

Figure 1.6. Last Stages of Core Uncovery — Maximum Fuel Damage Begins

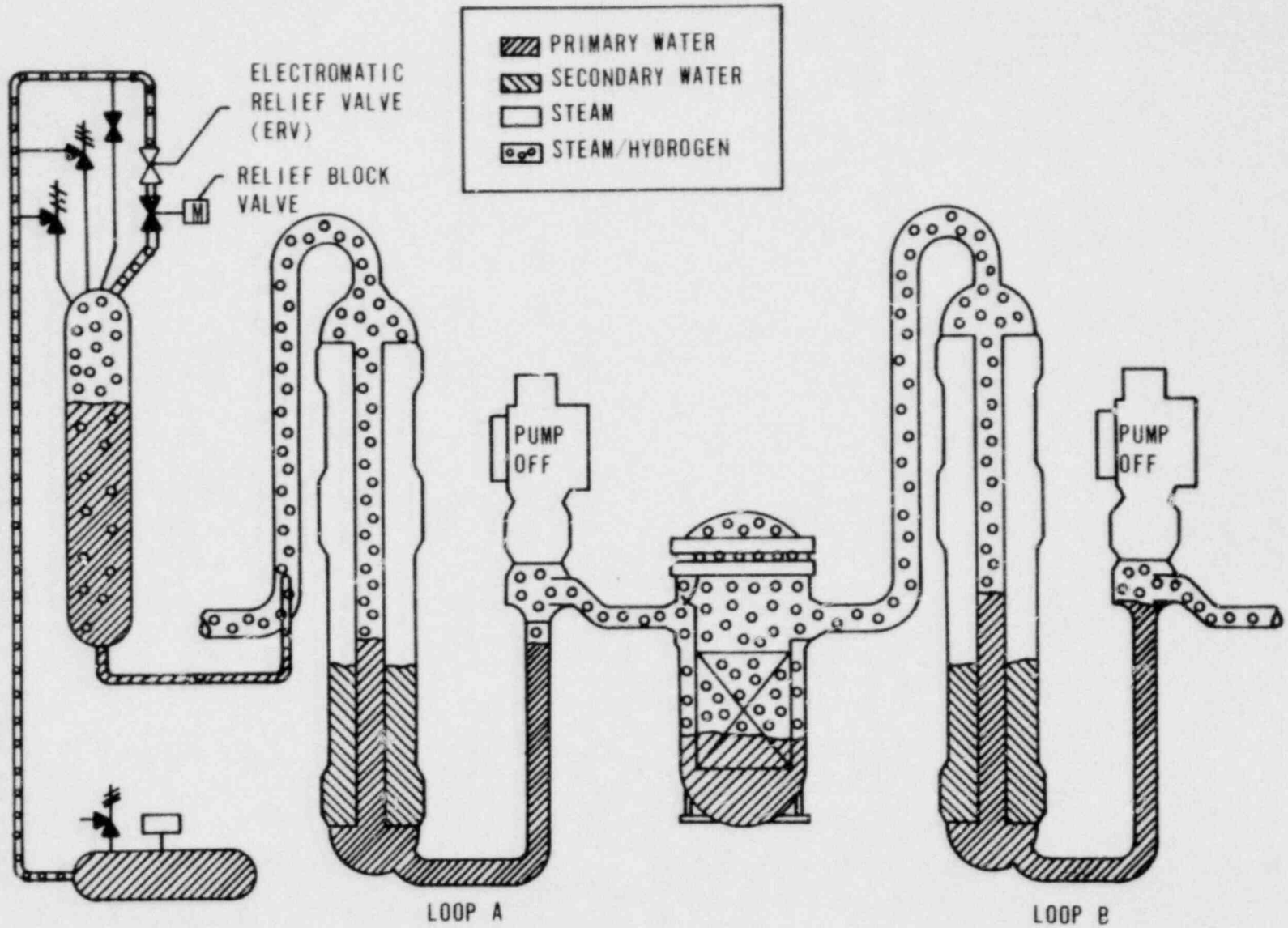

Figure 11-7. Appropriate Actions

1. CHECK AMOUNT OF ACTIVITY IN REACTOR COOLANT TO CONFIRM EXTENT OF DAMAGE

2. CHECK RATIO OF KEY NUCLIDES TO DISTINGUISH BETWEEN CLAD DAMAGE AND FUEL DAMAGE

APPENDIX 11-A

Fission Product Release From Fuel

WASH–1400
(NUREG 75/014)

RELEASE OF RADIOACTIVITY

in

REACTOR ACCIDENTS

APPENDIX VII

to

REACTOR SAFETY STUDY

by

R. L. Ritzman

E. F. Aber
C. Alexander
M. H. Fontana
D. K. Landstrom
D. L. Lessor
H. L. McMurry
D. L. Morrison
P. C. Owzarski
G. W. Parker
L. F. Parsly
M. Pobereskin
A. K. Postma
H. S. Rosenberg
W. A. Yuill

Contract W-7405-eng-92
Battelle Columbus Laboratories

U.S. NUCLEAR REGULATORY COMMISSION

OCTOBER 1975

Section 1

Fission Product Release From Reactor Core Material

Fission product release from core material during accidents involving meltdown would probably occur more or less continuously until the system finally cools. During this period, release rates should vary over wide limits depending on fission product properties, system temperatures, and the surface to volume ratio of the molten material. However, it is possible to identify four conditions or times at which major driving forces for release exist. These periods of high rates should account for most of the total release. The four major release components are:

a. Gap release - fission product release which occurs when the claddings experience initial rupture. It consists mostly of activity that was released to void spaces within the fuel rods during normal reactor operation and rapid depressurization of contained gases provides the driving force for escape.

b. Meltdown release - fission product release which occurs from the fuel while it first heats to melting and becomes molten. High gas flows in the core during this period sweep the activity out of the core region.

c. Vaporization release - fission product release which occurs after large amounts of molten core material fall into the reactor cavity from the pressure vessel. Turbulence caused by internal convection and melt sparging by gaseous decomposition products of concrete produce the driving forces for escape.

d. Oxidation release - fission product release which occurs just after and is a result of a steam explosion event. Finely divided fuel material is scattered into an oxygen atmosphere and undergoes extensive oxidation which liberates specific fission products.

By concentrating on the processes and factors which will control these four components, it was decided that release terms for representative accident sequences could be developed. Each one pertains to a specific, identifiable time period in the core meltdown scenario of either water reactor type. Therefore, PWR and BWR analyses both can utilize the same set of release components but the particular number of components and the timing of the releases will depend on the reactor type and the particular accident sequence being examined. The subsections which follow describe each component in more detail and present the release values that were arrived at on the basis of the current interpretations of fission product behavior that are contained in appendices to this report. The relevant appendices are cited within the text.

1.1 GAP RELEASE COMPONENT

For the purposes of this work, gap release is defined as the fission product inventory that is free to escape in gaseous or vapor form from core fuel rods if the cladding ruptures. The number of core fuel rod claddings that will rupture depends on the effectiveness of the emergency core cooling systems. For highly effective emergency cooling no claddings may rupture, while for degraded cooling conditions, leading to fuel rod melting, essentially all claddings will rupture during the temperature rise to melting. Between these two extremes there exist a large series of core cooling temperature conditions which can lead to various percentages of cladding ruptures.

Cladding rupture temperatures depend upon several factors; rate of temperature rise, internal gas pressure, and cladding physical and mechanical properties. However, rupture temperatures are likely to range from about 1400 to 2000 F. Fission products which have migrated to the surface of the fuel pellets or to the interior surface of the cladding during normal reactor operation can potentially be released. The driving force for escape comes from the rapid release of inert gases (helium and fission gas) stored in the plenum and gas gap spaces of the fuel rods. Internal gas pressures ranging from a few hundred psia to 2000 psia can exist.

Only fission product material which exists in vapor form should escape during the rod depressurization. Therefore, if vaporization from condensed phases or reaction layers within the fuel rod is incomplete when depressuri-

zation takes place, the potential release would not be realized. After the depressurization, very little driving force exists to carry fission product vapors along the narrow annulus to the rupture location in the cladding. Consequently, in this work the gap release component will be confined to an estimate of the release that occurs at the time of cladding rupture only. For accident conditions which are less severe than core meltdown, the gap release component values developed here may be reduced according to the percentage of the fuel rod claddings that are expected to experience rupture.

Two fractions make up the gap release component: (1) the release fraction, and (2) the escape fraction. The release fraction defines the potential for release from UO_2 fuel and is the result obtained from most fission product release models. The escape fraction represents an estimate of the degree of volatility of the fission product at fuel rod cladding rupture. The processes and reactions that need to be considered in estimating the escape fraction include physical condensation and reactions with fuel material, cladding, other fission products and gaseous impurities in the rods.

1.1.1 THE RELEASE FRACTION

The three sets of gap release calculations which are reported in Appendices A, B, and C produced the release fraction estimates shown in Table VII 1-1. These results are based on PWR core properties but results for a BWR are so similar that Table VII 1-1 values will be used for both reactor types. The values in Table VII 1-1 also represent best estimate releases for the several species and these contain different uncertainties depending upon the release models used, variations in basic parameters, or differences in methods to compute temperature profiles in operating fuel. Inspection of results given in Appendices A, B, and C show that uncertainties range from factors of ± 2 for some species to factors ± 10 or more for others. As a rule, the magnitude of the uncertainty tends to decrease as the decay half-life increases.

The ultimate use of these release fractions in total accident release calculations demands that a single value be assigned for each chemical group; that is, isotopic dependent release behavior must be ignored. Consequently, in the last column of Table VII 1-1, average release values are listed which will be used for all isotopes of each of the applicable chemical elements. The average values in each case are the simple arithmetic means of the three calculated releases for the particular isotope. This isotope was selected on the basis that it represents the radiologically important one for the element. Note that no direct calculations of tellurium releases were made. Results of out-of-pile experiments (Ref. 2) indicate that its release should be similar to iodine and cesium, and on this basis the value of 0.10 for the principal isotope, Te-132, was selected. Since the isotopes that were selected to represent each chemical group have relatively long half lives, the uncertainties in the average release fractions should be nearer the lower end of the uncertainty range as noted above. This was the basis for the uncertainty factors that are specified in Table VII 1-1.

The data in Table VII 1-1 represent the best effort that can be made with current mathematical models in calculating fission product releases during reactor operation. Due to lack of basic information for some species or parameters, simplifying assumptions are often made which tend to overestimate rather than underestimate releases. Therefore, the results should be interpreted as current state-of-the-art and not as absolute values. Future experimental and theoretical study may indicate lower releases, and when this occurs the models and results used here can be modified.

1.1.2 THE ESCAPE FRACTION

The rationale used to select escape fraction values will be discussed on an element by element basis.

1.1.2.1 Noble Gases.

The noble gases are gaseous at room temperature and are known to be very unreactive chemically. At cladding rupture the only mechanism which could retard their escape would be flow restrictions along the gas gap to the hole or split in the cladding. Since this constitutes only a delay process, which depends on very specific details of fuel rod structure, no retention of released noble gases in the fuel rod gas space can be claimed.

1.1.2.2 Halogens.

Elemental iodine would be entirely gaseous at normal reactor fuel rod operating temperatures and particularly at the cladding rupture temperatures. However, iodine readily reacts with

metals to form iodides which have different volatilities. Possibilities include zirconium iodides (reaction with cladding), cesium iodine (reaction with fission-product cesium), and hydrogen iodide (reaction with trace hydrogen or water vapor).

Experimental work by Feuerstein (Ref. 3) has shown that a series of zirconium iodides can form when iodine in Zircaloy capsules is heated, and several minutes is required to volatilize appreciable fractions of the reaction product at a temperature of 800 C (1472 F). Indirect evidence of iodine reaction with Zircaloy in operating fuel rods has been obtained by Weidenbaum (Ref. 4). Collins, et al (Ref. 5) performed puncture tests with irradiated Zircaloy-2 clad UO_2 in steam at about 1000 C (1832 F) from which it was concluded that only 10 percent of the iodine that was expected to be free within the cans escaped through the puncture hole. Lorenz and Parker (Ref. 6) have conducted a pair of in-reactor fuel rod failure transient tests with pressurized Zircaloy-2 clad fuel rods. The fission product release data for the two experiments indicated 25 percent and 100 percent escape of the free iodine relative to free noble gases. These limited studies suggest that iodine retention by Zircaloy cladding could limit the escape of iodine from the gas spaces of fuel rods during rupture. The escape fraction value cannot be specified very accurately but would be expected to fall within the range 0.1 to 1.

Contrary to the cladding reaction mechanism, thermodynamic analyses of the fuel-cladding fission product system consistently predict that CsI would be the most stable chemical form for iodine at elevated temperatures (see Appendix E). Since the fission yield for cesium isotopes is more than ten times that for iodine isotopes, there is sufficient cesium for complete conversion of the iodine. If CsI is the dominant iodine species in fuel rods then iodine would exhibit a significantly lower volatility at cladding rupture temperature i.e., a vapor fraction in the range of 0.01 to 0.1 would be expected. As shown above, experimental escape data do not coincide with these low values. In addition there is limited evidence that cesium may undergo compound formation with UO_2 and thus prevent formation of CsI (Refs. 7,8). Thermodynamic analyses have not considered this reaction. Finally, there appears to be no experimental confirmation of the presence of CsI in irradiated fuel rods. Therefore, the possibility of CsI being a major chemical form is not sufficiently established to justify consideration in this work. However, additional experimental work in this area would be useful.

The formation of hydrogen iodide, which might be significant at high temperatures, also has not been verified by experimental work on irradiated fuel rods. The existence of HI as a major species would not alter iodine volatility at cladding rupture temperatures appreciably. Therefore HI will not be considered an important iodine form in this analysis.

In summary the escape fraction for iodine gap release should be based on available experimental evidence that indicates at least partial retention by Zircaloy cladding. On the basis of the range indicated a best estimate value of 1/3 with an uncertainty factor ± 3 is appropriate.

1.1.2.3 Alkali Metals.

The normal boiling point of cesium metal is about 960 K (1270 F) and if the fission product exists in this elemental form, the gap release fraction could be completely vaporized at cladding rupture temperatures. On the other hand the thermal transient may be too rapid and incomplete vaporization would have occurred at this point. Also, compound formation with the fuel (noted above) or with the cladding (possibly with corrosion products) could result in significantly reduced volatility. There is almost no experimental data related to escape of fission product cesium under these conditions. The in-pile transient tests of Lorenz and Parker (Ref. 6) provide the only known experimental estimate. The results of two tests indicate an escape fraction value of about 2/3. Because of the approximate nature of these measurements, it was decided to use the same escape fraction for cesium that is used for iodine; i.e., 1/3 with an uncertainty factor of ± 3.

1.1.2.4 Alkaline Earths.

Depending upon the oxygen activity in the system, fission product strontium would predominately exist as either the metal or the monoxide. However, neither condensed phase has appreciable volatility at clad rupture temperatures. The metal which exhibits the higher vapor pressure should limit vapor fractions to less than 10^{-4} of the total strontium. The ANC fission product release model calculation for strontium, which considers thermodynamic equilibrium in the

fuel body, obtained a maximum release fraction of 4×10^{-5} (Appendix B). The in-pile transient test data of Lorenz and Parker (Ref. 6), while quite crude for strontium, indicate escape fractions ranging from about 10^{-4} to 10^{-6}. On the basis of this evidence, it appears that in conjunction with a release fraction of 0.01, a best estimate value for the escape fraction would be 10^{-4} with an uncertainty factor of ± 100.

1.1.2.5 Tellurium.

Thermodynamic calculations indicate that tellurium can exist as either the element or an oxide in the fuel. The stable vapor form at cladding rupture temperatures is probably Te_2, but several experimental studies indicate that tellurium will react with Zircaloy. Genco, et al. (Ref. 9) demonstrated extensive reaction of tellurium vapor with zirconium at temperatures above 400 C (752 F). The in-pile transient tests of Lorenz and Parker (Ref. 6) while very limited indicate an escape fraction for tellurium of between 10^{-1} and 10^{-5}. A complex kinetic situation involving competition among vaporization, reaction with cladding, and escape in the gaseous puff probably determines the escape fraction. Therefore, the value was set at 10^{-3} with an uncertainty factor of ± 100.

1.1.2.6 Other Species.

The volatilities of other fission product species, besides those which are chemical analogs of the elements discussed above, are expected to be so low that their escape at cladding rupture can be considered negligible. Therefore, the results of all the gap release component analysis can now be summarized. Table VII 1-2 presents such a summary showing the gap release fractions, the escape fractions, and the product of these two - the gap release component. The release and escape fractions listed here may be somewhat different from values obtained or recommended by the individual laboratories that contributed to the analyses. This is because current knowledge does not clearly show one analytical approach is superior to the others.

1.2 MELTDOWN RELEASE COMPONENT

The conditions pertaining to this release period begin with rapid boiloff of the water coolant which uncovers the reactor core. Steam, flowing up through the heating core, initiates Zr-H_2O reaction and this accelerates the rate of temperature rise. The cladding begins to melt within one minute and in a few more minutes fuel-melting temperatures are approached in the hotter regions. The process spreads throughout the core and within 30 minutes to 2 hours (Ref. 1) nearly the whole core is molten at temperatures ranging from roughly 2000 to 3000 C. During the later stages of this process molten core material can run through or melt through the grid plate and fall into the bottom of the pressure vessel. If a steam explosion does not occur when residual water is contacted in the lower portion of the pressure vessel, partial quenching and temporary solidification of portions of the molten mass can take place. However, the internal heat generation causes remelting and the inevitable downward migration continues until the pressure vessel fails, probably by meltthrough. Pressure vessel failure is expected to require about 1 hour after most of the core has melted (Ref. 1). Prior to this the high internal temperatures have caused melting of some of the pressure vessel steel and interior structural components. The molten iron is not miscible with the core material (oxide phase) although partial conversion to iron oxides could produce some dissolution in and dilution of the core material. Nevertheless some fission products (i.e., the noble metals) would tend to distribute to the metallic iron phase.

Initial fuel melting is expected to occur in only the center regions of the rods on almost a pellet by pellet scale. Thus the melting fuel will offer a relatively high surface area for release of fission products. As the melting front moves outward, the melting of the individual pellets may continue, but it is also conceivable that larger sections of fuel may collapse into the molten mass. If this fuel melts within the mass rather than at the edge, then fission product release could be inhibited by the time required for transport to a free surface. On the other hand, gaseous fission products, present as bubbles in the UO_2 could rise quickly to the surface of the molten mass and escape. It appears that most of the fission product release that does occur will take place early in the melting period at each core location. Then as the melted fuel mixes with the rest of the molten mass and the mass increases in size, fission product release rates will become much slower. The melting of structural steel in the pressure vessel during this later period is expected to produce a layer of molten iron above the molten core material which would offer a further barrier to

fission product release. Other factors which can inhibit release during meltdown in the pressure vessel include the possibility of crust formation at the melt surface and partial quenching when melt runs or falls into water that may be left in the bottom of the vessel.

The atmosphere in the core region and pressure vessel during meltdown is expected to be a steam-hydrogen mixture with small concentrations of fission product and core material vapors and aerosols. This may be classified a nonoxidizing atmosphere for most fission products, and it, of course, results from partial consumption of steam by metal-water reaction, yielding H_2 in the core region. Although the metal-water reaction that does occur is steam supply limited, some steam flow passes through cooler portions of the core region without complete reaction. It is estimated that during the meltdown phase only about half the Zircaloy is reacted and other metal-water reaction produces only about 50 percent more H_2. Thus total metal-water reaction is only the equivalent of 75 percent $Zr-H_2O$ reaction.

Thermal analyses of core meltdown provide only generalized data on core temperature profiles, geometry changes, and melt behavior versus time. This, combined with the uncertainties which exist in fission product properties at very high temperatures, argue against construction of a highly mechanistic model to calculate fission product release during the meltdown phase. Therefore, in this work, fission product release is treated as being simply proportional to the fraction of core melted.

Mathematically,

$$RCFx(t) = [RFx] \cdot [FCM(t)]$$

where RCFx(t) = Core release fraction for fission product x as a function of time (t):

RFx = Release fraction of fission product x from melted fuel

FCM(t) = Fraction of core melted as a function of time (t)

It is important to note that this approach assigns all release, which is expected to occur during the time core material remains in the pressure vessel, to the early period of first melting. This is consistent with two key observations; (1) the highest steam flows and (2) the highest fuel surface areas are expected during the early period. Thus this should be the period of maximum driving force for fission product escape from the core region. The release fractions (RFx) for the various fission products were estimated by considering:

a. The limited data that are available from small-scale experiments with UO_2 (Appendix D), and

b. The predictions of limited thermodynamic analyses of fuel-cladding-fission product system at high temperature (Appendix E)

The results are summarized in Table VII 1-3 and a short description of the rationale connected with each value is given in the following paragraphs.

a. Noble Gases (Xe, Kr) - Experimental work shows that nearly total release of these essentially chemically inert gases would be expected during the meltdown period if the surface-to-volume ratio of melting material remains high. Although this seems likely and considerable release should occur even before the fuel melts, some gases could become trapped as the molten mass enlarges during the later stages of meltdown. Accordingly, a range of 50 to 100 percent release is considered reasonable but 90 percent should be assumed probable.

b. Halogens (I, Br) - Again nearly total release is expected due to the high volatility, but the rate of release could be limited by transport in the melt to an external surface. Therefore, the same range (50-100 percent release) should apply and 90 percent is considered the probable value.

c. Alkali Metals (Cs, Rb) - Nearly total release would be expected but experimental data on cesium release from molten UO_2 and thermodynamic studies show that the alkali metals are not so highly volatile as the noble gases or halogens. Therefore, the release rate could be somewhat affected by internal transport in the melt or by the possible tendency toward compound formation. Experimental evidence indicates a range of 40 to 90 percent with a probable value of 80 percent.

d. Tellurium - Simple thermodynamics indicate that Te should volatilize almost completely from melting core material in the elemental form. However, experimental data indicate

extensive reaction with unoxidized Zircaloy cladding would tend to hold tellurium in the melt, even though much of the cladding may oxidize during the meltdown period. The tellurium apparently migrates farther into the cladding to react with remaining free metal rather than diffuse out through the oxide layer. Release of the tellurium from a particular core region will occur when nearly all or all of the cladding has been oxidized. Since an average of 50 percent of the core cladding is expected to become oxidized during meltdown, this represents an upper limit for release. However, the oxidation is spread unevenly over the core and a smaller amount of cladding undergoes complete reaction. On this basis tellurium release is estimated to range from 5 to 25 percent.

e. Alkaline Earths (Sr, Ba) - The chemical form and the volatility of these two fission products are very sensitive to the oxygen partial pressure in the system. Strontium metal is more volatile than barium metal but barium oxide is more volatile than strontium oxide. Thermodynamic analyses produce conflicting estimates of volatility and chemical form due to variations in oxygen activities. Experimental data on release from molten fuel material indicate that the two elements would experience about the same release. Data obtained with zirconium clad UO_2 showed up to 20 percent release of strontium and barium over several minutes in a neutral atmosphere, while only a few percent loss was found for bare or stainless steel clad UO_2. The lower volatility of these elements and the probable existence of unoxidized cladding suggest that releases in the range of 2 to 20 percent would occur. Since incomplete cladding oxidation is expected, the probable release value should lie above the geometric mean for this range. Hence, 10 percent is used as the probable value.

f. Noble Metals (Ru, Rh, Pd, Mo, Tc) - Although these elements probably volatilize as the oxides, thermodynamic calculations suggest that the volatile oxide forms are not very stable at the high temperatures and the lower oxygen partial pressure that are expected to be associated with the core meltdown. The first three elements probably exist in the metallic form in the fuel, while the latter two are probably in the form of lower oxides. The metallic species could partially distribute to the molten iron phase and be retained. Experimental data on ruthenium release from molten UO_2 in an oxygen-deficient atmosphere indicate low release. Releases in the range of 1 to 10 percent are considered possible, and 3 percent (the approximate geometric mean) is used as the probable value.

g. Rare Earths (including Y and Np, Pu) - The rare earth elements will generally exist in the fuel as the sesquioxides (M_2O_3) while the actinides, neptunium and plutonium, should form the dioxides (MO_2). The oxides characteristically exhibit low volatility but an estimate of the release fraction is difficult to make. Experimental data for cerium release from small specimens of molten UO_2 indicate losses of several tenths of a percent over a few minutes, or about the same as the UO_2 vaporization loss. In Appendix H, estimates of fuel vaporization rates indicate losses in the range of 0.01 to 1 percent. This range can also be used for the rare earth species but the probable value, 0.3 percent, reflects caution in selecting a characteristic release when the estimate is so approximate.

h. Refractory Oxides (Zr, Nb) - The oxides of these elements are so stable and of such low volatility that they probably would experience less release than the rare earths. However, for simplicity the same release definitions are used here as for the rare earths.

1.3 VAPORIZATION RELEASE COMPONENT

When the molten core and iron penetrate the pressure vessel and fall (or run) into the reactor cavity, the material will be exposed to oxygen from the containment atmosphere, steam from contact with water or vaporized from concrete, and carbon dioxide from thermal decomposition of the limestone aggregate in the concrete. Passage of steam and carbon dioxide through the molten mass will produce a gas sparging effect. In addition these gases or their dissociation products will create highly oxidizing conditions. One can speculate that the iron phase would be (at least partially) converted to oxide which could then dissolve in the core melt. The melt should also contain products of the concrete decomposition; silica, calcium

silicates, or calcium oxide. The products would eventually reduce the density of the oxide phase and the then heavier iron phase might sink to the bottom of the mass (Ref. 10). Conversely, incomplete dissolution could leave a relatively pure UO_2 phase which would continue penetrating downwards (Ref. 11). Lower melting mixed oxide phases forming ahead of the UO_2 would tend to rise and cover the UO_2. Thus, development of several immiscible or partially miscible phases is conceivable. Internal convection would promote mixing within and exchange between phases. Depending upon their solute properties, fission product oxides could distribute to these phases thereby altering the heat source distribution and the temperature profile in the melt system (Ref. 10). Vaporization of fuel and structural materials from the upper surface of the molten mass should produce dense aerosol clouds (smokes) above the melt and buildup of condensation products on nearby surfaces. Agglomeration and growth of smoke particles is expected to cause some vaporized material to settle back. Thus much of the vaporized material should be retained in the reactor vessel cavity. Vaporized fission products, mixed with the much larger quantities of structural material vapors and smoke, should generally follow the distribution of the bulk material. Exceptions to this would be the high volatility species which could escape into the upper part of the containment.

Only highly simplified analyses of the physical situation just outlined have been performed (Refs. 10,11,12). There are many unknown details concerning most of the chemical, physical, thermal, mechanical, and metallurgical properties of the complex system. Analytical results are dependent on basic assumptions which differ among models. No large-scale experimental work on the relevant system has been performed to guide modeling. Concrete penetration rates cannot be estimated accurately because of uncertainties in heat transfer mechanism, melt interaction effects, and/or boundary limit definitions. Release calculations can and have been performed, but the assumptions and data extrapolations needed, lead to estimates that are usually upper limit values (Ref. 11) (See Appendices E and G). The release models are useful in identifying key release processes and species that have a high potential for release by one or more of these processes.

To a first approximation, the extent of release will depend upon species volatility and the rate of transport in the molten mass to an external surface. For the large molten masses that result from core meltdown, the latter process should control release for all except the very low volatility species. For example, estimates have shown that pure diffusion transport would require several hundred hours to achieve significant release fractions, regardless of volatility (Ref. 13). However, additional estimates indicated that thermally induced internal convection currents might increase mass transfer rates such that corresponding releases would occur within several hours (Ref. 13). Very recent approximations based on gas sparging assumptions suggest total release for volatile species in fractions of an hour (Appendix G). The release rates that would actually occur would probably be some mixture between the latter two processes. Also, gross vaporization of the melt could assist the release by creating a receding surface. The uncertainties of the problem require that a simple approach be used to specify fission product releases for this portion of the accident.

1.3.1 VOLATILE FISSION PRODUCTS

The very volatile fission products will escape the melt if they can reach an external surface. The gas sparging process offers a mechanism for inducing mixing and creating a large effective external surface area. The convective mass transfer process offers an alternative and usually slower rate for transport to surfaces where vaporization can occur. Both processes would result in an exponential decrease in the volatile fission product inventory with time. In each case the half-time for release might range from less than one hour to many hours, depending on the gas flow or mass transfer conditions.

Other work on the Reactor Safety Study has resulted in an estimated time for core penetration of the concrete base of about 18 hours (Ref. 1). The analyses also indicate that considerable spalling and decomposition of the concrete would occur within the first half-hour of contact. This would be a period of rapid gas (steam and carbon dioxide) generation during which the sparging process could be a dominant driving force for escape of volatile fission products. Subsequently, lower rates of release would be expected as gas flows decrease but sparging could still efficiently deplete the melt of volatile species (See Appendix G). Thermally induced internal convection and also surface evaporation might assist in the release.

The potential importance of gas sparging to the release of volatiles from the massive melt dictated that treatment of the vaporization release component should be based on this process. Accordingly, a pseudo-exponential rate expression was designed which required only a single input parameter, the characteristic release half-time. Mathematically,

$$VLF(t) = 1 - \exp[-0.693t/\tau]$$

where

VLF(t) = The vaporization loss fraction after time (t)

τ = The characteristic release half-time

In order to avoid excessive calculations during actual accident sequence analyses, a cut-off time for the expression, equivalent to four half-time intervals, was selected. In practice the rate expression was used exactly as written for the first three half-time intervals, but then complete escape of the remaining activity was compressed into the fourth interval. Since this last step involves only 12.5% of the total vaporization release, the approximation should produce only slight perturbations in results.

The value of the characteristic release half-time would be a function of the fission product volatility, the gas sparging rate, and other kinetic factors. In a rigorous sense, there would be a unique value for each fission product species which would vary continuously with the sparging conditions. This complexity is not warranted here and so the half-time value was assigned only to roughly match the period of high sparge gas flow. This period, as noted earlier, has been estimated to last on the order of one-half hour. Thus the best estimate half-time value is considered to be 30 minutes. Use of this uniform value for all fission products probably produces underestimates of the rate of release for the most volatile species and overestimates of the rate of release for species of lesser volatility. Also, the sparging process may not be fully effective in sweeping volatile fission products from the melt either because some sections of the melt are not exposed to sparge gas or because mass transfer limitations inhibit vapor saturation of sparge gas bubbles. Due to uncertainties such as these the 30 minute half-time value which is used in calculations should be considered uncertain by at least an order of magnitude.

The fission products that are sufficiently volatile to experience total loss during this vaporization phase are Xe, Kr, I, Br, Cs, Rb, Te, Se, and Sb. The meltdown release of the first six of these is expected to be quite large, because of their high volatilities, and so little will be left to contribute to the vaporization release component. This is not true for the tellurium group elements, whose meltdown release is considered inhibited by compound formation with Zircaloy cladding. However, by the time the vaporization release begins most of the free zirconium, which exists during core meltdown, should be oxidized (probably from reaction with UO_2). If not, then the oxidizing sparge gases (steam and CO_2) should quickly eliminate free zirconium so that tellurium and its chemical analogues, selenium and antimony, will become very volatile and also experience total release.

1.3.2 LOW VOLATILITY FISSION PRODUCTS

Essentially all the remaining important fission product species must be considered low volatility components. Thus total release of these species should not occur. With one exception this group of elements should be present as oxides in the oxide phase. The noble metals (Ru, Rh, Pd) and to a lesser extent Mo and Tc probably exist as the metals and would be expected to partition into the metallic iron phase of the molten system (Ref. 14). Low release (less than 1 percent) of these species is expected unless complete oxidation of the iron should occur (Appendix G). Although this is not considered likely, localized oxidation could lead to some release and a value of 5 percent is considered to be a realistic estimate. This is probably uncertain by a factor of $\pm$ 5. The other fission products (alkaline earth oxides and rare earth oxides) should be dissolved in the oxide phase of the melt (Ref. 14). Under the generally oxidizing conditions which persist over this period these species are less volatile than UO_2 (Appendix E). The vaporization of UO_2 and of other oxide materials in the melt is very difficult to estimate owing to uncertainties in composition and temperature. High vaporization rates (high temperatures and oxygen pressures) should produce dense aerosol clouds above the melt which would tend to settle out, carrying condensable fission products back down. Low vaporization rates (lower temperatures) would also indicate low losses for these fission products. Considering these limiting processes it is doubtful that more

than 1 percent of these fission product species could be distributed to the atmosphere in the containment over the course of the reactor melt-through period. This estimate is also probably uncertain by a factor of ±5.

The rate of release of the low volatility fission products, for lack of better definition, is assumed here to follow the same exponential function that is used to describe the release rate of the volatile species. On this basis the percentage release values given in Table VII 1-4 indicate the amount of each fission product, remaining in the core material after gap release and melt-down release have occurred, that will escape to the containment atmosphere during the vaporization period.

1.4 OXIDATION RELEASE COMPONENT

A steam explosion event will result in the scattering of finely divided UO_2 (containing fission products) into the atmosphere outside the containment or into the air-steam atmosphere inside containment. In either case, the UO_2 particles will cool and undergo reaction with oxygen to form U_3O_8 at temperatures below about 1500 C (Ref. 15). The reaction is exothermic and is accompanied by release of fission products that are volatile under these conditions. Oak Ridge work on measurement of fission product release during fuel oxidation by air at elevated temperatures is directly applicable (Ref. 16). These data summarized and discussed in Appendix F show large releases of rare gases, iodine, tellurium, and ruthenium during 10 to 15 minute exposures to air at temperatures of 1100 and 1200 C. Since the data indicate positive temperature coefficients for each species, comparable releases should occur in much shorter times at higher temperatures. On this basis the release percentage given in Table VII 1-5 may be treated as essentially instantaneous values. Note, however, that the releases apply only to the fraction of the UO_2 fuel that is expected to be dispersed into an air (oxygen)-containing atmosphere.

1.5 USE OF RELEASE COMPONENT VALUES

The four release components described above would occur more or less sequentially during a reactor meltdown accident. In all cases, the gap component would occur first, followed by the meltdown component, and then by the vaporization component. However, steam explosions could potentially occur any time after appreciable amounts of the core have melted. Thus, the oxidation component is somewhat randomly time oriented.

In using the release component values from Tables VII 1-2 through VII 1-5 to specify release source terms for a particular accident sequence, it should be obvious that proper inventory balances for each fission product must be maintained. For example, the fraction of the total inventory that experiences gap release is then not available for release by any of the other three processes. Consequently, care must be exercised in setting up release source terms. To illustrate this point, a basic release source summary is provided in Table VII 1-6. Here individual core release fractions are given for each component and fission product assuming that, except for the steam explosion fraction, the total core is involved in the release processes. That is, all fuel rod claddings rupture to give the gap release fraction, total core melting occurs, and all of the core melt contributes to the vaporization release fraction (unless preceded by a steam explosion). It is also implicitly assumed that a steam explosion will not precede total meltdown release.

It is emphasized that the single values listed in Table VII 1-6 are based on the best estimate values taken from Tables VII 1-2 through 1-5. Each of the values contains uncertainties as noted in those Tables and should, therefore, not be considered absolute release fractions.

References

1. Carbiener, W. A., et al "Physical Processes in Reactor Meltdown Accidents", WASH-1400, Appendix VIII, October, 1975.

2. Parker, G. W., et al., "Out-of-Pile Studies of Fission Product Release from Overheated Reactor Fuels at ORNL, 1955-1965", ORNL-3981, p 81 (July, 1967).

3. Feuerstein, H., "Behavior of Iodine in Zircaloy Capsules", ORNL-4543 (August, 1970).

4. Weidenbaum, B., et al., "Release of Fission Products from UO_2 Operating at High Power Rating", CONF-650407, Vol. 2, p 885-904, USAEC (1965).

5. Collins, R. D., et al., "Air Cleaning for Reactors with Vented Containments", CONF-660904, Vol. 1, p 419-452 (1967).

6. Lorenz, R. A., and G. W. Parker, "Final Report on the Second Fuel Rod Failure Transient Test of a Zircaloy-Clad Fuel Rod Cluster in TREAT", ORNL-4710 (January, 1972).

7. Chen, H., and P. E. Blackburn, "ANL Reactor Development Program Progress Report for September, 1969", ANL-7618, p 117 (October, 1969).

8. Crouthamel, C. E. and I. Johnson, "ANL Reactor Development Program Progress Report for July, 1971", ANL-7845, p 522 (August, 1971).

9. Genco, J. M., et al., "Fission-Product Deposition and Its Enhancement Under Reactor Accident Conditions: Deposition on Primary System Surfaces", BMI-1865, p 38 (March, 1969).

10. Jansen, G. and D. D. Stepnewski, "Fast Reactor Fuel Interactions with Floor Material After a Hypothetical Core Meltdown", Nucl. Tech. 17, 85-95 (1973).

11. Morrison, D. L., et al., "An Evaluation of the Applicability of Existing Data to the Analytical Description of a Nuclear Reactor Accident-Core Meltdown Evaluation", BMI-1910, Appendix B (July, 1971).

12. Ergen, W. K., et al., "Emergency Core Cooling: Report of Advisory Task Force on Power Reactor Emergency Cooling (USAEC).

13. Fontana, M. H., "An Estimate of the Enhancement of Fission Product Release from Molten Fuel by Thermally Induced Internal Circulation", Nucl Appl, 9, 364-375 (1970).

14. Fischer, J., J. D. Schilb, and M. G. Chasonov, "Investigation of the Distribution of Fission Products Among Molten Fuel and Reactor Phases. Part I - The Distribution of Fission Products Between Molten Iron and Molten Uranium Dioxide", ANL-7864 (October, 1971).

15. Parker, G. W., et al., "Out-of-Pile Studies of Fission Product Release from Overheated Reactor Fuels at ORNL, 1955-1965", ORNL-3981, p 4 (July, 1967).

16. Parker, G. W., et al., "Out-of-Pile Studies of Fission Product Release from Overheated Reactor Fuels at ORNL, 1955-1965", ORNL-3981, p 85 (July, 1967).

TABLE VII 1-1 FRACTIONS RELEASED TO GAP (TOTAL CORE)

Fission Product (decay half-life)	Calculated Fractions ANC[a]	BCL[b]	ORN[c]	Chemical Groups	Average Release Fraction
Xe, Kr (long lived)	0.06	0.10	0.08		
Xe-133 (5.27 day)	0.04	0.02	0.02	Noble Gases	0.03[d]
Xe-135 (9.2 hour)	0.0002	0.004	0.004		
I, Br (long lived)	0.06	0.10	0.14		
I-131 (8.06 day)	0.06	0.03	0.05	Halogens	0.05[d]
I-132 (2.3 hour)	0.0007	0.005	0.006		
I-133 (20.8 hour)	0.007	0.01	0.02		
Cs, Rb (long lived)	0.20	0.05	0.21		0.15[e]
Cs-138 (32 minutes)	0.00001	0.0005	0.005	Alkali Metals	
Sr, Ba (long lived)	0.000004[f]	0.02	0.02		0.01[d]
Sr-89 (51 day)	-	0.01	0.015		
Sr-91 (9.7 hour)	-	0.002	0.01	Alkaline Earths	
Te-132 (78 hour)	(estimated value)			Tellurium	0.10[d]

(a) See Appendix B

(b) See Appendix A

(c) See Appendix C

(d) Values can be higher or lower by a factor of 4

(e) Value can be higher by a factor of 2 or lower by a factor of 4

(f) This value results from thermodynamic restrictions not considered in the other two models. See discussion of the escape fraction for this species.

TABLE VII 1-2 GAP RELEASE COMPONENT VALUES

Fission Product Species	Gap Release Fraction	Gap Escape Fraction	Total Gap Release Value
Xe, Kr	0.03[a]	1	0.03
I-Br	0.05[a]	1/3[c]	0.017
Cs, Rb	0.15[b]	1/3[c]	0.05
Sr, Ba	0.01[a]	10^{-4}[d]	0.000001
Te, Se, Sb	0.10[a]	10^{-3}[d]	0.0001
Others	-	-	Negligible[e]

(a) Values can be higher or lower by a factor of 4

(b) Value can be higher by a factor of 2 or lower by a factor of 4

(c) Values can be higher or lower by a factor of 3

(d) Values can be higher or lower by a factor of 100

(e) While no numerical value was developed for these various species, the number should not exceed that used for strontium-barium.

TABLE VII 1-3 MELTDOWN RELEASE COMPONENT VALUES

Elements	Release Range (percent)	Best Estimate (percent)
Xe, Kr	50-100	90
I, Br	50-100	90
Cs, Rb	40-90	80
Te[a]	5-25	15
Ba, Sr	2-20	10
Noble Metals[b]	1-10	3
Rare Earths[c]	.01-1	0.3
Zr, Nb	.01-1	0.3

(a) Includes Se, Sb
(b) Includes Ru, Rh, Pd, Mo, Tc
(c) Includes Y, La, Ce, Pr, Nd, Pm, Sm, Eu, Np, Pu

TABLE VII 1-4 VAPORIZATION RELEASE COMPONENT VALUES[a]

Fission Product	Release, Percent
Xe, Kr	100
I, Br	100
Cs, Rb	100
Te, Se, Sb	100
Ru, Rh, Pd, Mo, Tc	5[c]
Refractory Oxides[b]	1[c]

(a) Releases for the amount that remains after the gap and meltdown releases have occurred. The rate is approximated by an exponential function with a half-time of 30 min although this value is considered uncertain by an order of magnitude.

(b) Includes Sr, Ba, Y, La, Ce, Nd, Pr, Eu, Pm, Sm, Np, Pu.

(c) Values can be higher or lower by a factor of 5.

TABLE VII 1-5 FISSION PRODUCT RELEASES DURING STEAM EXPLOSIONS

Fission Product	Release From Oxidation, Percent	
	Range	Best Value
Xe, Kr	80-100	90
I, Br	80-100	90
Te, Se (Sb)	20-80	60
Ru (Mo, Tc, Pd, Rh)	80-100	90

TABLE VII 1-6 FISSION PRODUCT RELEASE SOURCE SUMMARY-BEST ESTIMATE TOTAL CORE RELEASE FRACTIONS

Fission Product	Gap Release Fraction	Meltdown Release Fraction	Vaporization Release Fraction[d]	Steam Explosion Fraction[e]
Xe, Kr	0.030	0.870	0.100	(X)(Y) 0.90
I, Br	0.017	0.883	0.100	(X)(Y) 0.90
Cs, Rb	0.050	0.760	0.190	--
Te[a]	0.0001	0.150	0.850	(X)(Y) (0.60)
Sr, Ba	0.000001	0.100	0.010	--
Ru[b]	--	0.030	0.050	(X)(Y) (0.90)
La[c]	--	0.003	0.010	--

(a) Includes Sn, Sb

(b) Includes Mo, Pd, Rh, Tc

(c) Includes Nd, Eu, Y, Ce, Pr, Pm, Sm, Np, Pu, Zr, Nb

(d) Exponential loss over 2 hours with halftime of 30 minutes. If a steam explosion occurs prior to this, only the core fraction not involved in the steam explosion can experience vaporization.

(e) X = Fraction of core involved in the steam explosion. Y = Fraction of inventory remaining for release by oxidation.

(Draft - may contain errors not yet corrected)

TECHNICAL BASES FOR ESTIMATING FISSION PRODUCT BEHAVIOR DURING LWR ACCIDENTS

Prepared by:

Battelle Columbus Laboratories
Oak Ridge National Laboratory
Sandia National Laboratory
U. S. Nuclear Regulatory Commission
Office of Nuclear Regulatory Research
Office of Nuclear Reactor Regulation

March 6, 1981

4. FISSION PRODUCT RELEASE FROM FUEL

4.1 Fission Product Behavior in Fuel

Understanding of the initial state of iodine and other fission products in the fuel pellet is helpful in tracing its subsequent movement into the primary and secondary system under accident conditions. The fuel pellet forms the initial boundary for fission products, and their chemical form on leaving the pellet governs the initial behavior in an accident environment.

4.1.1 Precursor Effects

Fission products in their radiologically important form are born as elements of slightly higher atomic number and decay to progresively more stable elements emitting a β-particle. Table 4.1 summarizes this situation for the mass numbers 127 through 138 which includes isotopes of the elements tin (Sn), antimony (Sb), tellurium (Te), iodine (I), xenon (Xe), cesium (Cs), and barium (Ba). The second column of Table 4.1 denotes the yield for each mass number, i.e., the number of atoms of that particular mass produced in 100 fissions. The [brackets] denote the element at birth, with β-decay at each mass number producing the elements to the right at a rate depending on the half-life of the specie. From Table 4.1 we note the following:

Relatively stable Cs fission products isotopes (half-lives greater than one day) exceed relatively stable iodines by a factor of 4.7 This ratio is increased by significant amounts of ^{134}Cs and ^{136}Cs which build in by activation via

$$\text{fission} \rightarrow {}^{133}Xe(n,\beta){}^{134}Cs, \ (21\ y)$$

$$\text{fission} \rightarrow {}^{135}Xe(n,\beta){}^{136}Cs, \ (13\ d)\ .$$

Therefore, the total amount of cesium significantly exceeds iodine. All important iodine isotopes (except ^{135}I) spend significant time from 25 min to 78 h) as tellurium. Therefore, tellurium mobility and chemistry could play a role in the overall picture of iodine release, especially since it is relatively volatile and shows a chemical affinity for cesium (Cs_2Te). The yield for relatively stable Te species ($T_{1/2} > 1$ day) is 2.3 times that for relatively stable I species. (If one counts ^{133}I with $T_{1/2}$ = 21 h, this ratio falls to 0.63.)

Precursor effects for cesium may be significant only for the formation of ^{134}Cs which spends 21 h as ^{133}I before decaying to ^{133}Xe (5.3 d) and subsequent activation to ^{134}Cs. Therefore, we should not be surprised to find ^{134}Cs behaving differently from the other cesium isotopes.

4.1.2 Fission Product Behavior in the Fuel Pellet

The average fission fragment begins its life with a kinetic energy of about 40 MeV, which is roughly 10^7 times the energy of a typical chemical bond. Therefore, each fragment causes considerable lattice dislocation before either coming to rest within the UO_2 crystal (or adjacent

Table 4.1. Iodine, xenon, and cesium fission product isotopes showing yields and half-lives. The bracket denotes elements at birth

Mass No.	Total yield (%)	β-decay						
		Sn	Sb	Te	I	Xe	Cs	Ba
127	0.14	[4.4 m]	3.8 d	9.4 h	∞			
128	0.46	[60 m]	10 m	∞				
129	1.0	[7.5 m]	4.3 h	70 m	~∞			
130	2.0	[3.7 m]	[6.3 m]	∞				
131	2.93		[23 m]	[25 m]	8.0 d	∞		
132	4.31		[2.8 m]	[78 h]	2.3 h	∞		
133	6.69		[2.7 m]	[55 h]	21 h	5.3 d	∞	
134	7.92			[42 m]	53 m	∞		
135	6.43			[18 s]	[6.6 h]	9.1 h	~∞	
136	6.45			[21 s]	[46 s]	∞		
137	6.18				[25 s]	[3.8 m]	30 y	∞
138	6.71				[62 s]	[14 m]	32 m	∞

crystal) or being expelled from the pellet surface. The initial state of fission products are then as individual atoms in interstitial locations in the UO_2 lattice. The precise manner in which these individual atoms move to either microbubbles, metal phase inclusions, or to phases including chemical combination with UO_2 is quite complex and imperfectly understood. Yet this initial phase in the life of a fission product is very important since it represents the major resistance to transport to the pellet exterior.

However, some general characteristics of this early state of fission products in UO_2 are as follows:

Above some critical temperature (between 1100° and 1400°C) general lattice mobility exists, allowing the individual atoms to move easily to more stable thermodynamic states. For atoms inert to UO_2 (the gases Kr, Xe, and probably I and Te and the noble metals, Ru, Tc, Rh, Pd), this means moving from the interstitial location to either a microbubble or a metallic phase. Other elements (Zr, Nd, and the rare earths) move to locations in the UO_2 lattice to form true solutions. The alkaline earths (Sr, Ba) would migrate to form a separate oxide phase. Cesium would tend to form a separate cesium uranate phase when such is stable ($T < \sim 1500°C$), but its high vapor pressure over cesium uranate would probably remove Cs from high temperature locations by migration with the other gaseous species. If sufficient Cs is available from the Cs/cesium uranate equilibrium, the balance may combine with I to form CsI.

Below the temperature of general mobility in the UO_2 lattice, large atoms inert in UO_2 (Xe, I, Te) probably migrate as complexes with one U- and two O-vacancy locations. This rather odd behavior is only supposition, but these large atoms are too firmly wedged in interstitial locations to move in a more conventional way.

The manner in which a more active atom, like Cs, moves under these conditions is even more unclear. It is important though to point out that at this phase of life of a fission product, the laws of chemical equilibria (and indeed chemistry) may not apply. The Cs and I atoms here migrate as a complex with a set of lattice vacancies. There may or may not be opportunity for significant chemical combinations even when equilibria considerations so dictate.

4.1.3 Predicted Chemical Behavior of Iodine and Cesium in UO_2

Under normal chemical circumstances, and if the opportunity occurs, iodine prefers to exist predominantly as stable species CsI and ZrI_4 rather than either atomic I or the molecule I_2. However, some hedging is necessary here because some features of the environment within a fuel rod differ significantly from conditions forming the basis of usual chemistry or equilibrium chemical thermodynamics.
Iodine and cesium atoms are born separately within the UO_2 lattice and initially have quite different chemical tendencies in UO_2. Iodine, having no chemical affinity for UO_2, would tend to migrate into the gas

phase along with the noble gases, whereas cesium, with its higher chemical affinity for its surroundings, could behave quite differently. There is no way of predicting whether or not cesium at this stage has an opportunity for combining with iodine, or whether iodine is effectively "swept" from cesium by the migration to the noble gas bubbles.

Assuming an aproximately conventional equilibration of Cs, I, O_2, and UO_2, two general categories of reactions need to be considered: (1) dissociation reactions, and (2) vaporization reactions.

Dissociation reactions

$$\langle Cs_2UO_4 \rangle = (2Cs) + (O_2) + \langle UO_2 \rangle \qquad (4.1)$$

$$\langle Cs_2O \rangle = (2Cs) + 1/2(O_2) \qquad (4.2)$$

$$(CsI) = (Cs) + (I) \qquad (4.3)$$

Vaporization reactions

$$\{CsI\} = (CsI) \qquad (4.4)$$

$$\{I_2\} = 2(I) \qquad (4.5)$$

$$\{Cs\} = (Cs) \qquad (4.6)$$

The brackets signify the assumed state; < >, { }, and ( ) signify solid, liquid, and gas phases, respectively. The above six reactions are perhaps the most significant ones of the dozens that need to be considered on the determination of equilibrium compositions. In particular, the formation of zirconium compounds, ZrO_2 and ZrI_4 may be significant near the cladding. At any rate, these six reactions are selected here to illustrate the types of interrelatinships which may occur between competing reactions.

Reactions (4.1) through (4.6) plus many others form a set of competing reactions, the net result of which is an equilibrium composition of the gas phase plus various amounts of the condensed phases. The manner in which this estimate is performed falls within the realm of chemical thermodynamics. Here we should point out the following interrelationships:

(1) All dissociation and vaporization reactions are coupled, for example, by the following illustration: If conditions favor CsI dissociation [reaction (4.3)] to a degree which would yield an iodine partial pressure greater than the vapor pressure at that temperature [reaction (4.5)], then CsI dissociates and all the iodine transfer to a condensed iodine phase via

$$(CsI) \rightarrow (Cs) + (I) \; ; \qquad (I) \rightarrow 1/2\{I_2\} \; .$$

Alternatively, if a condensed iodine phase possesses a vapor pressure greater than the dissociation pressure of iodine over CsI under a particular set of conditions, the condensed phase iodine would vaporize and combine with Cs to form CsI by the reverse procedure. A similar discusion would apply as well for Cs dissociation pressures via reactions (4.1) and (4.2) and Cs condensation via reaction (6).

(2) If CsI formation by the reverse of reaction (4.3) tends to generate a cesium iodide partial pressure higher than the vapor pressure at that temperature [reaction (4.4)], liquid or solid CsI would form to a degree which equalizes the pressures:

$$P_{CsI}[\text{reaction (4.3)}] = P^{*}_{CsI}[\text{reaction (4.4)}] .$$

(The asterisk denotes vapor pressure above a pure substance.) Conversely, if the association pressure of CsI via reaction (4.3) is less than the vapor pressure of CsI, no condensed phase CsI would form.

(3) Reactions (4.1) and (4.2) illustrate the key role played by the level of the oxygen pressure. Within the UO_2 lattice, the oxygen pressure is imposed by the degree of hyperstoichiometry, i.e., by the value of x in UO_{2+x}. In fresh LWR fuel, the oxygen excess is such that the chemical potential of oxygen, RT ln P_{O_2}, is normally ~-300 kj/mol. Burnup tends to increase the oxygen pressure, but LWR burnup even at discharge does not change it significantly. Under conditions of high heat rating (>43 kW/m), the oxygen pressure is drastically reduced in the vicinity of the clad due to formation of ZrO_2.

In addition, progressively higher oxygen pressure tends to favor the formation of cesium uranate (reverse of reaction (4.1)) tending to make cesium unavailable for cesium iodide. Therefore, high oxygen pressure tends to destabilize CsI by

$$CsI + O_2 + UO_2 \rightarrow \text{cesium uranate} + I_2 .$$

However, chemical thermodynamic estimates predict this to occur at fairly high oxygen pressure (~-100 kJ/mol), in the region where O_3 is stable, rather than UO_2.

Some key properties of the materials in Eqs. 4.1-4.6 are given in Table 4.2. The free energy of formation at 1000 K, given in the first column, is a measure of chemical stability in the presence of their elements, the more negative values indicate greater stability for these conditions. We note also that CsI is a compound of intermediate volatility. If present, it would be predominantly gaseous at central rod temperatures, a liquid at intermediate locations, and a solid near the cladding surface. Cesium oxide (Cs_2O plus other oxides) also fall into this range of intermediate volatility. Cesium uranate (Cs_2UO_4) would tend to decompose into (Cs), $\langle UO_2 \rangle$, and (O_2) at elevated temperatures (>~1500°C). The cesium uranate phase would be liquid throughout much of the pellet volume and be a separate solid phase near the clad surface.

Methods based on chemical thermodynamics can often be quite helpful in predicting the chemical composition of complex mixtures, but as with all idealized calculations, it is essential to emphasize its inherent limitations. These limitations include the following: (1) kinetic effects frequently determine composition rather than chemical equilibria; (2) conditions within the fuel pellet differ in many respects from that

Table 4.2. Charateristics of some key materials

	Free energy of formation at 1000 K[a] (kJ/mol)	Melting point (°C)	Boiling point (°C)
$\langle UO_2 \rangle$	-907	2830	
$\langle Cs_2UO_4 \rangle$	-1511	940	Decomposes
$\langle Cs_2O \rangle$	-220	490	Decomposes
(CsI)	-289	626	1280
(Cs)	-13.8	30	700
(I_2)	-82.1	114	183

[a]As the pure solid for UO_2, Cs_2UO_4, and Cs_2O; for the gas phase of CsI, Cs, and I_2 at standard state.

normally encountered, i.e., intense radiation field, large temperature gradients, (3) the solubility of some condensed phases in UO_2 at high temperature is not well known and can cause an uncertain degree of error.

These limitations mean that prediction based on equilibrium chemical thermodynamics, while they are of interest, do not carry the force of direct observation and must be considered as being uncertain. Bearing this in mind, we note that calculations of this type were performed[4.1] to determine the chemical forms of I and Cs in UO_2 predicted up to ~950°C in three atmospheric environments: normal in-reactor conditions, steam, and for a 50-50 steam-air mixture. The value of the oxygen pressure for the normal atmosphere case was assumed to be that imposed by the preponderant UO_{2+x}. The approach was first to estimate the composition of the cesium species in these environments. Subsequently, a representative amount of I was added to the calculation to determine the composition of I-species. In each case, the addition of Cs to UO_2 or the addition of I to Cs + UO_2, the addition was assume to cause negligible perturbation of the preponderant host environment.

Some results of this study[4.1] are the following:

(1) The major form of Cs in UO_2 under normal conditions appears to be the cesium uranate, Cs_2UO_4, at least up to 950°C. "Normal conditions" means an oxygen potential of between -350 and -300 kJ/mol, corresponding to an oxygen level in UO_2 of from $UO_{2.0001}$ to $UO_{2.001}$. A higher uranate, $Cs_2U_2O_7$, may exist at lower temperatures, $T \lesssim 800$ K.

(2) The major form of a representative quantity of I in the stable Cs_2UO_4 zone is CsI. At somewhat higher oxygen pressures (~-280 kJ/mol at 1200 K) or lower temperatures (<800 K at -300 kJ/mol), a higher uranate form exists ($Cs_2U_2O_7$) over which the cesium pressure is lower, but not to the extent of destabilizing CsI.

(3) It is thought that oxygen potentials as high as ~-100 kJ/mol would be required to destabilize CsI by

$$UO_2 + \{CsI\} \rightarrow \text{cesium uranate} + (I) \ .$$

This would occur in the region where UO_3 is the stable form of uranium oxide, which is highly unlikely in LWR fuel.

(4) Conditions in a steam environment are predicted to be about the same as for the normal environment case; i.e., the addition of pure steam does not significantly alter the oxygen potential in UO_{2+x}.

(5) When a 50-50 steam/air environment is assumed, higher cesium uranates, e.g., $Cs_2U_{15}O_{46}$, are predicted to be the stable form of Cs. These essentially lock up the available Cs, rendering CsI unstable. The stable iodine under these conditions is therefore I_2 or I.

It should be emphasized that these predictions are from an idealized computation based on chemical thermodnamics. There are a number of ways that error an be introduced into these estimates, and they grow more uncertain as temperatures extend above 950°C.

4.1.4 Observed Behavior in Fuel

Observations regarding the state of cesium and iodine in fuel pellets fall into three categories: (1) measured concentration profiles and observed solid phases on discharged fuel; (2) thermonigration experiments performed using fresh UO_2 and simulated fission products; and (3) fission product release experiments.

Concentration profiles and observed solid phases in discharged fuel

Radial concentration profiles in discharged fuel pellets may be determined using electron microprobe or micro-rollimated, gamma spectroscopy. Occasionally, the chemical form of the fission product may be inferred from the nature of the measured profile. For example, Kleykamp (in ref. (4.2)) observed that a cesium concentration peak at the outer radial edge of a pellet extracted from a high heat rated rod (43 kW/m) coinsided with concentration peaks of Zr, Sn, and O. For this case then, a chemical association is inferred involving a Cs-Zr-Sn-O compound.

Unfortunately, no similar distinct features in iodine radial profiles have been found from which its chemical state in the fuel may be deduced. Peehs et al. (in ref. (4.2) measured ^{137}Cs and ^{139}I radial profiles in fuel irradiated at 23, 42, and 56 kW/m. The lowest heat-rated fuel showed essentially no radial redistribution. At the higher heat ratings, radial redistribution in the fuel did occur, and the redistribution of iodine and cesium followed similar trends. However, no conclusions regarding the chemical state of either cesium or iodine can be drawn from observed radial concentration profiles.

Numerous distinct chemical phases may be observed in discharged fuel pellets using metallographic techniques. Determination of the elemental composition of these phases by use of an electron microprobe can lead to an understanding of the chemical nature of fission products in each phase. A summary of phases observed in discharged fuel has been presented by Kleykamp(4.3) which represents the state-of-knowledge in this area as of 1972.

Kleykamp observed 22 distinct fission product phases of which three contained cesium. None contained iodine, which probably means that iodine was uniformly distributed throughout the UO_2 and did not segregate in any separate solid phase. The same is true for cesium; the observed cesium-bearing phases were found near the clad and contained cladding material. No distinct cesium-bearing phase was found in the interior of the pellet. However, crystalline deposits containing cesium and iodine have been observed on internal cladding surfaces.

Therefore, we came to an uncertain conclusion regarding direct observations of disharged fuel. Neither published concentration profile measurements nor observed phase compositions have shed light on the chemical form of cesium or iodine in the fuel element.

Thermomigration experiments

In these experiments, fission product simulants are added to UO_2 in a manner calculated to approach the environment of a degree of burnup. The UO_2 is then placed in a temperature gradient, and the movement of the fission product simulants followed by gamma spectrometry. The physicochemical state of the fission products is inferred from the extent of its movement. In this way a completely sealed system may be used, thereby preserving the intended oxygen pressure in the fuel pin. A significant disadvantage of this method is that the simulated fission products are applied to the exterior of the UO_2 grain. For refractory fission products, pellet sintering creates some diffusion into the grain, thereby approaching a more realistic initial condition. This is not possible with volatile fission products which would have to be applied to either the UO_2 powder or nonsintered pellet. Therefore, thermomigration experiments exclude a significant chapter in the life and transport of the volatile fission products.

Peehs et al. (in ref. 4.2) conducted several types of thermomigration experiments. In the first I and Cs were uniformly applied to an 11 mm length of UO_2 powder which was placed in an axial temperature gradient between ~1400°C and ~200°C. These tests showed that (1) the Cs and I both migrated to the 300-320°C temperature zone; and (2) a detailed analysis of the measured profiles showed that the I migrated more rapidly than Cs, from which it was concluded that significant amounts of CsI did not form.

The influence of in-grain diffusion of iodine was investigated using trace-irradiated UO_2. In these tests, the tendency for migration of I was much less, supporting the conclusion that the primary resistance to migration of I exists during its initial state within the UO_2 grain. (In these tests, I remained relatively immobile even at ~1900°C.)

Other tests were conducted to determine the influence of oxgyen pressure on Cs and I movement. At near-usual oxygen pressures (corresponding to a formulation of $UO_{2.02}$), the Cs and I both migrated, at first, to the 1000°C location; later, after ~10 h, the Cs and I peaks moved down to the 700°C location. A quite different migration pattern occurred at higher oxygen pressures, corresponding to $UO_{2.1}$. Under these conditions, the I migrated quickly to 200°C whereas the Cs stabilized at 1000°C. A possible explanation for this behavior is that CsI formed at the lower oxygen pressure and did not form at the higher. At the higher oxygen pressure, cesium uranate formation undoubtedly stabilized the Cs at ~1000°C.

Adamson et al. (in ref. 4.2) studied the movement of Cs, I, Te, and Mo in UO_2 by applying these fission products to one end of ~10-in. length of discharged LWR fuel and placing the length in a temperature gradient ranging from 1400°C to 400°C. The stated conclusions of this study are as follow:

(1) Cesium migration depends critically on the oxygen pressure, which in the UO_{2+x} regime, depends on the value of x. Cesium tends to combine with UO_2 to form at least two types of uranates, but at low oxygen pressure ($Cs/O_x < \sim 1$), some Cs remains in the metallic state.

(2) Iodine does not react with UO_2, but forms CsI when excess Cs is present. CsI is more stable than either Cs-U-O or Cs-Si-O compunds.

(3) Tellurium migration is complicated in the presence of Cs because both Te and Cs may associate with UO_2.

Evidence from thermomigration experiments is therefore also somewhat uncertain. In one set of tests (Peehs) CsI apparently did not form in UO_2. A second test series by the same experiments using a fuel composition of $UO_{2.02}$ seemed to indicate CsI formation at least initially. Adamson's tests with low oxygen clearly indicated CsI formation. Subtle differences in technique undoubtedly caused these different results. It is agreed, however, that excess oxygen (in a degree forming $UO_{2.1}$) tends to make iodine appear in the molecular form.

Fission product release-from-fuel experiments

In principle, at least, the chemical form of volatile fission products, like iodine, may be inferred by observing the rate of evolution from overheated fuels relative to the evolution rate of noble gases. If, for example, the observed release rate of iodine matched closely that of xenon, especially at lower temperatures, (1000°-1400°C), it would speak strongly for iodine being in a highly volatile form in the fuel, i.e., molecular instead of cesium iodide. In fact, in the experiments conducted by Parker(4.4) on bare chunks of low-burnup fuel annealed in purified helium, the iodine evolution rate consistently exceeded that of xenon. This bias has been adopted by the ANS 5.4 release rate model in which the recommended diffusion coefficient for iodine is seven times higher than the value for xenon.

On the contrary, however, in Lorenz's(4.5-4.7) experiments using discharged fuel heated in steam, release of iodine was substantially slower than krypton up to 1400°C. However, we would expect more rapid evolution of noble gases at lower temperatures because surface deposits would be removed in this range, which could not be distinguished experimentally from diffusional release. Therefore, relative release rate data are not useful at this time as an indicator of the nature of the evolved specie.

Lorenz's experiments did, however, contain an approximate means for direct chemical specie identification. This was done by observing the

location in the apparatus where the evolved iodine and cesium deposited. Iodine deposit locations above 200°C were presumed to be CsI. The amount of "reactive iodine," which includes I_2, HI, and CH_3I, was given by the sum of that found on the charcoal, the filter train (excluding the first filter) plus other cool, nonparticulate deposits. Iodine on particulates was determined principally by the amount on the first filter. (This description is an oversimplification since "reactive iodine" would, to a degree, also deposit on the filter while particulate iodine can deposit in locations besides the filter).

A summary of Lorenz's results is given in Table 4.3, which lists the percent of evolved iodine found as "presumably CsI," "presumably molecular iodine," and as particulates for each test run. We note that for the gap purge tests, which were run in helium (BWR-4 and HBU-12), more than 91% of the released iodine appeared as CsI. The balance of the tests were run on steam and showed smaller percentages of iodine as CsI, ranging from a low of 4% in HBU-8 to 79% in BWR-2. For the steam tests, the molecular iodine ranged from 0.1 up to 88%, and iodine in particulates ranged from 6 to 56%.

Clearly, the fraction of evolved iodine which appeared as CsI was lower in the steam tests than the tests using helium. At least three reasons for this behavior are possible: (1) the iodine evolved as CsI but reacted with steam to form CsOH and HI; (2) the steam contained some air as an impurity which enhanced formation of Cs_2O, thereby destabilizing CsI; and (3) evolved CsI reacted with quartz to release I_2 in the steam experiments, but had less opportunity to do so in the gap purge tests.

4.2 Fission Product Release from Fuel Data

4.2.1 Release Rate Mechanisms

Five principal mechanisms control the rate of release of fission products from LWR fuel under accident conditions. They are (1) burst release, (2) diffusional release of the pellet-to-cladding gap inventory, (3) grain boundary release, (4) diffusion from the UO_2 grains, and (5) release from molten material. Each mechanism becomes dominant at a succeedingly higher temperature.

The burst release occurs when the overheated fuel rod cladding ruptures. In a LOCA this can be expected to occur in the temperature range 750 to 1100°C depending upon the amount of fission gas and prepressurizing helium in the fuel rod, the primary vessel pressure, and the rate of heatup or time at temperature. When the cladding ruptures the entire amount of noble fission gases previously accumulated in the plenum and open voids in the fuel rod can be assumed to be released. This amount can range from ~0.25% to ~25% of the total amounts of stable and long half-life fission gas isotopes. Isotopes of gases with half-lives less than 30 days will be present in significantly lower amounts. For instance, the amount of ^{133}Xe might be a factor of 5 to 9 less in the burst-released plenum gas.(4.8) Approximately 1 to 1.5% of the total

Table 4.3. Summary of iodine release species in Lorenz's(4.5, 4.6, 4.7) experiments

Test No.	Temperature (°C)	Gaseous Environment	Test duration (min)	Amount of I released (mg)	% of each form		
					Presumably CsI	Presumably mainly I_2	Particulate
BWR-4[a]	700-1100	helium	300	4800	99.99	0.005	0.02
HBU-12[a]	700-1200	helium	480	170	91.2	0.27	8.6
HT-1	1300	steam	10	71	70	10	20
HT-2	1445	steam	7	990	90	0.1	9.9
HT-3	1610	steam	3	5400	86	0.2	14
HT-4	1440	steam	0.4	750	78	0.3	22
HBU-1	700	steam	300	0.9	18	72	10
HBU-2	900	steam	120	1.8	14	73	13
HBU-4	500	steam	1200	0.1	40	44	16
HBU-11	1200	steam	27	20	34	8	58
HBU-7[b]	900	steam	1	11	71	4	25
HBU-8[b]	900	steam	61	14	4	88	8
HBU-9[b]	1000	steam	10	17	6	88	6
HBU-10[b]	1050	steam	11	14	26	53	20
BWR-1[b]	960	steam	1	490	67	0.4	33
BWR-2[b]	850	steam	1	1000	79	0.1	21
BWR-3	1200	steam	25	1200	44	0.7	56

[a]Gap purge tests

[b]Burst release tests

fuel rod fission gas inventory is released with or shortly after the burst release in addition to the previously described plenum and void space gas. This amount is believed to be gas atoms shallowly embedded in fuel and cladding surfaces and is released as these surfaces heat up.(4.5)

Cesium and iodine are also released when the fuel rod ruptures, but the quantity carried out with the vented gases is considerably less than for the noble fission gases. The burst release of cesium and iodine depends upon the fuel rod temperature, the total volume of gas vented, and the amount of cesium and iodine initially in the pellet-to-cladding gap space. The LOCA source term model describes the quantitative calculation of their release.(4.8) Usually only a small fraction of the gap inventory of cesium and iodine is released with the burst.

For a PWR, typical burst releases might be 3% of the stable noble fission gases, including embedded gas release, 0.02% of the total stable cesium, and 0.04% of the total stable iodine. For short half-lived isotopes, the burst releases would be a factor of 3 or more lower than the above.(4.8) For BWRs the releases might be twice the above. Individual high burnup, high heat-rated fuel rods might release ten times the above amounts with the burst.

Following the burst release, the amount of cesium and iodine remaining in the gap space will diffuse out of the rupture opening. This diffusional escape of the gap contents is a slow process and is quantitatively considerably smaller than the burst release unless the fuel rod temperature is raised several hundred K above the burst temperature and held for times longer than 10 min. The LOCA source term model(4.8) provides a method for calculating diffusional release from the gap space.

Beginning at ~1350°C, fission gases, cesium, and iodine previously accumulated at the grain boundaries are released. Higher temperatures are probably required for low burnup fuel in which the concentration of fission products is lower. The mechanism is driven by the formation, swelling, and coalescence of bubbles of fission gases. At the temperatures involved (>1350°C), the bubbles probably include vaporized cesium and iodine species as well as the noble fission gases. The expanded bubbles work to mechanically separate the grains allowing escape of gas and vapor, and also link together to form tunnels, many of which apparently reach open voids. Approximately equal amounts (percentages of total inventory basis) of noble fission gas, cesium, and iodine are released from the grain boundaries.(4.6) For a high burnup fuel rod, ~20% of the total initial fuel rod inventory of stable isotopes of the above elements would be released. Release from the grain boundaries of lower burnup fuel would probably be less, and temperatures as high as 1800°C might be required.

At completion of the burst release, diffusional escape of the gap inventory, and release of the grain-boundary inventory, ~60 to 90% of the noble fission gases, cesium, and iodine remain in the UO_2 grains. This mechanism follows solid state diffusion mechanics in which the fraction

briefly below, provide fission product behavior information that will require more detailed analysis.

Tests of R. A. Lorenz et al. - commercial fuel rod segments(4.5-4.8)

Fifteen tests were performed with 30.5-cm segments of fuel rods from the H. B. Robinson-2 PWR and the Peach Bottom-2 BWR in steam atmosphere. Holes were drilled in the Zircaloy cladding or the test segments were pressurized and ruptured in the temperature range 850 to 960°C to allow escape of fission products. The test matrix ranged from 20 h at 500°C to 3 min at 1610°C. Released fission products were carried in the flowing stream into a collection system composed of a thermal gradient tube, high efficiency filter papers, and both heated and cold charcoal traps. Tests were performed with purified helium in which the pellet-to-cladding gap space was purged of the readily releasable fission products while heated incrementally from 700 to 1100 or 1200°C. Heating was by either a tubular electrical resistance furnace or by direct induction heating of the Zircaloy cladding. The fission product species monitored were ^{85}Kr, ^{134}Cs, ^{137}Cs, and ^{129}I. Frequently ^{106}Ru and ^{125}Sb were detected.

Tests of G. W. Parker et al. - crucible heating of UO_2 in helium(4.4,4.9)

G. W. Parker et al. investigated the release of fission products from bare UO_2 in purified helium. Trace-irradiated whole PWR-type pellets and pieces of pellets with 1000 and 4000 MWd/MT burnup reirradiated to trace levels were tested. The trace-irradiated whole pellets were 7 g each, and the chunks of higher irradiated material weighed 0.1 to 0.2 g each with ~10 pieces used in each test. The UO_2 samples were located in an induction-heated tantalum crucible so that there was no temperature gradient; the time at temperature was usually 5.5 h and the range 980 to 2270°C was investigated. The fission gas isotope ^{133}Xe was monitored continuously for release; the release of other fission product isotopes was measured only at the end of each test. Parker et al. also measured fission product release from trace-irradiated UO_2 pellets melted in tungsten crucibles in purified helium. The test parameters included molten times from 0.4 to 10 min, two different helium flow rates, and two different pellet densities.

Tests of H. Albrecht et al. - SASCHA fuel melting tests(4.10,4.11)

In these tests 150 g of Zircaloy-clad fuel pellets and stainless steel are melted in a ThO_2 crucible in atmospheres of flowing argon, air, or steam. Because of eutectics formed between the various components, the mixture becomes essentially completely molten at about 2300°C. An induction heated tungsten cylinder surrounds the crucible and heats the test sample by conduction and radiation. The usual heatup rate is ~110°C/min.

The UO_2 pellets are especially fabricated to contain a variety of radioactively traced fission product simulants in concentrations equivalent to a burnup of 44,000 MWd/MT. The cladding and stainless steel may

have been irradiated to provide tracers for typical neutron activation products. Most of the released material forms a dense smoky aerosol. Roughly half of the released material settles (by gravity or diffusion) on the glass container and half reaches the filter papers that are monitored continuously by a multichannel GeLi detector. A higher percentage of the more volatile species (i.e., Cs and I) reach the filter papers whereas most of the less volatile materials (U and Zr) deposit on the

Power Burst Facility (PBF)(4.12,4.13)

The PBF is a specialized test reactor designed to test nuclear fuel and components under off-normal operating conditions. The facility is made up of an open pool reactor which is used to drive the nuclear operation of test fuel in a separate in-pile coolant loop. The experiments are mounted in a in-pile tube and cooled by a separate high pressure coolant loop. An experiment consists of one or more LWR-type fuel rods, 0.91 m in length, each mounted in individual coolant flow shrouds inside an instrumented test train. The loop coolant system provides the experiment with water at pressures, temepratures, and flow rates typical of normal operation in a BWR or PWR and any off-normal conditions necessary to simulate a particular accident.

Fuel rods that fail as a result of testing, or rods that may be defective and allow fission products to leak from their interior, produce a fission product source term to the circulating water. A sample of the loop coolant is taken from a tap just upstream of the loop strainer and directed to a shielded detector enclosure. The identity and quantity of radioactive fission products released from test fuel rods can be monitored using on-line gamma spectroscopy techniques to provide an indication of rod failure, the time of the rod failure, and concentration histories of the short-lived fission products within the loop coolant.

Other current in-reactor tests - Halden and SILOE

In the Halden reactor, the test assembly IFA-430 contains four 1.28 m long fuel rods loaded with 10% enriched UO_2 pellet fuel.(4.14) Two of the rods are used in fission gas release experiments; each is instrumented with a centerline thermocouple and three axially spaced pressure sensors. These two rods are of typical LWR design with diametral gap sizes representing beginning of life and end of life conditions, respectively. The rods are connected to a gas flow system which permits the fission gases released to the gap to be swept out of the fuel rods to a gamma spectrometer where the isotopic content is quantitatively measured. Only the gaseous isotopes can be measured directly because of the cool sampling lines. The release of ^{135}I can be measured by counting the ^{135}Xe daughter following reactor shutdown. Measurements of ^{131}I and ^{133}I release are also made but with somewhat less accuracy.

In the SILOE reactor in Grenoble, France,(4.15) the emission of fission products from PWR fuel rods containing small defects is being measured in a pressurized water loop. Test parameters include hole location and type, fuel rod linear power, and power cycling effects. A loss-of-coolant accident (LOCA) test series has been initiated.

of initial inventory released increases with the square root of time. Release from the grains is insignificant at cladding burst temperatures (750-1100°C), but the fractional release rate doubles approximately every 100°C so that by 2000°C the fraction of remaining inventory released is about 10%/min for fission gas, cesium, and iodine.

The fifth major release mechanism is escape from molten fuel. The formation of molten material begins with the melting of iron and nickel based alloys (if present), and low melting-point materials in control rods, followed by the melting of Zircaloy and the formation of eutectics. The details of the melting process are complex and imperfectly understood partly because chemical transformations occur simultaneously with the melting process which alter the melting points of key materials. For example, while Zircaloy melts at ~1800°C, oxidation to ZrO_2 occurs at the same time during many accidents, producing a material with a melting point of ~2700°C. Therefore, whether clad melting or clad oxidation occurs more quickly in an accident sequence can profoundly affect the subsequent course of events.

Similarly, both physical and chemical processes occur during fuel pellet melting, some of which are described in Section 4.4. The presence of molten cladding has a prominent effect on the pellet material as it approaches its melting point. At elevated temperatures, zirconium diffuses into the pellet, reducing a part of the UO_2 to form a metallic phase with much lower melting point. Therefore, fission products whose chemical affinities would cause them to move into the metallic phase would evolve more rapidly during melting than those that are retained in the higher melting UO_2 phases. Thus, the melting process has some struture, and the simple model employed by the commonly used code, where the amount of fission product released was assumed proportional to the fraction of the core melted, must be seen as a provisional oversimplification. A mechanistic model for fission product release from melting fuel would be based upon (1) the vapor pressure of fission products in their appropriate chemical form and in the appropriate phase (metallic or oxidic), and (2) transport effects from the melting surface to bulk of the gas phase.

A mechanistic analysis of noble gas movement in the UO_2 pellet has been incorporated into the GRASS code.[4.31] A series of mechanisms effecting migration are postulated in this code including bubble nucleation and resolution, bubble diffusion, bubble coalescence, channel formation, fuel microcracking, and grain boundary diffusion. Therefore, this code may be used to provide an insight regarding the effect of noble gas concentration on these principally mechanical processes in the fuel. At present, extension of the GRASS code to reactive, volatile fission products is in an early, formulative stage.

4.2.2 Fission Product Release Experiments

Three sets of experiments (Lorenz et al., Parker et al., and Albrecht et al., described below) have been selected to provide the data base for fission product release from LWR fuel rods. Many other tests, described

Older in-reactor tests

Most of the earlier in-reactor fission product release tests emphasized the measurement of release of long half-life isotopes from pre-irradiated fuel. On-line monitoring capability was limited so that little was learned about the release of short half-life fission products. Several specialized sweep-gas facilities existed for the continuous measurement of fission gas release which did emphasize measurement of short half-life species as do the current in-reactor tests (PBF, Halden, and SILOE).

Parker et al.(4.16) conducted two LOCA fuel rod failure test in TREAT reactor with bundles containing six LWR fuel rods 60 cm long prepressurized with helium. Fission heat in the pellets simulated the LOCA decay heat; fission product release from the preirradiated center rod was measured following the Zircaloy cladding expansion and rupture. Parker et al.(4.17,4.18) also measured fission product release from short low-burnup fuel pins transient-heated to melting under water in the TREAT reactor. More than 20 tests were performed with miniature fuel pins heated by internal fissioning in the Oak Ridge Research Reactor (ORR).(4.19) Test parameters included cladding material (stainless steel or Zircaloy), atmosphere (dry air, moist air, dry helium, moist helium, steam-air, and steam-helium-hydrogen mixtures) burnup (20 to 26,500 MWd/tonne), gas flow rate, and temperature (estimated 2000 to 2900°C).

Other out-of-reactor tests

Castleman and Tang(4.20) measured fission product release from trace-irradiated uranium (metal) and uranium-molybdenum alloy fuels in air and helium. A quartz thermal gradient tube was used in an attempt to characterize the chemical forms of the released cesium and iodine. D. Davies et al.(4.21) measured the release of fission products from trace-irradiated UO_2 in hydrogen in the temperature range 930 to 2200°C. Many of the UO_2 samples were powders or in other high surface-area forms. The apparatus permitted the periodic measurement of released xenon cesium, iodine, and tellurium. Hillary and Taylor(4.22) performed tests with stainless-steel clad UO_2 fuel pins with various defects releasing fission products into a CO_2/CO mixture. Burnup ranged from 10 to 10,000 MWd/tonne. Decay time was usually 1 month so that short half-life isotopes could be measured. The emphasis was on comparing xenon, iodine, and cesium releases. Collins et al.(4.23) measured release from low burnup Zircaloy clad UO_2 heated to ~2000°C. Seven tests were performed at 1000°C in steam. The emphasis was on testing systems for trapping iodine, not on fission product release. G. W. Parker et al.(4.24) performed tests in the Containment Mockup Facility (CMF) and the Containment Research Installation (CRI) using either irradiated fuel or simulated fission products. Most tests were conducted in steam-air atmospheres; the emphasis was on fission product behavior in containment vessels. Other fission product release experiments(4.4) included the oxidation of LWR fuels, melting of LWR fuels, and a variety of tests with non-LWR fuels.

4.2.3 Best-Estimate Fission Product Release Rates

As discussed in Section 4.2.2, fission product release occurs as a composite of at least five different mechanisms, each of these mechanisms is dependent on many variables. The parameters controlling release include burnup (concentration), fuel density, grain size, and power (temperature) cycling, but the most important are temperature and time.

For simplicity we expressed the data from the first three sets reviewed in Section 4.2.3 (Lorenz et al., Parker et al., and Albrecht et al.) in terms of time and temperature by calculating a fractional release rate coefficient, k, (fraction of remaining isotope released per min) defined as

$$k = \frac{df}{dt}$$

where f = fraction of current inventory and
t = time (min) .

In most experiments the release rate, df/dt was not monitored continuously, for these the value of k was estimated from the test end point, the total fractional release and total time:

$$k = \frac{-\ln(1-F)}{t}$$

where F = total fraction released and
t = total test time (min) .

For tests in which the temperature was changed incrementally or continuously and the fission product release monitored continuously, we calculated the release rate coefficient in this manner:

$$k = \frac{\Delta f}{\Delta t}$$

where Δf = fraction of current inventory released, and
Δt = increment of time for which Δf was measured (min) .
The burst release amounts were not included in determining the release rate coefficients.

The results of these release rate coefficients are shown in Figs. 4.1 and 4.2. The large extent of scatter in results is not surprising. In order to obtain the best estimate release for typical reactor fuel rods, the following guidelines were observed.

(1) The H. B. Robinson results for temperatures <1200°C were considered to be very low because of the small pellet-to-cladding gap space and the low inventory of fission products in the gap space.

(2) The H. B. Robinson results at 1200°C were considered to be low because of the low gap inventory. (This test segment and the Peach Bottom-2 test segment used at 1200°C had been ruptured previously so that the pellet-to-cladding gap was opened to a realistic size for a ruptured fuel rod.)

ANOTHER REF.
DAVE COLLINS
J. NUC. ENG (1966)

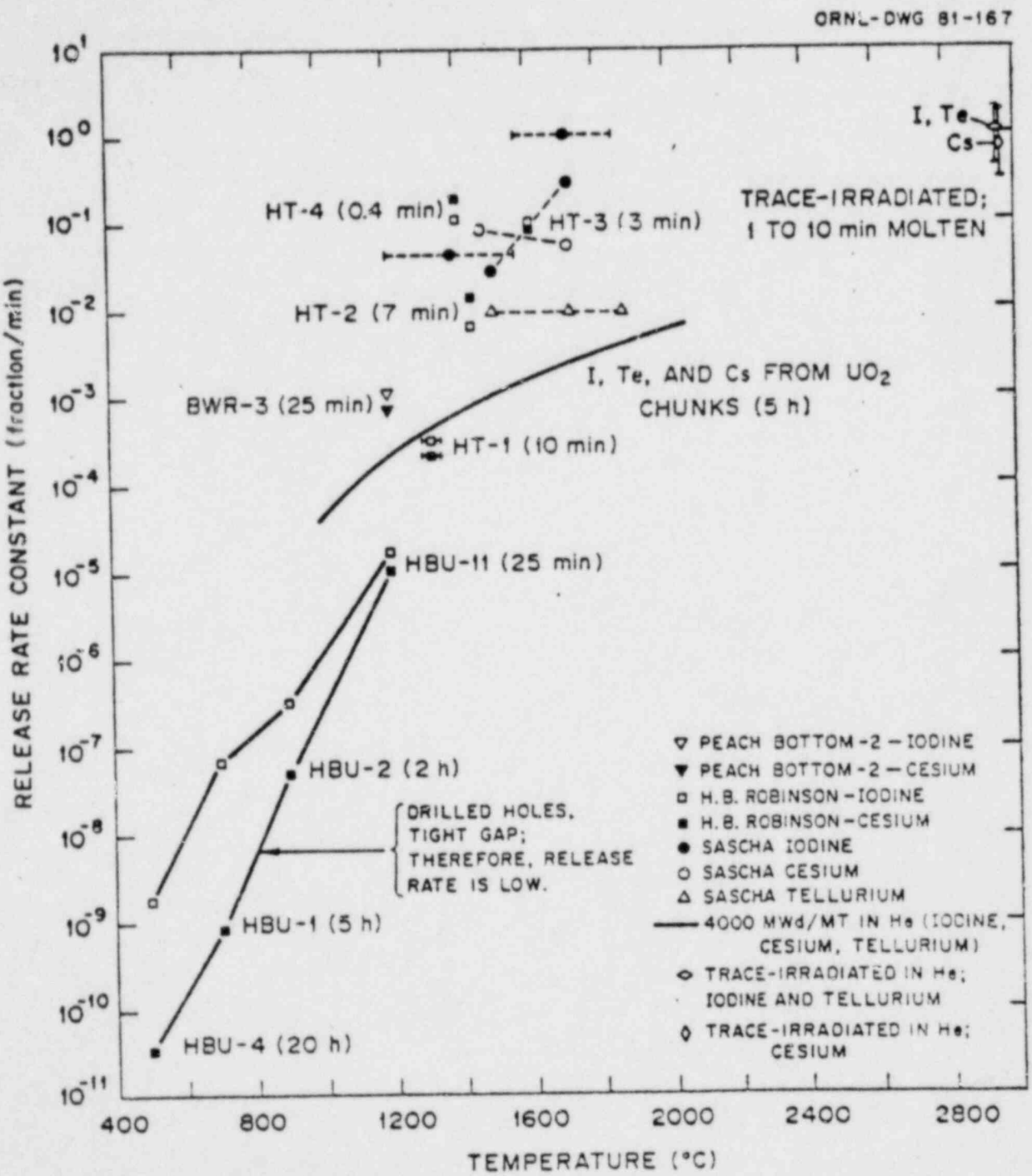

Fig. 4.1. Release rate constants from fuel — noble gases and volatiles.

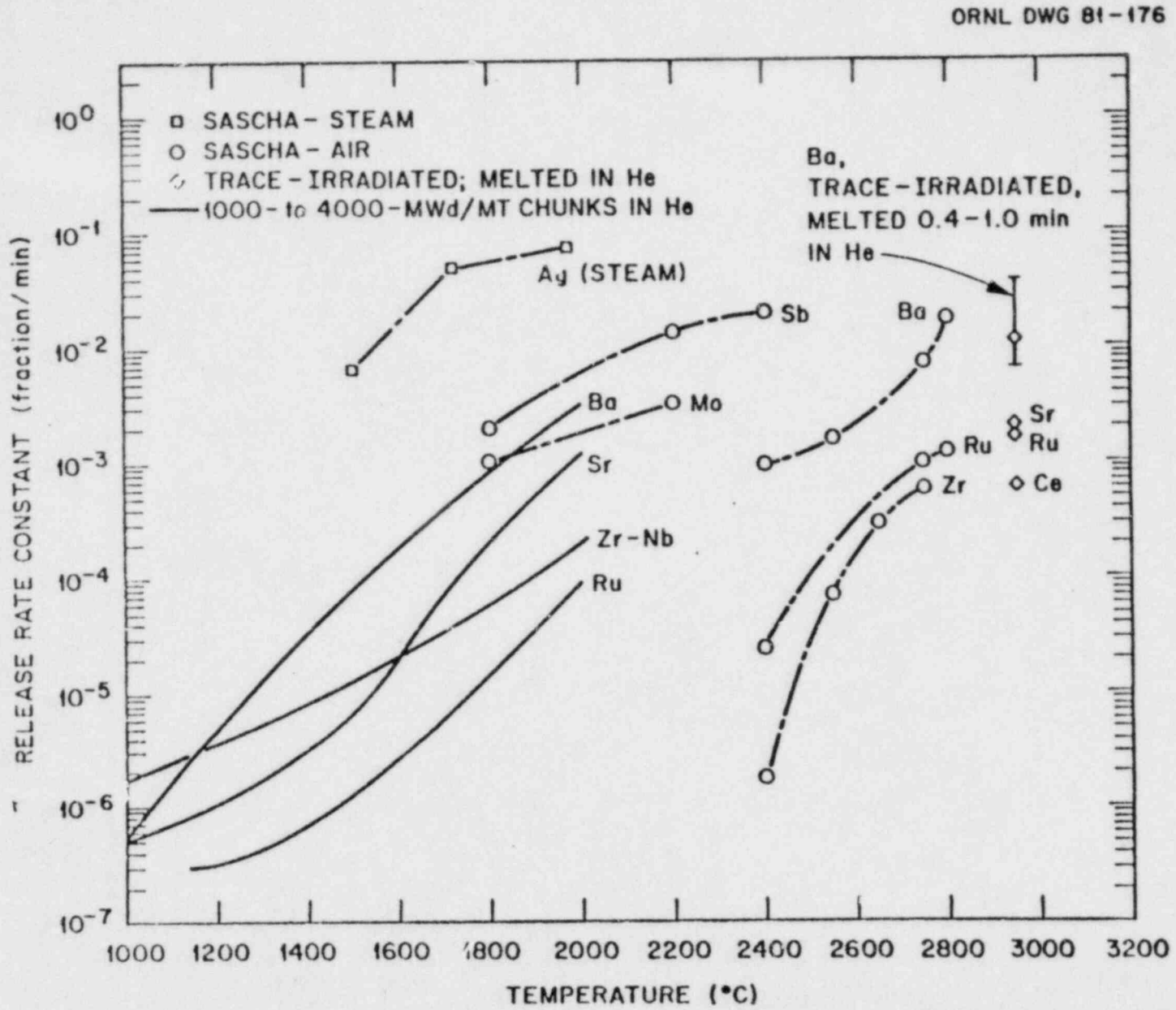

Fig. 4.2. Release rate constants from fuel – low volatiles.

4.20

(3) The Peach Bottom-2 results at 1200°C were high because of the high gap inventory.

(4) The H. B. Robinson results at 1300-1350°C might be somewhat low because of the low gap inventory.

(5) The H. B. Robinson results at 1400, 1445, and 1600°C were high because of the short heating times and the one-time rapid release of the grain boundary inventory.

(6) The SASCHA results for iodine and cesium were high because of the method of incorporating the simulants in the pellets.

(7) The results of Parker et al. between 1000 and 2200°C were for an overall time period of 330 min and would probably have been lower for shorter heating times. No Zircaloy was present for possible trapping.

(8) Release results from Parker's melting tests were probably low because of low concentration.

(9) No special compensation was made for differences in atmosphere.

The best estimate results for release from typical LWR reactor fuel in steam are shown in Fig. 4.3. These release rate coefficients strictly apply only to fuel rod amounts equivalent to 20 or 30 cm in length and for heating times of 10 to 50 min.

As seen in Fig. 4.1, the scatter on the value of the fuel release coefficient for cesium and iodine is about plus or minus one order of magnitude. The smoothed curve through these points in Fig. 4.3 may therefore be taken to be accurate to this degree. (However, we should emphasize that a large uncertainty in the value of the release rate coefficient does not infer that total fission product releases are uncertain to this degree. The uncertainty effects only the rate of release from fuel; i.e., the amounts released up to a specified temperature in for given heatup rate. There exists an insufficient body of data to approximate an accuracy for the low volatiles (Fig. 4.2). In this absence, we assume that roughly the same accuracy exists for the low volatiles, i.e., plus or minus one order of magnitude. It should be emphasized that the factors shown in Fig. 4.3 represent the slower release mechanisms; noble gas burst release of ~3% for PWRs and ~4% for BWRs is not included.

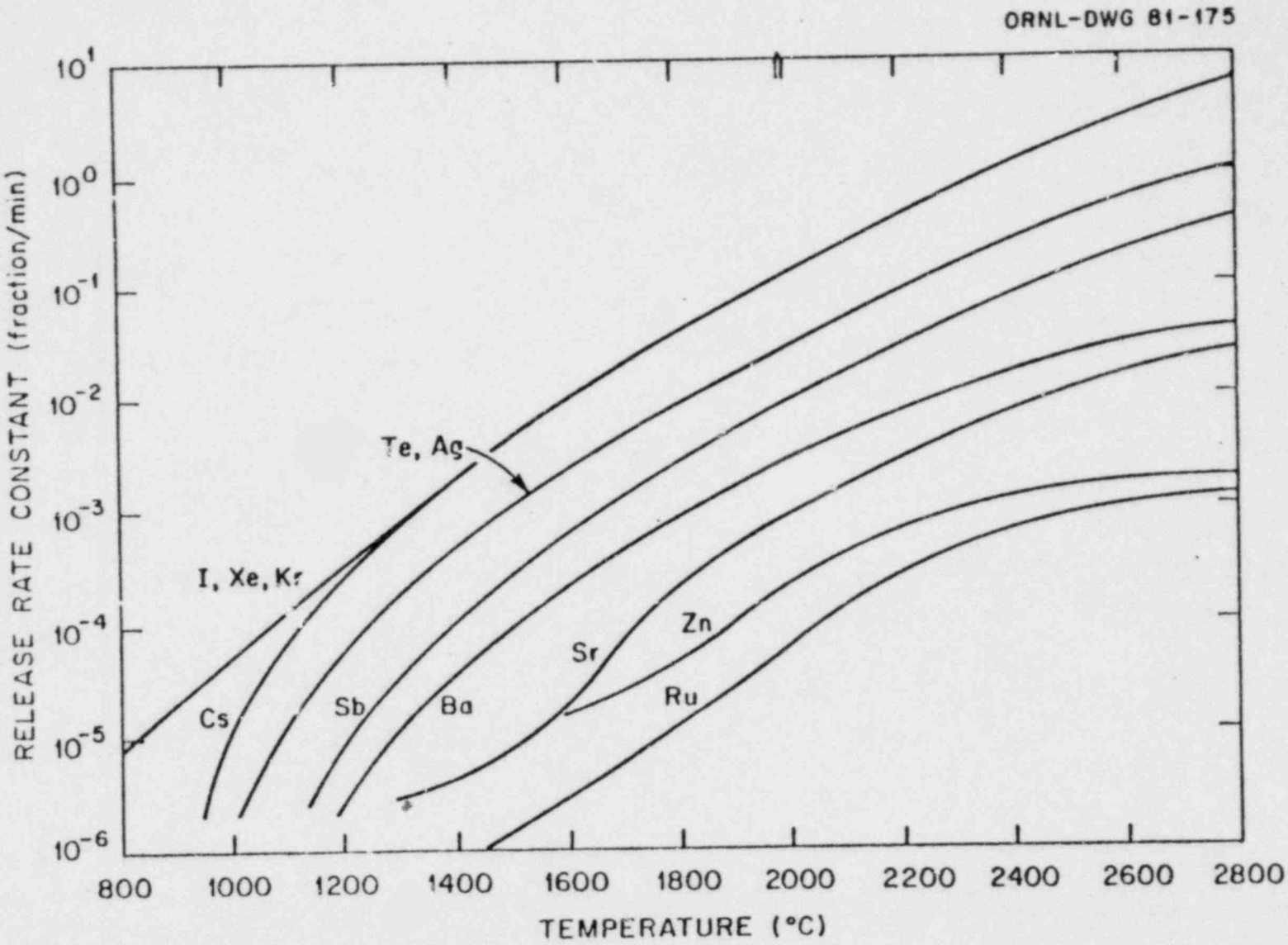

Fig. 4.3. Fission product release rate constants from fuel – smoothed curves.

4.22

Lesson 12 — FISSION PRODUCT TRANSPORT
CHARACTERISTICS AND RELEASE PATHWAYS

Introduction

1. Lecturer —

2. Purpose — To describe the basic chemical characteristics that affect the transport of several groups of key fission product nuclides and to identify potential pathways for the release of these fission products to the containment or to the environment.

Objectives

The following material is covered in Lesson 12:

1. The basic chemical characteristics (qualitative) that affect the transport of key fission product nuclides.

2. Basic facts on how fission products will behave following a reactor accident.

3. Identification of potential pathways for the release of fission products into the containment or into the environment.

4. Rapid identification of fission product release pathways so that they can be expeditiously terminated.

The following key points are to be retained:

1. The noble gases will follow the steam and will accumulate wherever there is a gas phase, i.e., the pressurizer steam space, the makeup tank gas space, or the containment atmosphere.

2. The iodine activity can exist in many forms, but in general if water is readily available, 99.9%$^{+}$ will tend to be in the liquid phase.

3. If for some reason the accident is a dry one, i.e., no water in the reactor and no steam in the containment atmosphere, there is likely to be a very large source of iodine and cesium aerosols airborne in the containment, which should be removed as quickly as possible using the reactor building sprays.

4. The activity re ease pathways that develop during a reactor accident are not necessarily the intuitively obvious pathways but are more likely to be obscure, forgotten pathways.

LESSON OUTLINE

1. Chemical and Transport Characteristics of Fission Products
   - 1.1. Noble Gases
   - 1.2. Iodine
     - 1.2.1. Elemental Iodine
     - 1.2.2. Hypoiodous Acid
     - 1.2.3. Organic Iodide
     - 1.2.4. Cesium Iodide
     - 1.2.5. Particulates
   - 1.3. Cesium
2. Fission Product Release Pathways
   - 2.1. Pathways From RCS to Containment
   - 2.2. Pathways Into Auxiliary Building
   - 2.3. Pathways to the Environment
   - 2.4. Release Pathways Identified at TMI-2
3. Summary

Lesson 12 — FISSION PRODUCT TRANSPORT CHARACTERISTICS AND RELEASE PATHWAYS

1. Chemical and Transport Characteristics of Fission Products

The basic purpose of this section is to give the reactor operating staff a better understanding of how key fission products will behave following a major accident.

1.1. Noble Gases

The noble gas nuclides — primarily Kr-85, Kr-88, Xe-131m, Xe-133m, and Xe-133 — will always follow the steam and/or coolant flow and will accumulate wherever there is a gas phase, i.e., in the pressurizer steam space, in the makeup tank cover gas, or in the containment atmosphere. A significant fraction of all noble gas nuclides will be soluble in the reactor coolant while the system is at a high pressure, but the gas will rapidly leave the liquid phase upon depressurization. After 10 to 20 minutes at atmospheric pressure, less than a few percent will remain in solution. All noble gases are chemically inert, so there is no effective way to remove them following a reactor accident other than to attempt to contain them and wait for decay, which should take 60 to 70 days. After this period, the remaining noble gas activity is so small that it no longer presents a significant offsite radiological risk.

1.2. Iodine

The behavior of iodine nuclides — primarily I-131, I-133, and I-135 — is complicated by the fact that the iodine can exist in several different chemical forms, each of which has somewhat different behavior characteristics.

1.2.1. Elemental Iodine

Elemental iodine in a dry environment is very volatile at all temperatures above room temperature. If water is present, the elemental iodine will quickly react with it in the following manner:

$$I_2 + H_2O \rightarrow H^+ + I^- + HOI$$

$$3HOI \rightarrow 3H^+ + 2I^- + IO_3^-$$

The first of these reactions is very rapid; the second is much slower. There are several things to note about these reactions:

1. They produce H^+, which tends to make the solution more acid, so the reaction will proceed more rapidly if the solution is alkaline (basic).

2. If the reactions went to completion, there would be no iodine activity in the gas phase; however, in most reactor environments some iodine (0.01 to 0.1%) is always detectable in the gas phase. There is speculation that HOI (which is called hypoiodous acid) is somewhat volatile, and since the HOI concentrations are so low, the second reaction proceeds very, very slowly and does not go to completion.

In some plants sodium hydroxide or trisodium phosphate is added to the containment sump water or the reactor building spray solution to make the solution more basic and to increase the iodine removal rates.

If elemental iodine (I_2) becomes airborne as a vapor, it can be removed very quickly by the reactor building sprays. The removal half-time is approximately 2 to 3 minutes. Charcoal filters also remove elemental iodine very effectively. The previous operating history of the charcoal filters does affect the removal effectiveness to some degree, but in general the removal effectiveness remains high. Of course, if gross condensation occurred in the charcoal bed, the pore structure would become clogged with water and the absorption effectiveness of the charcoal would be destroyed. (An important point to remember about charcoal is that it acts to lower the vapor pressure of materials passing through it; therefore, condensation could occur at relative humidities of about 90%.)

1.2.2. Hypoiodous Acid

The formation of hypoiodous acid was discussed previously. The small fraction which may become airborne is not removed very effectively by the reactor building sprays but does seem to be retained reasonably well by dry charcoal (90 to 95% retention efficiency).

1.2.3. Organic Iodide

The exact source of organic iodides is not known, but since the bulk of the organic iodide is known to be methyl iodide (CH_3I), it is believed that the iodine reacts with the methane (CH_4) in air. The containment air has many times more methane than needed to react with all the iodine in the core. The classic reaction is written as follows:

$$I_2 + CH_4 \rightarrow CH_3I + HI.$$

However, there is some evidence that this reaction is improbable in the gas phase and that the reaction might actually be

$$HOI + CH_4 \rightarrow CH_3I + H_2O.$$

In any event, the end product is the formation of methyl iodide or another organic iodide, e.g., ethyl iodide.

It appears as though only about 2% of the iodine released from the fuel ever appears in the form of methyl iodide. This is fortunate because methyl iodide has a high volatility, is not very soluble, is not very reactive, and is difficult to remove from the containment atmosphere. The containment sprays are relatively ineffective for removing methyl iodide (removal half-times of 1 to 2 days). Charcoal filters are relatively effective at removing methyl iodide (90 to 98% efficient) if the charcoal is fresh and dry. If the charcoal is old or if the relative humidity is 70 to 80%, the efficiency will be much lower, probably 30 to 60%.

1.2.4. Cesium Iodide

As discussed in Appendix 11-A, there are some relatively new data that suggest that the elemental iodine produced in the fuel rapidly reacts with the fission product cesium to form cesium iodide (CsI). Cesium iodide is volatile at high temperatures (2200 to 2400F). Under dry conditions, the vapor would condense to CsI aerosol particles as soon as it cooled. Under moist conditions, the CsI would probably condense as cesium oxide particles. The dispersed aerosols are removed more slowly by the reactor building sprays than elemental iodine would be, but the removal half-time is still relatively fast (15 ± 5 minutes). The real importance of the CsI premise is that cesium iodide is extremely soluble in water and thus whenever the release pathway is wet (i.e., via the RC quench tank) or wherever steam is condensed to water,

the CsI will be retained in the water and will not escape from the containment with other gases. The formation of cesium iodide is one possible explanation of why the iodine release from the TMI-2 accident was so low. (Of the almost 40 million Ci of I-131 released from the fuel, 3 million escaped into the auxiliary building. Only about 400 Ci of the 3 million volatilized. Ninety-five percent of the 400 Ci volatilized was collected by the charcoal filters in the exhaust ventilation system. Thus, only 15 Ci escaped into the atmosphere.)

1.2.5. Particulates

Particulate iodine forms consist of either CsI aerosol particles formed by the condensation of CsI vapor or iodine activity adsorbed on the surface of other aerosol particles. As previously stated, aerosol particles are removed reasonably well by the reactor building spray system. Aerosols can be removed by HEPA filters with a 99.9%$^{+}$ efficiency (assuming, of course, that the accident or its environment has not damaged the filter system).

1.3. Cesium

Like cesium iodide, cesium is volatile at high temperatures (1200 to 1300F). Once volatilized, it will condense as Cs aerosol particles when the vapor cools. In moist environments, Cs reacts with water to form cesium oxide or cesium hydroxide depending on the conditions. In any event, the Cs will almost always be in the liquid phase except during a dry release pathway event, when it is produced in aerosol form.

2. Fission Product Release Pathways

2.1. Pathways From RCS to Containment (Figure 12-2)

There are actually only two different types of pathways from the reactor coolant system (RCS) to the containment — isolable LOCAs and non-isolable LOCAs.

1. Isolable LOCAs can occur at relatively few locations since they require a remotely operated isolation valve to be in the line between the RCS and the source of the discharge into the containment. Typical examples of where isolable LOCAs can occur are as follows:

   a. Failure of the pressurizer's pilot-operated relief valve (PORV) to close; this results in a discharge via the reactor coolant drain tank rupture disc.

   b. Pipe break in the letdown line downstream of the letdown cooler inlet.

   c. Pipe break in the RC pump seal flow return line downstream of the inlet to the flow transmitters.

   d. Failure of the pressurizer sample lines downstream of the isolation valve.

   e. Failure of one or more steam generator tubes.

   Most isolable LOCAs can result in either wet or dry release pathways depending on how long it takes to isolate the leak and on the availability of either makeup or HPI flow.

2. Non-isolable LOCAs can occur due to the failure of any component in the RCS, e.g., the following:

   a. Rupture of a primary coolant loop pipe.

   b. Failure of an RC pump seal or seal flow line.

   c. Failure of a steam generator manway or hand hole or their gaskets.

   d. Rupture of the makeup or decay heat piping connected directly to the RCS.

   e. Rupture of the pressurizer surge line.

   f. Failure of pressurizer safety valves (stuck open or blown off).

   g. Rupture of a control rod drive housing.

   Non-isolable LOCAs have a greater potential for resulting in dry release pathways, but will normally result in a wet release pathway as long as adequate makeup or HPI flow is available.

2.2. Pathways Into Auxiliary Building (Figure 12-3)

Pathways for the release of activity into the auxiliary are isolable provided that the source of the leakage can be determined. Typical examples of these pathways are as follows:

1. Letdown line leakage or overpressurization of its relief valve.
2. Decay heat cooling system leakage or overpressurization of its relief valve.
3. Reactor building spray system leakage or overpressurization of its relief valve.
4. Overfilling of the miscellaneous waste tank or auxiliary building sump tank.
5. Makeup tank leakage or overpressurization of its relief valve.
6. Waste gas system leakage or overpressurization of its relief valve.

In some cases the operator may feel that he cannot isolate the release pathway because he needs the system to safely bring the plant to a stable condition. At TMI-2, the letdown line was probably the largest source of activity release but was never intentionally isolated.

2.3. Pathways to the Environment (Figure 12-4)

The release pathways to the environment are relatively few but are all difficult to isolate once established. Typical examples of these pathways are the following:

1. Leakage in the containment purge valves into the auxiliary building exhaust ventilation system.
2. Leakage via containment closures, e.g., the equipment hatch.
3. Steam safety valve and atmospheric dump valve releases (whenever there is primary-to-secondary leakage).
4. Condenser vacuum pump discharges.
5. Auxiliary building exhaust ventilation system discharges.
6. Liquids discharged via non-radioactive sump drains. (At TMI-2, radioactive liquid entered systems that were typically non-radioactive, e.g., diesel generator building sumps, and were subsequently discharged with non-radioactive wastes.)

7. Leakage of radioactive liquids via cracks in the basement floor of the containment or auxiliary building.

2.4. Release Pathways Identified at TMI-2

1. The pathway via the RC drain tank (RCDT) discharge piping is shown in Figure 12-5. Prior to the rupture of the RCDT rupture disc (which occurred 15 minutes after the accident), the RCDT could have contained pressures of 120 to 190 psig. Depending on the various valve positions, flow from the RCDT could have passed through the four isolation valves and into one or more of the bleed holdup tanks, or it could have overpressurized the relief valve and drained to the auxiliary building sump. If the transfer pumps were running this pathway could have been flowing for about 4 hours.

2. The pathway via the RCDT vacuum breaking system is shown in Figure 12-6. This system is automatically isolated whenever the RCDT pressure is greater than 10 psig. When the RCDT rupture disc blew, the pressure dropped below 10 psig and the isolation valves automatically opened. This pathway then remained open until the reactor building was isolated 3 hours and 40 minutes later.

3. The pathway via the RCDT vent piping is shown in Figure 12-7. This is a potential pathway only if the four valves were open or were leaking. If these valves were open, the pressure in the RCDT before the rupture disc blew (120 to 190 psig) could have forced water into the vent header piping and could have jammed the water drain tap (WDG-U8A) in the open position. In any event, this pathway could have resulted in continuous leakage of both liquid and gas into the auxiliary building. This leakage would have been stopped when the reactor building was isolated 4 hours after the accident.

4. The pathway via the reactor building (containment) sump is shown in Figure 12-8. The reactor building sump pumps were on from 4:08 a.m. until 4:38 a.m., when they were shut off by the operators. During that period approximately 8000 gallons of water was transported to the auxiliary building sump tank. The rupture disc on the auxilary building sump tank had failed several days before the accident, and the tank was completely full. Therefore, this water spilled on the floor of the auxiliary building and, via floor drains, to the auxiliary building sump. After the reactor building sump pumps were shut off, a siphon may have been established between the reactor building sump and the auxiliary building sump tank. This is because, even though there is a 35-foot loop seal and the top of the auxiliary sump tank is approximately 6 feet above the top of the reactor building sump, there was a 2 to 4 psi positive pressure in the reactor building (a driving head of 5 to 10 feet of water) between 6:30 and 7:56 a.m. Also, there was an accumulation of contaminated water on the

reactor building floor, which effectively raised the water depth above the top of the reactor building sump. This flow path was finally isolated at about 8:00 a.m., approximately 4 hours after the accident, when high pressure in the containment caused the isolation of the reactor building.

5. The pathway via the letdown line and makeup tank is shown in Figure 12-9. This pathway is the one most likely to have led to the release of 13 million curies* of Xe-133, not to mention lesser amounts of other noble gases. Essentially all of the offsite dose consequences were the result of this noble gas release. (*Curies all corrected to time of reactor trip.)

   There were probably several release points from time to time along this pathway. The basic cause of the release was the high pressures generated by the large volume of hydrogen contained in the reactor coolant entering the letdown line.

   The most generally accepted release point is associated with the operation of the makeup tank vent valve (MU-V13), which was suspected to be leaking before the accident. Large quantities of hydrogen accumulated in the makeup tank, and thus, the tank had to be vented frequently to avoid excessive pressure. Each time the valve was opened, high radiation alarms in the auxiliary building occurred. What probably happened was that the flow characteristics (C_v) of the valve permitted the gas to vent too quickly. This overpressurized the vent header (which may have had some water loop seals) and caused the radioactive gas to leak out through poorly vented vacuum breaker valves on tanks connected to the vent header or to overpressurize the relief valve on the vent header compressors.

   The next most probable release point was the letdown line relief valve (MU-R3). When the letdown filters plugged, the line would overpressurize and would relieve the excess pressure via MU-R3. The discharge from this relief valve was supposed to be routed to the bleed holdup tanks, but the piping to accomplish this may not have actually been installed.

   Another possible release point could have been the relief valves on the purification demineralizers. When the demineralizers were isolated, the gas pressure could have pressurized the vessels enough to open their relief valves. A similar isolation of the bleed holdup tanks could have resulted in the opening of relief valve WDL-R10.

3. Summary

The key points of this lesson can be summarized as follows:

1. The noble gases will follow the steam and will accumulate wherever there is a gas phase, i.e., the pressurizer steam space, the makeup tank gas space, or the containment atmosphere.

2. The iodine activity can exist in many forms, but in general, if water is readily available, 99.9%$^{+}$ will tend to be in the water phase.

3. If for some reason the accident is a dry one, i.e., no water in the reactor and no steam in the containment atmosphere, there is likely to be a very large source of iodine and cesium aerosols airborne in the containment, which should be removed as quickly as possible using the reactor building sprays.

4. The activity release pathways that develop during a reactor accident are not necessarily the intuitively obvious pathways but are more likely to be obscure, forgotten pathways.

Figure 12-1. Transport Characteristics of Key Fission Products

NOBLE GASES

- WILL FOLLOW STEAM

IODINE

ELEMENTAL (I_2)

- MOST WILL FOLLOW COOLANT DURING WET RELEASE
- MOST WILL BE AIRBORNE DURING DRY RELEASE

CESIUM IODIDE (CsI)

- WILL FOLLOW COOLANT DURING WET RELEASE
- WILL FORM AEROSOLS DURING DRY RELEASE

ORGANIC IODIDE (METHYL IODIDE, CH_3I)

- SMALL FRACTION OF TOTAL IODINE IN AIRBORNE VAPOR FORM

HYPOIODOUS ACID (HOI)

- FORMS IN LIQUID BUT A SMALL FRACTION MAY VOLATILIZE

PARTICULATES

- ELEMENTAL IODIDE OR Cs I AS AIRBORNE DUST PARTICLES

CESIUM

- WILL FOLLOW LIQUID COOLANT DURING WET RELEASE
- WILL FORM AEROSOLS DURING DRY RELEASE

Figure 12-2. eakage Pathways Into Containment

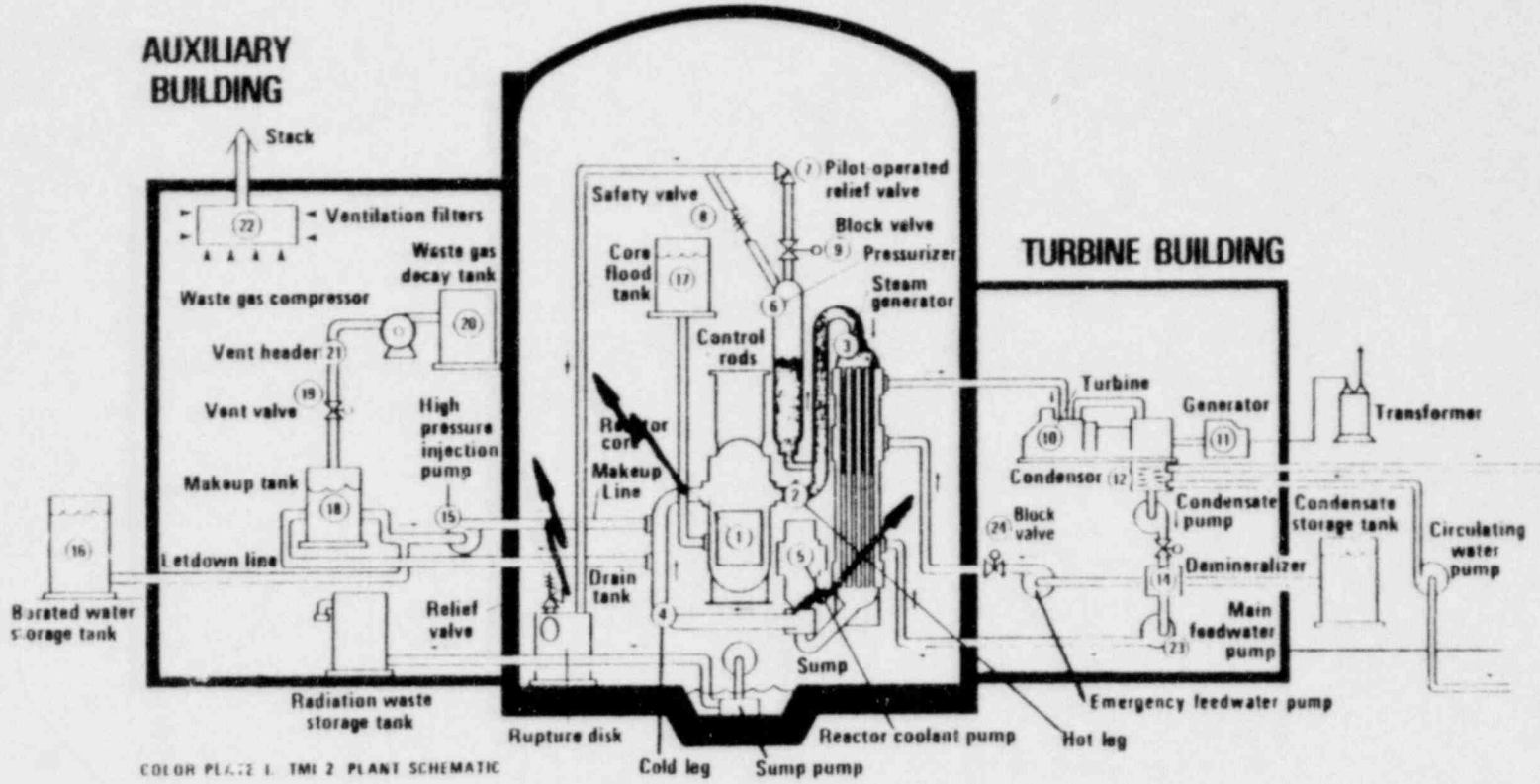

COLOR PLATE I. TMI 2 PLANT SCHEMATIC

Figure 12-3. Leakage Pathways Into Auxiliary Building

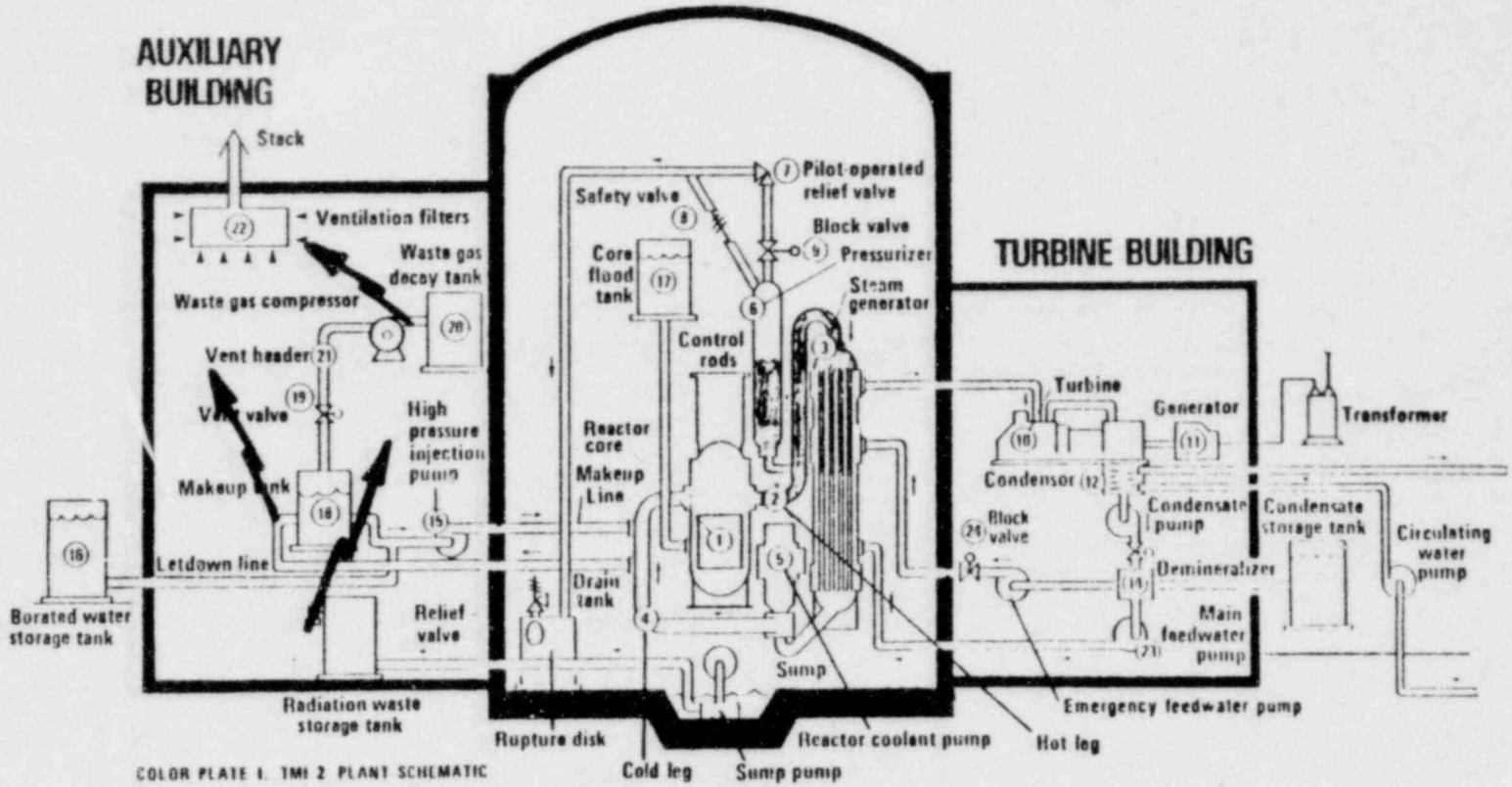

Figure 12-4. Leakage Pathways to the Environment

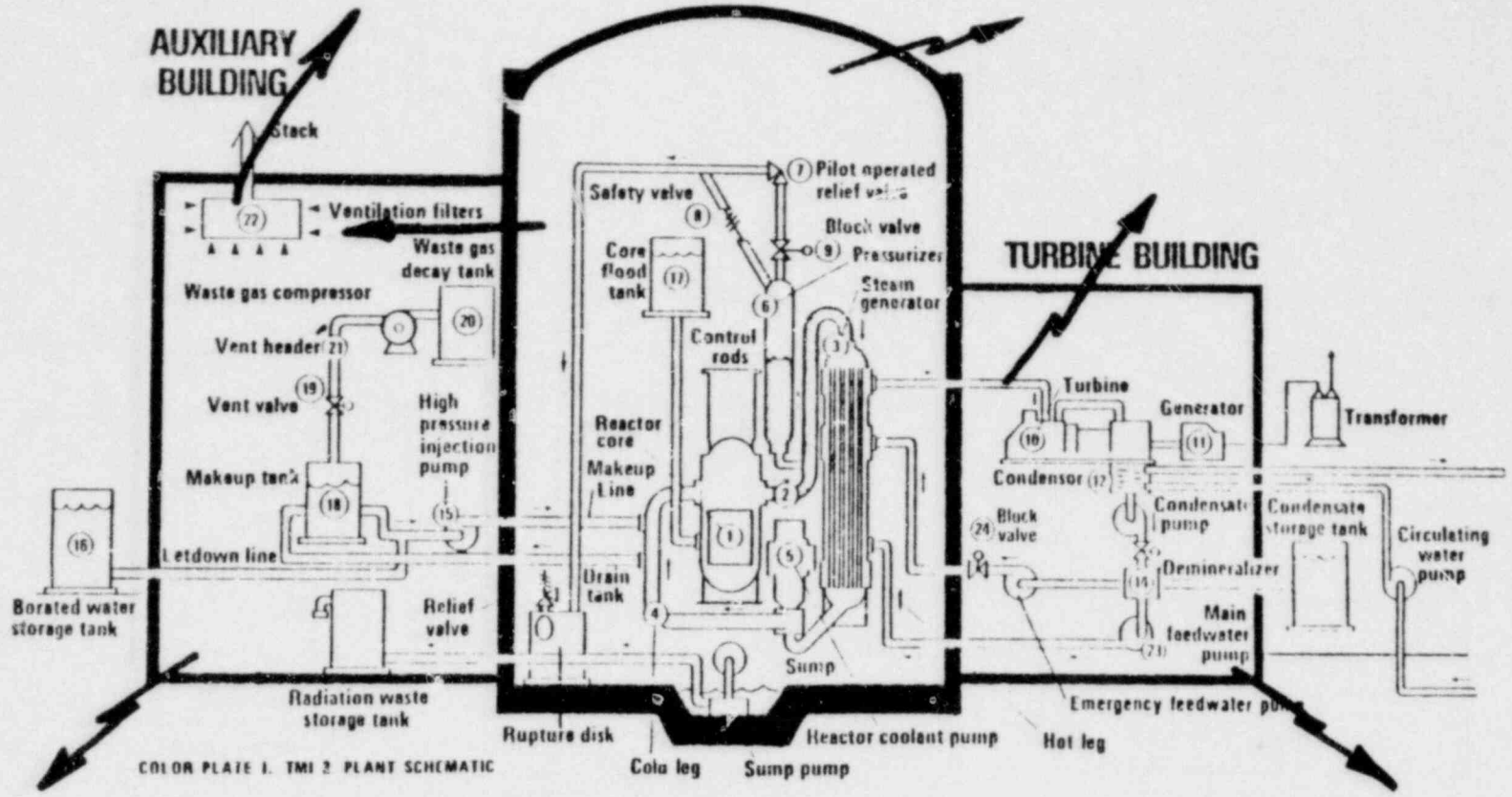

Figure 12-5. Pathway Via RC Drain Tank Discharge Piping

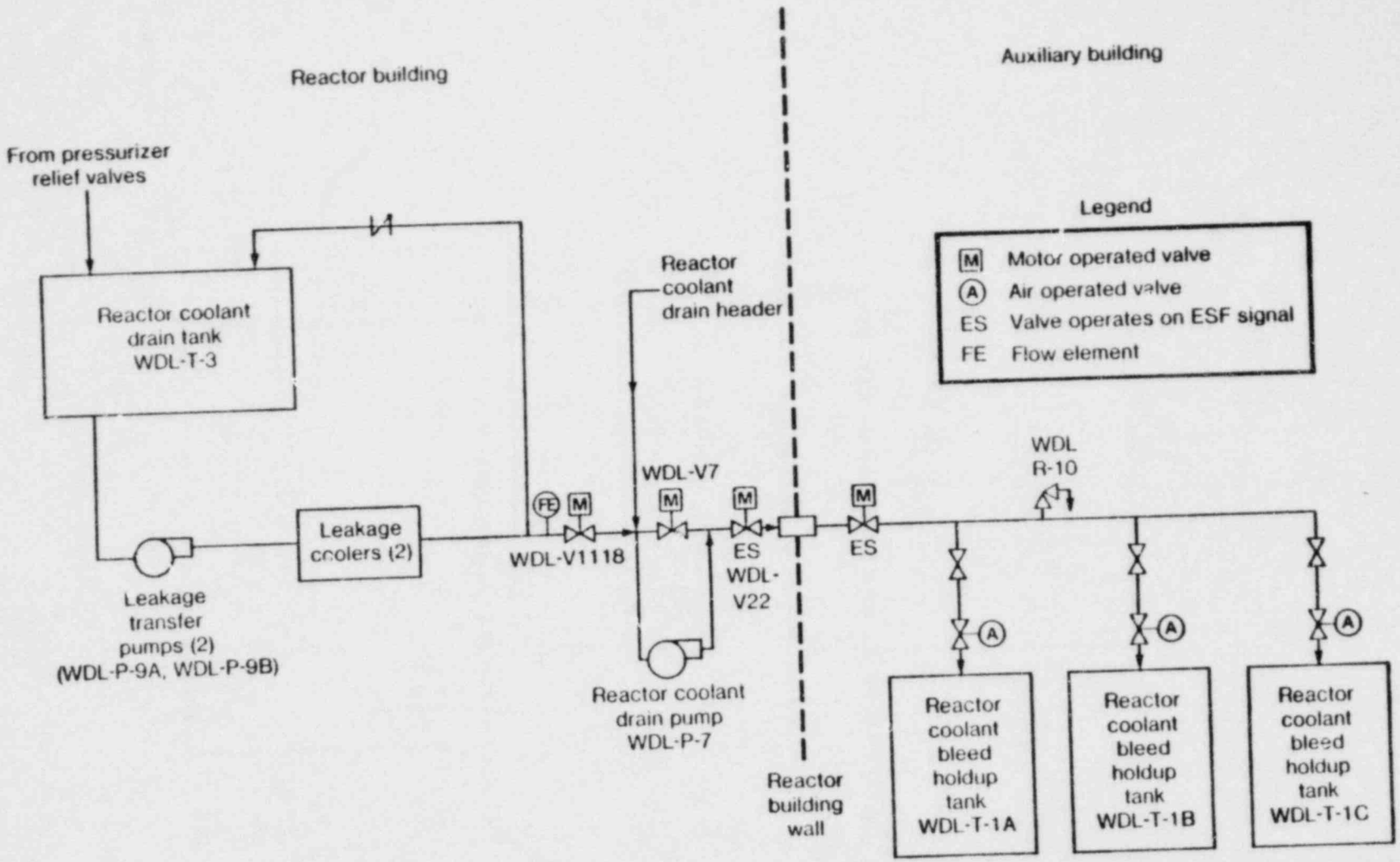

Figure 12-6. Pathway Via RC Drain Tank Vacuum Breaking System

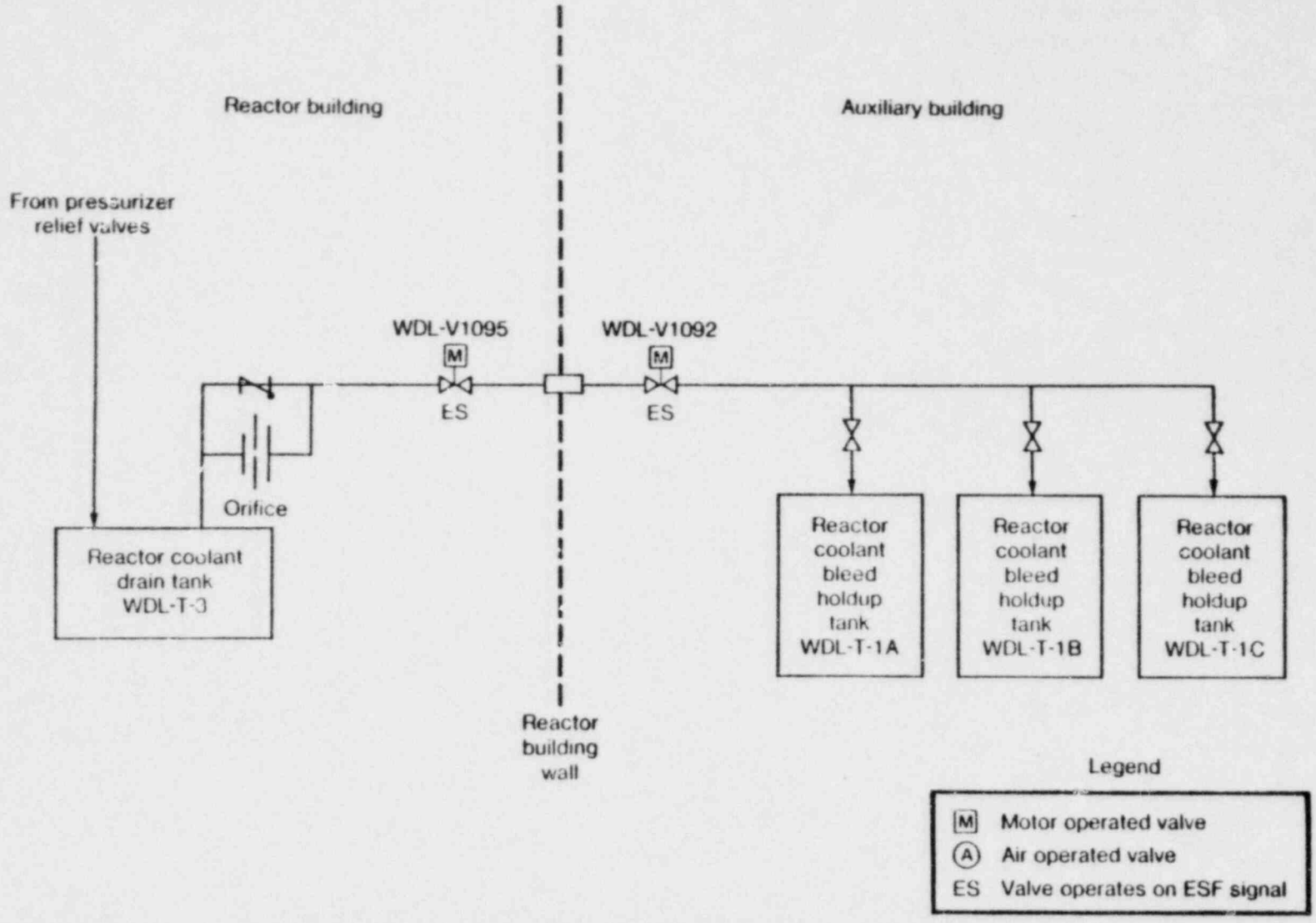

Figure 12-7. Pathway Via RC Drain Tank Vent Piping

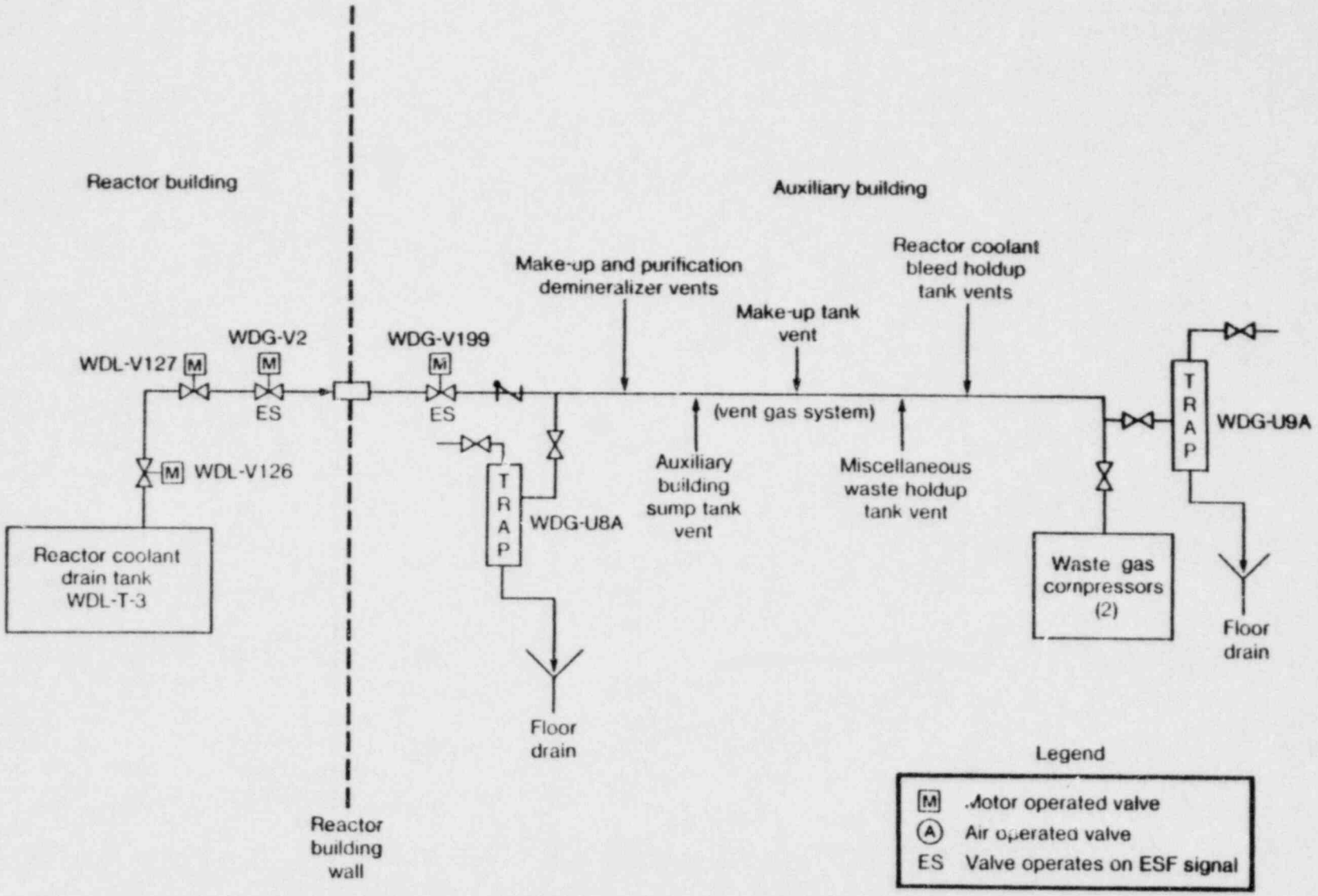

Figure 12-8. Pathway Via the Reactor Building Sump

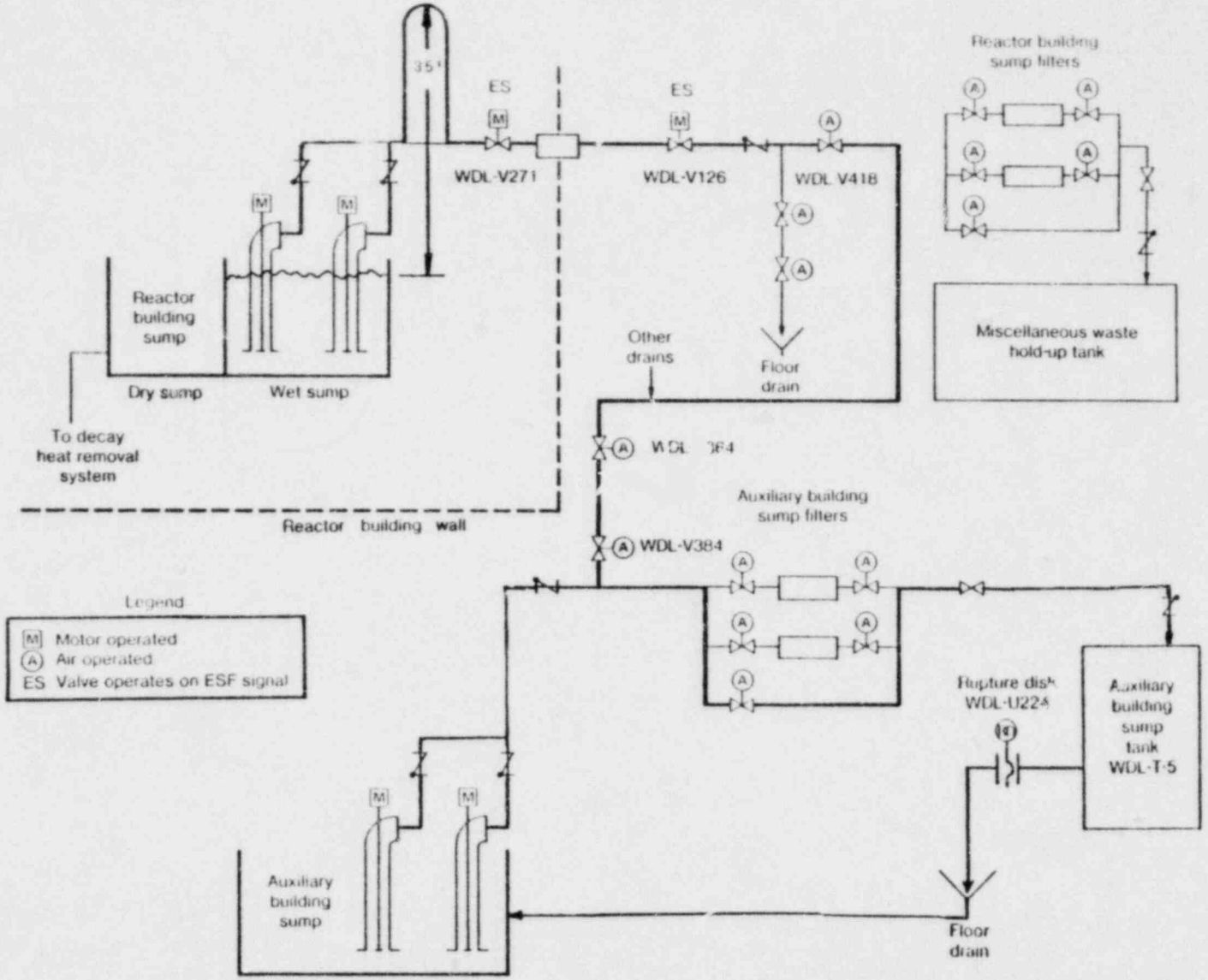

Figure 12-9. Pathway Via the Letdown Line and Makeup Tank

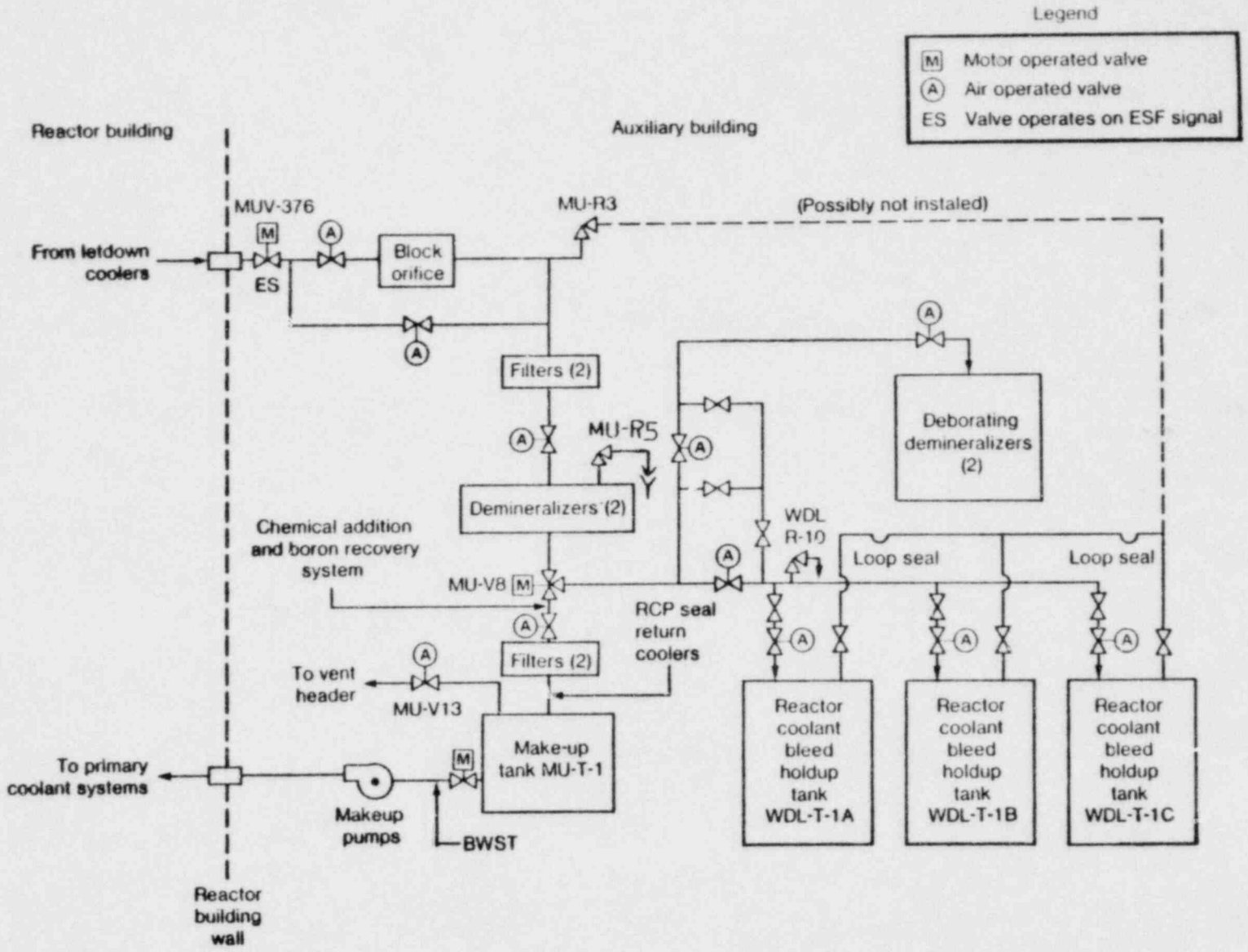

Lesson 13 – RESPONSE OF GAMMA RADIATION MONITORS

Introduction

1. Lecturer –

2. Purpose – To describe the responses that should be expected from various gamma radiation monitors following a reactor accident and to alert the operators to anomalous readings that may occur due to high background radiation, instrument failure, improper calibration, and source concentration gradients.

Objectives

The following material is covered in Lesson 13:

1. The magnitude of the letdown line monitor response as an indication of the degree of core damage.

2. Anomalous readings that have occurred in process radiation monitors and area radiation monitors following the TMI-2 accident and the CR-3 loss of non-nuclear instrumentation event.

The following key points are to be retained:

1. Expected letdown monitor response.

2. Effects that can cause anomalous readings:
   a. High background radiation.
   b. Scale and calibration errors.
   c. Shielding of detectors.
   d. Mixture of fission product nuclides.
   e. Source concentration gradients.
   f. Electrical power supply failures.
   g. Electronic component failures.

LESSON OUTLINE

1. Letdown Line Monitor
2. Process Monitors
3. Area Monitors
4. Reactor Building Dome Monitor
5. Failure Modes
6. Summary

Lesson 13 — RESPONSE OF GAMMA RADIATION MONITORS

The response of gamma radiation monitors to various reactor accident conditions can provide valuable information to the reactor operator which will help him to diagnose the post-accident conditions. Unfortunately, the response of these same instruments can be the source of considerable confusion if the operator is not prepared for the abnormal responses that are associated with accident conditions. This lesson describes typical post-accident responses that might be expected from various gamma radiation monitors in order to alert reactor operators to anomalous readings that may occur due to high background radiation, instrument failure, improper calibration, and nonuniform distribution of the source.

1. Letdown Line Monitor

The letdown line monitor is normally expected to be the first monitor to indicate the release of fission product activity from the fuel; however, as will be shown later in this lesson, the letdown line monitor at TMI-2 did not respond until about 30 minutes after fuel damage had occurred. Notwithstanding the delayed response at TMI-2, the letdown line monitor has the potential (with an expanded monitoring range) of providing the operator with the fastest, most timely means of assessing the amount of fuel damage. Figure 13-1 was constructed based on relative gamma source strength calculations and shows the expected letdown line monitor response to a range of releases. The operator can use this figure to estimate the type and amount of fuel damage asosciated with a particular event. Although most letdown line monitors seem to be designed to cover the range from 10 to 10^6 counts per minute (cpm), it can be seen from the figure that, in order for the reactor operator to gain any useful information regarding significant amounts of fuel damage, the range of the monitor needs to be extended by 5 orders of magnitude (from 10^6 to 10^{11}). The current instrumentation seems to adequately cover the normal operating range of a reactor system. It appears that, if the reactor were operating at its Technical Specification limit on reactor coolant activity,

the shutdown iodine spike might come close to "pegging" the current monitors. Useful information regarding any significant amount of fuel damage cannot be obtained with present instrumentation. If the range were extended to 10^{11}, the operator would be able to promptly identify any additional fuel damage and to promptly make a semi-quantitative assessment as to whether the release corresponds to the gap activity from a few percent to 100% of the fuel rods in the core or whether the release corresponds to a release of activity from 0.2 to 20% of the fuel material in the core.

Notwithstanding the desirability of having a letdown line monitor with sufficient range to respond to accident conditions, the operator must be ever-alert to situations that might prevent the monitor from responding as expected. The most obvious and the most common reason for the monitor not responding as expected (assuming proper maintenance and calibration practices) is that the coolant at the monitor location is not representative of the coolant in the RCS. This can occur for many reasons, e.g., the letdown flow has been manually or automatically stopped, the letdown line block orifice or filter may be plugged, or, as was the case at TMI-2, steam bubbles in the hot legs prevented circulation in the RCS; thus, the coolant entering the letdown line was not mixed with the coolant containing the fission product release.

The response of the TMI-2 letdown line monitor is shown in Figure 13-2. Note that the monitor did not respond until 3 hours after the reactor trip. Fuel damage occurred about 2 hours and 25 minutes after trip, but the monitor did not respond because of lack of circulation in the RCS. The RC pump that was jogged at about 2 hours and 55 minutes after trip enabled the monitor to respond by transporting a slug of activity into the cold leg leading to the letdown line monitor. Also shown in Figure 13-2 is the response of the Crystal River 3 (CR-3) letdown line monitor following the loss of non-nuclear instrumentation trip on February 25, 1980. In the CR-3 event, the RCS circulation was maintained and HPI flow was initiated. The letdown line monitor response was prompt and could be analyzed to show that the decrease in signal was due entirely to HPI dilution and that no additional activity was released due to the transient.

2. Process Monitors

The responses of some of the process monitors following the TMI-2 accident are shown in Figure 13-3. A study of this figure will show that it properly reflects many important events of the TMI-2 transient, but for many reasons this information was more a source of puzzlement than of enlightenment for the reactor operators. In order to facilitate the presentation of this figure, 30 inches of recorder chart were compressed into about 8 inches, and some of the less interesting monitors were eliminated to simplify the figure; thus, certain features are more clearly visible on this figure than on the actual recorder chart.

Note that the first process monitor to respond to the TMI-2 transient was the intermediate cooler monitor for the letdown line in the reactor building. This monitor is primarily intended to detect leakage of radioactive reactor coolant into the intermediate cooling water system, which is non-radioactive but which is apparently at a location where it can respond to the nitrogen-16 activity in the reactor coolant. The time of trip is clearly shown by the sudden decrease in the monitor's signal. This monitor is also located relatively close to the reactor building sump and appears to respond to activity sources in the sump, e.g., when the reactor coolant drain tank (RCDT) rupture disc blew at about 4:12, this monitor reflected the flooding of the sump area with reactor coolant. At about 6:30 this monitor responded to the higher activity water being added to the sump following gross fuel failure at about 6:25 a.m. The letdown line monitor, as previously discussed, only saw pre-accident coolant from the stagnated cold leg; it did not respond to the fuel failure until after an RC pump was jogged, thus sending a slug of highly radioactive coolant into the cold leg feeding coolant to the monitor. The nuclear service cooling monitor and the intermediate cooler monitor are two process monitors in the auxiliary building that are intended to detect leakage of radioactivity into non-radioactive systems. These two monitors, like the intermediate cooler monitor and many other gamma monitors throughout the plant, did not respond to their "nameplate" source but rather to an external source which increased the radiation level in the vicinity of the monitors. The nuclear service cooling monitor apparently responded to the highly radioactivt gas in the vent header in the vicinity of the waste gas decay tanks. The intermediate cooler monitor apparently responded to the highly radioactive

material beginning to accumulate on the purification demineralizers. The plant liquid effluent monitor was intended to monitor the activity in cleaned-up coolant being prepared for the evaporator condensate test tank to the plant discharge, but it is located near the auxiliary building sump tank, which was overflowing onto the floor because the reactor building sump pumps were automatically trying to reduce the level of the water flooding the basement of the reactor building.

In retrospect, the response of the process monitors seems relatively clear, but the reactor operator did not have the luxury of abundant time during the accident to analyze the source to which each monitor might be responding. If he believed the "nameplates" on each monitor, he would rapidly be led to the erroneous conclusion that most heat exchangers in the plant developed a sudden leak and that somehow activity was bypassing the cleanup system and being discharged from the plant.

Reactor operators should thus become intimately familiar with the idiosyncracies of each radiation monitor in the plant, i.e., its location, its range, its failure modes, its response to other sources or potential sources in the vicinity of the monitor.

3. Area Monitors

The response of some of the area radiation monitors following the TMI-2 accident are shown in Figure 13-4. This figure, like the previous one, was compressed and simplified to improve its clarity and readability. The operator had to glean his information from approximately 30 inches of recorder chart that had twice as many monitor traces, all of which were printing poorly due to inadequate inking.

The first area monitor to respond to the TMI-2 transient was the incore instrument tank monitor. Apparently, this monitor is located in such a position that it responds to N-16 activity coming through the secondary shield. Thus, upon reactor trip the monitor showed a marked reduction in dose rate due to the decay of N-16 activity. This response seems to be typical because the incore instrument tank monitor at CR-3 also responed to the N-16 decay following the February 26, 1980, transient.

Most area monitors showed little initial response to the accident transient, which resulted in flooding much of the containment and auxiliary building basements with reactor coolant water. The instrument tank monitor responded promptly to the release of fission products when the fuel failed at about 6:25 a.m. Since the letdown line monitor did not respond promptly to this fission product release, the instrument tank monitor may have been responding primarily to noble gas activity in the steam generator (loop A).

The south refueling bridge monitor and the reactor building dome monitor responded almost simultaneously to the high radiation levels due to the release of fission product activity into the containment. The makeup tank area monitor, which is located between the makeup tank and the purification demineralizers, responded at about 6:40 a.m. (which is surprising because the letdown line monitor did not respond until 7:00 a.m.).

The letdown line monitor is located less than 10 feet from the makeup tank area monitor, so one would have expected to see similar radiation levels except that the letdown line monitor is heavily shielded from external radiation, whereas the area monitors are not.

The intermediate cooling pump area monitor, which is located in the vicinity of the purification demineralizers in the same general area of the auxiliary building as the makeup tank monitor, also began to respond at about 6:40 a.m.

but did not show a marked increase until about 7:10 a.m. Finally, at about 7:20 a.m., the emergency cooling pump area monitor, which is located near a bleed holdup tank, responded to high radiation levels caused by either the bleed holdup tank or the flooding of the auxiliary building basement.

As with the process radiation monitors, the operator should be familiar enough with the response of each area radiation monitor so that he will not be led to erroneous conclusions.

4. Reactor Building Dome Monitor

One source of puzzlement to the TMI-2 operating staff was why the RB dome monitor, which is housed in a 2-inch-thick lead shield, yielded almost identical radiation dose rates to the 200 mR/h indicated by the south refueling bridge monitor (see Figure 13-4), which is unshielded. A considerable effort was expended to resolve this question. Figure 13-5 (which is the same as 13-4 except that it only has the dome monitor response) shows that the dome monitor was recorded on a 5-decade log scale recorder chart. All the area radiation monitors provide a 5-decade log signal to this recorder except the dome monitor, which provides an 8-decade signal. Rather than provide a separate recorder just for the dome monitor, the plan was to provide a separate auxiliary scale that the operator could use to interpret the readings from the recorder chart. Unfortunately, the scale was never installed and was probably lost. Figure 13-6 shows that on an 8-decade log scale, the dome monitor was reading 10^4 mR/h inside its shield and not the 200 mR/h previously believed. Further investigation revealed that the dome monitor output was not really an 8-decade log signal but rather an 8-decade signal that was linear within any decade. The calibration curve for this output signal is shown in Figure 13-7. This calibration curve for the instrument revealed that the dome monitor's instrumentation, which includes an integral indicator, was out of calibration and that a full 8-decade response on the indicator only produced a 3.8-decade response on the recorder instead of a full 5-decade response. Using this calibration curve, Figure 13-8 was constructed to show the dome monitor's "true" dose rate reading of about 7×10^5 mR/h. Figure 13-9 compares the dome monitor's response based on the correct interpretation of the recorder charts with the dome monitor indicator readings recorded on the operating logs. Several interesting features are shown in this figure:

1. The large dose rate reduction produced by the reactor building sprays.
2. The large increase in dose rate between March 29 and April 1 when the RCS was degassed by venting steam to the containment.
3. The increase in dose rate on April 6, when the waste gas tanks were vented into the containment.
4. The series of linear decreases in dose rate indicating exponential removal rates, which surprisingly did not relate to radioactive decay but rather to other removal processes (e.g., the large decrease on or about May 1 seemed to relate to operationn of the RB coolers).

5. The constant dose rate, about 40 R/h, after May 15, which may be anomalous and indicative of instrument failure. (This failure is discussed in the "Failure Modes" section.)

All dome monitor dose rates discussed up to this point have been those at the detector, which is inside a 2-inch-thick lead shield. The dose rate of interest to the operators is that in the containment building. The dome monitor shield was specified to provide a dose rate reduction factor of 100 based on the Cs-137/Ba-137m gamma energy (0.662 MeV). Figure 13-10 shows the calibration curve for the dome monitor shield. As can be seen, the shield does provide a dose rate reduction factor of 100 for 0.662 MeV gammas; however, the energy spectrum of a mixed source of unknown fission products is not known, and it changes continuously with time. Thus, if the accident produced a gamma source with an average energy of 1 MeV, the shield might only reduce the dose rate by a factor of about 10, whereas if the average energy were only 0.1 MeV, the shield might provide a reduction factor of 700. Because of the strong dependence on source energy which is introduced by the shield, the dome monitor can only provide a gross indication of containment doses to reactor operators following a major accident that releases activity into the containment.

Figure 13-11 shows the response of the CR-3 reactor building dome monitor following their February 26, 1980, transient. The CR-3 detector is unshielded and thus showed the correct dose rate response relative to the other detectors in the reactor building. There are several other important observations that can be made based on Figure 13-11:

1. The fuel handling bridge monitor was reading about a factor of 500 lower than the RB dome monitor, similar to the anomalous behavior observed at TMI-2. Apparently, the hot steam and air carry the activity to the top of the containment; thus, even though the bridge monitor and dome monitor are both exposed to large gas volumes in the containment, there is not enough mixing to prevent radiation dose rates several orders of magnitude different.

2. The RB incore instrument area monitor responded to the decay of the N-16 activity immediately after reactor trip, then eventually climbed to correspond to the dome monnitor reading. The decrease in both the dome monitor reading and the RB incore instrument area monitor reading corresponds to the mixing rate provided by the RB fan-coolers.[1]

Based on these results, it seems clear that the reactor buildings at both TMI-2 and CR-3 had significant concentration gradients for several hours and that the assumption of a well mixed building atmosphere cannot be justified on the basis of the fan-cooler operation.

Reference

[1] "Analysis and Evaluation of Crystal River Unit 3 Incident," NSAC-3, March 1980.

5. Failure Modes

One of the most interesting failure modes analyses that has been performed since the TMI-2 accident was done at Sandia National Laboratory. One of the TMI-2 area radiation monitors inside the containment, the personnel hatch monitor (HP-R-211), was removed during one of the first post-accident containment entries and sent to Sandia for analysis. The results of the analysis showed that a rubber boot on the instrument's cable connector was not on securely; thus, when the RB sprays were on, a drop of water caused a short between two high-voltage connections. This short caused one transistor to have a cathode-to-emitter short. The instrument was calibrated before and after the failed transistor was replaced. After the transistor was replaced, the detector responded within specifications. Figure 13-12 shows the corrected response of the post-accident dose rates at the personne' hatch.

The failure mode of the TMI-2 dome monitor was predictable. The manufacturers knew that the most radiation-sensitive component in the detector was a field-effect transistor; they knew at what doses the transistors began to fail; and they knew that failure would be indicated by a periodic quiver with about a 1-second period. All of these are consistent with the May 15, 1979, failure date shown in Figure 13-9. Failures that leave the indicator needle on scale are particularly confusing to the operator because they quite often indicate believable values (e.g., TMI-2 dome monitor indicating a constant 40 R/h after about 2 months of decay).

A similar problem arose during the CR-3 incident caused by the loss of power to the non-nuclear instrumentation. Since the power supply was a -10 V to +10 V system, the loss of power produced 0 V, which corresponded to a mid-scale reading. The mid-scale reading is usually very close to the normal reading for that process variable, so the operators have difficulty identifying which instruments are functioning properly and which have failed.

Based on the experience to date, it seems as though much can be done to better understand the normal and abnormal operating characteristics of the plant instrumentation and to predict likely failure modes.

6. Summary

The following highlights are the important points of this lesson:

1. The present letdown line monitors have a useful range that is only suitable for nuclear plants operating within their design envelope. However, if the range of the letdown line monitor were expanded to monitor source strengths 100,000 times more intense than they currently can, they would enable the operator to make a prompt semi-quantitative assessment of the amount of fuel damage within minutes of establishing circulation in the reactor coolant system.

2. All process and area radiation monitors respond to all gamma radiation sources and do not respond exclusively to the source on their nameplate. Operators, therefore, should study each radiation monitor to learn its individual idiosyncracies with respect to:

   a. Potential external radiation sources.

   b. Invalid or non-representative sample flowing through or stagnant in the monitor.

   c. Effects of local shielding.

   d. Effects of different nuclide mixtures following a major accident.

   e. Failure modes (due to loss of power, loss of signal, excessive radiation, excessive temperature, electrical shorts, and the like).

Figure 13-1. Estimate of Letdown Line Monitor Response to Various Amounts of Fuel Damage

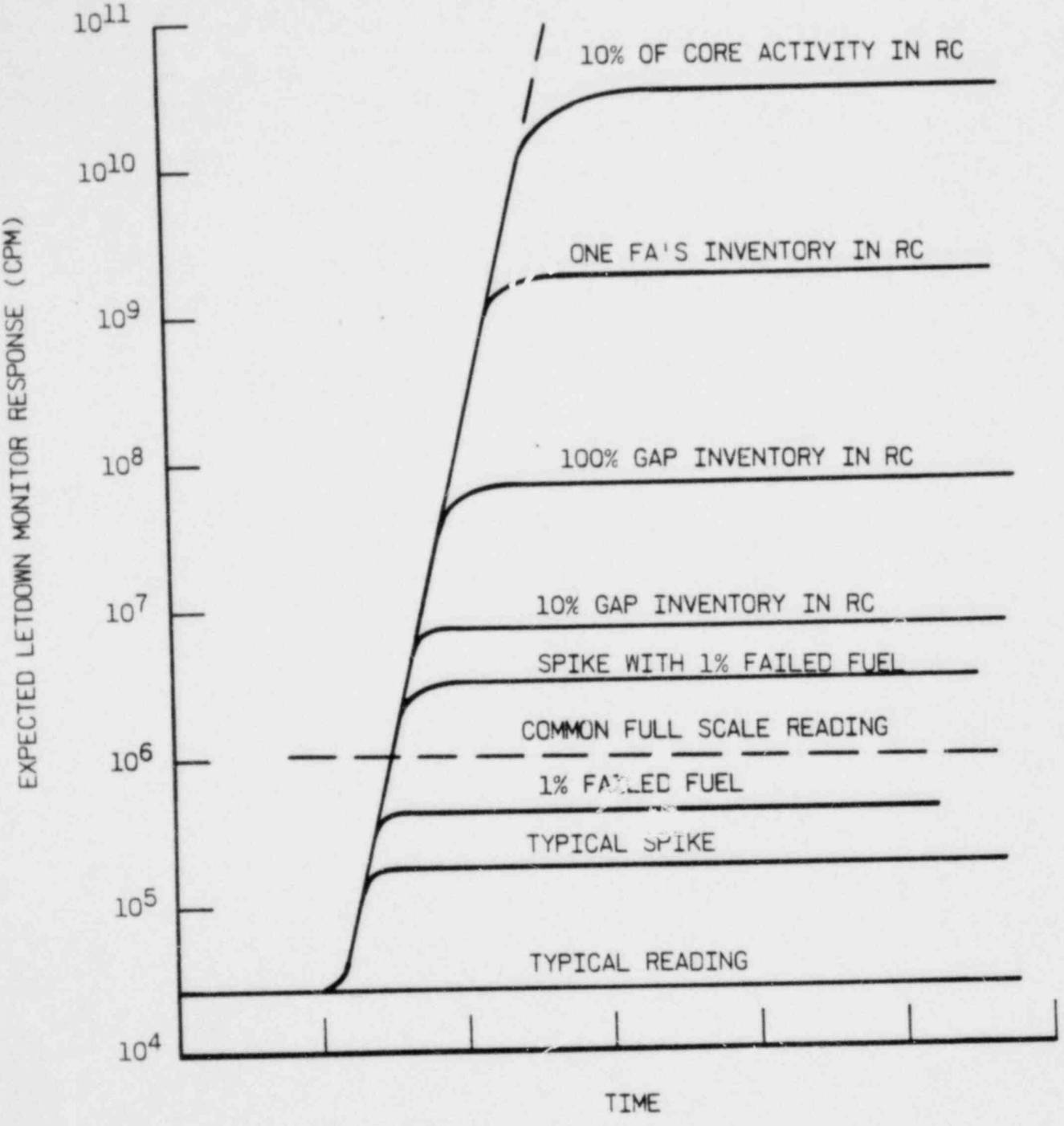

Figure 13-2. Letdown Line Monitor Response

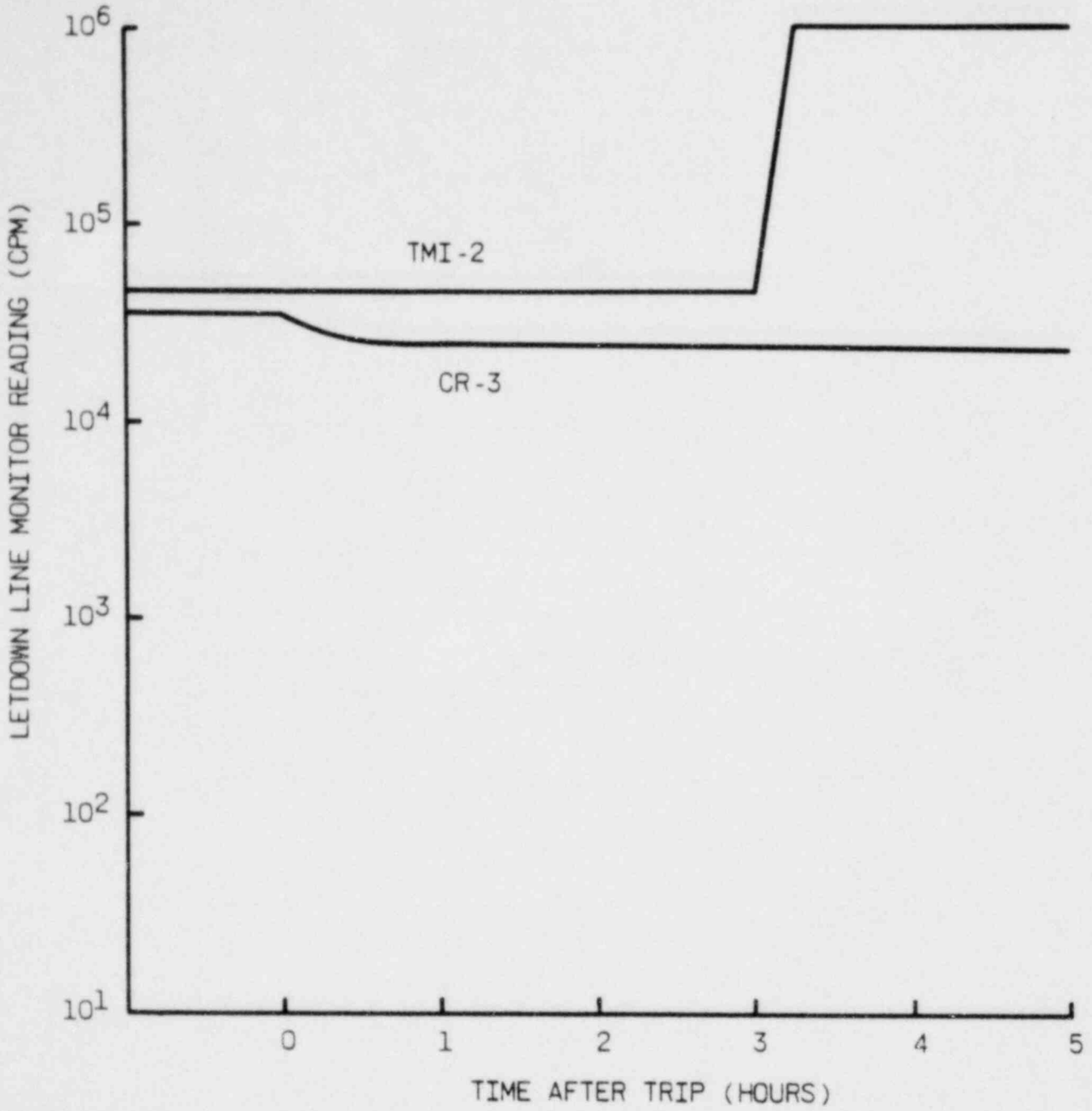

Figure 13-3. Process Radiation Monitor Responses Following TMI-2 Accident on March 29, 1979

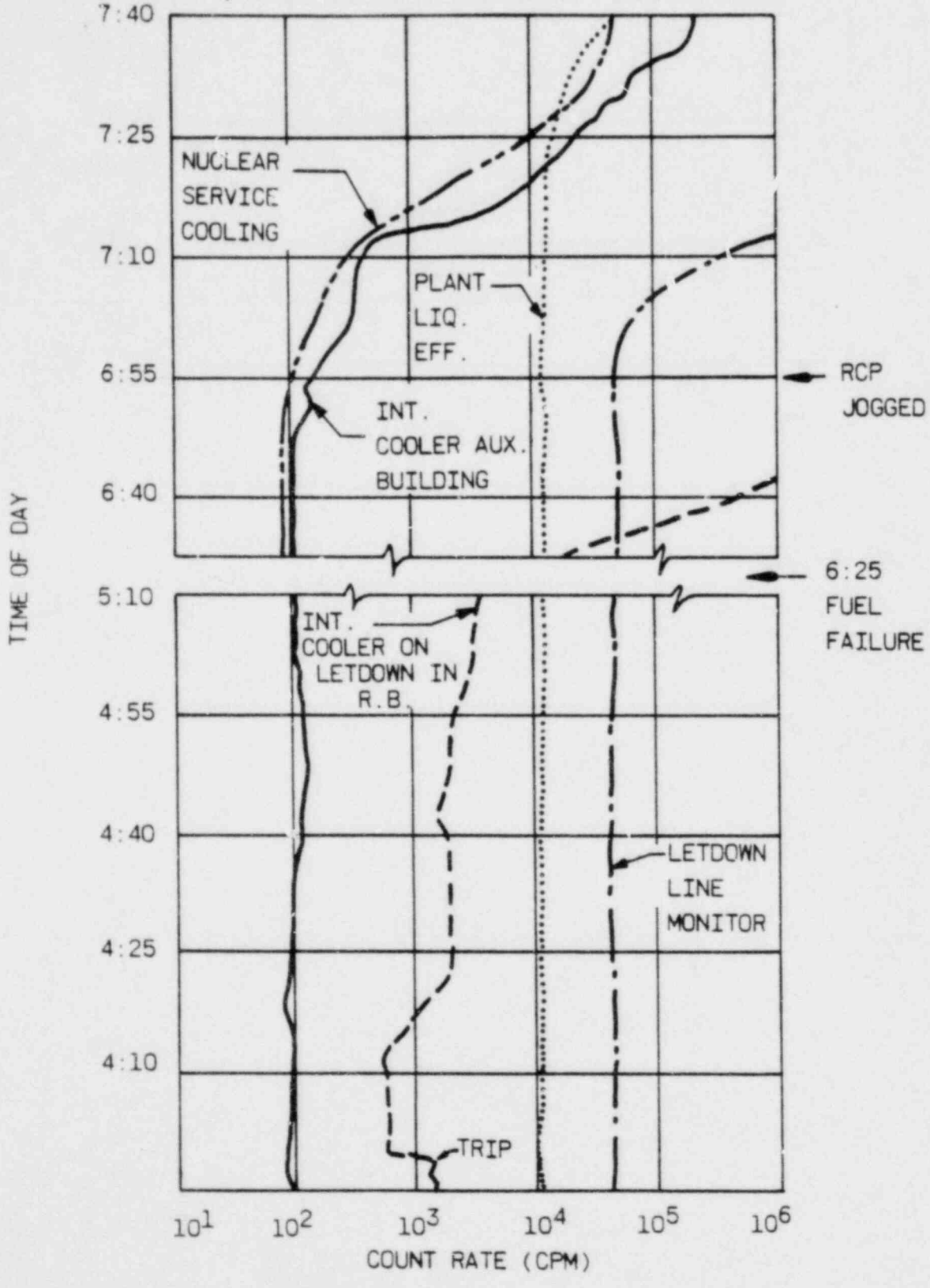

Figure 13-4. Area Radiation Monitor Responses Following TMI-2 Accident on March 29, 1979

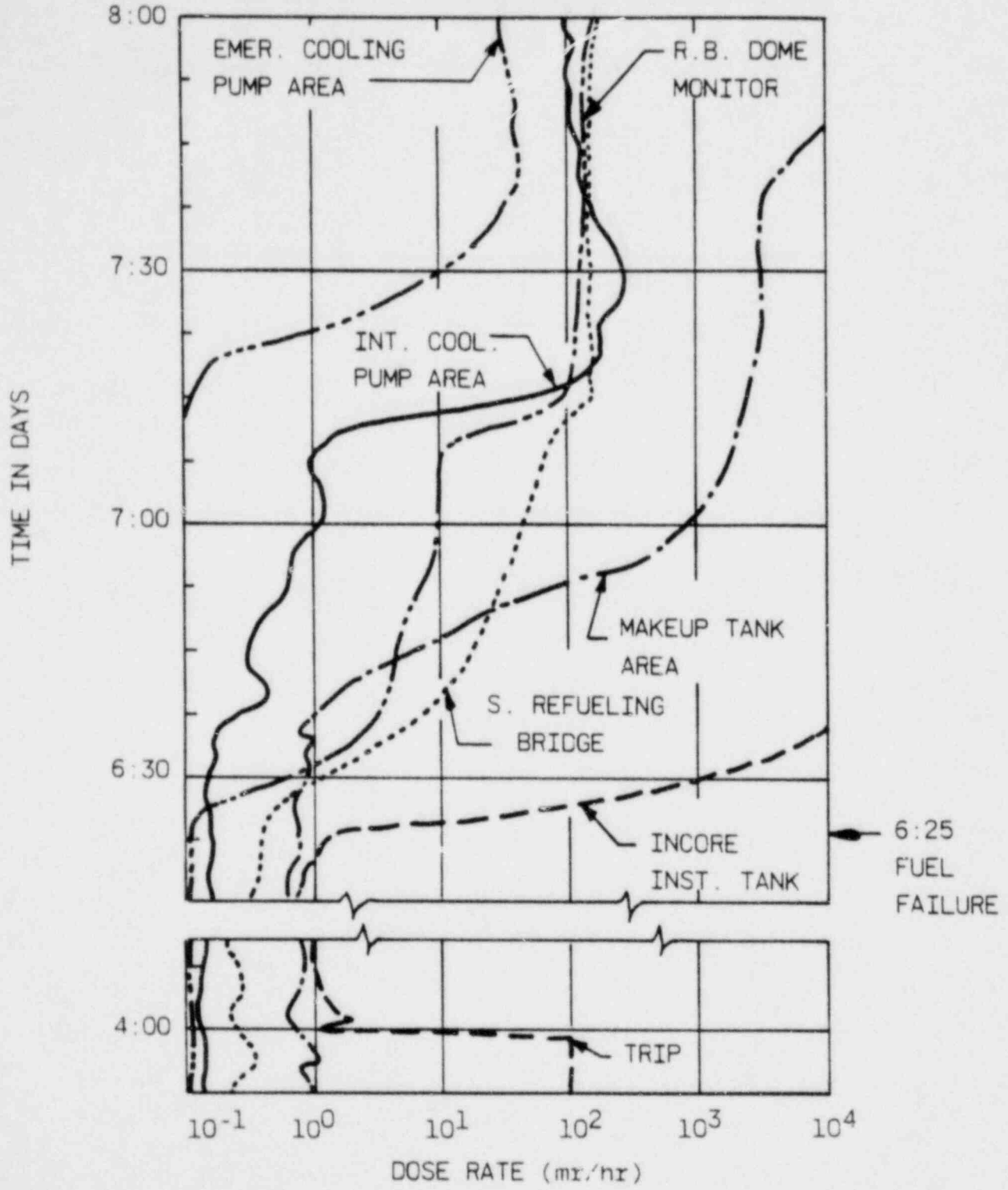

Figure 13-5. Area Radiation Monitor Responses Following TMI-2 Accident on March 29, 1979

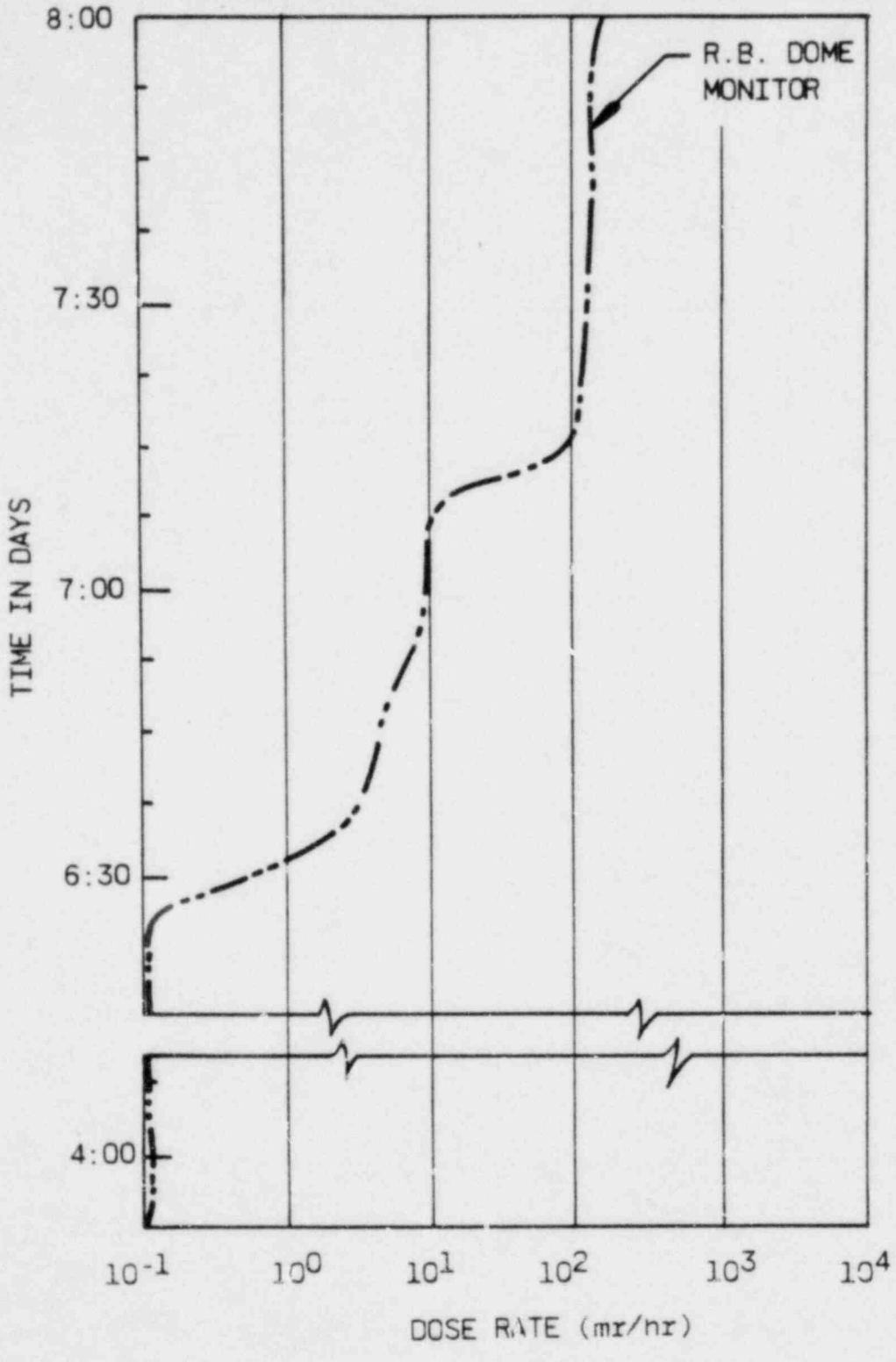

Figure 13-6. Area Radiation Monitor Responses Following TMI-2 Accident on March 29, 1979

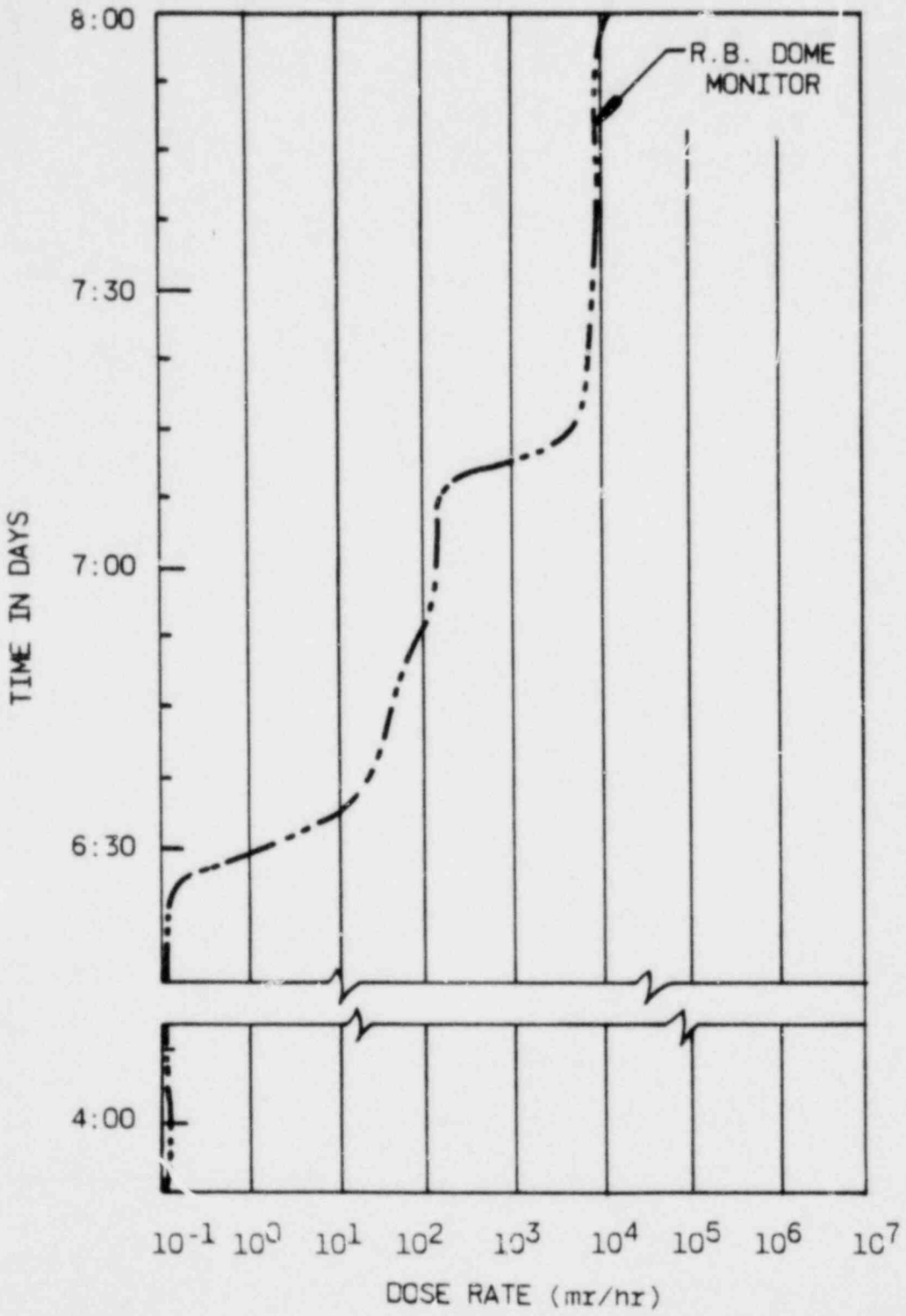

Figure 13-7. Scale Conversion for TMI-1 Dome Monitor Recorder

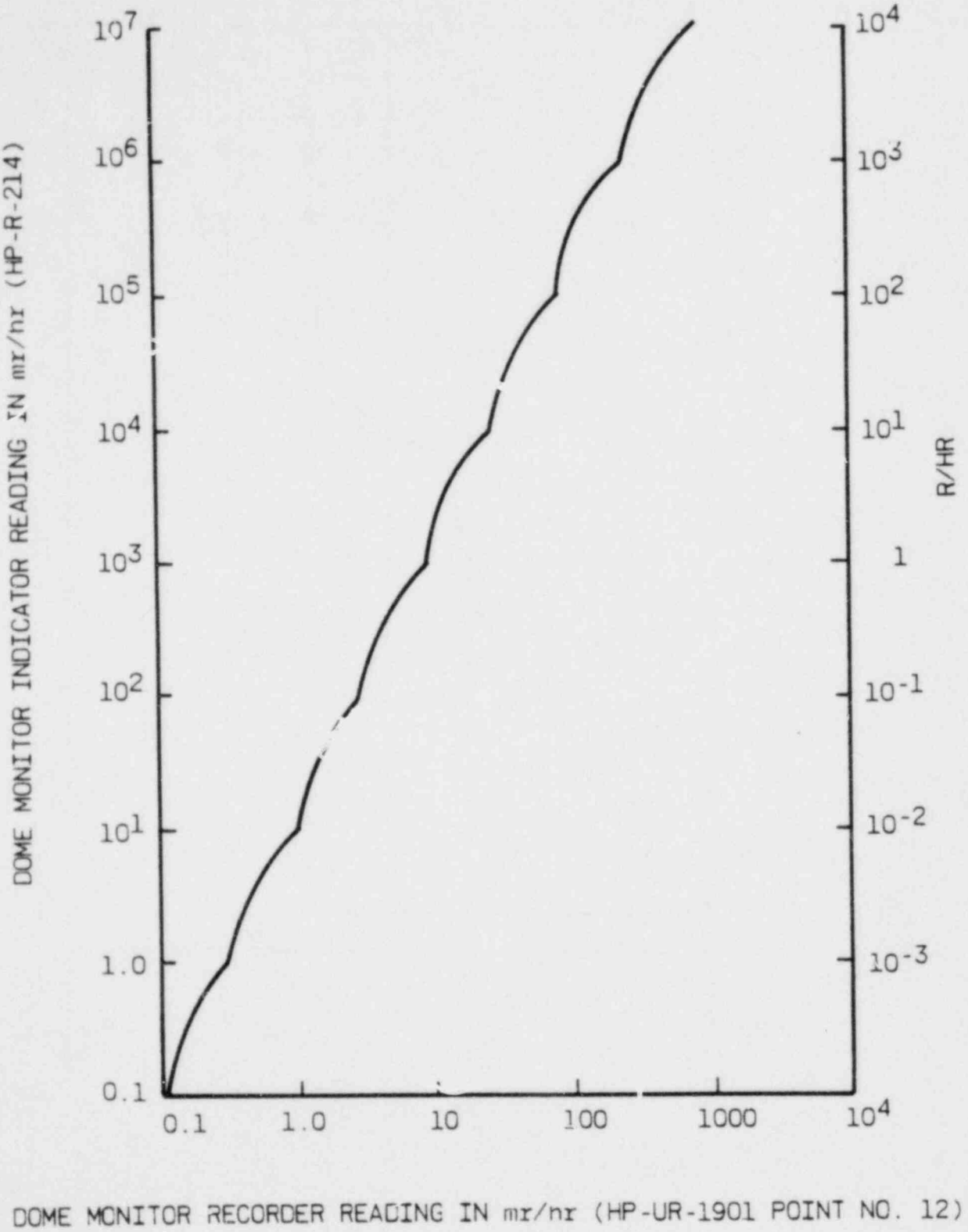

Figure 13-8. Area Radiation Monitor Responses Following TMI-2 Accident on March 29, 1979

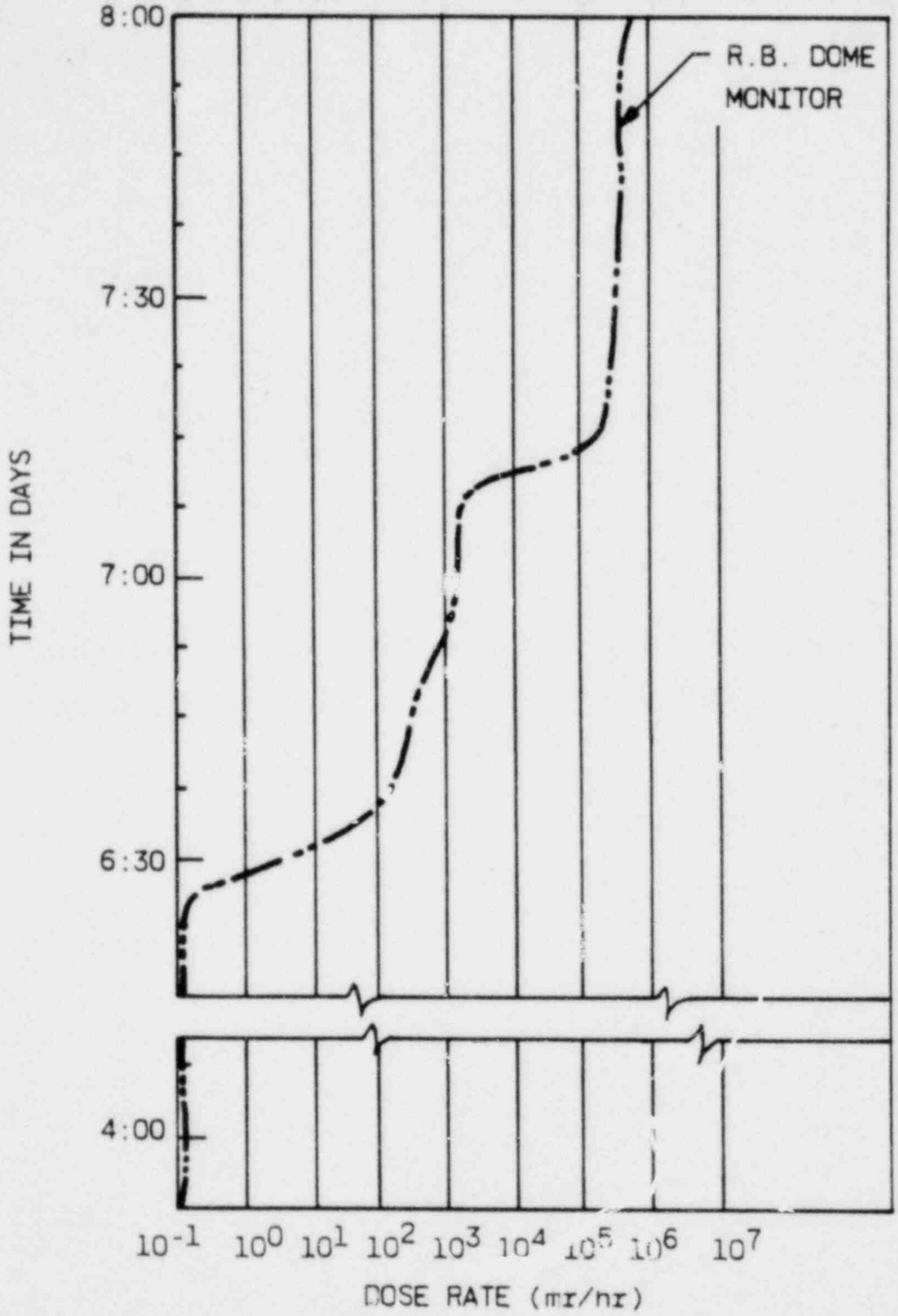

Figure 13-9. TMI-2 Dome Monitor Readings (Inside Shielded Housing)

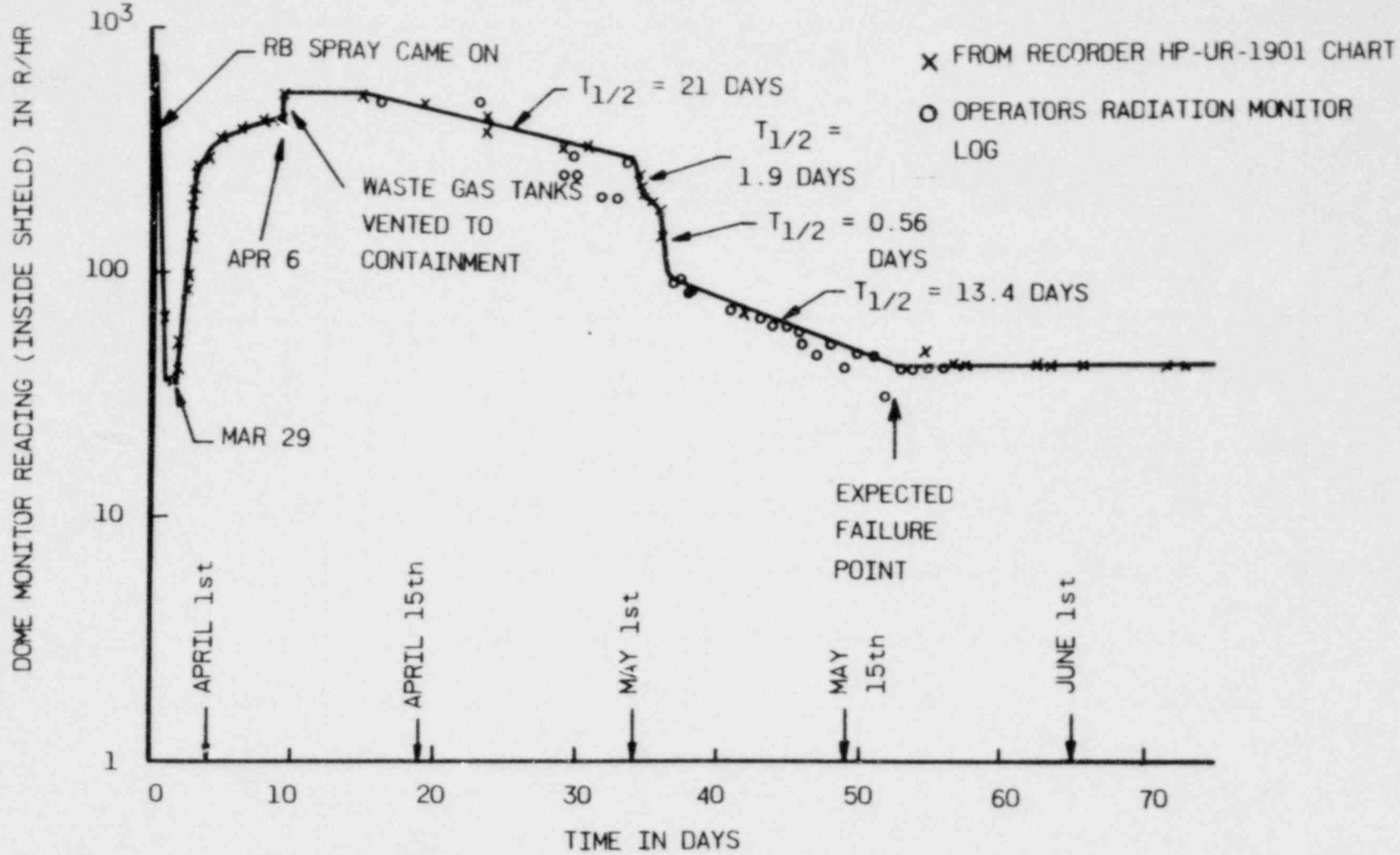

Figure 13-10. TMI-2 Dome Monitor Shield Calibration

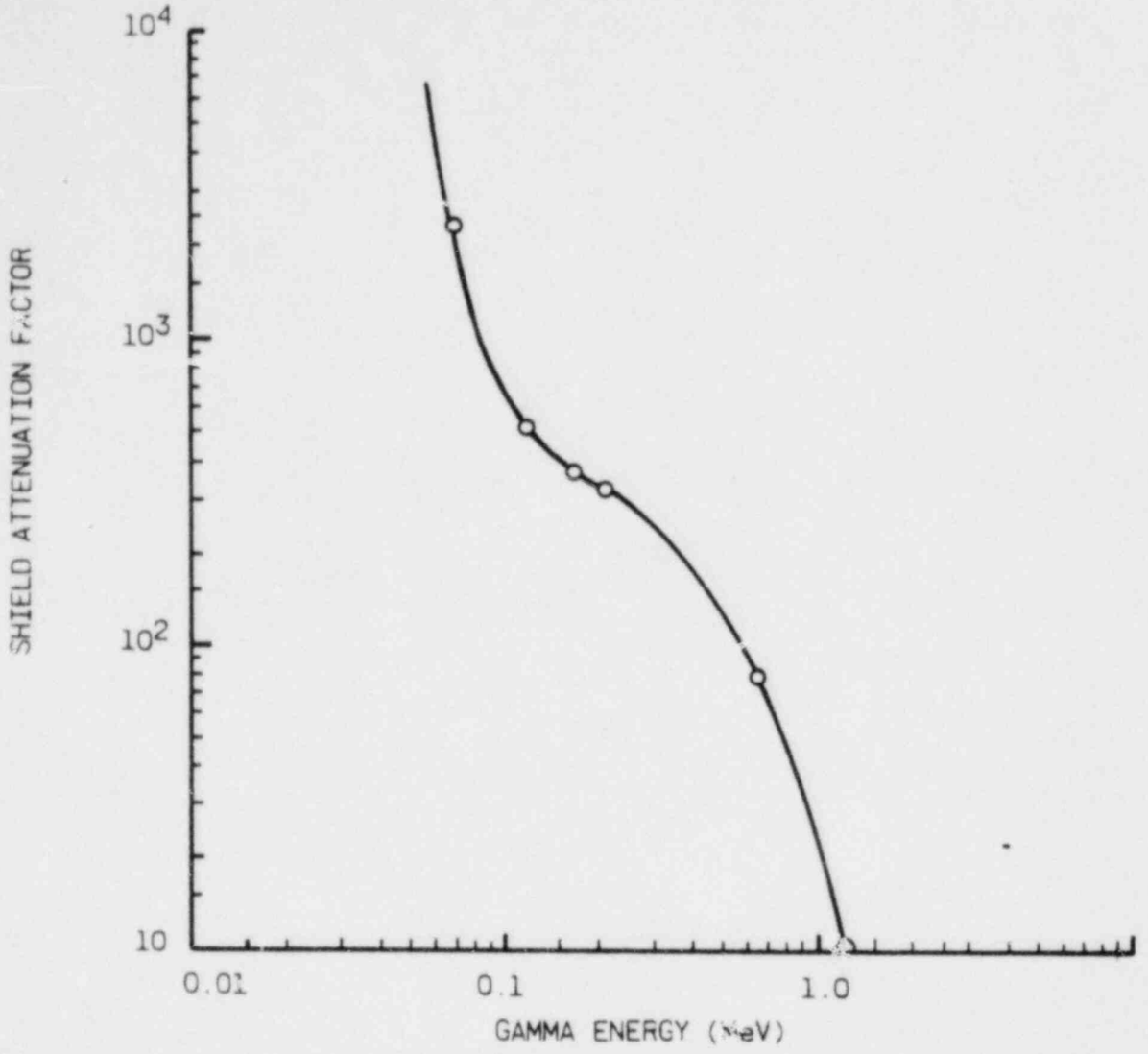

Figure 13-11. Reactor Building Radiation Monitor Response Following CR-3 Event

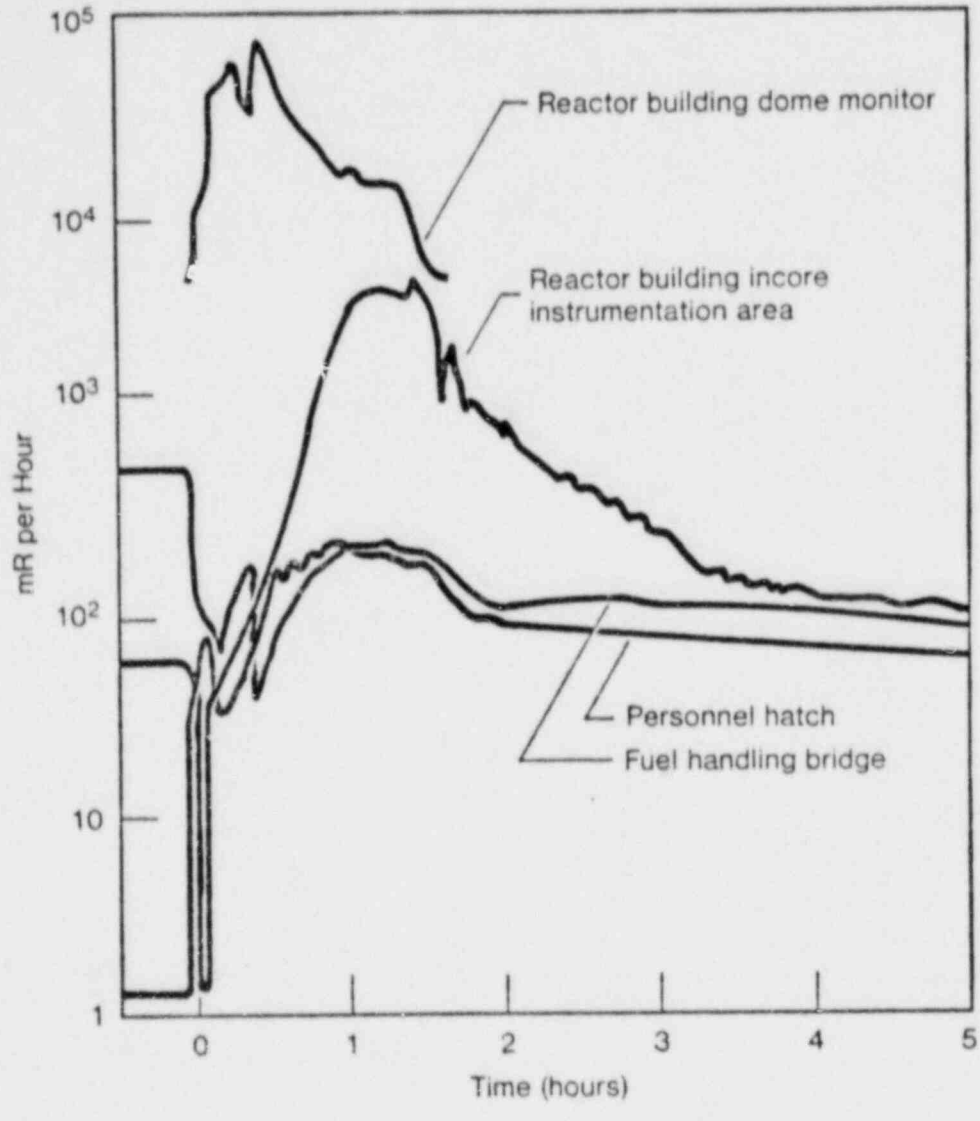

Figure 13-12. Response of RB Gamma Monitor (HP-k-211)

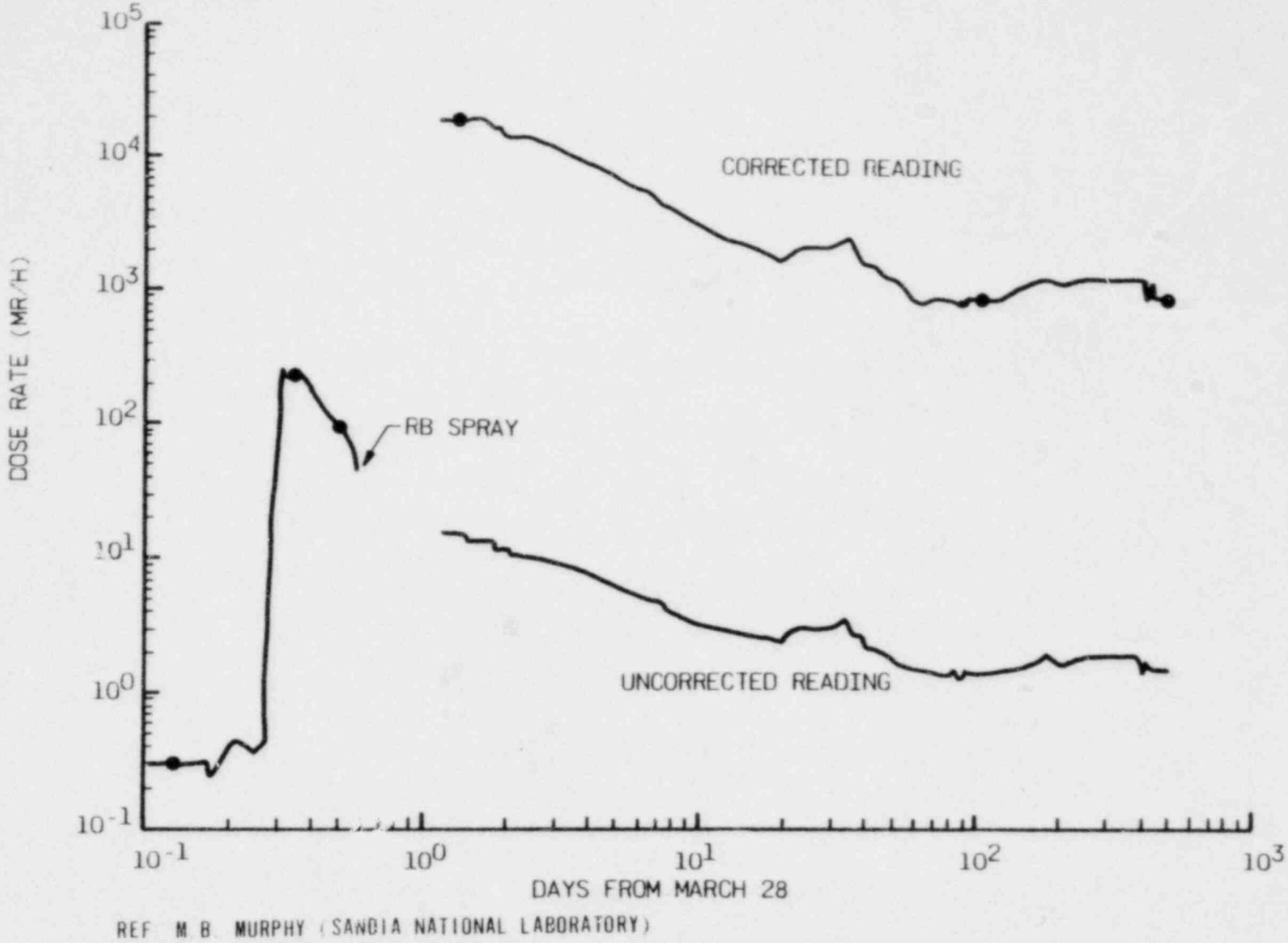

REF M.B. MURPHY (SANDIA NATIONAL LABORATORY)

Figure 13-13. Summary

1. CHECK LETDOWN MONITOR RESPONSE TO ASSESS MAGNITUDE OF DAMAGE (MAY NOT BE VALID IF RC PUMPS ARE NOT RUNNING)

2. CONSIDER POSSIBILITY OF ANOMALUS READINGS
   - HIGH BACKGROUND DUE TO ANOTHER SOURCE
   - MOBILITY OF SOURCE CAUSING CONCENTRATION GRADIENTS
   - DETECTOR'S RESPONSE TO SOURCES WITH DIFFERENT ENERGY SPECTRUMS
   - POWER SUPPLY FAILURES

3. PRE-ACCIDENT ACTIONS
   - AVOID SPECIAL SCALES & CALIBRATION ERRORS
   - AVOID SHIELDED DETECTORS
   - ANTICIPATE EFFECTS OF ELECTRIC COMPONENT FAILURES

Lesson 14 — CHEMICAL AND RADIOCHEMICAL PROBLEMS

Introduction

1. Lecturer —

2. Purpose — To describe some of the chemical and radiochemical problems that can occur following a reactor accident that results in degraded core conditions.

Objectives

The following material is presented in Lesson 14:

1. Chemical and radiochemical problems to be expected following reactor accidents that result in degraded core conditions.

2. Interpreting the analytical results, which will appear to be anomalous if compared to normal operating conditions.

3. How to avoid making operational or procedural errors that might lead to plant and equipment contamination as excessive radiation exposure to operating personnel.

4. Avoiding both sampling problems and the use of incorrect analytical methods.

Lesson 14 — CHEMICAL AND RADIOCHEMICAL PROBLEMS

1. Reactor Coolant System Conditions With a Degraded Core (Table 14-1)

During normal reactor operation, the reactor coolant pumps provide sufficient flow to transfer core heat to the steam generators. The coolant has a loop transient time of about 12 seconds, so the coolant is well mixed and homogeneous (Figure 14-1). Since these normal conditions exist year after year, it is easy to develop a mindset based on normal conditions, and it is difficult to adjust ones thinking to the unusual conditions that arise during rare accident events. One of the major purposes of this lesson is to stimulate thinking about the unusual conditions associated with reactor accidents that lead to degraded core conditions.

For example, a depressurization event, like the delayed closing of the pilot operated relief valve on the pressurizer could cause the reactor coolant system (RCS) pressure to drop to saturation and create steam bubbles in the top of the hot legs, as illustrated in Figure 14-2. High pressure injection (HPI) will be automatically initiated under these conditions, and the reactor coolant pumps (RCP) will be tripped upon loss of adequate subcooling margin with the intent of initiating a natural circulation cooling mode. Unfortunately, under these conditions natural circulation would be prevented because of the steam bubbles. There are two important points to be remembered in relation to this condition.

1. The pressurizer (PRZ) will only control pressure when it contains the hottest water in the RCS. If the water in the hot leg becomes hotter than the water in the pressurizer, the hot leg conditions will control RCS pressure.

2. A steam bubble once formed can not be collapsed by increasing the pressure; it can only be collapsed by cooling it.

Figure 14-3 shows that when subcooled water is depressurized below its saturation pressure some of the water flashes to steam and a two-phase system

exists. A subsequent repressurization of the two-phase system merely compresses the steams to a superheated condition. The only way to collapse a steam bubble is to condense it by cooling it (i.e., reduce its enthalpy). Of course, given sufficient contact area and contact time, the superheated steam in contact with subcooled water will eventual condense and return to their original starting point on Figure 14-3 (assuming no other heat losses).

The most effective way to condense the steam bubble is to jog or start the reactor coolant pumps (RCP) and thus condense the steam in the steam generators (SG). The only other alternative is to maximize HPI flow and open high point vents until natural circulation begins.

In the event that neither the RCP or HPI are available, the core region will control the RCS pressure and raise the pressure until steam is relieved via the pressurizer safety valves. Thus, the heat will be removed by the boiloff of reactor coolant. If the water level on the secondary side of the steam generators is sufficiently high, the decreasing water level on the primary side may expose enough condensing surface that boiloff of reactor coolant may stop at some level. If the water level drops to the point where significant amounts of fuel are uncovered, large quantities of hydrogen gas can be generated very quickly by the metal-water reaction between the hot Zircaloy and steam. This condition is illustrated in Figure 14-4. It shows that both coolant loops are stagnant and that although the remaining liquid in the core has been concentrated considerably by boiloff of coolant and boiloff of HPI flow, the liquid in the cold legs could be primarily condensate from steam condensing in the steam generators. Thus, reactor coolant samples taken via the letdown sample line (which is on the cold leg) will not be representative samples. One should therefore expect the analytical results to be puzzling; they will probably show low boron concentrations, low xenon and krypton activity, and relatively high iodine concentration in comparison to other nuclides.

The amount of hydrogen that was estimated to be in the TMI-2 reactor coolant system is shown in Figure 14-5. It can be seen that 173,000 SCF was generated in the period between 2 and 4 hours after the accident. At least 63,000 SCF was released into the containment and exploded approximately 9 hrs. 50 mins. after the accident causing a 28 psig pressure pulse inside the containment. The remaining hydrogen was slowly removed from the RCS over the next several days either by a combination of venting the pressurizer into the containment

and degassing the letdown flow in the makeup tank or by a small fortuitous leak in the area of the control rod drives. The hydrogen contrentration in the containment building subsequently reached a maximum concentration of 2.3 volume percent on April 3rd (6 days after the accident). A 95 CFM recombiner operated frequently during the period April 2nd to May 1st and slowly reduced the hydrogen concentration to about 0.8 percent.

It can be seen that even if all of the plants waste gas storage tanks were empty, they could only accommodate a small fraction of the hydrogen generated. Thus, the capability to vent these tanks into containment is highly desirable, especially if the vent stream could be passed through a recombiner. Other important facts to be considered are:

1. The hydrogen in the reactor coolant system does not present a explosion hazard, and if the RCS pressure is kept high, the hydrogen occupies a relatively small volume (e.g., 173,000 SCF = 2125 cu. ft. @ 2200 psig and 450F) and should not interfere with forced circulation cooling; however, it can interfere with natural circulation cooling if it blocks the top of the hot legs. If the pressure is not kept high the gas can expand to fill the entire RCS.

2. If all the hydrogen is vented to the containmet too rapidly, the potential for an explosion more violent than TMI's is quite high.

Table 14-2 list some of the recommended actions and factors to be considered in order to deal with large volumes of hydrogen in the RCS.

At some point in the recovery from an accident that generates large volumes of hydrogen , the RCS is likely to be in the state shown in Figure 14-6, i.e., one loop circulating and a sizable gas bubble trapped in the reactor vessel head. The installation of high point vents and a reactor vessel head vent will greatly expedite the elimination of indicated gas pockets. However, if vents are not available it may be necessary to measure the volume of gas voids in the RCS to determine if it is safe to begin depressurization. At TMI-2 the volume of gas void in the system was measured by taking a set of data before and after subjecting the RCS to a pressure increase of at least 100 psi (if the pressure change is too smalll the accumulation of instrument errors destroy the accuracy of the calculation). The data was then used in conjunction with the following equation to calculate the volume of gas based on the net ammount of compression.

$$V_1 = \frac{P_2}{P_1 - P_2}\left[C_p\left(\frac{v_{r_2}}{v_{p_2}} L_{p_2} - \frac{v_{r_1}}{v_{p_1}} L_{p_1}\right) + C_m \left(\frac{v_r}{v_m}\right)\left(L_{m_2} - L_{m_1}\right)\right.$$

$$\left. - M_r \alpha_r (T_{r_2} - T_{r_1}) - M_r \beta_r (P_2 - P_1) + M_r \gamma_r (P_2 - P_1)\right]$$

where

V = volume of gas bubble in RCS at P_{r_1} and T_{r_1},

P = RCS pressure,

C = volume of vessel per unit height,

v = specific volume of water at T,

L = level in component,

M = mass of water in RCS,

α = change in RCS specific volume per °F (at constant pressure),

β = change in RCS specific volume per psi (at constant temperature),

γ = change in hydrogen solubility per psi (at constant temperature),

T = temperature of liquid in system or component,

Subscripts:

1 = initial condition,

2 = final condition after pressure increase,

r = reference to RCS,

p = reference to pressurizer,

m = reference to makeup tank.

The data necessary to perform this calculation were tabulated on a data sheet structured as follows:

Sample Data Sheet for Bubble Size Calculation

Date:

RCS Pressure
P_1 = psia
P_2 = psia

PZR Level
L_{p_1} = inches
L_{p_2} = inches

Makeup Tank Level
L_{m_1} = inches
L_{m_2} = inches

RCS Temperature
T_{r_1} = °F
T_{r_2} = °F

PZR Temperature
T_{p_1} = °F
T_{p_2} = °F

Makeup Tank Temperature
T_{m_1} = °F
T_{m_2} = °F

Time Pressure Increase Began:
Time Pressure Increase Stopped:

It can be seen from Figure 14-7 that, at high RCS pressures, the hydrogen is so soluble that the gas solubility correction must be included to obtain an accurate measurement of the gas bubble volume.

Even after the bubble volume has been reduced to zero, care must be exercised in depressruizing the reactor coolant system because of the large volume of dissolved gas that would be liberated during the depressurization. Figure 14-8 shows the solubility of hydrogen as a function of temperature and pressure. It can be seen from the figure that at 2200 psig and approximately 540F there would be as much as 7000 cc(S.T.P.) hydrogen per kg of coolant, i.e., 5.2 std. liters of hydrogen per liter of coolant. If the RCS is to be cooled by natural circulation, the dissolved gas concentration would have to be reduced by a factor of about 1000 to 2000 before depressurization to low pressures, whereas if it is to be cooled by the decay heat system, a reduction by a factor of 100 to 200 would surfice. Figure 14-9 shows the degassing rate as a function of the "effective degassing flow rate" (K). This figure shows that under optimum conditions the degassing process would take 2 to 3 days to remove the dissolved gas, but under conditions similar to those at TMI-2 ($20 \leq K \leq 50$), the degassing could take 2 to 3 weeks.

If HPI flow is only sufficient to makeup for the steam loss, the boiloff process can continue for a long period of time and the boric acid concentration can increase many fold. Figure 14-10 shows the boric acid solubility as a function of temperature. It also shows the solubility of borax. Borax is formed by the addition of sodium hydroxide to the boric acid to aid in the removal of iodine or to adjust the solution pH. Borax is less soluble than boric acid at low temperatures. Thus, if the system only contains boric acid, there is no need for concern about precipitating solids until the boron concentration exceeds 5200 ppm; however, if sodiun hydroxide is present in the coolant precipitation can occur at boron concentrations as low as 2800 ppm. Although there is little concern about precipitation at temperatures above 120°F, precipitation can occur as a concentrated solution is cooled. This effect is illustrated in Figure 14-11 for a boric acid solution with 12,000 ppm boron. Precipitation of boric acid begins when the solution is cooled to 90F and continues until it reaches the temperature of the cooling water (60F); thereafter, the solution remains saturated at 7200 ppm boron.

2. Sampling Problems (Table 14-3)

In addition to the previcusly mentioned problem of not being able to obtain representative samples of reactor coolant because of stagnated loops, localized dilution, and solutions concentrating in the core due to boiloff, there are other problems associated with obtaining reactor coolant samples following a core degrading accident.

Figure 14-12 schematically shows the arrangement of a typical sampling system. Note that the sample line taps into the letdown line upstream of the letdown cooler; thus the sample is usually cooled in the sample cooler. Since the concentration of boric acid in the sample to be taken is not known at the time of sampling, there is some risk that it might exceed the 5200 ppm boron value for a boric acid solution (or 2800 ppm boron for borax solution) and thus solids may precipitate in the sample cooler and plug the sample system valves thereby precluding the ability to obtain subsequent samples without excessive delay and radiation exposure. Thus, at least the first sample taken after a major accident should bypass the sample cooler and flow through a 2500 psig sample bomb. The purge flow should be routed back to the makeup tank and not to the sample sink. After an appropriate purge time, the sample bomb can be isolated and cooled in-place with a wet towel or by other appropriate means.

The most hazardous aspect of post-accident sampling is caused by the high dissolved gas content in the reactor coolant. As can be seen from Figure 14-8, the partial pressure of dissolved hydrogen can be quite high. At TMI-2 the dissolved hydrogen was about 400 cc (S.T.P.) per Kg which at room temperature can generate approximately 1200 psia. The person taking the first reactor coolant sample following the TMI-2 accident was unprepared for the effects of pressure created by the dissolved gas, so he attempted to quickly obtain an atmospheric sample via the sample sink valve. Much to his surprise, when he opened the valve, the coolant sprayed form the top similar to the way water is sprayed from a faucet when there is air in the pipes except at TMI the gas pressure was ten times higher. The result was that coolant droplets were atomized to aerosol particles which spread throughout the radiochemical laboratory facilities which were shared jointly by both TMI units. Contamination of these facilities precluded any further onsite analysis which were so essential to the accident recovery phase. Furthermore, the person was immediately

engulfed in a cloud of radiation from the dissolved xenon and krypton nuclides and received a radiation dose well in excess of allowable limits.

It is therefore essential that the sample bomb be disconnected in a manner which precludes the spray of coolant or gas trapped in the lines between the valves and that the bomb be vented into an appropriate container or system which is designed to accommodate the large volume of high pressure gas. Similarly, liquid samples withdrawn from the bomb may not be completely degassed, so they should not be sealed into low pressure containers because gas pressure could buildup and rupture the sample containers. Liquid samples withdrawn from bomb should be stored in containers with adequate gas space to accommodate any hydrogen that may evolve and the cap should be left loose for the first few hours.

The radiation fields associated with reactor coolant samples taken after a core damage accident will be extremely intense, so smaller sample bombs should be available to help reduce the amount of activity handled, the appropriate long handle tools and carriers should be readily available, and an adequate supply of temporary shielding lead bricks and lead glass window blocks should also be available.

3. Analytical Problems (Table 14-4)

The routine chemical and radiochemical analyses performed year after year under normal conditions at a nuclear plant help to create a mindset wherein the analyst is unprepared to efficiently analyze the range of samples and sample conditions that are generated by a major accident which severely damages the core. Furthermore, the laboratory's equipment and supplies are sized and calibrated to normally expected samples. These higher radioactive samples need special considerations which include vessels for smaller samples, provisions for additional dilutions, isotopic separations, and calibration for different counting geometrics. In addition, there will also be a need to analyze these highly radioactive samples for non-radioactive constituents which may have never been needed before the accident. Several situations arose during the TMI-2 accident which illustrated the need for diverse analytical capability.

The first reactor coolant sample, had it been obtained and analyzed correctly, would have been found to contain 60,000-70,000 microcuries of Xe-133 per gram (μCi/g), 20,000 μCi/g I-131, and 300 μCi/g Cs-137 not to mention an equivalently high concentrations of many other shorter half-life nuclides. The sample also contained traces of Ag, In and Cd from melted control rod alloy, some impurities found in Susquhanne River water, and high concentrations of sodium hydroxide (the chemical additive for the reactor building spray system).

Silver-indium-cadmium control rods melt between 1700 and 1800F which is the lowest melting point material in the core; therefore if the core becomes hot enough to cause the stainless steel cladding on the control rods to fail, the Ag-In-Cd will surely be molten and thus will leak into the RCS. It is suspected that the silver from the control rods eventually reacted with a significant fraction of the iodine release from the fuel. The reason for this supposition is that about 70% of the total noble gas activity in the core was released and accounted for; one would thus expect about 60 to 70% of the iodine to be released, but only about 42% could be accounted for. The missing 18 to 28% of the iodine inventory in the core is suspected to have reacted with the silver and precipitated within the RCS.

The river water was accidentally introduced into the reactor coolant system via the bleed holdup tanks. A large inventory of river water was in the auxiliary building sump tank from a pre-existing leak in a service water pump.

The large volume of water pumped form the RB sump after the accident caused the auxiliary building sump tank to overflow and flood the auxiliary building basement level. Since the only available tankage at the time was in a bleed holdup tank (BHT), the radioactive liquid was pumped from the floor to a BHT. Eventually, the river water entered all three BHT via a common overflow header.

The river water introduced many impurities into the reactor coolant. The full impact of these impurities may never be known. It did create high chloride levels in the RCS, and it introduced carbonates which are suspected to have caused the precipitation of some strontium activity within the RCS.

The high sodium hydroxide concentration in the coolant could have interfered with the boric acid analysis if it was not properly neutralized prior to titrating for the boric acid content.

5. Conclusions (Table 14-5)

The key points of the lesson are as follows:

1. The initial reactor coolant samples should be taken in 2500 psig sample bombs with the sample stream bypassing the sample cooler.

2. The vapor pressure from large quantities of dissolved gas can over pressurize isolated equipment (including sampling vessels) unless appropriate provisions are made to accomodate the evolution of the dissolved gas.

3. Interpret sample analyses carefully — consider the potential effects of stagnation, dilution, boiloff, unusual impurities, and the suitability of the usual analytical methods.

4. Keep RCS pressure high and coolant temperature below 500F.

5. Try to keep hydrogen and radioactivity contained within the RCS and containment building.

6. Bleed hydrogen from RCS into containment at the maximum possible rate consistent with avoiding explosive conditions within the containment .

7. Try to keep the reactor coolant pump running in the cold leg with the pressurizer spray line to expedite coolant degassing.

8. The volume of hydrogen will greatly exceed the waste gas storage capacities, so waste gas storage tanks should be quickly purged of low activity gas to make room for high activity hydrogen. The operator needs the capability to vent the waste gas storage tanks and the makeup tank directly into the containment at a controlled rate and preferably via a hydrogen recombiner.

9. The amount of reactor coolant letdown should be kept to a minimum to avoid plugging the letdown line and to avoid over pressurizing the makeup tank.

Table 14-1. Sampling Problems During Core Damage Accidents

- Poor circulation or stagnation
- Localized dilution by makeup water
- Volatilization during boiloff (Xe, Kr, I, ^{3}H)
- Concentration of non-volatiles during boiloff (Boric Acid, Cs, etc.)

Table 14-2. Dealing With Large Volumes of Hydrogen in RCS

1. Keep RCS pressure high
   - Compress hydrogen into smaller volume
   - Increases gas solubility
2. Immediately start recombiners and all reactor building fans
3. Empty all waste gas storage tanks to make room for the highly radioactive hydrogen
4. Degas the RCS using
   - High point vents
   - Pressurizer PORV
   - Letdown to makeup tank
5. Continuously monitor hydrogen concentration in containment to avoid explosion hazard
6. Try to keep activity and hydrogen in containment rather than transfer to auxiliary building
7. Dissolved gas in reactor coolant will over pressurize letdown and makeup system
   - Don't isolate individual components
   - Vent makeup tank frequently
8. Try to start RC pumps (the one in cold leg with PZR spray line greatly improves degassing rate)
9. Measure gas content of RCS by observing the PZR. Level decrease corresponding to pressure increases
10. Preplan and provide capability to vent makeup tank and waste gas storage tanks into containment

Table 14-3. Potential Sampling Difficulties

- Spraying of coolant and activity from atmospheric sampling taps due to effervesence caused by dissolved gas
- Vapor pressure of dissolved gas could rupture sealed sample container if inadequate gas expansion space is not provided
- Concentrated boric acid could plug the sample cooler and/or sample system valves
- High radiation fields from sample and from gases volatilizing from sample.

Table 14-4. Potential Analytical Problems

- Silver from failed control rods could reduce the observed iodine activity
- Sodium hydroxide could interfere with boron analysis it not properly neutralized
- Other impurities could interfere with both chemical and radiochemical results (e.g., carbonates from river water may have precipitated strontium activity in the TMI-2 reactor coolant system)

Table 14-5. Conclusions

- Be prepared to take reactor coolant samples in 2500 psig sample bombs
- Don't use sample cooler on initial samples (cool sample in sample bomb, after isolating the bomb)
- Be prepared to collect large quantities of highly radioactive gas from sample bomb
- Interpret sample results carefully — consider potential effects of stagnation, dilution, boiloff, unusual impurities, and suitability of the usual analytical methods
- Keep RCS pressure high and coolant temperature below 500F
- Try to keep hydrogen and activity contained in RCS and containment building
- Try to keep RC pump running in cold leg with PZR spray line
- Volume of hydrogen could far exceed waste gas storage capabilities
- Bleed hydrogen into containment at maximum rate without creating an explosion hazard
- Minimize letdown flow to avoid plugging letdown line and over pressurizing makeup tank

Figure 14-1. Initial Conditions – System Steady

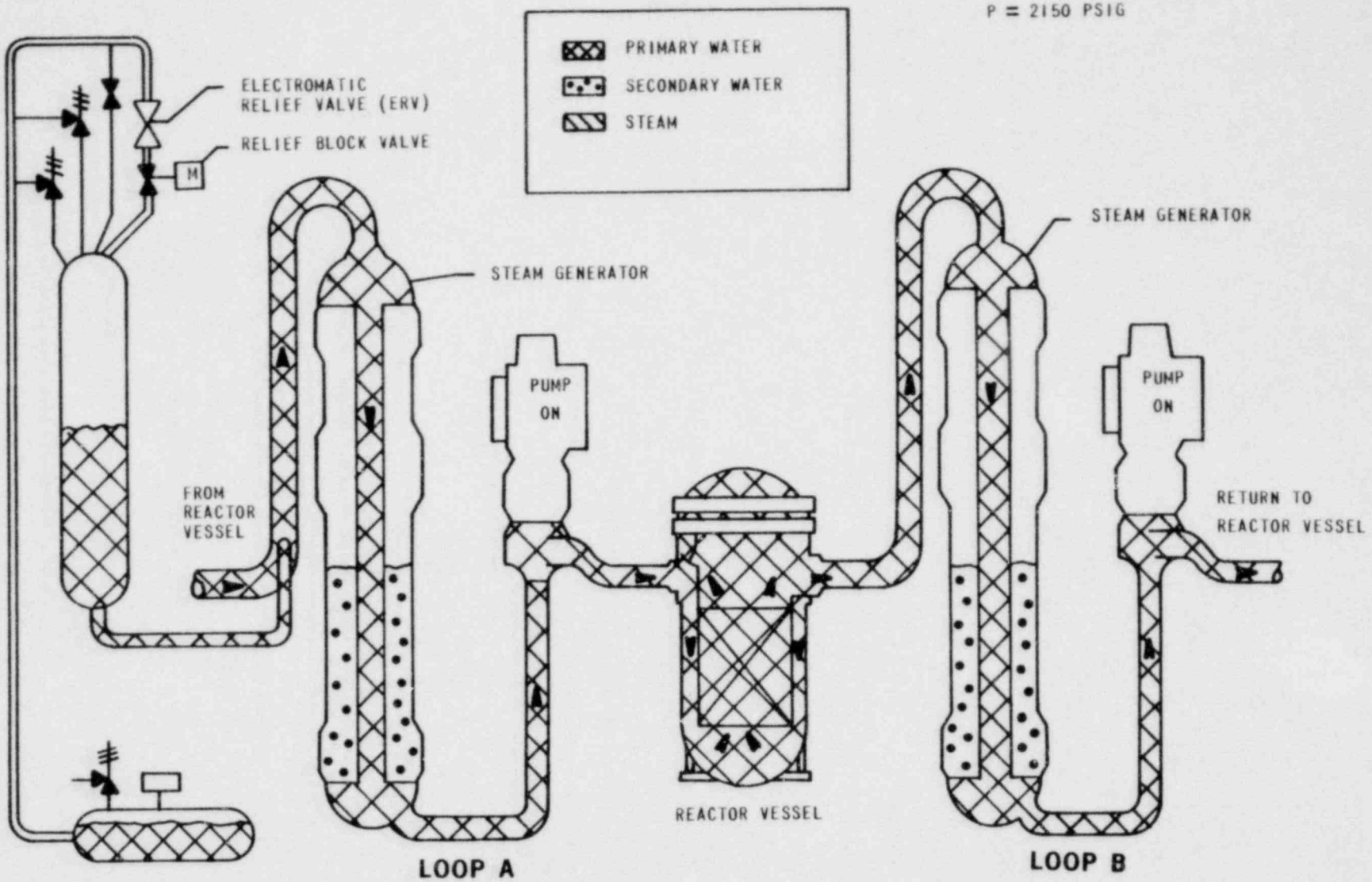

Figure 14-2. Steam Binding in Hot Legs

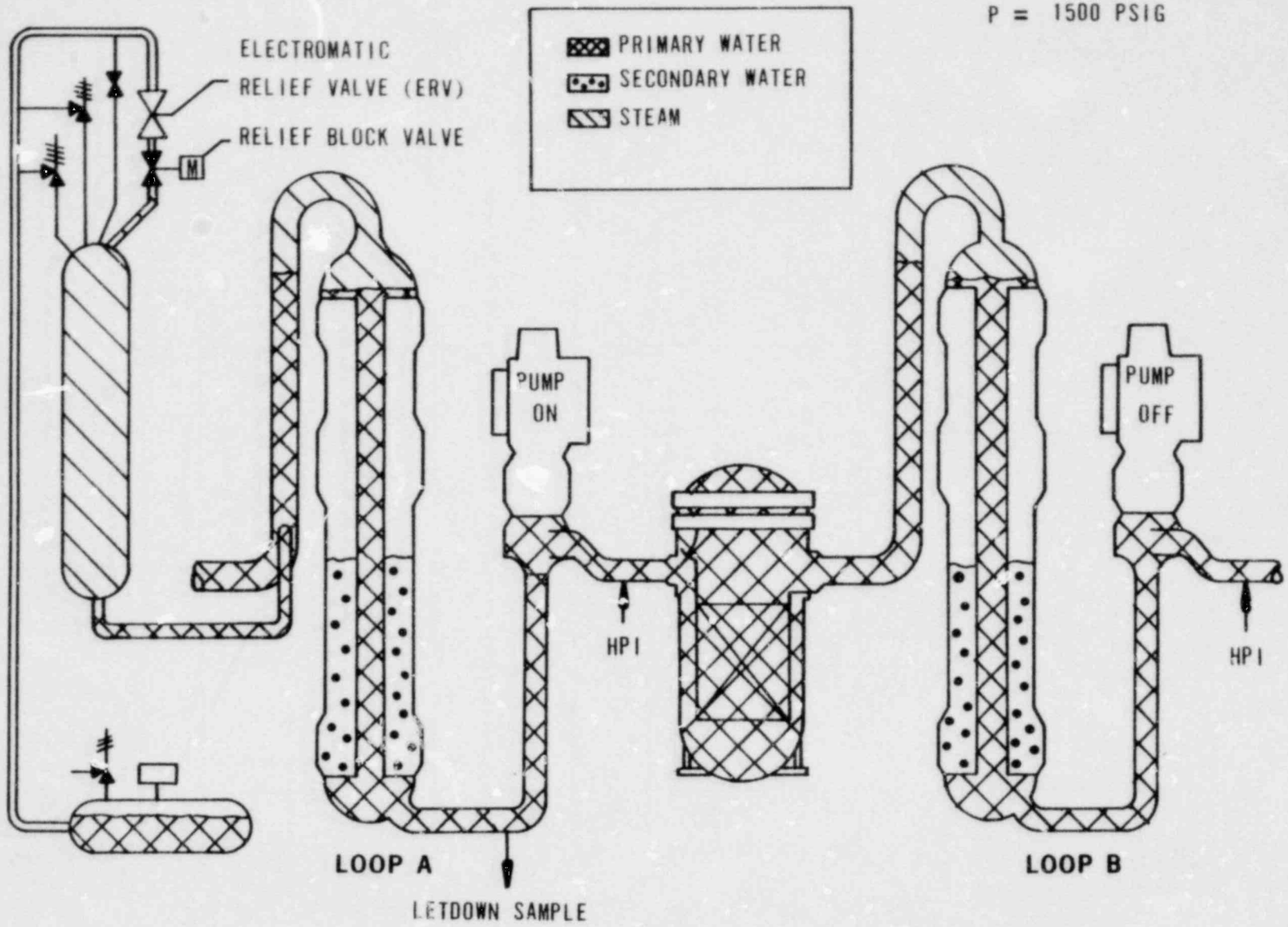

Figure 14-3. Behavior of H_2O During Depressurization/Repressurization

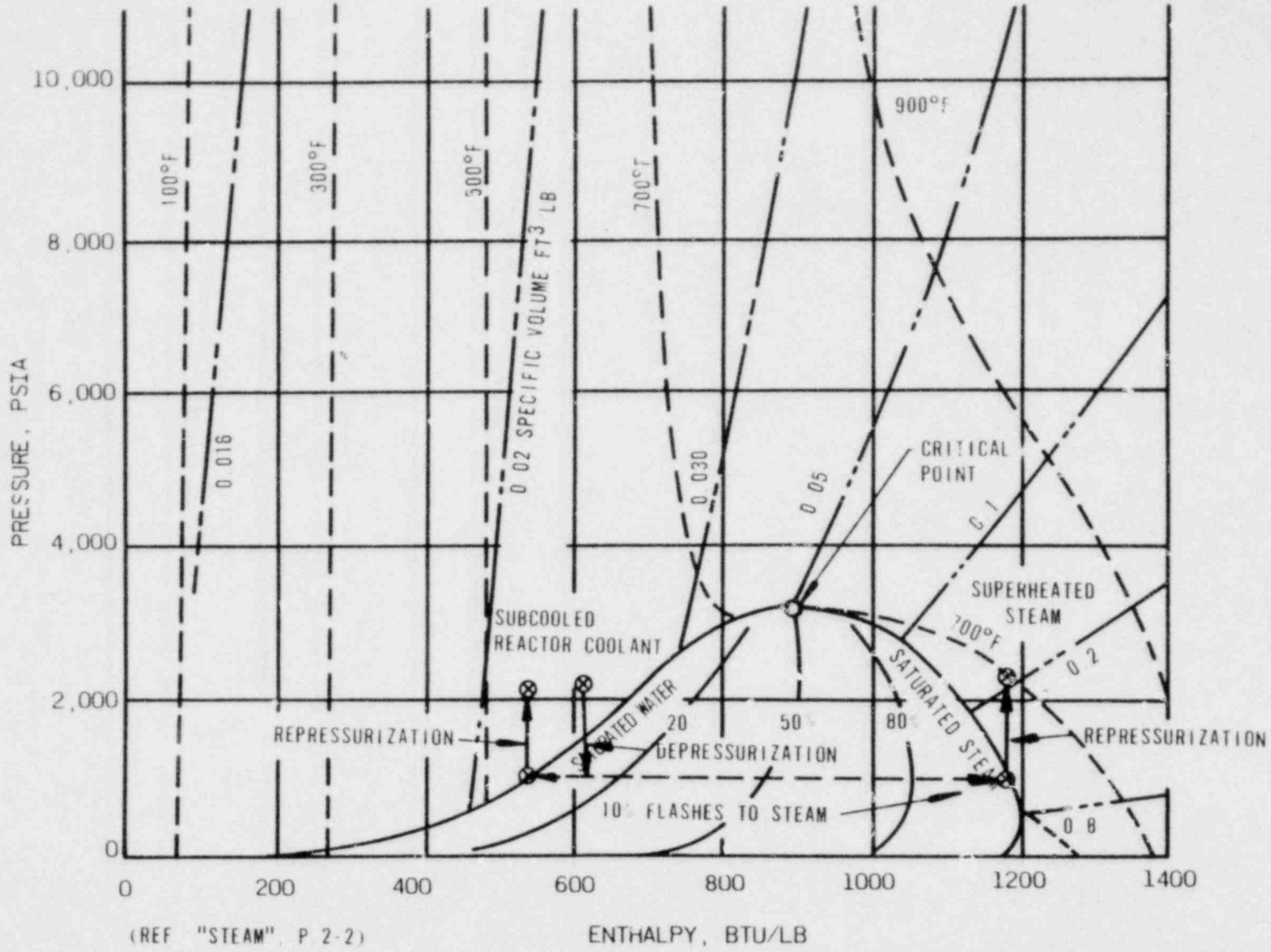

Figure 14-4. Hydrogen Generation by Zirconium/Water Reaction (Letdown Sample not Representative)

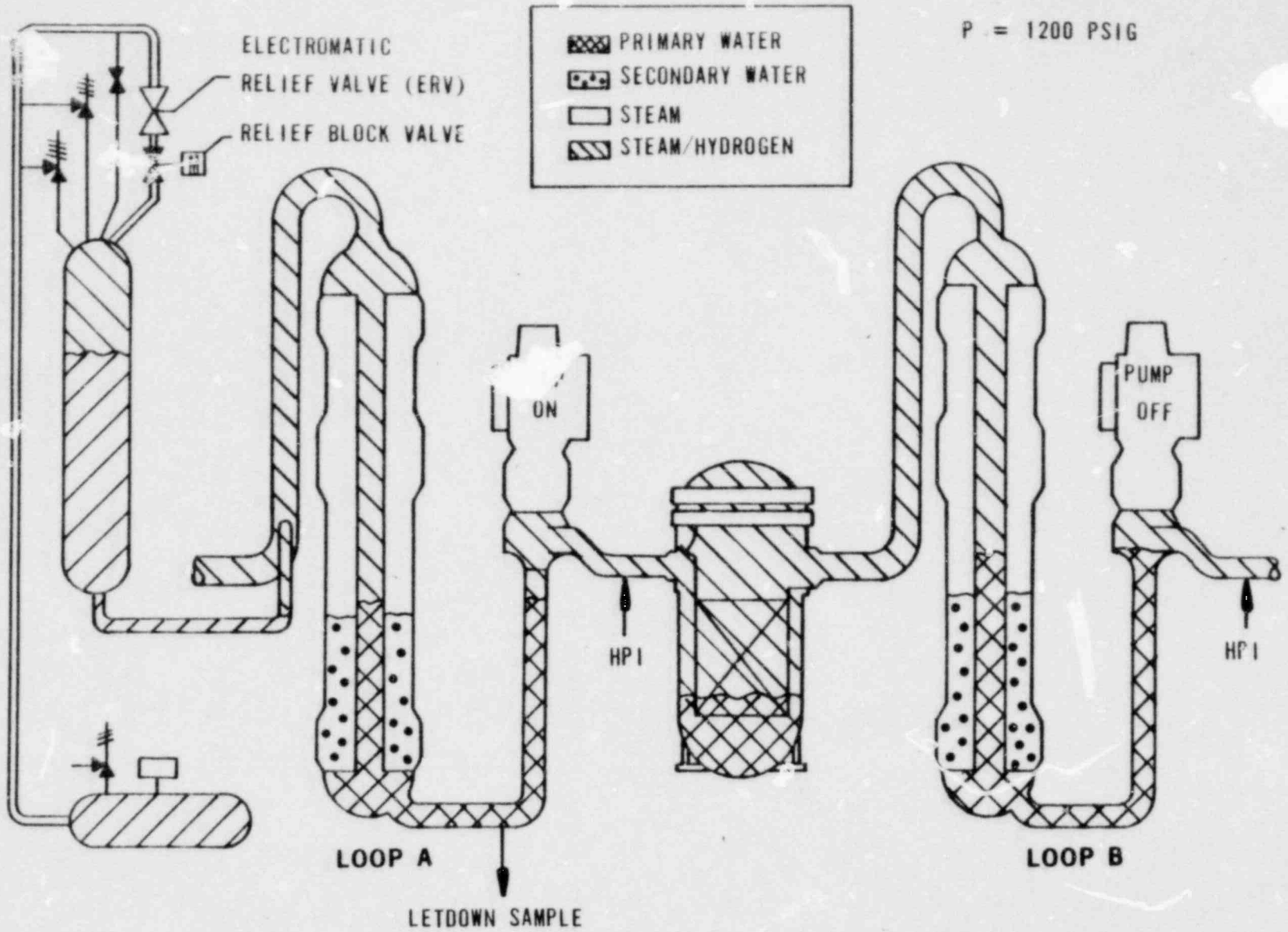

Figure 14-3. Estimate of Total Hydrogen Volume in RCS of TMI-2

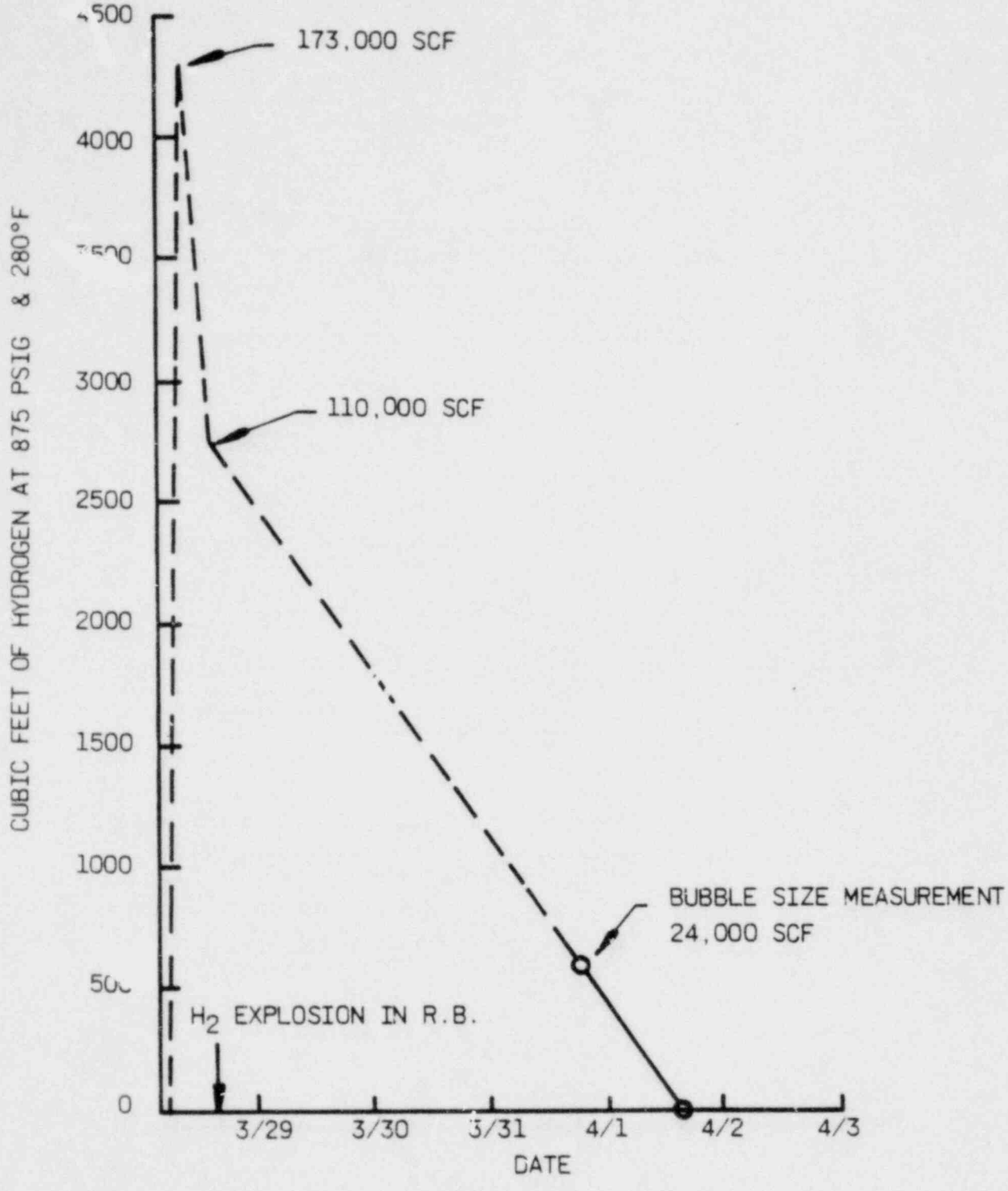

Figure 14-6. Gas Bubble Trapped in Reactor Vessel Head

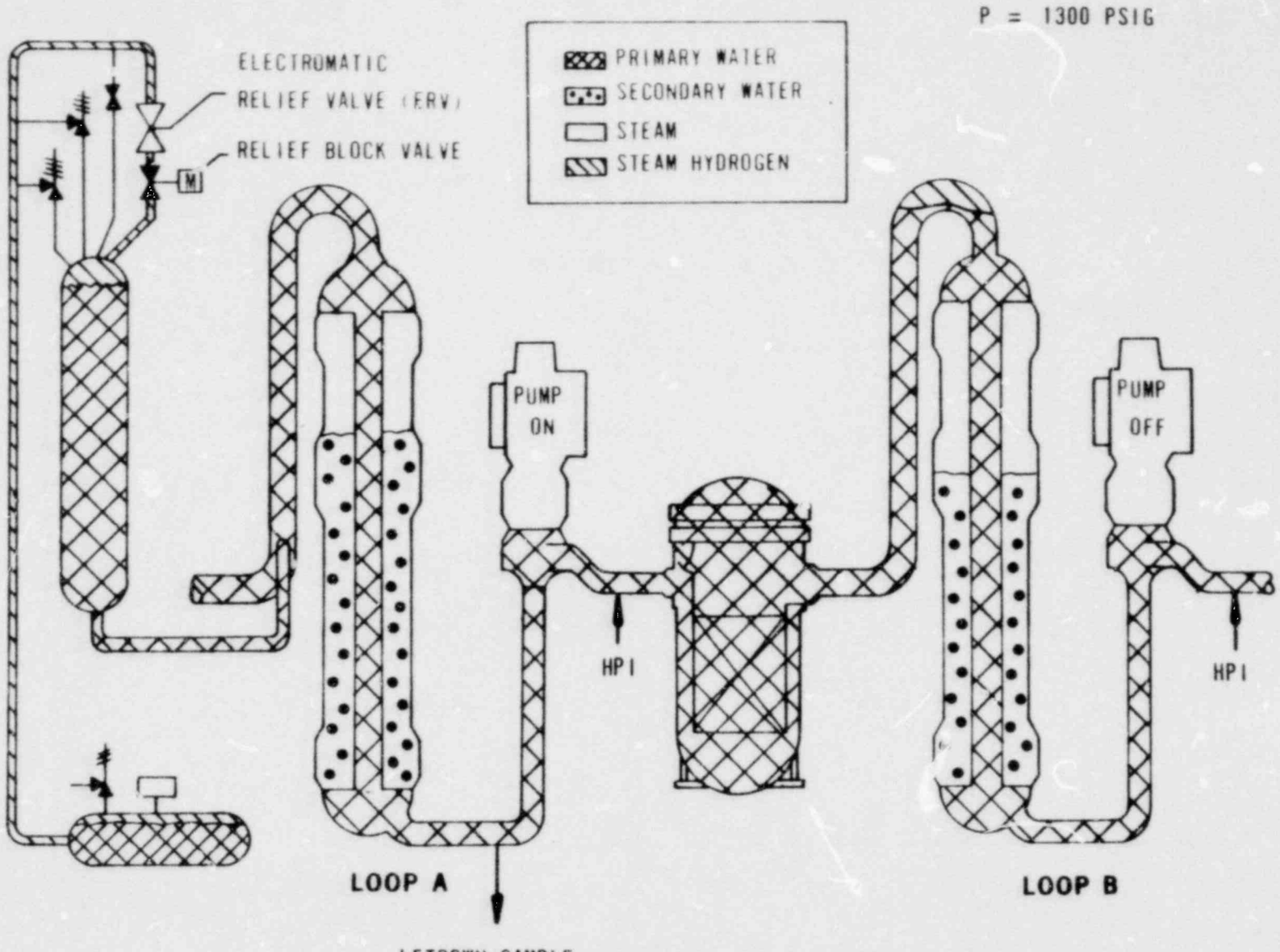

Figure 14-7. Estimate of Gas Bubble Volume in TMI-2 Reactor Vessel

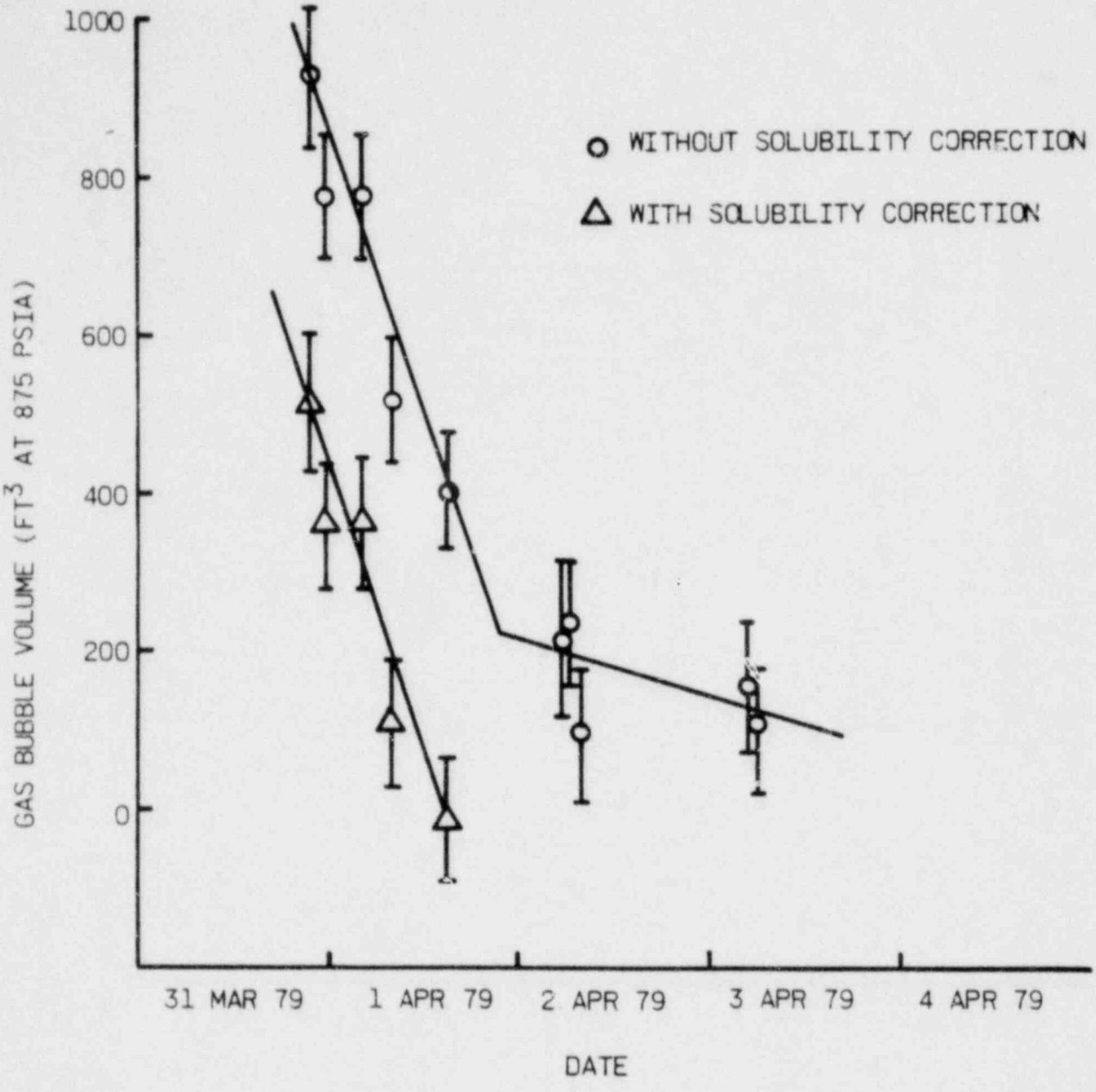

Figure 14-8. Solubility of Hydrogen in Reactor Coolant

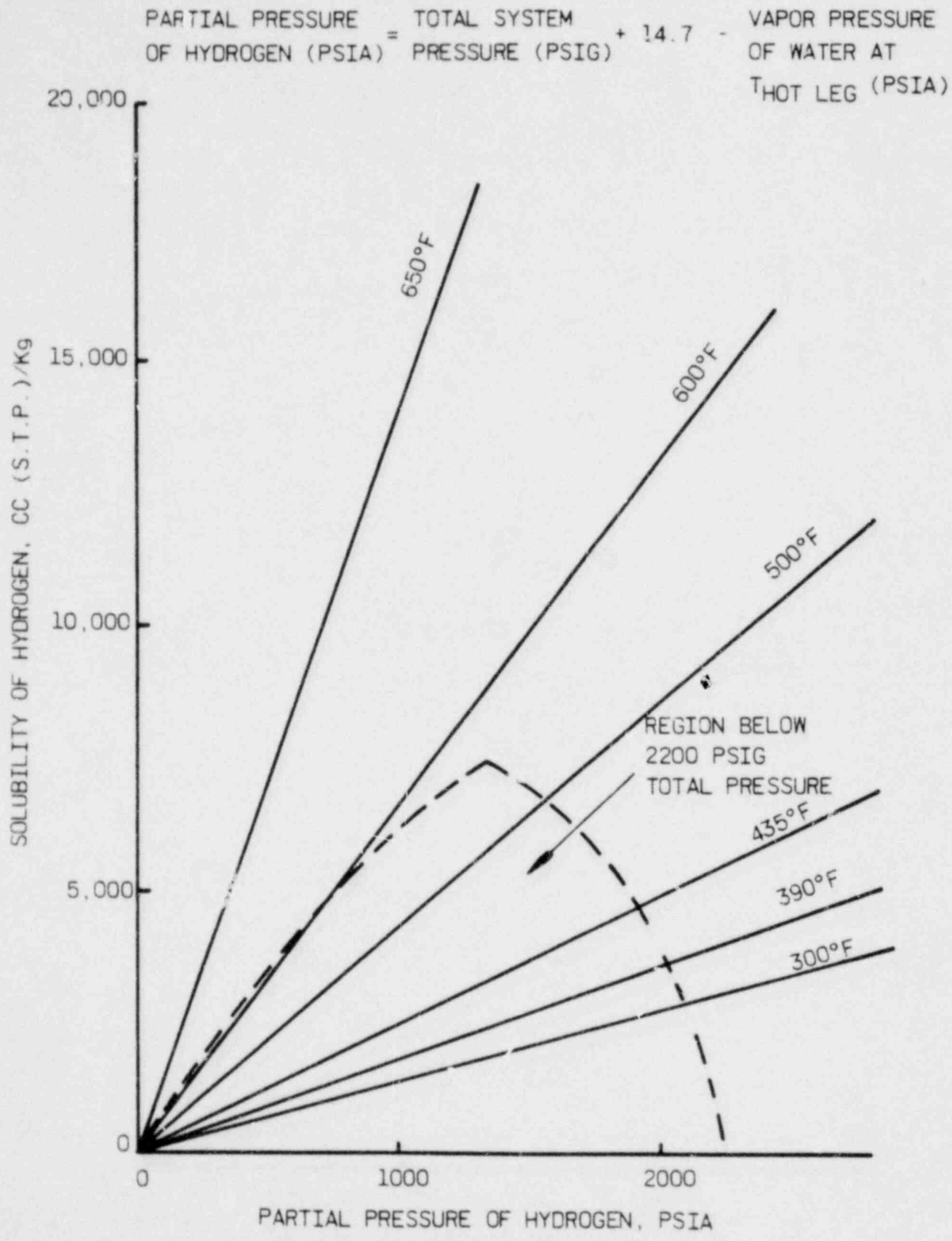

Figure 14-9. Reactor Coolant Degassing Rate After Gas Bubbles are Dissolved

EFFECTIVE DEGASSING FLOW RATE

$K(GPM) = E_1F_1 + E_2F_2 + F_3$

WHERE

E_1, F_1 = EFFICIENCY AND FLOW RATE FOR PRESSURIZER SPRAY FLOW

E_2, F_2 = EFFICIENCY AND FLOW RATE OF LETDOWN TO MAKEUP TANK

E_3 = REACTOR COOLANT LEAK RATE

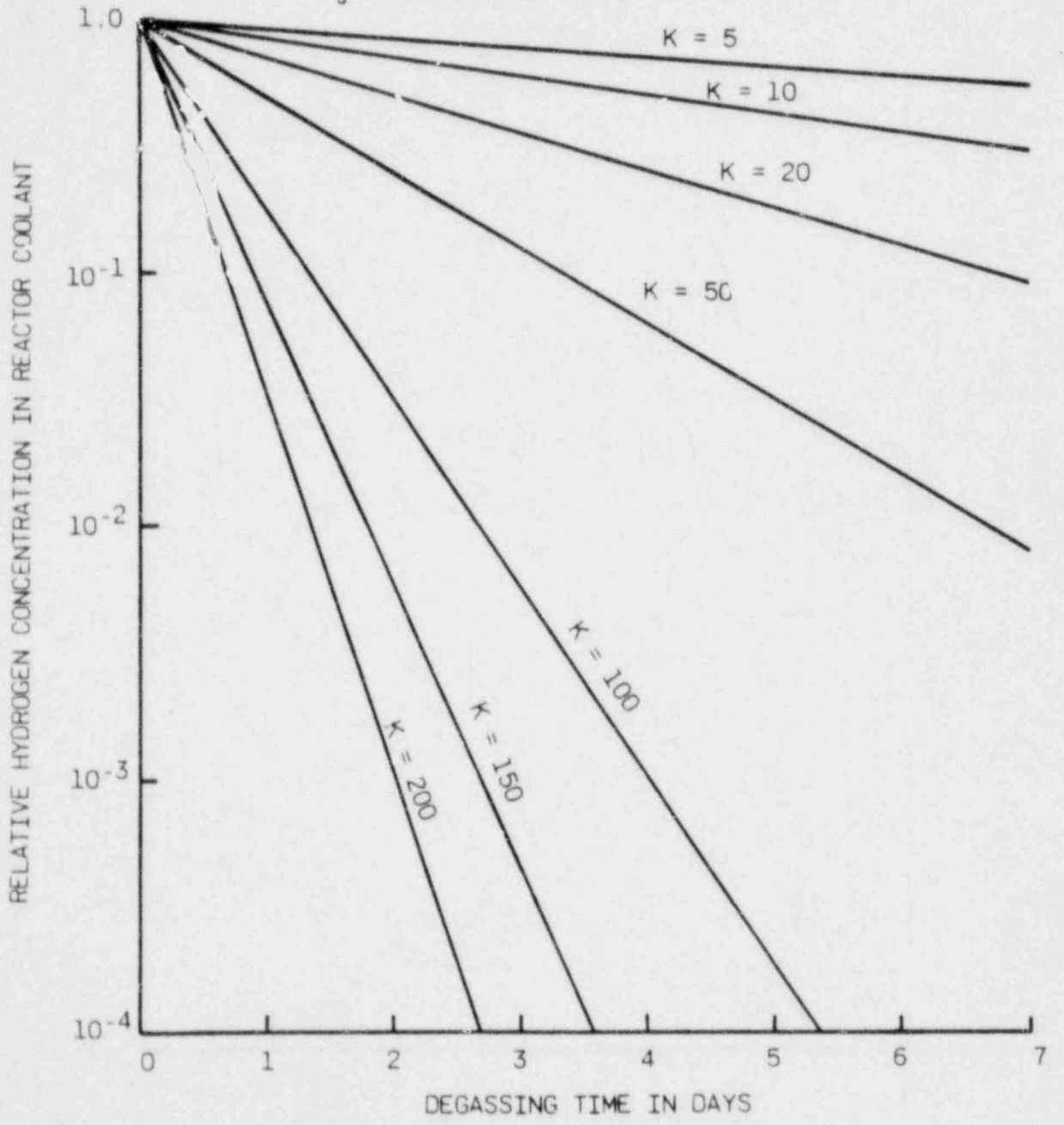

Figure 14-10. Boric Acid Solubility Limit

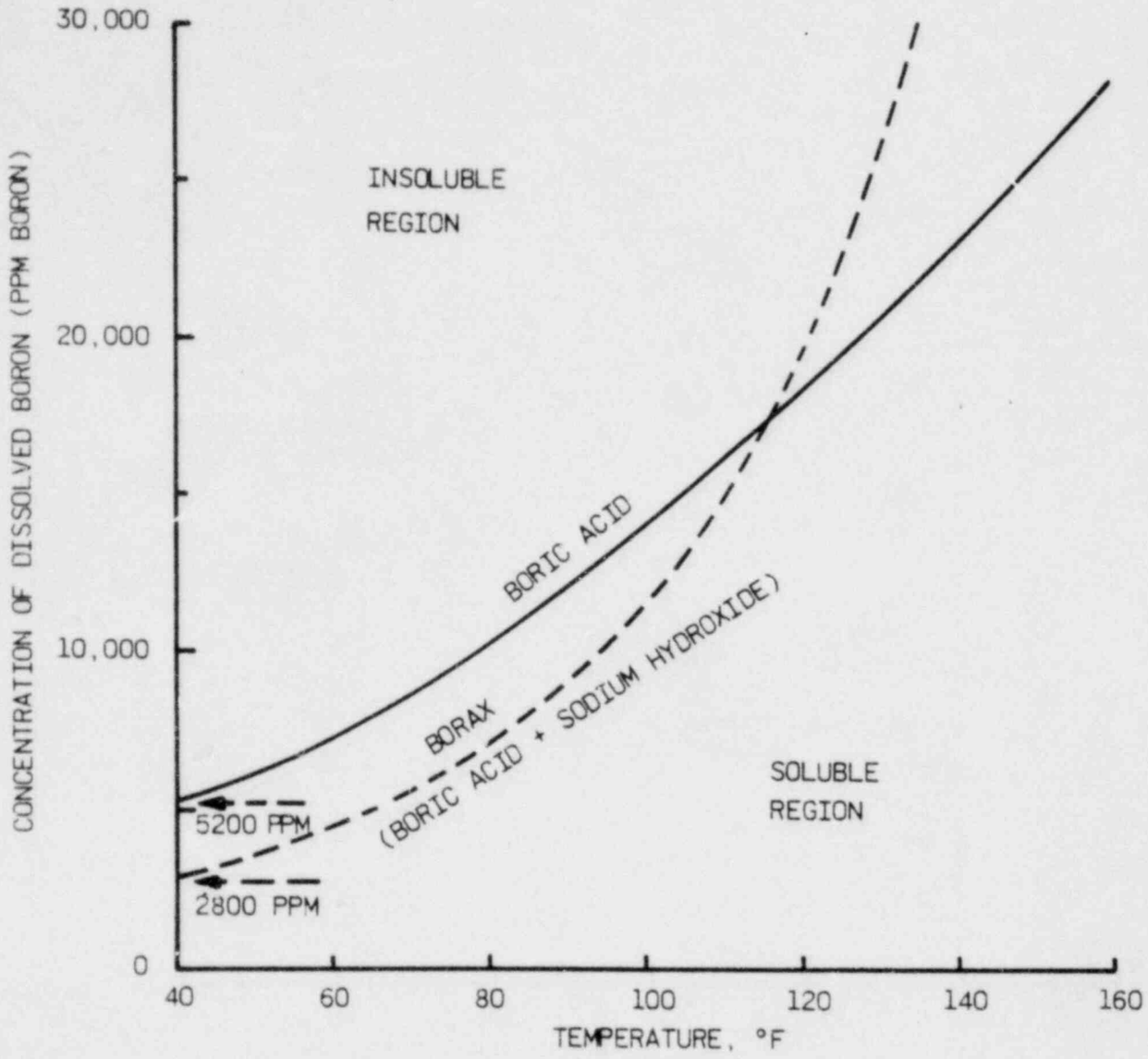

Figure 4-11. Example of Error Introduced By Cooling Concentrated Boric Acid

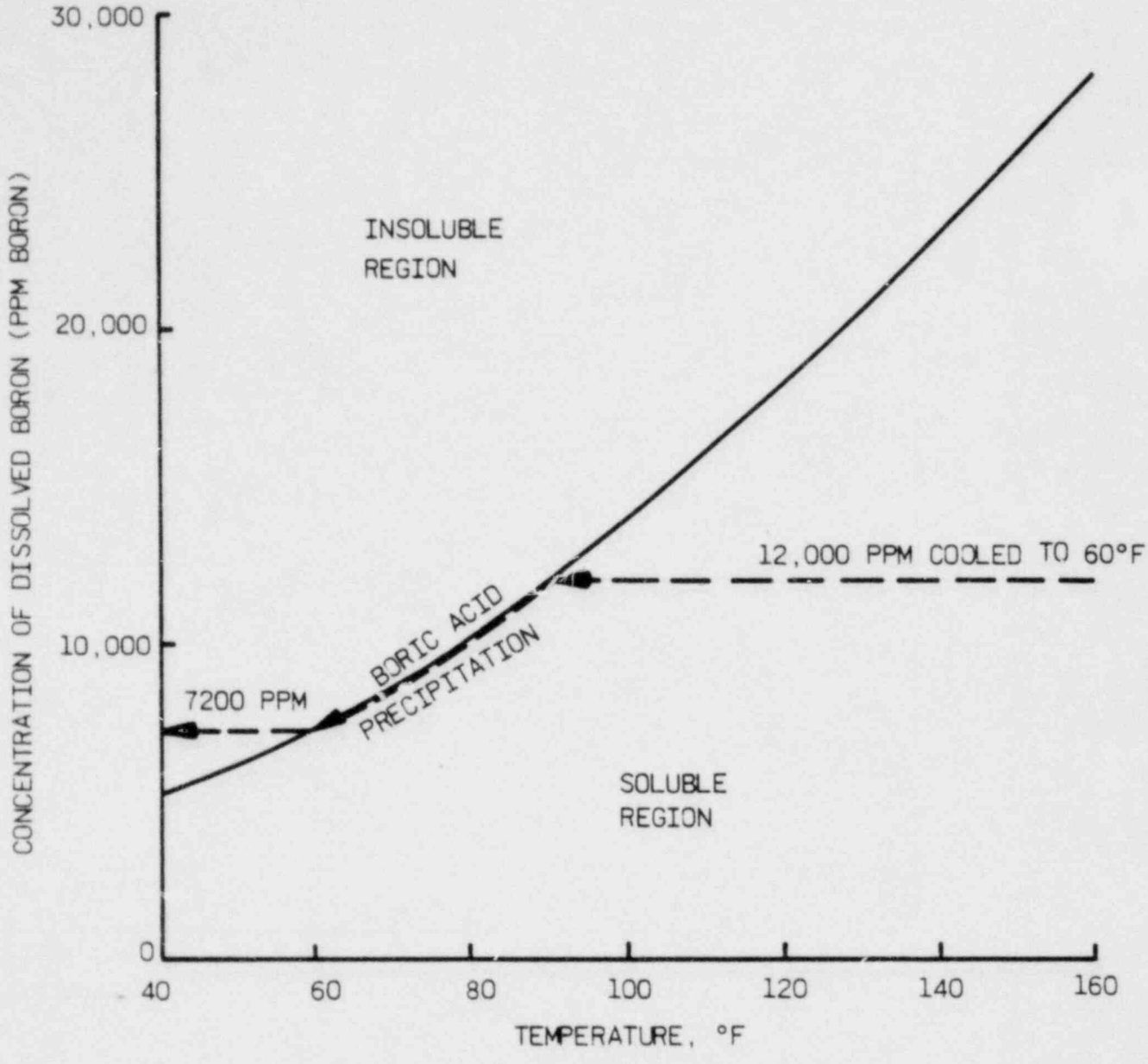

Figure 14-12. Typical Sampling System